frontiers | Research Topics

Third window syndrome, volume II

Edited by
P. Ashley Wackym, Carey David Balaban, Tetsuo Ikezono, Konstantina M. Stankovic and Todd Mowery

Published in
Frontiers in Neurology

ISSN 1664-8714
ISBN 978-2-8325-5720-4
DOI 10.3389/978-2-8325-5720-4

About Frontiers

Frontiers is more than just an open access publisher of scholarly articles: it is a pioneering approach to the world of academia, radically improving the way scholarly research is managed. The grand vision of Frontiers is a world where all people have an equal opportunity to seek, share and generate knowledge. Frontiers provides immediate and permanent online open access to all its publications, but this alone is not enough to realize our grand goals.

Frontiers journal series

The Frontiers journal series is a multi-tier and interdisciplinary set of open-access, online journals, promising a paradigm shift from the current review, selection and dissemination processes in academic publishing. All Frontiers journals are driven by researchers for researchers; therefore, they constitute a service to the scholarly community. At the same time, the *Frontiers journal series* operates on a revolutionary invention, the tiered publishing system, initially addressing specific communities of scholars, and gradually climbing up to broader public understanding, thus serving the interests of the lay society, too.

Dedication to quality

Each Frontiers article is a landmark of the highest quality, thanks to genuinely collaborative interactions between authors and review editors, who include some of the world's best academicians. Research must be certified by peers before entering a stream of knowledge that may eventually reach the public - and shape society; therefore, Frontiers only applies the most rigorous and unbiased reviews. Frontiers revolutionizes research publishing by freely delivering the most outstanding research, evaluated with no bias from both the academic and social point of view. By applying the most advanced information technologies, Frontiers is catapulting scholarly publishing into a new generation.

What are Frontiers Research Topics?

Frontiers Research Topics are very popular trademarks of the *Frontiers journals series*: they are collections of at least ten articles, all centered on a particular subject. With their unique mix of varied contributions from Original Research to Review Articles, Frontiers Research Topics unify the most influential researchers, the latest key findings and historical advances in a hot research area.

Find out more on how to host your own Frontiers Research Topic or contribute to one as an author by contacting the Frontiers editorial office: frontiersin.org/about/contact

Third window syndrome, volume II

Topic editors

P. Ashley Wackym — Department of Head and Neck Surgery & Communication Sciences, Rutgers Robert Wood Johnson Medical School, United States

Carey David Balaban — University of Pittsburgh, United States

Tetsuo Ikezono — Saitama Medical University, Japan

Konstantina M. Stankovic — Stanford University, United States

Todd Mowery — Rutgers, The State University of New Jersey, United States

Citation

Wackym, P. A., Balaban, C. D., Ikezono, T., Stankovic, K. M., Mowery, T., eds. (2024). *Third window syndrome, volume II*. Lausanne: Frontiers Media SA.

doi: 10.3389/978-2-8325-5720-4

Table of contents

frontiers | Frontiers in Neurology

TYPE Editorial
PUBLISHED 20 March 2025
DOI 10.3389/fneur.2025.1554737

OPEN ACCESS

EDITED AND REVIEWED BY
Michael Strupp,
Ludwig Maximilian University of Munich, Germany

*CORRESPONDENCE
P. Ashley Wackym
wackym@neurotology.org

RECEIVED 02 January 2025
ACCEPTED 05 February 2025
PUBLISHED 20 March 2025

CITATION
Wackym PA, Balaban CD, Stankovic KM, Ikezono T and Mowery TM (2025) Editorial: Third window syndrome, volume II. *Front. Neurol.* 16:1554737. doi: 10.3389/fneur.2025.1554737

Editorial: Third window syndrome, volume II

P. Ashley Wackym[1]*, Carey D. Balaban[2], Konstantina M. Stankovic[3], Tetsuo Ikezono[4] and Todd M. Mowery[1]

[1]Department of Head and Neck Surgery & Communication Sciences, Rutgers Robert Wood Johnson Medical School, New Brunswick, NJ, United States, [2]Department of Otolaryngology, University of Pittsburgh, Pittsburgh, PA, United States, [3]Department of Otolaryngology – Head and Neck Surgery, Stanford University School of Medicine, Palo Alto, CA, United States, [4]Department of Otolaryngology and Neuro-Otology, Saitama Medical University Hospital, Saitama, Japan

KEYWORDS

dizziness, headache, migraine, otic capsule dehiscence, perilymph fistula, superior semicircular canal dehiscence, third window syndrome, vestibular migraine

Editorial on the Research Topic
Third window syndrome, volume II

This Research Topic, *Third window syndrome volume II*, compiles the latest discoveries on the mechanisms underlying the spectrum of symptoms and dysfunction associated with Third Window Syndrome. It presents novel diagnostic tools and interventions aimed at identifying and resolving this condition.

Nearly a century ago, Tullio described the physiologic outcomes of creating a third mobile window in the semicircular canals of pigeons (1, 2). Although third mobile windows have been identified subsequently at other sites in the labyrinth, the "Tullio phenomenon" eponym Is applied generally to sound-induced dizziness and/or nystagmus. Superior semicircular canal dehiscence is clearly the best-known and most thoroughly characterized type of a third mobile window. In 1998, Minor and coworkers first reported sound- and/or pressure-induced vertigo due to bone dehiscence of the superior semicircular canal, confirmed on CT scans (3). Minor later distinguished both an inner ear conductive hearing loss (i.e., bone-conduction hyperacusis), and a reduced cervical vestibular myogenic potential (cVEMP) threshold with increased amplitude responses in patients with superior semicircular canal dehiscence. While the clinical phenotype associated with the superior semicircular canal dehiscence is well-recognized; third window syndrome with the same clinical phenotype has been reported in patients without radiographic evidence of a frank superior semicircular canal dehiscence (4–9). Such a CT-negative third window syndrome is associated with an inner ear conductive hearing loss and an abnormally reduced cVEMP threshold, among other objective findings typically found in patients with superior semicircular canal dehiscence (4–9). The more general term of Third Window Syndrome has gained acceptance recently because the same spectrum of symptoms, signs on physical examination and audiological diagnostic findings are associated with mobile third windows at different otic capsule loci. These locations includes superior semicircular canal dehiscence, superior semicircular canal dehiscence-superior petrosal vein dehiscence, superior semicircular canal dehiscence-sub-arcuate artery dehiscence, lateral semicircular canal-superior semicircular canal ampulla dehiscence, posterior semicircular canal dehiscence, posterior semicircular canal-endolymphatic sac dehiscence,

posterior semicircular canal-jugular bulb dehiscence, cochlea-internal carotid artery dehiscence, cochlea-internal auditory canal dehiscence, cochlea-facial nerve dehiscence, modiolus, perilymph fistula, vestibule-middle ear dehiscence, lateral semicircular canal-facial nerve dehiscence, wide vestibular aqueduct in children, posttraumatic hypermobile stapes footplate and in patients with CT negative Third Window Syndrome [review see (4–9)]. Pathological third mobile window at an otic capsule defect is the common structural finding in all of these conditions.

Over the past 70 years, our understanding of Third Window Syndrome has advanced significantly. Contributions from objective diagnostic studies, descriptions of clinical features, assessment of clinical outcomes with validated survey instruments, and neuropsychology testing have expanded the disciplinary scope diagnosis and treatment of these disorders. One restricted to the hallmark symptoms of sound-induced otolithic dysfunction (dizziness) and autophony, consequences of Third Window Syndrome are recognized to encompass manifestations of anxiety, migraine, spatial disorientation and cognitive dysfunction. The collection of papers featured in this Research Topic offers valuable insights for both scientists and clinicians working in the fascinating fields of peripheral vestibular dysfunction and its related central pathophysiology.

This Research Topic was truly global in effort and representation with four continents: Asia, Australia/Oceania, Europe, and North America. However, three were not represented: Africa, Antarctica, and South America. There were five countries represented: USA; Japan, France, Canada, and New Zealand. There were 68 authors.

In this editorial, we present an overview of the 12 published studies included in this Research Topic, organized into the following categories: New Animal Model; Diagnostic Studies and New Diagnostic Tools; Sites of Dehiscence; Surgical Advances; and Surgical Outcomes.

New animal model

Wackym et al. have developed and reported a gerbil model of superior semicircular canal dehiscence, displaying reversible diagnostic findings that are characteristic of patients with the disorder, such as an inner ear conductive hearing loss and increased amplitude cervical positive vestibular evoked myogenic potentials. Using this animal model, Mowery et al. demonstrated reversible impairments in specific auditory and visual behavioral tasks that assess decision-making performance. Specific and reversible cognitive deficits were associated with vestibular dysfunction in the presence of the otic capsule deficit. Specifically, the animals with a surgically-induced, superior semicircular canal dehiscence displayed reversible deficits in a spatial two-alternative forced-choice task, in which they must choose between a left or right option to receive a food reward. Together, these findings show how an otic capsule defect can disrupt normal decision-making behaviors. Most recently, Hong et al. used the same gerbil superior semicircular canal dehiscence model to confirm that aberrant asymmetric vestibular output results in reversible balance impairments, similar to those observed in patients after superior semicircular canal dehiscence plugging surgery. Together, these findings show how a unilateral mobile third window can disrupt normal cognitive functions and behaviors, and the methodology used to establish the gerbil animal model can be employed in other species to systematically investigate the influence of vestibular function on peripheral ear and central cognitive processing.

Diagnostic studies and new diagnostic tools

Third Window Syndrome has emerged as a significant clinical diagnosis, benefiting thousands of patients globally through its discovery and the development of effective treatments. Moreover, this syndrome serves as valuable pathologic phenomenon that enhances our understanding of the physiology of the vestibular end organs, and aids in the development and refinement of diagnostic tools that probe various aspects of the vestibular system.

Kileny et al. studied the diagnostic utility of electrocochleography (EcochG) relative to the inner ear conductive hearing loss in 20 patients with confirmed superior semicircular canal dehiscence. Eleven patients had unilateral superior semicircular canal dehiscence, and nine patients had bilateral superior semicircular canal dehiscence demonstrated by high-resolution temporal bone CT scanning. There were 29 ears with superior semicircular canal dehiscence and 11 normal ears included in their study. They found that all confirmed superior semicircular canal dehiscence ears presented with an abnormal EcochG summating potential to action potential (SP/AP) ratio value and that there was a statistically significant difference between normal and dehiscent ears. There was no statistically significant relationship between inner ear conductive hearing loss air-bone gap and SP/AP ratio in the ears diagnosed with superior semicircular canal dehiscence. Further, there was no significant difference in the inner ear conductive hearing loss air-bone gap at three frequencies between the normal and dehiscent ears. The authors concluded that EcochG remains a valuable diagnostic tool for superior semicircular canal dehiscence. They also emphasized that the variability in the air-bone gap associated with inner ear conductive hearing loss should not drive the decision to include EcochG in the diagnostic test battery for patients suspected of having this condition.

Ito et al. reported the case of a 27-year-old female who complained of hearing disturbance in her right ear and recurrent vertigo after sudden onset of hearing loss with vertigo. She had reduced vestibular function in the affected ear demonstrated by caloric testing and video head impulse testing. The innovative diagnostic testing reported used a contrast-enhanced MRI technique using hybrid of reversed positive image of endolymph signal and a negative image of perilymph signal which they interpreted as a collapsed endolymphatic space. After failed medical management and with persistent vestibular symptoms, an exploratory right tympanotomy was performed and both the round and oval windows were sealed with connective tissue. The patient's vestibular symptoms improved rapidly after surgery, accompanied by imaging improvement of the collapsed endolymphatic space in a postoperative contrast-enhanced MRI. A unilateral weakness persisted in the caloric test postoperatively, but the VOR gain on the vHIT improved to normal on the right side. Thus, these findings

are consistent with concept a collapsed endolymphatic space may contribute to recurrent symptoms caused by a perilymph fistula. They speculated that a ruptured Reissner membrane contributed to the collapsed endolymphatic space and further hypothesized that sealing the fistula resulted in normalization of the perilymph pressure by promoting healing of the ruptured Reissner membrane. This case added to the existing literature on the occurrence of the *"double-membrane break syndrome."*

Kubota et al. investigated the diagnostic performance of endoscopic middle ear examination compared to testing for cochlin-tomoprotein test (newly developed perilymph specific protein detection test) in diagnosing idiopathic perilymphatic fistula. Diagnosing this condition is particularly difficult when patients present with sudden sensorineural hearing loss or vestibular symptoms without any clear prior incidents. The study examined five patients who initially received intratympanic dexamethasone treatment for sudden sensorineural hearing loss, during which a cochlin-tomoprotein test was also conducted. For those who did not respond to corticosteroids, endoscopic perilymph fistula repair was performed, sealing the oval and round windows using connective tissue and fibrin glue. The researchers assessed cochlin-tomoprotein levels preoperatively and intraoperatively, findings from endoscopic surgery, and changes in hearing and vestibular symptoms both before and after the procedure. Results showed varied cochlin-tomoprotein levels: three patients had positive pre-operative and intermediate intraoperative values, one patient had positive preoperative but negative intraoperative values, and one showed negative preoperative but positive intraoperative values. No patient displayed clear endoscopic evidence of a fistula or perilymph leakage during surgery. Hearing improvement was minimal, with only two patients showing slight recovery. Of the four patients who experienced disequilibrium before surgery, two reported resolution of these symptoms post-operatively. The study concluded that a positive cochlin-tomoprotein test can provide confirmation of perilymph fistula in cases lacking obvious intraoperative findings.

Sites of dehiscence

Ionescu et al. published an interesting series of complex superior semicircular canal dehiscence patients whose outcomes were not as successful as expected. They initially considered both errors in surgical repair technique and the possibility of co-existing sites of otic capsule defects as factors contributing to the poorer-than-expected clinical outcomes. A review of the radiological and clinical files, they discussed possible surgical technique issues in one case and the likelihood of other undetected dehiscence sites. They completed a retrospective analysis of high-resolution temporal bone CT scans from 157 patients (314 ears), collected over a 5-year period, to examine the prevalence of both symptomatic and asymptomatic Third Window Syndrome. They detected multiple suspected sites of otic capsule dehiscence in the ipsilateral ear in 29 of 157 patients (18.47%).

These findings were similar to those reported in 2019 by Wackym et al. in the original Research Topic focused on Third Window Syndrome. A dehiscence was found in 463 temporal bones of ears with Third Window Syndrome symptoms (57.7% [463/802]). The single sites included superior semicircular canal dehiscence, near-superior semicircular canal dehiscence, CT negative Third Window Syndrome, cochlea-facial nerve, cochlea-internal auditory canal, wide vestibular aqueduct, lateral semicircular canal, modiolus, and posterior semicircular canal, superior semicircular canal dehiscence and superior petrosal sinus, superior semicircular canal dehiscence, and subarcuate artery dehiscence. After excluding temporal bones from cases with no CT evidence of a dehiscence, the remaining 402 bones included 366 cases (91.0%) with a single temporal bone dehiscence site. Multiple sites of dehiscence were observed less frequently, For example, a two site dehiscence was observed in 9.38% of cases (superior semicircular canal dehiscence and cochlea-facial nerve dehiscence, cochlea-facial nerve dehiscence and cochlea-internal auditory canal, cochlea-facial nerve dehiscence and wide vestibular aqueduct canal dehiscence, superior semicircular and cochlea-internal auditory canal, superior semicircular canal dehiscence and posterior semicircular canal-jugular bulb). The most prevalent combination. A superior semicircular canal dehiscence and cochlea-facial nerve dehiscence, accounted for 6% of all cases. The combination of (30/502). Thus, the Ionescu et al. study and the earlier Wackym et al. study agree that the prevalence of multiple-site findings is important to consider when faced with recurrent or incompletely resolved Third Window Syndrome symptoms after plugging a superior semicircular canal dehiscence. Both studies also emphasize the prudence of careful assessment of the potential additional dehiscence sites prior to determining the surgical approach for managing superior semicircular canal dehiscence.

In this Research Topic, Seo et al. reported a case of a microfissure near the round window niche that communicated between middle ear and the ampulla of the posterior semicircular canal. They reported the first case of a patient successfully treated with perilymph fistula repair surgery, presenting with ipsilateral hearing loss, tinnitus described as a flowing-water sound, and a floating sensation triggered by pressing the left tragus, which was caused by an inner ear microfissure. An exploratory tympanotomy was performed 8 days after onset of his symptoms, revealing intraoperative findings of a microfissure and an accumulation of clear fluid in the floor of the round window niche. The site of leakage was sealed with connective tissue. One month after surgery, clinical improvement in his hearing and disequilibrium suggested that the microfissure contributed to his auditory and vestibular symptoms.

Surgical advances

Sawada et al. described "a multilayer round window reinforcement technique" in managing patients with superior semicircular canal dehiscence (SSCD). This technique involved making an incision within the external auditory canal, and collecting loose areolar tissue, which was compressed using a fascia press and cut into 3 to 5-mm pieces. Cartilage and perichondrium were obtained from the tragus, then thinned and shaped into approximately 2–3 mm circular sections. A CO_2 laser was employed to remove mucosa from the area around the round window niche. A thin piece of cartilage with perichondrium was positioned within the bony overhang, with the perichondrium side

facing the round window to prevent damage to its membrane. Small cartilage fragments, about 0.25 mm in size, were added around the initial cartilage to fill gaps and stabilize the structure. Thinned connective tissue was layered over this structure, adhering to the exposed bone, while additional cartilage pieces were placed on top to secure the reinforcement. Finally, fibrin glue was used to hold everything in place.

To illustrate the outcomes of this technique, Sawada et al. shared two case studies where their "multilayer round window reinforcement technique" was applied to patients with SSCD. The procedure led to significant symptom relief, including diminished autophony, reduced hypersensitivity to bone-conducted sounds, decreased pulsatile tinnitus, and fewer vestibular disturbances triggered by sound or pressure. Patients also reported a lessening of aural fullness. Post-surgical assessments indicated notable improvements in scores from the Dizziness Handicap Inventory, Vertigo Symptom Scale Short Form, and the Niigata Persistent Postural-Perceptual Dizziness Questionnaire.

Altamami et al. developed a manual neuronavigation technique to more consistently identify the superior semicircular canal and the site of dehiscence in superior semicircular canal dehiscence. While a computer-assisted neuronavigation system is useful to precisely identify the location of a superior semicircular canal dehiscence, there are several limitations regarding the cost of purchasing these systems and the need to charge patients for their use during the surgery. Additional limitations of computer-assisted neuronavigation systems are that more surgical time is required to set up, calibrate and use during middle cranial fossa superior semicircular canal dehiscence plugging, which is exacerbated when the surgeon's experience is limited. The study reported by Altamami et al. demonstrated a simple manual neuronavigation technique that can help neurotologic surgeons identify the superior semicircular canal dehiscence accurately and efficiently. They demonstrated that the use of *"line A"* on the preoperative high-resolution temporal bone CT axial cut, which measures the distance from the superior semicircular canal dehiscence to the lateral cortical part of the supra-auricular squamous bone, provides a precise distance that can be measured during surgery. These findings were supplemented by two instructional videos that explained and demonstrated the technique.

Surgical outcomes

Matsuda et al. presented a retrospective analysis involving 22 patients who underwent surgical treatment for perilymph fistula after conservative treatment had failed. The study explored case characteristics and assessed the effectiveness of the procedure in alleviating both vestibular and auditory symptoms. It was observed that patients with prior triggering events had a significantly shorter duration between symptom onset and surgery. Post-operatively, 82% of the patients experienced substantial relief from vestibular symptoms within a week, even among those with long-standing conditions. Although the study lacked a control group, the marked improvement in vestibular function and the significant reduction in Dizziness Handicap Inventory scores suggest that these outcomes were likely a result of the surgical intervention. Additionally, early surgical intervention showed improvements in hearing, with some positive effects also noted in cases with delayed surgery. By utilizing cochlin-tomoprotein, a perilymph-specific protein, as a biomarker, the study confirmed that the presence of a perilymph fistula contributed to both balance and auditory issues in these patients. Furthermore, the authors introduced a new hypothesis, referred to as the "Hyperactive Utricular Movement Theory," suggesting that chronic imbalance in these cases may result from increased utricular mobility rather than endolymphatic hydrops.

Benchetrit et al. sought to identify predictors of symptom persistence after surgical management of superior semicircular canal dehiscence. They conducted a retrospective study of 132 ears in 126 patients who underwent superior semicircular canal dehiscence plugging via the middle cranial fossa or transmastoid approach. The authors used a previously published standardized symptomatology questionnaire from their preoperative and postoperative visits. The questionnaire asked patients to identify if their most bothersome complaint is hearing-related or balance-related. Binary (yes/no) responses were recorded for the subjective experience of 11 auditory symptoms [hearing loss, aural fullness, pulsatile tinnitus, non-pulsatile tinnitus, autophony (hearing your voice too loudly), hyperacusis, hearing your voice echo, hearing your footsteps, hearing your eyeballs moving or hearing hair brushing, or shaving sounds too loudly] and eight vestibular symptoms (general dizziness, sense of imbalance, Tullio phenomenon, straining causing dizziness, physical activity causing dizziness, blowing your nose/sneezing/coughing causing dizziness, oscillopsia, and positional dizziness). Information regarding postoperative resolution of primary (most bothersome) symptom complaint was obtained from reviewing the electronic medical record and stratified to the categories of resolved, improved and persisted. The preoperative vs. post-operative survey results, demographic and clinical characteristics, operative characteristics, audiometric data and cervical vestibular evoked myogenic potential (cVEMP) thresholds were compared via univariate χ^2 and multivariate binary logistic regression analyses between those patients reporting full post-operative resolution of symptoms and persistence of one or more symptoms. The authors found that of the 132 ears in 126 patients, 119 patients (90.2%) reported postoperative resolution ($n = 82$, 62.1%) or improvement ($n = 37$, 28.0%) of primary (most bothersome) symptoms, while 13 patients (9.8%) reported persistence of primary symptoms. The median (interquartile range) and range between surgery and questionnaire completion were 9 months (4–28), 1–124 months, respectively. Analyzing all symptoms (primary and non-primary) 69 (52.3%) and 68 (51.1%) patients reported complete postoperative auditory and vestibular symptom resolution, respectively. They found that the most likely persistent symptoms included imbalance (33/65, 50.8%), positional dizziness (7/20, 35.0%), and oscillopsia (44/15, 26.7%). Factors associated with persistent auditory symptoms included history of seizures (0% vs. 7.6%, $p = 0.023$), auditory chief complaint (50.0% vs. 70.5%), higher PTA (mean 19.6 vs. 25.1 dB, $p = 0.043$) and higher cervical vestibular evoked myogenic potential (cVEMP) thresholds at 1,000 Hz (mean 66.5 dB vs. 71.4 dB, $p = 0.033$). A migraine diagnosis (14.0% vs. 41.9%, $p < 0.010$), bilateral radiologic superior semicircular canal dehiscence (17.5% vs. 38.1%, $p = 0.034$), and revision cases (0.0% vs. 14.0%, $p = 0.002$)

were associated with persistent vestibular symptoms. They also found that neither superior semicircular canal dehiscence size nor location were significantly associated with symptom persistence ($p > 0.05$). The authors concluded that surgical plugging of a superior semicircular canal dehiscence results in a meaningful reduction in the majority of auditory and vestibular symptoms; however, the persistence of certain, mostly non-primary, symptoms, and the identification of potential associated factors including migraines, pure tone average thresholds, cVEMP thresholds, bilateral superior semicircular canal dehiscence, and patients representing revision cases underscore the need for individualized patient counseling and management strategies.

Conclusions

In this Editorial, we highlight the 12 published studies included in this Research Topic and organized them in the following categories: New Animal Model; Diagnostic Studies and New Diagnostic Tools; Sites of Dehiscence; Surgical Advances; and Surgical Outcomes.

Research on new diagnostic tools indicates that Third Window Syndrome can provide valuable insights into the mechanisms of the inner ear. There are three key symptoms and physical signs that are essential for identifying Third Window Syndrome, regardless of specific location of the dehiscence: (1) sound-induced dizziness; (2) hearing internal sounds; and (3) hearing or feeling low frequency tuning forks in an involved ear when applied to a patient's knee or elbow. The sound-induced auditory and vestibular activity is distinct from other balance disorders because the transient vestibular afferent activity is uncoupled from motion of the head or body in space (allocentric reference frame) or from motion of the environment around the head and body (egocentric reference frame). The sound-induced auditory and vestibular activity will also be uncorrelated with contextual visual, somesthetic and interoceptive sensory information and on-going (or planned) motor activity. While the studies examining cognitive and spatial orientation in Third Window Syndrome shed light on important cognitive outcome measures for researching patients with vestibular impairments, neither their measures nor validated survey instruments for symptoms—such as the Dizziness Handicap Inventory—are specifically tailored to account for the distinctive perceptual incongruities present in Third Window Syndrome compared to other conditions. Although current tools may be useful for monitoring patient outcomes in the management of Third Window Syndrome, there is potential for improvement and refinement. The studies included in this Research Topic provided useful conceptual and state-of-the-art frameworks to better understand peripheral bases for the signs and symptoms of common forms of Third Window Syndrome. In addition, a series of basic research studies developing a new animal model of superior semicircular canal dehiscence creates the opportunity to study the fundamental neuroanatomic circuitry underlying the changes in cognitive dysfunction and other central nervous system phenomena that patients with Third Window Syndrome experience. These frameworks are essential for designing specific diagnostic tests and new, potentially therapeutic approaches. Finally, rare and newly identified sites of dehiscence creating a third mobile window were presented and surgical advances to manage various sites resulting in Third Window Syndrome were reported. Together, these 12 studies provide a comprehensive overview of our current knowledge, as well as gaps that remain in understanding, diagnosing and managing of patients with Third Window Syndrome.

Author contributions

PAW: Conceptualization, Project administration, Supervision, Writing – original draft, Writing – review & editing. CDB: Conceptualization, Writing – review & editing. KMS: Conceptualization, Writing – review & editing. TI: Conceptualization, Writing – review & editing. TMM: Conceptualization, Writing – review & editing.

Funding

The author(s) declare that financial support was received for the research and/or publication of this article. Funded via the Rutgers Health Chancellor Scholar (PAW).

Conflict of interest

The authors declare that the research was conducted in the absence of any commercial or financial relationships that could be construed as a potential conflict of interest.

The author(s) declared that they were an editorial board member of Frontiers, at the time of submission. This had no impact on the peer review process and the final decision.

Publisher's note

References

1. Tullio P. *Das Ohr und die Entstehung der Sprache und Schrift*. Berlin, Germany: Urban & Schwarzenberg (1929), p. 1–455.

2. Huizinga E. The physiological and clinical importance of experimental work on the pigeon's labyrinth. *J Laryngol Otol.* (1955) 69:260–8. doi: 10.1017/S0022215100050635

3. Minor LB, Solomon D, Zinreich JS, Zee DS. Sound- and/or pressure-induced vertigo due to bone dehiscence of the superior semicircular canal. *Arch Otolaryngol Head Neck Surg.* (1998) 124:249–58. doi: 10.1001/archotol.124.3.249

4. Wackym PA, Wood SJ, Siker DA, Carter DM. Otic capsule dehiscence syndrome: Superior canal dehiscence syndrome with no radiographically visible

dehiscence. *Ear Nose Throat J.* (2015) 94:E8–24. doi: 10.1177/014556131509400802

5. Wackym PA, Balaban CD, Mackay HT, Wood SJ, Lundell CJ, Carter DM, et al. Longitudinal cognitive and neurobehavioral functional outcomes after repairing otic capsule dehiscence. *Otol Neurotol.* (2016) 37:70–82. doi: 10.1097/MAO.0000000000000928

6. Wackym PA, Balaban CD, Zhang P, Siker DA, Hundal JS. Third window syndrome: surgical management of cochlea-facial dehiscence. *Front Neurol.* (2019) 10:1281. doi: 10.3389/fneur.2019.01281

7. Wackym PA, Balaban CD, Mowery TM. History and overview of third mobile window syndrome. In: Gianoli GJ, Thomson P. editors. *Third Mobile Window Syndrome of the Inner Ear*. Switzerland AG: Springer Nature (2023). p. 3–25. doi: 10.1007/978-3-031-16586-3_1

8. Mowery TM, Balaban CD, Wackym PA. The cognitive/psychological effects of third mobile window syndrome. In: Gianoli GJ, Thomson P. editors. *Third Mobile Window Syndrome of the Inner Ear*. Switzerland AG: Springer Nature (2023). p. 107–119. doi: 10.1007/978-3-031-16586-3_6

9. Wackym PA, Balaban CD, Mowery TM. Migraine, headache and third mobile window syndrome. In: Gianoli GJ, Thomson P. editors. *Third Mobile Window Syndrome of the Inner Ear*. Switzerland AG: Springer Nature (2023). p. 421–433. doi: 10.1007/978-3-031-16586-3_25

frontiers | Frontiers in Neurology

TYPE Original Research
PUBLISHED 19 January 2023
DOI 10.3389/fneur.2022.1035478

OPEN ACCESS

EDITED BY
Vincent Van Rompaey,
University of Antwerp, Belgium

REVIEWED BY
Wei Gao,
The Fourth Military Medical University, China
Erin Gillikin Piker,
James Madison University, United States
Alexandre Bisdorff,
Hospital Center Emile Mayrisch, Luxembourg

*CORRESPONDENCE
Todd M. Mowery
tm692@rwjms.rutgers.edu

†These authors share first authorship

SPECIALTY SECTION
This article was submitted to Neuro-Otology, a section of the journal Frontiers in Neurology

RECEIVED 02 September 2022
ACCEPTED 15 November 2022
PUBLISHED 19 January 2023

CITATION
Wackym PA, Balaban CD, Van Osch OJ, Morris BT, Tamakloe M-A, Salvatore VL, Duwadi S, Gay JD and Mowery TM (2023) New model of superior semicircular canal dehiscence with reversible diagnostic findings characteristic of patients with the disorder. *Front. Neurol.* 13:1035478. doi: 10.3389/fneur.2022.1035478

New model of superior semicircular canal dehiscence with reversible diagnostic findings characteristic of patients with the disorder

P. Ashley Wackym [1,2†], Carey D. Balaban [3†], Olivia J. Van Osch[1], Brian T. Morris[1], Mark-Avery Tamakloe[1], Victoria L. Salvatore[1], Sudan Duwadi[1], Jennifer D. Gay[1] and Todd M. Mowery [1,2*]

[1]Department of Otolaryngology – Head and Neck Surgery, Rutgers Robert Wood Johnson Medical School, New Brunswick, NJ, United States, [2]Rutgers Brain Health Institute, New Brunswick, NJ, United States, [3]Departments of Otolaryngology, Neurobiology, Communication Sciences and Disorders, Bioengineering and Mechanical Engineering and Materials Science, University of Pittsburgh School of Medicine, Pittsburgh, PA, United States

Background: Third window syndrome is a vestibular-cochlear disorder in humans in which a third mobile window of the otic capsule creates changes to the flow of sound pressure energy through the perilymph/endolymph. The nature and location of this third mobile window can occur at many different sites (or multiple sites); however, the most common third mobile window is superior semicircular canal dehiscence (SSCD). There are two essential objective diagnostic characteristics needed to validate a model of SSCD: the creation of a pseudoconductive hearing loss and cVEMP increased amplitude and decreased threshold.

Methods: Adult Mongolian gerbils ($n = 36$) received surgical fenestration of the superior semicircular canal of the left inner ear. ABR and c+VEMP testing were carried out prior to surgery and over acute (small 1 mm SSCD, 1–10 days) or prolonged (large 2 mm SSCD, 28 days) recovery. Because recovery of function occurred quickly, condenser brightfield stereomicroscopic examination of the dehiscence site was carried out for the small SSCD animals *post-hoc* and compared to both ABRs and c+VEMPs. Micro-CT analysis was also completed with representative samples of control, day 3 and 10 post-SSCD animals.

Results: The SSCD created a significant worsening of hearing thresholds of the left ear; especially in the lower frequency domain (1–4 kHz). Left (EXP)/right (CTL) ear comparisons *via* ABR show significant worsening thresholds at the same frequency representations, which is a proxy for the human pseudoconductive hearing loss seen in SSCD. For the c+VEMP measurements, increased amplitude of the sound-induced response (N1 2.5 ms and P1 3.2 ms) was observed in animals that received larger fenestrations. As the bone regrew, the c+VEMP and ABR responses returned toward preoperative values. For small SSCD animals, micro-CT data show that progressive osteoneogenesis results in resurfacing of the SSCD without bony obliteration.

Conclusion: The large (2 mm) SSCD used in our gerbil model results in similar electrophysiologic findings observed in patients with SSCD. The changes observed also reverse and return to baseline as the SSCD heals by bone resurfacing (with the lumen intact). Hence, this model does not require a second surgical procedure to plug the SSCD.

KEYWORDS

cognitive dysfunction, dizziness, memory, perilymph fistula, spatial disorientation, superior semicircular canal dehiscence, third window syndrome, vestibular evoked myogenic potential

Introduction

While it was nearly a century ago that Tullio described the physiologic outcomes of creating a third mobile window in the semicircular canals of pigeons (1, 2), it was a quarter century ago that Minor et al. first described superior semicircular canal dehiscence (SSCD) in two patients (3). However, this is not a new clinical entity as SSCD has been observed after CT imaging of Egyptian mummy heads (4). Since 1998, many locations of third mobile windows have been described [for review see (5–7)]. The sound-induced dizziness and/or nystagmus due to a third mobile window has been memorialized by the eponym "Tullio phenomenon." Clinically, the most thoroughly characterized third mobile window is SSCD. Minor later reported a conductive hearing loss, which was recognized as a pseudoconductive hearing loss (bone-conduction hyperacusis) (8), as well as a reduced cervical vestibular myogenic potential (cVEMP) threshold in patients with SSCD to 81 ± 9 dB nHL (9). We, and others, have proposed the more general term of third window syndrome because the same spectrum of symptoms, signs on physical examination, and audiological diagnostic findings, e.g., pseudoconductive hearing loss and the abnormally reduced cVEMP threshold with increased amplitude, are encountered with SSCD as well as the other 14 known third mobile window locations that can be seen with high-resolution temporal bone CT [for review see (5–7)].

There are two essential objective diagnostic characteristics needed to validate a model of SSCD: the creation of a pseudoconductive hearing loss and VEMP increased amplitude and decreased threshold. Because unilateral bone-conduction ABR thresholds in rodents cannot be measured, it is not possible to measure the pseudoconductive hearing loss, but the proxy finding of worsened ABR thresholds is adequate, particularly, when the hearing loss recovers once the surgically created SSCD recloses after bone regrowth. The two previous animal models tried to record cVEMP responses, but they did not appreciate that the sternocleidomastoid evoked potentials (cVEMP) are relaxation potentials, and this explains why the animal SSCD literature has no convincing cVEMP responses shown in the models published to date (10–12). In contrast, it is well-known that sound-induced otolithic neck extensor responses are excitatory potentials (13); therefore, we developed a c+VEMP method that demonstrates increased c+VEMP amplitudes and decreased c+VEMP thresholds after surgically creating a SSCD in our model, just as we see in patients with SSCD.

Patients with third window syndrome, including SSCD, also report symptoms of autophony, cognitive dysfunction, spatial disorientation, anxiety, and autonomic dysfunction (7, 14–16). To varying degrees, patients with SSCD describe cognitive dysfunction (impaired memory and concentration, word finding and name finding difficulty, occasional slurred speech and for women, the loss of the ability to listen to more than one person speaking at a time), spatial disorientation (trouble judging distances, sense of detachment, sometimes perceiving the walls moving/breathing or the floor moving, and less commonly out of body experiences), and anxiety (sense of impending doom). In children and young adults continuing their education, their academic performance typically drops; they miss days of school and are often assigned a psychiatric or neurobehavioral diagnosis (5–7, 14–16). SSCD and other third window syndrome patients with other sites of dehiscence frequently experience migraine headaches as well as the three variants of migraine: ocular migraine [an older term which has been replaced with migraine with aura (bilateral visual field loss) with or without headache], hemiplegic migraine, and vestibular migraine (5–7, 14–19). Retinal migraine (unilateral visual field loss) has not been reported in patients with SSCD or other third window syndrome sites of dehiscence. Ward et al. reported that many patients with SSCD also have migraine, but they commented that this may represent the high prevalence of migraine in the general population and that SSCD is an effective migraine trigger (19). Naert et al. completed a systematic review of SSCD symptoms and after combining synonymous terms, 22 symptoms were derived by consensus that also included headache (20). These additional symptoms typically resolve or markedly improve after surgically managing the third mobile window (5–7, 14–19, 21, 22). However, for reasons that are not understood,

the pseudoconductive hearing loss typically does not resolve after plugging the SSCD (23–25). The value of developing an animal model of SSCD in a rodent well-known for inner ear similarities with humans and capability to be trained to perform complex behavioral tasks designed to measure decision-making is that the basic electrophysiologic, neural plasticity, and molecular events subserving the cognitive dysfunction can be studied and understood. With this knowledge, new translational interventions to treat patients with SSCD can be discovered. It was for this purpose that we sought to develop this SSCD model in adult Mongolian gerbils. Consequently, we hypothesized that the creation of bony dehiscence of the SSC would result in diagnostic findings that resemble patients with SSCD. For example, we expect to see changes in otolithic stimulation as measured by VEMPs and pseudoconductive hearing loss as measured by ABR as a proxy since bone-conduction thresholds cannot be measured in gerbils due to small skull size.

Materials and methods

Animals

A total of 36 adult Mongolian gerbils *Meriones unguiculatus* (19 males and 17 females) were used in this study. All animals were housed in the same vivarium facility under a 12/12 dark cycle with *ad libitum* access to food and water. Animals were randomly divided into two groups, which received either small (1 mm) or large (2 mm) semicircular canal fenestrations. The Rutgers University IACUC reviewed and approved this research protocol (PROTO202000179).

Surgical creation of the superior semicircular canal dehiscence

Animals were anesthetized with isoflurane and prepared for stereotaxic surgery. Figure 1 shows the detailed surgical method for creating a left SSCD. Figure 1A is a cartoon that shows the middle/inner ear and the location of the surgically created SSCD "third mobile window." The inset (Figure 1A) shows the site of dehiscence. The skull (top left) and nuchal muscles (center and bottom right) are exposed (Figure 1B). After the muscles were taken down from the bulla, the superior bulla is exposed (Figure 1B, inset). The superior bulla was opened widely with a 1.5-mm diamond bur, and the dissection was carried near, but not into the surrounding sinus, to avoid bleeding (Figure 1C). Through the open bulla, the intact superior semicircular canal was visualized. Using a 1-mm diamond bur, a controlled fenestration of the superior (anterior) semicircular canal was completed (Figure 1D). It should be noted that the bone of the superior semicircular canal, including the endosteum, was precisely removed. The endolymphatic duct was seen to be intact and surrounded by perilymph illustrating the precise surgical creation of the SSCD (Figure 1D). Sterile physiologic saline was used to irrigate away bone debris; however, it was not possible to remove the bone debris at the margins of the fenestration by irrigation, likely contributing to the bone regrowth. After the fenestration was completed, the perilymph was open and exposed without egressing, just as patients with SSCD have their perilymph exposed. The open bulla was then sealed/partitioned with Sterile Silastic (Dow Chemical Company, Midland, MI) to partition the air-filled bulla from the overlying neck muscles thereby restoring the normally air-filled middle ear (Figure 1E) and avoiding a true conductive hearing loss. Condensation on the interior surface of the Silastic seal was deemed indicative of this restoration of function. Finally, the reattached muscles were glued to the skull with Medbond tissue glue (Stoelting Co., Wood Dale, IL), which allowed c+VEMP testing as soon as the day after the surgical creation of the SSCD (Figure 1F). Condenser brightfield stereomicroscope and micro-CT analysis were performed *post-hoc* to assess the SSCD site and bone regrowth.

Auditory brainstem responses

Animals were anesthetized with isoflurane (1.0%) and placed in a small sound chamber (IAC, Sound Room Solutions, Inc, Glen Cove, NY). As shown in Figure 2A, ABR recordings were made by inserting pin electrodes subcutaneously at the vertex of the skull and just caudal to the right pinna; the ground electrode was inserted into the base of the tail. BioSigRZ software and the TDT ABR system (Tucker-Davis Technologies, Alachua, FL) were used to collect ABR data. A 10-cm tube (closed field) was inserted into the ear and placed at the opening of the ear canal. The left ear of the animal was stimulated *via* multi-field speaker (MF1, Tucker-Davis Technologies, Alachua, FL) at 1, 2, 4, 8, and 16 kHz tones [90 to 20 dB SPL (10 dB steps)], 5 ms, 2 ms linear ramp rise-fall times at 25 Hz. Traces were averaged across 500 (threshold) sweeps. Thresholds for each frequency were measured as the last dB SPL (i.e., 10 dB SPL resolution stimulus level) that elicited a tone-induced ABR.

Sound-induced cervical positive potential vestibular evoked myogenic potentials

As shown in Figure 2B, sound-induced otolithic stimulation and evoked intramuscular excitatory potential recordings were made by inserting pin electrodes into the neck extensor muscles (splenius capitus m.) and the reference electrode in the vertex of the skull. BioSigRZ software and the TDT ABR system were used to collect c+VEMP data. A 10-cm tube capable of delivering 100 dB SPL (see TDT specs, Closed Field) was inserted into the ear and placed at the opening of the ear canal. The

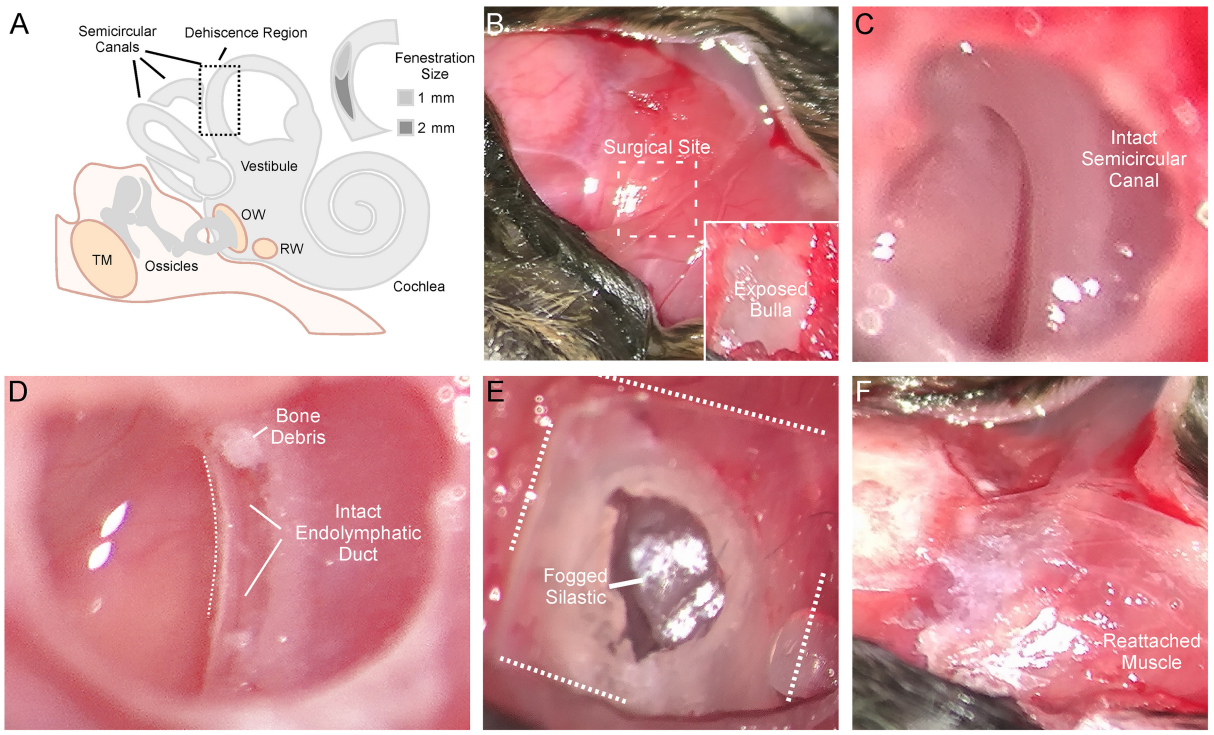

FIGURE 1
Detailed surgical method for creating left semicircular canal dehiscence (SSCD). **(A)** Cartoon showing the middle/inner ear and the location of the surgically created SSCD "third mobile window." The inset shows the dehiscence site. **(B)** Photomicrograph showing the exposed skull (top left). The exposed nuchal muscles can be seen (center and bottom right). In the inset, after the muscles are taken down from the bulla, the superior bulla is exposed. **(C)** The superior bulla is opened widely with a 1.5-mm diamond bur and the dissection is carried near, but not into the surrounding sinus, to avoid bleeding. Through the open bulla, the intact superior semicircular canal can be seen. **(D)** Using a 1-mm diamond bur, a controlled fenestration of the superior (anterior) semicircular canal is completed. It should be noted that the bone of the superior semicircular canal, including the endosteum, is precisely removed. The endolymphatic duct can be seen to be intact illustrating the precise surgical creation of the SSCD. Sterile physiologic saline is used to irrigate away bone debris. Note, bone debris at the margins of the fenestration cannot be removed by irrigation. This no doubt contributes to bone regrowth. The perilymph is open/exposed just as patients with SSCD have their perilymph exposed. **(E)** Photomicrograph shows the sealing of the bulla with Silastic to partition the air-filled bulla from the overlying neck muscles thereby restoring the normally air-filled middle ear. Note condensation on the interior surface of the Silastic seal. **(F)** The reattached muscles are glued to the skull with Medbond. This allows c+VEMP testing beginning the day after the surgical creation of the SSCD.

left ear of the animal was stimulated *via* multi-field speaker (MF1, Tucker-Davis Technologies, Alachua, FL) at 2kHz [100 to 80 dB SPL (5 dB steps), 5 ms, 2 ms linear ramp rise-fall times sampled at 25 kHz]. Traces were averaged across 500 (threshold) sweeps. The c+VEMPs were recorded under low-isoflurane anesthesia (<1.5%), near conditions of wakefulness. The c+VEMP was measured when it appeared under the condition of stimulation of air-conducted sound at 2 kHz and 100 dB. Peak amplitudes were measured by subtracting the peak of the negative N1 wave (in μV) from the later positive P1 wave (see Supplementary Figure 1).

Condenser brightfield stereomicroscope

After the systematic ABR and c+VEMP recordings were collected, animals were euthanized (Euthasol 300 mg/kg) and perfused for histology. Each animal's heart was accessed through the diaphragm. The right atrium was cut, and 20 ml of room-temperature phosphate-buffered saline (1M) was perfused through the left ventricle. This was followed by 20 ml of cold paraformaldehyde (4%). After perfusion, the animals were decapitated. The left bulla was dissected and immersed in paraformaldehyde (4%). The superior (anterior) semicircular canal was imaged using a condenser brightfield stereomicroscope through the opening into the bulla on a Revolve R4 microscope (ECHO, San Diego, CA).

Micro-CT imaging

The bullae containing the inner ears of three adult gerbils (>P86) were dissected, fixed with paraformaldehyde (4%),

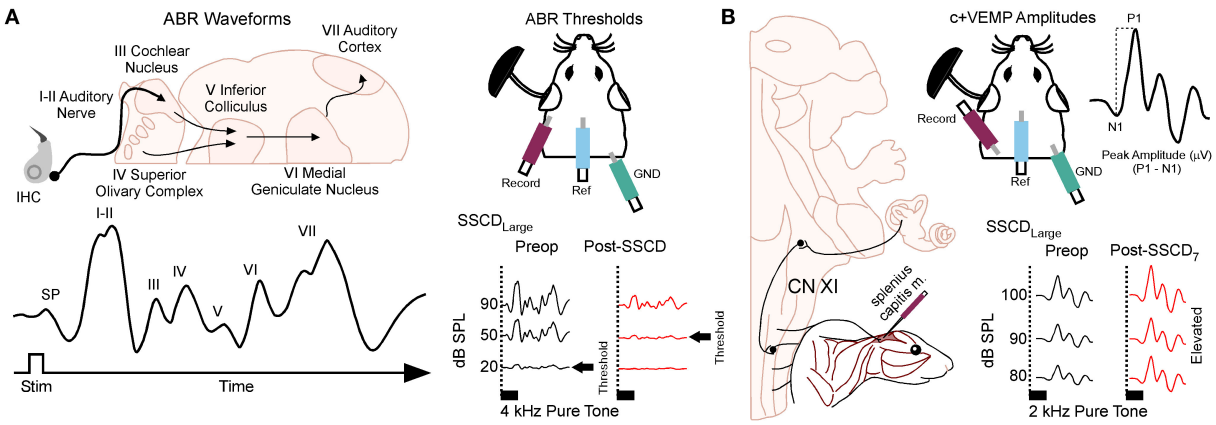

FIGURE 2
Semicircular canal dehiscence induces sound-induced changes to auditory and vestibular physiology. **(A)** Cartoon showing the configuration for closed field auditory brainstem responses (ABR) and threshold shifts that occur for 2 kHz tones after SSCD of the left ear. **(B)** Cartoon showing the configuration for the left ear when measuring the sound-induced cervical positive vestibular evoked myogenic potential (c+VEMP) in the anesthetized animal. Here, electrodes are inserted into the splenius capitus extensor muscles, and sound is delivered in a closed field to the ear with SSCD. The c+VEMP amplitude is calculated by subtracting the positive P wave 1 from the negative N wave 1. Pictured is the increase in c+VEMP amplitudes 7 days after surgical creation of a large SSCD.

and then stored in phosphate-buffered saline (1.0M). Serial micro-CT images of the specimens were acquired in the sagittal plane at a slice thickness of 5.0 μm [Bruker Skyscan 1,172 nanoCT (Bruker Corporation, Allentown, PA, USA)]. The high-resolution allows delineating of the semicircular canals and other inner ear structures. The 3D reconstructed images were rotated and oriented into the natural anatomical position. Micro-CT with maximum intensity projections (MIP), micro-CT with attenuated images, and serial section review through all six planes in the rectangular grid were created and reviewed using the Brucker CTvox software (Bruker Corporation). Specific regions of interest were selected, imaged, and exported for Figure creation in Canvas X (Canvas GFX, Inc, Boston, MA, USA).

Statistical analyses

Statistical analyses were performed using JMP software (SAS, Carey, NC) and SPSS (IBM, Armonk, New York). Figures were generated using JMP software. To test the main effects of SSCD over postoperative days, mixed model ANOVAs were generated. Where appropriate the Greenhouse–Geisser Adjustment test, the Kolmogorov–Smirnov tests, the Lilliefors Corrections, the Bonferroni corrections, and the Least Significant differences (LSD) multiple range tests were used to explore frequency, amplitude, and day-by-day interaction effects associated with the main effects. When comparing two unmatched data sets within groups (e.g., baseline to postoperative day), Student's *t*-test was utilized, and where appropriate *post-hoc* analysis using Tukey's Honestly Significant Difference (HSD) test was used to account for variance within and between groups. A matched *t*-test modeling was used for matched pair data sets that compared preoperative data to endpoint data within groups. A linear regression analysis was used to calculate adjusted R^2 scores when correlating data within groups. The mixed model ANOVA with repeated measures was used to analyze data between groups over days. For all analyses, significance was determined at $p < 0.05$ or greater. Data in the figures display group mean ± SEM or actual data points (e.g., regression analysis).

Results

Establishment of superior semicircular canal dehiscence induced changes to cochlear and vestibular output

We measured ABRs (Figure 2A) in animals ($n = 10$, 5M, 5F) with surgically created small (1 mm) SSCD fenestrations. In our pilot experiments, we found significant increases in ABR threshold compared to preoperative baselines 3 days after SSCD for all animals (mean ± SEM; baseline: 43.0 ± 8.8 vs. post-SSCD day 3: 67.25 ± 15.8; $t = 1.99$, $p < 0.0001$, Supplementary Figure 1A) suggesting that a pseudoconductive hearing loss accompanies SSCD in our model as it does in humans.

For the c+VEMP studies (Figure 2B), we first established the latency of N and P waves at descending sound intensities, as each organism differs in latency of nerve conduction based on size (e.g., human p latency is 13 ms and n latency is 23 ms, see Supplementary Figiure 1B). As we observed from ABR

measurements, c+VEMP characteristics [N1 latency (2.5 ms average), P1 latency (3.2 ms average), Supplementary Figure 1C; wave 1 duration, Supplementary Figure 1D] also were significantly altered by the SSCD.

Preoperative ABR and c+VEMPs

The preoperative ABR thresholds [$F_{(1,8)} = 3.27$, NS] and c+VEMPs [$F_{(1,8)} = 0.00$, NS] did not differ significantly between the animals that received small or large SSCD. The preoperative measurements of ABR thresholds showed a pattern of significant threshold differences as a function of frequency [$F_{(df=2.19,17.52)} = 26.07$, $p < 0.001$, Greenhouse–Geisser adjustment], The minimum threshold of 20 dB SPL was recorded from all subjects at 4 kHz: it was significantly lower ($p < 0.05$, Bonferroni correction) than the thresholds of 32.0 ± 2.0 dB SPL at 1 kHz, 32.0 ± 2.1 dB SPL at 8 kHz, and 43.0 ± 2.0 dB SPL at 16 kHz (mean ± SE). There were no significant variations in c+VEMP amplitudes across intensities in the preoperative assessments. The preoperative c+VEMP values at 90 dB SPL and 100 dB SPL stimuli were consistent with single Gaussian distributions (Kolmogorov–Smirnov tests and Lilliefors correction) with mean amplitudes and standard deviations of 604.72 ± 112.78 μV and 706.11 ± 159.71 μV, respectively.

Tracking prolonged peripheral impairment, recovery, and persistence after large superior semicircular canal dehiscence

The small SSCD group data showed a significant impairment in ABR and c+VEMP physiology. The effects were consistent with the major variability between animals being the latency of return toward baseline within 1 week of surgery (Table 1) [see supplementary results (Supplementary Figures 2, 3)]. Therefore, we hypothesized that larger fenestrations could expand this timeline and more appropriately map onto the human disorder. For this experiment, five animals (3M, 2F) had microsurgical creation of large SSCDs (2 mm) followed by ABR and c+VEMP measurements throughout 28 days of recovery. Recordings were carried out prior to surgery and 7, 14, 21, and 28 days after the microsurgical creation of the large SSCD. An analysis was carried out within animals across days and between animals across days.

As with the smaller fenestrations, there was significant variability between individual animals in the duration of the air-conduction increased ABR threshold as a proxy for the pseudoconductive hearing loss seen in patients with SSCD (Supplementary Figure 4). There was a general trend across frequencies in individual subjects such that ABR thresholds increased over the first 2 weeks followed by a return toward baseline over the next 2 weeks (Supplementary Figures 4B–F). The grand mean (Figure 3) of thresholds (across frequencies) was elevated significantly from the preoperative baseline on post-SSCD day 14 ($p = 0.05$) and reduced significantly from preoperative levels on post-SSCD day 28 ($p < 0.01$). LSD multiple range tests were used to make direct comparisons between pre-SSCD thresholds at each frequency (baseline) and the various day-by-day threshold changes post-SSCD. The time course of threshold changes varied with frequency. At 1 kHz, there were significant threshold decreases from the preoperative assessment at 7 days ($p < 0.01$), 14 days ($p < 0.01$), and 21 days ($p < 0.01$) after the creation of the large SCCD. The same pattern appeared at 2 kHz, with significant decreases from the preoperative baseline threshold at post-SSCD 7 days ($p < 0.01$), 14 days ($p < 0.05$), and 21 days ($p < 0.05$). At 8 kHz, though, significant threshold decrements (relative to preoperative value) were only found at 7 days ($p < 0.01$) and 14 days ($p < 0.05$) after the surgery, followed by a recovery to baseline. The pattern was the same at 16 kHz; significant reductions from the preoperative baseline were identified at 7 days ($p < 0.01$) and 14 days ($p < 0.05$) after the creation of the large SCCD. Table 2A shows the means and SEMs and significance tests for ABR thresholds in each individual animal that received large SSCD fenestrations.

In the same animals, c+VEMPs were measured after ABRs on each post-SSCD day. As with ABRs, the duration of changes in the peak amplitude varied between gerbils (Supplementary Figures 4H–L). LSD multiple range tests were used to make direct comparisons between preoperative peak amplitudes at 100 to 80 dB SPL stimulation (baseline) and the various day-by-day changes to peak amplitude after SSCD (Table 2B). The average c+VEMP amplitudes across frequencies were elevated significantly from preoperative values on post-SSCD day 7 ($p < 0.05$) and day 14 ($p < 0.05$), followed by a return to baseline levels. Subject 2 showed a continued impairment at post-SSCD day 28. Interestingly, the larger SSCD produced a sound-induced response (increased amplitude) in the opposite direction from the small SSCD response but is more similar to the cVEMP response in humans with SSCD that typically show larger cVEMP amplitudes and reduced thresholds in the affected ear. Table 2B shows the means and SEMs and significance tests for c+VEMP amplitudes in each individual animal that received large SSCD fenestrations. Between animal comparisons (Figure 3C) with repeated measures, ANOVA and LSD multiple range tests showed a significant increase in peak amplitude of c+VEMPs after post-SSCD 7 days at 80, 85, 90, 95, and 100 dB SPL ($p < 0.05$), which persisted at 14 days for stimulation at 90, 85, and 100 dB SPL ($p < 0.05$). The values did not differ from baseline after either 21 days or 28 days. As in the small SSCD group, the relationship between the ABR

TABLE 1 Recovery of ABR and c+VEMPs after Small SSCD.

1A: Small SSCD, ABR.					
	Post-SSCD 1	**Post-SSCD 3**	**Post-SSCD 5**	**Post-SSCD 7**	**Post-SSCD 10**
Subject 1	$p < 0.0001$	$p < 0.0001$	$p = 0.0006$	$p = 0.004$	$p = 0.099$
Subject 2	$p = 0.032$	$p = 0.016$	$p = 0.036$	$p = 0.14$	$p = 0.070$
Subject 3	$p = 0.004$	$p = 0.0003$	$p = 0.0005$	$p = 0.0010$	$p = 0.019$
Subject 4	$p = 0.010$	$p = 0.0006$	$p = 0.0028$	$p = 0.034$	$p = 0.099$
Subject 5	$p < 0.0001$	$p = 0.0041$	$p = 0.016$	$p = 0.117$	$p = 0.37$
1B: Small SSCD, c+VEMP.					
	Post-SSCD 1	**Post-SSCD 3**	**Post-SSCD 5**	**Post-SSCD 7**	**Post-SSCD 10**
Subject 1	$p = 0.0005$	$p = 0.0005$	$p = 0.053$	$p = 0.93$	$p = 0.23$
Subject 2	$p = 0.0011$	$p = 0.086$	$p = 0.28$	$p = 0.095$	$p = 0.102$
Subject 3	$p = 0.00015$	$p = 0.00011$	$p = 0.0003$	$p = 0.0002$	$p = 0.0234$
Subject 4	$p < 0.0001$	$p < 0.0001$	$p = 0.0007$	$p = 0.008$	$p = 0.0013$
Subject 5	$p = 0.0027$	$p = 0.0002$	$p = 0.65$	$p = 0.70$	$p = 0.88$

ABR, auditory brainstem response; c+VEMP, cervical positive vestibular evoked myogenic potentials; SSCD, superior semicircular canal dehiscence.

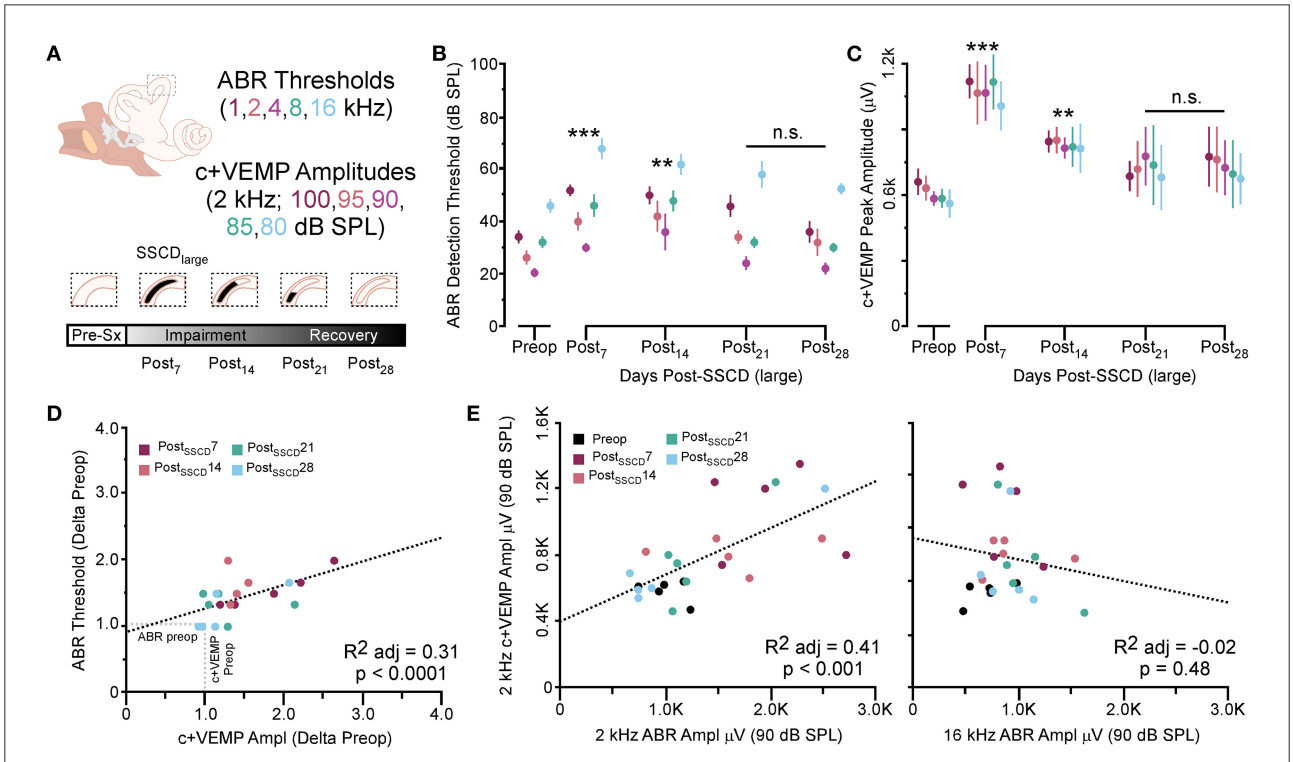

FIGURE 3
The correlated group changes to sound-induced ABR thresholds and c+VEMP amplitudes after large SSCD. **(A)** Diagram showing the theoretical recovery of ABR thresholds and c+VEMP amplitudes over days (post-SSCD 7, 14, 21, and 28). **(B)** Line chart shows the group means for ABR thresholds over postoperative days in animals that received the large SSCD. **(C)** Line chart shows the group means for c+VEMP amplitudes over post-SSCD days in animals that received the large SSCD. **(D)** Scatterplot showing a significant negative correlation between auditory thresholds and c+VEMP amplitudes throughout impairment and recovery from large SSCD. **(E)** Scatterplot showing a significant positive correlation between c+VEMP amplitudes and ABR amplitudes at 2 kHz (90 dB SPL) and a non-significant correlation between c+VEMP amplitudes and ABR amplitudes at 16 kHz (90 dB SPL) for large SSCD. $^{**}p \leq 0.001$, $^{***}p \leq 0.0001$. ns, not significant.

TABLE 2 Recovery of ABR and c+VEMPs after Large SSCD.

2A: Large SSCD, ABR.				
	Post-SSCD 7	**Post-SSCD 14**	**Post-SSCD 21**	**Post-SSCD 28**
Subject 1	$p = 0.016$	$p = 0.019$	$p = 0.373$	$p = 0.495$
Subject 2	$p = 0.016$	$p = 0.003$	$p = 0.016$	$p = 0.032$
Subject 3	$p = 0.008$	$p = 0.024$	$p = 0.37$	$p = 0.37$
Subject 4	$p = 0.004$	$p = 0.004$	$p = 0.70$	$p = 0.37$
Subject 5	$p = 0.024$	$p = 0.034$	$p = 0.099$	$p = 0.37$
2B: Large SSCD, c+VEMP.				
	Post-SSCD 7	**Post-SSCD 14**	**Post-SSCD 21**	**Post-SSCD 28**
Subject 1	$p < 0.0001$	$p = 0.0015$	$p = 0.79$	$p = 0.55$
Subject 2	$p = 0.006$	$p = 0.002$	$p = 0.006$	$p = 0.0001$
Subject 3	$p = 0.014$	$p = 0.45$	$p = 0.77$	$p = 0.14$
Subject 4	$p = 0.004$	$p = 0.010$	$p = 0.11$	$p = 0.10$
Subject 5	$p = 0.003$	$p = 0.0018$	$p = 0.085$	$p = 0.062$

ABR, auditory brainstem response; c+VEMP, cervical positive vestibular evoked myogenic potentials; SSCD, superior semicircular canal dehiscence.

amplitudes at 2 kHz and the c+VEMP amplitudes was explored with regression analysis. Results are shown in line charts for the 2 kHz data in Figure 3B and the 90 dB SPL c+VEMP data in Figure 3C. For this analysis, ratios were calculated to show changes above (>1.0) or below (<1.0) preoperative baselines. The relationship is linear [c+VEMP (μV) = 0.91 + 0.35*ABR Threshold (dB), adjusted $R^2 = 0.29$, $p < 0.01$]. Again, this correlation suggested a physiological inner ear coupling between the effects on sensory (ABR) and motor (c+VEMP) consequences of the large SCCD. The correlation between c+VEMP amplitudes at 90 dB SPL (Figure 3C) and ABR VEMP amplitudes at 90 dB SPL for 2 kHz and 16 kHz frequency measurements are shown in Figure 3B. For the 2 kHz correlation (Figure 3E, left), there was a significant linear relationship [c+VEMP (μV) = 401 + 0.27*ABR Amplitude (μV), adjusted $R^2 = 0.41$, $p < 0.001$]. Like the small SSCD, the 16 kHz correlation (Figure 3F, right) did not show a linear relationship between c+VEMP amplitude and ABR amplitude at 90 dB SPL [c+VEMP (μV) = 912–0.13*ABR Amplitude (μV), adjusted $R^2 = -0.02$, $p = 0.48$]. The comparison of the ABR threshold, ABR amplitude and latency, and c+VEMP amplitude, as well as latency showed a bimodal distribution of data around day 7 (see Supplementary Figures 5A–D and corresponding results). A clear relationship between elevated ABR thresholds and amplitude and c+VEMP amplitude emerges when data are grouped above and below thresholds of 40 dB SPL at 2 kHz based on SSCD size (see Supplementary Figures 5E–G and corresponding results). Lower thresholds were correlated with baseline and return to baseline, while increased thresholds were associated with significant impairments. Inspection of the waveforms in threshold-recovered animals suggested that there could be perseverative changes to ABR and c+VEMP latency. Therefore, we wanted to verify that returning thresholds were accompanied by similar returns in other physiological parameters. End-point analysis of the ABR and c+VEMP latency data suggested that persistent changes can remain after ABR thresholds, and c+VEMP amplitudes have returned to preoperative-like levels (Figure 3). Figure 4 compares preoperative waveform analysis data to ABR and c+VEMP data collected on the day of terminal recording. In Figure 4A, a matched pairs *t*-test demonstrated a significant decrease in superior semicircular canal wave 1 ABR latency at 2 kHz (preoperative latency vs. recovered latency: mean difference ± SEM; 0.165 ± 0.054; $t = 3.02$, $p < 0.01$). The c+VEMP N1 latency was significantly increased (matched pairs *t*-test: mean difference ± SEM; 0.70 ± 0.094, $t = 7.4$, $p < 0.0001$) after threshold recovery (Figure 4B). Inspection of the ABR waveform peaks (Figure 4C) showed a significant decrease in the number of identifiable peaks after threshold recovery [MANOVA with repeated measures; $F_{(1,13)} = 29.1$, $p < 0.001$]. Figure 4C shows the regression analysis of preoperative and endpoint ABR amplitudes at 2 kHz stimulation, as well as c+VEMP amplitude for large SSCD animals. There is no significant difference for ABR amplitudes at 2 kHz in large SSCD animals [$F_{(1,8)} = 0.008$, $p = 0.98$] or for c+VEMP amplitudes [$F_{(1,8)} = 0.776$, $p = 0.40$]. Thus, the changes in ABR/c+VEMP amplitudes do resolve with the return of ABR thresholds.

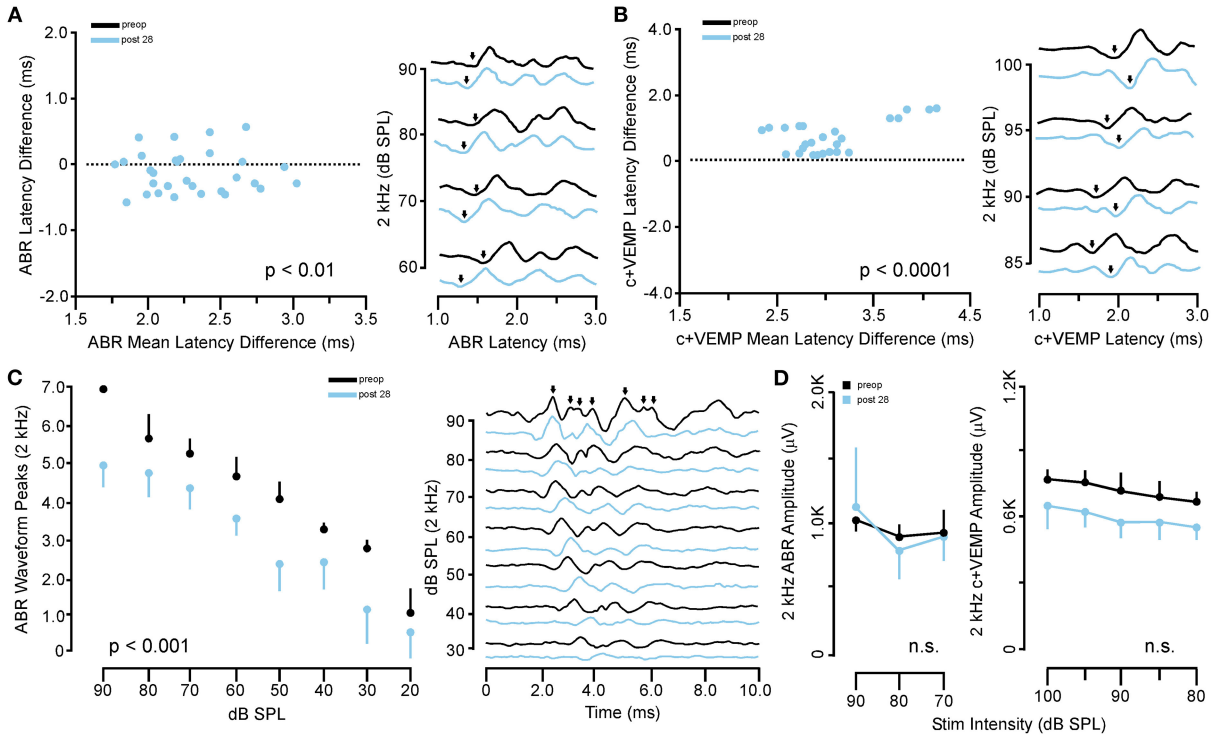

FIGURE 4
Persistent changes to ABR and c+VEMP waveform latency and expression after recovery from SSCD. **(A)** Scatterplot (left) showing the matched pair analysis of wave 1 ABR latency before SSCD (preoperative) and after recovery for the large SSCD group (post-SSCD 28) SSCD groups. A representative example of the persistent increase in ABR latency is shown on the right. **(B)** Scatterplot (left) showing the matched pair analysis of wave 1 c+VEMP latency before SSCD (preoperative) and after recovery for the large SSCD group (post-SSCD 28). A representative example of the persistent decrease in c+VEMP latency is shown on the right. **(C)** Line plot (left) comparing the average number of ABR waveform peaks present for 2 kHz stimuli at each dB SPL before (preoperative) and after recovery for large SSCD group (post-SSCD 28). Diagram (right) showing a representative example of ABR waveforms for 2 kHz stimuli before (preoperative) and after recovery (post-SSCD 28, dashed line) from large SSCD. **(D)** Left, line plot comparing ABR amplitudes between preoperative baselines and end point recordings for large SSCD group (post-SSCD 28) at 2 kHz stimulation levels. Right, line plot comparing c+VEMP amplitudes between preoperative baselines and end point recordings for large SSCD group (post-SSCD 28).

Condenser brightfield stereomicroscope: Evidence of bone regrowth correlates with returns to ABR threshold baseline

After both large and small SSCDs, we saw a trend in the changes to ABR and c+VEMPs wherein an impairment would emerge that was followed by a reversal of this impairment toward the baseline, i.e., preoperative, levels. This recovery in both groups suggested a conserved mechanism at work within both groups. As the major difference between the groups is the size of the fenestration we hypothesized that just like humans undergoing the old fenestration operations for otosclerosis, the site of bony dehiscence regrows into and obliterates the canal if the fenestration is too small or bone debris is left at the site of the fenestration (26–30). This is in contrast to patients who require direct surgical plugging of the SSCD to resolve the third window symptoms (14, 15, 21). To investigate this hypothesis, we carried out another acute experiment with eight animals (4M, 4F), where the experimental endpoint was the correlation of ABR and c+VEMP measurements with corresponding brightfield stereomicroscope evidence of bone regrowth. For all animals, the left ear was dissected, and the fenestration site was imaged with a condenser brightfield microscopy (Figure 5). Figure 5A shows a representative example of an animal with limited bone regrowth early after SSCD (post-SSCD day 3), with comparison to an animal with partial (post-SSCD day 7, Figure 5B) and full (post-SSCD day 10, Figure 5C) bone regrowth. Figures 5D, E show the ABR and c+VEMP data from the three animals shown in Figures 5A–C (Early. Partial, and Full Bone Regrowth, respectively). Illustrated is the SSCD-induced impairment and the data collected on the experimental endpoint (post-SSCD day 3, 7, or 10). Finally, Figure 5F shows the correlation between ABR and c+VEMPs as a function of the state of bone regrowth. This analysis suggests a strong correlation between bone regrowth and "recovery" of the physiological function of the inner ear

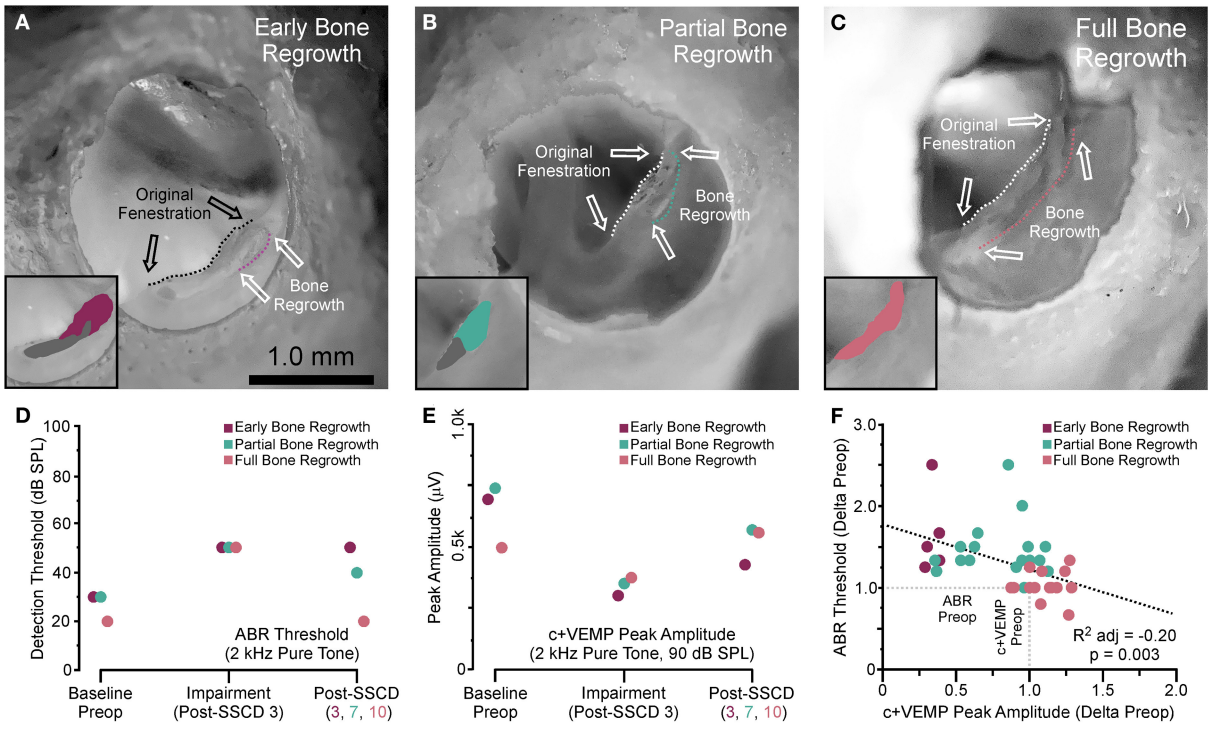

FIGURE 5
Photomicrograph correlation between ABR and c+VEMP thresholds/amplitudes at experimental endpoints and indicators of bone regrowth. **(A)** Photomicrograph showing early bone regrowth 3 days after SSCD. **(B)** Photomicrograph showing partial bone regrowth 7 days after SSCD. **(C)** Photomicrograph showing full bone regrowth 10 days after SSCD. **(D)** Chart showing the changes to ABR thresholds at 2 kHz for the animals shown in **(A–C)** at baseline, 3 days post-SSCD (impairment), and at the experimental endpoint (post-SSCD days 5–10). **(E)** Chart showing the changes to c+VEMP peak amplitudes at 90 dB SPL for the animals shown in **(A–C)** at baseline, 3 days post-SSCD (impairment), and at the experimental endpoint (post-SSCD days 5–10). **(F)** Scatterplot showing a negative correlation between ABR and c+VEMP based on bone regrowth status.

[ABR Threshold (dB) = 203–0.84*c+VEMP Amplitude (µV), adjusted $R^2 = 0.29$, $p < 0.001$].

Micro-CT scanning confirms that bone resurfacing and not canal obliteration is associated with bone regrowth

Based on the stereomicroscope, it was unclear whether the bone regrowth was accompanied by obliteration of the lumen, or if the bone resurfaced to form an intact canal. Therefore, we took the samples used in Figure 5 and completed micro-CT scans to visualize the site of surgically created SSCD and determine the outcome of bone regrowth (Figure 6). By comparing a control specimen (Figures 6A, B, I), the day 3 specimen (b), and the day 10 specimen (Figures 6G, H, J), it is clear that the bone resurfaces does not obliterate the canal. However, it does regrow as thicker bone (Figures 6H, I). Thus, unlike the most common surgical method in patients with SSCD, which plugs the dehiscence, our gerbil model repairs the SSCD by resurfacing the canal with qualitatively thicker bone. Hence, a second surgical procedure to plug the defect is unnecessary.

Discussion

For patients who are clinically suspected of having SSCD, there are three essential diagnostic features that are typically present: (1) high-resolution temporal bone CT demonstration of the dehiscence; (2) cVEMP increased amplitude and decreased threshold on the side of the SSCD; and (3) pseudoconductive hearing loss. In patients whose symptoms are severe enough to warrant surgical intervention, the most common way of accomplishing resolution of the SSCD and associated symptoms is a middle cranial fossa craniotomy and plugging of the SSCD. For an ideal model of this disorder, all of these features should be present, and resolution should follow the plugging of the SSCD.

Imaging

In our gerbil model, we used microsurgical techniques to create and measure the SSCD; therefore, CT imaging was not necessary. However, we used micro-CT to better understand the nature of the osteoneogenesis resulting in the reconstitution of the SSC (Figure 6).

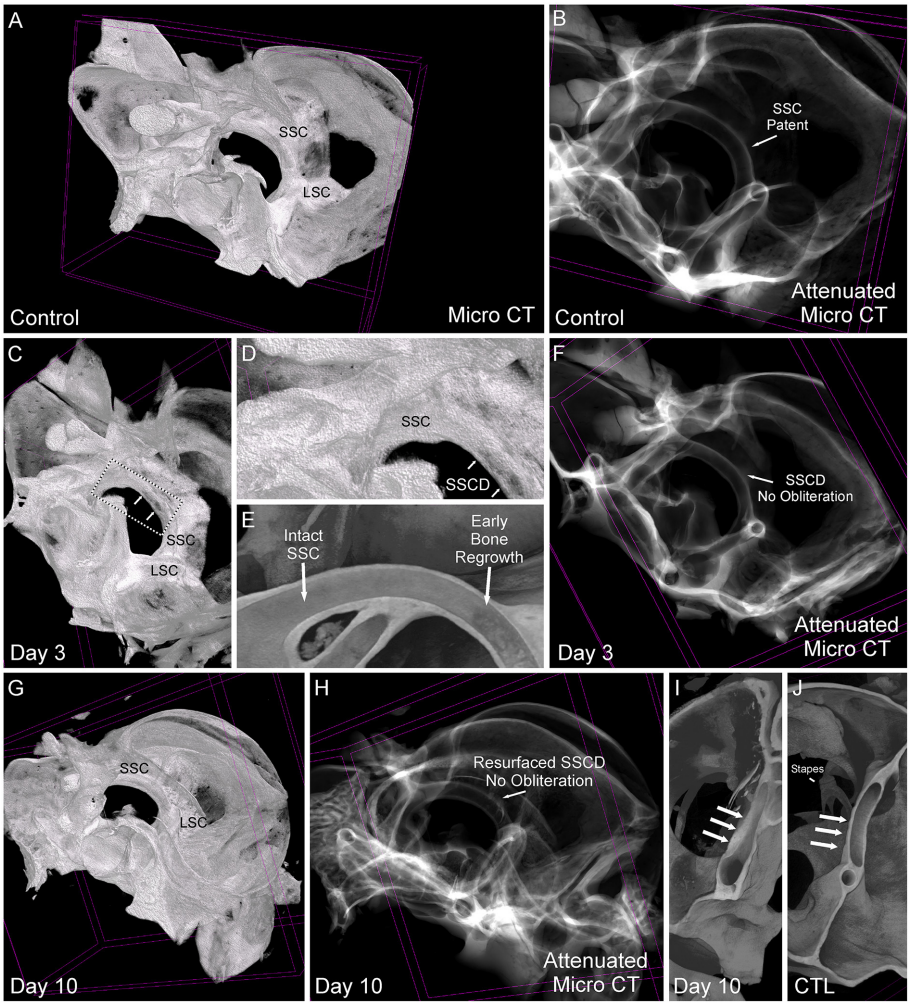

FIGURE 6
Comparative micro-CT analysis of control and post-SSCD day 3 and day 10. **(A)** Micro-CT scan of left control **(A, B, J)**, day 3 post-superior semicircular canal dehiscence (SSCD) **(C–F)**, and day 10 post-SSCD **(G–I)** after small (1 mm) SSCD surgery. **(A)** Micro-CT maximum intensity projections (MIP) with a 3D rendering of control left inner ear. Note the normal intact superior semicircular canal (SSC) and lateral semicircular canal (LSC). **(B)** Micro-CT with attenuated images shows that the lumen of the SSC is naturally patent. **(C)** Micro-CT MIP with 3D rendering shows the day 3 post-SSCD site of a small (1 mm) SSCD (double arrows). Note the position of the SSC and LSC. A bounding box containing the SSCD (double arrows) is shown in higher magnification in **(D)**. **(D)** The SSC with the beginning of osteoneogenesis within the SSCD can be seen (double arrows). **(E)** The micro-CT view inside of the intact SSC (left) reveals the adjacent early bone regrowth (right) at day 3 post-SSCD. **(F)** Micro-CT with attenuated images shows that the lumen remains patent at day 3 post-SSCD. **(G)** Micro-CT MIP with 3D rendering of a small (1 mm) SSCD on postoperative day 10. Note the positions of the SSC and LSC. **(H)** Micro-CT with attenuated images shows that the lumen remains patent and without bony obliteration, as is the normal condition shown in **(B)**. **(I)** Micro-CT view inside the left SSC on day 10 post-SSCD [small (1 mm) fenestration]. Note the increased thickness of the resurfaced SSC bone (triple arrows) compared to the control SSC has shown in **(J)**. **(I)** Micro-CT inside the left SSC shows that the natural SSC has uniform wall thickness (triple arrows) that is thinner than the resurfaced/regrown SSC. CTL, control.

c+VEMP

It was over a century ago that Robert Bárány began using caloric irrigation and his vertical axis rotational chair to assess horizontal canal function, yet it was not until 1994 that Colebatch and colleagues developed the sound-evoked cervical vestibular evoked myogenic potential (cVEMP) (31) to study the gravitational receptors. Sound-induced activation of the saccule leads to an inhibition of the sternocleidomastoid muscle, and this inhibitory potential can be recorded as the cVEMP [for review see (31–35)]. The evoked potentials recorded from a number of other muscles have been studied as well; however, it is the sternocleidomastoid muscle that is most consistently used in research and clinical applications. It has

also been shown that both ipsilateral and contralateral cVEMP can be recorded from the sternocleidomastoid muscle following ipsilateral stimulation (31–39). Bone-conducted stimuli have also been used to evoke cVEMP responses [for review see (33, 35)]. All of these cVEMP methods depend on voluntary contraction of the sternocleidomastoid muscle so that the evoked inhibitory potential can be measured, which is not possible in an anesthetized animal.

For a person without a mobile third window, the normal cVEMP threshold is 95 dB nHL. For patients with SSCD, there is typically an increased cVEMP amplitude and reduced cVEMP threshold to 81 ± 9 dB nHL (9); however, the threshold may be reduced as low as 60 to 65 dB nHL. In a small number of SSCD patients, particularly older patients, a cVEMP response cannot be measured. As outlined in the Introduction, it is not possible to record a cVEMP response in anesthetized animals since the voluntary contraction of the sternocleidomastoid muscle required to record the relaxation potential associated with sound-induced saccular stimulation cannot be accomplished. We have demonstrated that the c+VEMP response can be recorded in the gerbil and that the increased amplitude of the response after the creation of SSCD was observed. The c+VEMP was elicited at lower stimulus intensities than patients, and we were unable to measure the threshold as it was too low.

In patients with SSCD and other sites of dehiscence resulting in third window syndrome, cVEMPs are useful diagnostic indicators, with patients exhibiting abnormal responses to auditory clicks or tone bursts used in this test (7, 14–16, 36, 37). The cVEMP amplitudes in the affected labyrinth are increased, and thresholds are reduced (7, 9, 14–16, 34, 40). After surgical plugging of the SSCD, cVEMP thresholds and amplitudes were normalized (40). An ideal animal model of SSCD would show elevated amplitude responses and reduced thresholds in response to auditory stimulation of the sacculus that would normalize with the closure of the SSCD. A limitation of earlier animal models was the attempt to record cVEMP responses from the sternocleidomastoid muscle. The sound-induced VEMP is inhibitory for neck flexor muscles and excitatory in neck extensor muscles (13). Thus, it is required to have the SCM contracted to record the inhibitory relaxation potential, which is not possible in an anesthetized animal. However, we took advantage of the excitatory responses in the extensor muscles to record what we term c+VEMPs. In humans, the normal threshold for cVEMP is 95 dB HL. For gerbils, the c+VEMP threshold is 45 dB HL, so measuring a reduced threshold was not possible. However, just as in patients with SSCD, we recorded increased amplitude of the c+VEMP response in our surgically created large (2 mm) SSCD animals that remained elevated for 1–2 weeks before the amplitude returned to normal, in the same animal, with the closure of the SSCD *via* osteoneogenesis.

While not termed c+VEMPs, other investigators have studied the excitatory sound-induced VEMP recorded from the splenius capitus muscle of humans (41–44). This response from neck extensor muscles had not previously been reported in an animal model of SSCD but has been studied in multiple species for different experimental purposes.

Yang et al. used neck extensor muscle cVEMPs in a guinea pig model to monitor the vestibulotoxicity of gentamicin otic drops (45). The compound 3,3′-iminodiproprionitrile (IDPN) has been reported to be neurotoxic and vestibulotoxic resulting in loss of vestibular sensory epithelial cells in rats and mice and leading to irreversible loss of peripheral vestibular function (46). Negishi-Oshino et al. used neck extensor muscle cVEMPs, in addition to behavioral rotarod, beam crossing, and air-righting reflex tests in adult C57BL/6J mice to measure IDPN vestibulotoxicity and thereby create an *in vivo* model of adult mammalian vestibular dysfunction (47). Finally, neck extensor muscle VEMPs have been studied in mini-pigs and rats (48, 49).

On post-SSCD day 1 in the small (1 mm) group, there was a small increase in latency, and the amplitude of the c+VEMP response was greatly decreased along with an increase in the stretch reflex. These observations are consistent with acute otolithic dysfunction (50). Dyball et al. reported that, in normal humans, tapping the forehead delivering bone-conduction stimuli produces a cVEMP response and that the stretch receptors can also be activated by skull taps resulting in a later potential associated with the stretch reflex (58). They also found that patients with unilateral vestibular loss had larger late peaks on the affected than the normal side which in the context of our findings suggests these animals experienced transient acute otolithic dysfunction. As will be described shortly, this short-lived loss of c+VEMP function was not seen in the ABR data. Based upon the data reported herein, in all future experiments, the animal model will use 2-mm SSCD, and 1-mm SSCD will not be utilized.

Auditory brainstem response

Attias et al. (51) used bone-conduction ABR and air-conduction ABR to measure the pseudoconductive air-bone gap resulting from the surgical creation of a 0.6-mm SSCD in the sand rat. Attia et al. showed "significant deterioration of the air-conduction thresholds to clicks ($t_9 = 18.4$, $p < 0.001$) and tone bursts ($t_9 = 6.5$, $p < 0.001$) in the absence of a significant change in bone-conduction thresholds." This means that altered air-conducted ABR thresholds explained the increased air-bone gap in their model. We followed their established precedent and, therefore, we did not use a bone-conduction ABR approach. Delsmann et al. (52) used the same approach that we used in recording ear-specific air-conduction ABR as a proxy to measure the conductive hearing loss in the *Hyp* mouse model of X-linked hypophosphatemia caused by hypomineralization of the auditory ossicles.

For our data, we found that for the large SSCD group, while the data were variable, there was a recovery of ABR thresholds as

the SSCD closed, suggesting that surgical disruption of cochlear function was not due to hair cell loss and irreversible hearing loss and that the spontaneous bone regrowth and closure of the SSCD obviate the need of a second surgical procedure to surgically plug the SSCD. This not only avoids unnecessary animal surgeries but also allows the reversal of the SSCD and recovery of function in a more holistic way.

Evidence of bone regrowth and physiological return to baseline

The regrowth of bone to close the surgically created SSCD and reverse the physiologic dysfunction without a second surgical procedure is another strength of our animal model. The micro-CT data showed that the defect heals by resurfacing rather than bony obliteration of the canal (Figure 6). Initially, we did not expect the observed differences in the small vs. large SSCD cohorts, or the reversal of the c+VEMP and ABR findings over time. However, we reviewed the literature regarding an operation no longer performed in patients, the one-stage fenestration surgery for otosclerosis, to gain insight into our experimental observations. With otosclerosis, the stapes footplate becomes fused to the otic capsule effectively dropping from the physiologically necessary two mobile windows down to one. The lateral semicircular canal fenestration operation was developed to create a new second mobile window to improve the conductive hearing loss these patients experienced. Although many others contributed to the development of the fenestration procedure, Julius Lempert was the first to develop the one-stage fenestration operation (26–30). As the technique evolved, two critical issues emerged related to preventing bone regrowth and closure of the new surgically created second mobile window: (1) avoiding a fenestration that was too small and (2) removing the bone dust from the area surrounding the fenestration (27, 28, 30). Dewyer et al. reported the temporal bone pathology of a woman who had bilateral fenestration operations performed for otosclerosis (30). On the left side, there was histologic evidence of osteoneogenesis within the fibrous tissue sealing the lateral semicircular canal fenestration. In the context of our new animal model, the small SSCD proved to be too small and facilitated early closure of the fenestration. Because of the small diameter of the gerbil SSC and the associated surface tension between the surgically exposed perilymph, surrounding bone, and bone dust, it is very difficult to wash the bone dust away from the SSCD. For these reasons, in future experiments, we will use gerbils with large (2 mm) SSCDs for our longer-term behavioral studies.

Normally, the endochondral bone of the otic capsule calcifies in its adult conformation and does not undergo remodeling (53). Osteoblast–osteoclast bone remodeling units have not been normally seen in normal otic capsule bone (54). The bone lining cells of mammals form a membrane-like layer physically partitioning the bone matrix from the extracellular fluid, which in the cochlea, semicircular canals, and rest of the labyrinth, is perilymph. Chole and Tinling (55, 56) reported that in gerbil endosteal cochlea there was a relatively high ratio of bone lining cells to bone surface of 71.1 ± 15.1 (ulna was 100). However, they did not study the superior semicircular canal. The bone lining cells are thought to play an important role in the recruitment of osteoclasts and in turn osteoneogenesis to a local site after injury, in our animals by the surgical creation of the SSCD, by exposing the surface of the bone that initiates a signal for the chemoattraction of osteoclasts and/or their progenitors (55, 56). There are other well-known examples of injuries of the otic capsule that result in osteoneogenesis including transverse temporal bone fractures and cochleostomy with the placement of a cochlear implant electrode array. Nager (57) histologically demonstrated that the entire superior semicircular canal can become obliterated by bone by osteoneogenesis induced by a transverse temporal bone fracture. Surgical cochleostomy for cochlear implant electrode insertion in humans and animal models can induce osteoneogenesis. Quesnel et al. (58) reported postmortem histopathologic evidence of osteoneogenesis after cochleostomies, in an anterior–inferior location relative to the round window, and placement of bilateral hybrid electro-acoustic stimulation cochlear implants. In an experimental guinea pig cochlear implant model, O'Leary et al. (59) reported cochleostomy and electrode insertion-induced osteoneogenesis. In a subsequent study, using the same animal model, they found that systemic dexamethasone (a glucocorticosteroid) reduced this osteoneogenesis (60). This later observation may delay the time of bony obliteration in our SSCD model which would extend the time available for additional experimental studies of the sequelae, particularly with cognitive dysfunction and sound-induced vestibular dysfunction, seen in patients with SSCD.

Future studies will focus on the histopathologic response to the surgical creation of the SSCD in our model and the basic mechanisms associated with this osteoneogenesis.

Evidence for persistent changes to cochlear and vestibular function after c+VEMP amplitudes and abr thresholds return to baseline

ABR thresholds and wave morphology

There was strong evidence for the correlation between the closure of the SSCD by osteoneogenesis and the resolution of cochlear and vestibular impairments; however, deeper analysis of the data suggested that persistent changes can remain after ABR thresholds have returned to preoperative-like (non-significant difference) levels (see Supplementary Figures 2–4; Figure 3B). Figure 4 shows that latency to ABR wave I and the 7 peaks (waves I–VII) associated with activation of ascending central auditory neuraxis was persistently altered by

the surgical creation of and/or physiologic changes associated with the SSCD. Figure 4A shows a significant effect of superior semicircular canal fenestration on wave I ABR latency at 2 kHz and a persistently altered c+VEMP N1 latency (preoperative vs. recovered latency). Together, these data demonstrate that despite resurfacing of the SSCD and return of ABR thresholds and amplitudes as well as c+VEMP amplitudes, significant changes to the timing of nerve activation as well as the relative strength of central auditory neuraxis activation persist after recovery.

In patients with SSCD who have their superior semicircular canal plugged by either the middle cranial fossa approach or the transmastoid approach, persistent pseudoconductive hearing loss is well-known, but not understood (23–25). In our animal model, an inspection of the number of visible ABR peaks, which signify activation along with the neuraxis [cochlear nucleus (CN), superior olivary complex (SOC), inferior colliculus (IC), medial geniculate nucleus (MGN), and auditory cortex] (see Figure 2A) at each decibel stimulus level (90 db SPL to 20 dB SPL) showed a significant decrease in auditory neuraxis potentials evoked at each stimulus level compared to preoperative ABR waveforms. In the preoperative waveforms, there was increased activation at peaks II through VII compared to each experimental endpoint. Thus, the preoperative 40 dB SPL 2 kHz stimulus activates higher up the auditory neuraxis than 40 dB SPL 2 kHz stimulus in the same animal after the: (1) SSCD has closed by osteoneogenesis; and (2) ABR and c+VEMPs measures returned to a non-significant difference from preoperative levels. The medial geniculate nucleus and auditory cortex activation ABR potentials seem to be affected the most. This might drive the persistent hearing loss if the thalamus and the cortex have diminished activation at the same dB SPL stimulus level. Together, these could suggest that there are persistent changes in both peripheral function due to hair cell injury/dysfunction (e.g., latency) and central (ABR waveforms) or even that central circuit plasticity has altered signal propagation/amplification, which has altered some aspects of cochlear physiology (e.g., efferent system) after short-term diversion of sound pressure flow to the third mobile window (i.e., SSCD).

The noise produced by a surgical drill is a confounding factor in the interpretation of transient and persistent hearing loss after the creation of an experimental dehiscence. From an otologic drill perspective, both a temporal craniotomy (middle cranial fossa) approach and a transmastoid plugging of an SSCD are comparable clinical procedures that can result in postoperative high-frequency sensorineural hearing loss. Ward et al. reported the hearing outcomes after surgical plugging of SSCD patients using a middle cranial fossa approach and found that a mild high-frequency sensorineural hearing loss was present and persisted in 25% but there was no change in speech discrimination (24). A similar experience was reported by Ellsperman et al. after surgical plugging of SSCD patients using either a middle cranial fossa approach or a transmastoid approach (25). Both approaches could produce high-frequency hearing loss (8 kHz) because the surgical drill delivers high-frequency acoustic energy to the cochlea *via* the temporal bone. Since it is well-known the temporal bone dissection with contemporary microsurgical drills can result in high-frequency sensorineural hearing loss (61), it is not surprising that persistent hearing loss, measured by ABR, was found in our animal model at 16 kHz. However, drill noise alone cannot explain the greater ABR threshold elevation for the small dehiscence group (relative to the large dehiscence group) at 7 days post-SSCD, given the longer drill exposure in the latter group.

c+VEMP amplitudes

Initially, an increase in latency was observed in N1 of the c+VEMP for both small and large SSCD; however, there were no significant differences between the large and small SSCD c+VEMP latency after recovery. In both the small and large SSCD cohorts, the elevated c+VEMP amplitudes returned to preoperative-like (non-significant difference) levels (see Supplementary Figures 2G–L, 3C; Figure 3C), just as they do in patients with SSCD after plugging the dehiscence (40). Welgambola et al. studied cVEMP responses of 20 normal volunteers, 10 newly diagnosed subjects with SSCD, and 12 subjects who underwent successful plugging of their SSCD using a middle cranial fossa approach (40). In the subjects who had to plug their SSCD, the thresholds for evoking cVEMPs using air-conducted tones were pathologically lowered, and the amplitudes were elevated. Successful canal plugging resulted in normal cVEMP thresholds and reduced amplitudes. We were unable to measure reduced thresholds of the c+VEMP response in gerbils because of their naturally low c+VEMP thresholds; however, the elevated c+VEMP amplitudes returned to preoperative-like (non-significant difference) levels (Supplementary Figures 2G–L, 3C; Figure 3C) after the closure of the SSCD by osteoneogenesis (see Figures 5, 6).

Conclusion

The large (2 mm) SSCD used in our gerbil model resulted in electrophysiologic findings that mirror findings in patients with SSCD. Our animal model improves upon the fidelity to the human findings from previously reported models (10, 11) and provides a more detailed view of the healing process and associated physiological findings. The advances are in several areas. First, although the earlier studies reported elevated ABR thresholds after the experimental SSCD-induced elevations to ABR thresholds, we have provided evidence that effects differ markedly with SSCD size and document timelines of impairment and recovery. Second, we have added a functional vestibular measure that showed correlated

impairment, recovery, and persistence between cochlear and vestibular physiology. This is a key feature that will allow a detailed study of the functional connectivity between vestibular and cochlear input/output at the peripheral and central levels. Third, this animal model has been developed explicitly for compatibility with a wide range of behavioral paradigms to test cognitive and perceptual impairments as a function of SSCD status (impairment/recovery). Finally, we have documented that the SSCD-related changes recovered to baseline as the defect heals *in situ* by bony resurfacing of the SSCD without obliteration. Hence, there is no need for a second surgical procedure to plug the SSCD. Because peripheral vestibular disorders and associated asymmetric input to the central nervous system have been reported to provide a unique window to study cognitive dysfunction (62), this SSCD model will provide the opportunity to perform the behavioral as well as electrophysiological, cell, and molecular biology studies that are needed to understand the cognitive dysfunction seen in patients with SSCD and other vestibular disorders.

Data availability statement

The datasets are available upon reasonable request and with permission of the Institutional Animal Care and Use Committee.

Ethics statement

The animal study was reviewed and approved by the Rutgers University IACUC (research protocol PROTO202000179).

Author contributions

PAW and TMM contributed to the conception, design of the study, and wrote the first draft of the manuscript. TMM organized the database and performed the statistical analysis. OJVO, BTM, PAW, M-AT, VLS, SD, JDG, CDB, and TMM wrote sections of the manuscript. All authors contributed to manuscript revision, read, and approved the submitted version.

Funding

The Rutgers Biomedical Health Sciences Chancellor Scholar Award to PAW provided funding to support this work. The Skyscan 1272 NanoCT at the Rutgers Molecular Imaging Core was supported by the National Science Foundation through a Major Research Instrumentation (MRI) grant (Award#: 1828332).

Acknowledgments

We thank Patricia Buckendahl, Ph.D., and the Rutgers Molecular Imaging Center for completing the micro-CT scanning. DICOM files for each specimen were provided to the authors for creating the 3D reconstructed images and completing the analysis.

Conflict of interest

The authors declare that the research was conducted in the absence of any commercial or financial relationships that could be construed as a potential conflict of interest.

Publisher's note

Supplementary material

The Supplementary Material for this article can be found online at: https://www.frontiersin.org/articles/10.3389/fneur.2022.1035478/full#supplementary-material

References

1. Tullio P. *Das Ohr und die Entstehung der Sprache und Schrift*. Berlin: Urban & Schwarzenberg (1929). p. 1–455.

2. Huizinga E. The physiological and clinical importance of experimental work on the pigeon's labyrinth. *J Laryngol Otol.* (1955) 69:260–8. doi: 10.1017/S0022215100050635

3. Minor LB, Solomon D, Zinreich JS, Zee DS. Sound- and/or pressure-induced vertigo due to bone dehiscence of the superior semicircular canal. *Arch Otolaryngol Head Neck Surg.* (1998) 124:249–58. doi: 10.1001/archotol.124.3.249

4. Dalchow CV, Schmidt C, Harbort J, Knecht R, Grzyska U, Muenscher A. Imaging of ancient Egyptian mummies' temporal bones with digital volume tomography. *Eur Arch Otorhinolaryngol.* (2012) 269:2277–84. doi: 10.1007/s00405-012-2011-x

5. Wackym PA, Balaban CD, Ikezono T, Agrawal Y. *Third Window Syndrome*. Lausanne: Frontiers Media SA (2021).

6. Wackym PA, Agrawal Y, Ikezono T, Balaban CD. Editorial: third window syndrome. *Front Neurol.* (2021) 12:704095. doi: 10.3389/fneur.2021.704095

7. Wackym PA, Balaban CD, Zhang P, Siker DA, Hundal JS. Third window syndrome: surgical management of cochlea-facial nerve dehiscence. *Front Neurol.* (2019) 10:1281. doi: 10.3389/fneur.2019.01281

8. Merchant SN, Rosowski JJ. Conductive hearing loss caused by third-window lesions of the inner ear. *Otol Neurotol.* (2008) 29:282–9. doi: 10.1097/MAO.0b013e318161ab24

9. Minor LB. Clinical manifestations of superior semicircular canal dehiscence. *Laryngoscope.* (2005) 115:1717–27. doi: 10.1097/01.mlg.0000178324.55729.b7

10. Songer JE, Rosowski JJ. The effect of superior canal dehiscence on cochlear potential in response to air-conducted stimuli in chinchilla. *Hear Res.* (2005) 210:53–62. doi: 10.1016/j.heares.2005.07.003

11. Tong BS, He ZY, Ding CR, Yang JM, Wang J, Han Z, et al. Mechanisms of hearing loss in a guinea pig model of superior semicircular canal dehiscence. *Neural Plast.* (2018) 2018:1258341. doi: 10.1155/2018/1258341

12. Iversen MM, Rabbitt RD. Biomechanics of third window syndrome. *Front Neurol.* (2020) 11:891. doi: 10.3389/fneur.2020.00891

13. Uchino Y. Connections between otolith receptors and neck motoneurons. *Acta Otolaryngol.* (1997) 528:49–51.

14. Wackym PA, Wood SJ, Siker DA, Carter DM. Otic capsule dehiscence syndrome: superior canal dehiscence syndrome with no radiographically visible dehiscence. *Ear Nose Throat J.* (2015) 94:E8–24. doi: 10.1177/014556131509400802

15. Wackym PA, Balaban CD, Mackay HT, Wood SJ, Lundell CJ, Carter DM, et al. Longitudinal cognitive and neurobehavioral functional outcomes after repairing otic capsule dehiscence. *Otol Neurotol.* (2016) 37:70–82. doi: 10.1097/MAO.0000000000000928

16. Wackym PA, Mackay-Promitas HT, Demirel S, Gianoli GJ, Gizzi MS, Carter DM, et al. Comorbidities confounding the outcomes of surgery for third window syndrome: outlier analysis. *Laryngoscope Invest Otolaryngol.* (2017) 2:225–53. doi: 10.1002/lio2.89

17. Mozaffari K, Ghodrati F, Pradhan A, Ng E, Ding K, Rana S, et al. Superior semicircular canal dehiscence revision surgery outcomes: a single institution's experience. *World Neurosurg.* (2021) 156:e408–14. doi: 10.1016/j.wneu.2021.09.083

18. Mozaffari K, Willis SL, Unterberger A, Duong C, Hong M, De Jong R, et al. Superior semicircular canal dehiscence outcomes in a consecutive series of 229 surgical repairs with middle cranial fossa craniotomy. *World Neurosurg.* (2021) 156:e229–34. doi: 10.1016/j.wneu.2021.09.038

19. Ward BK, Carey JP, Minor LB. Superior canal dehiscence syndrome: lessons from the first 20 years. *Front Neurol.* (2017) 8:177. doi: 10.3389/fneur.2017.00177

20. Naert L, Van de Berg R, Van de Heyning P, Bisdorff A, Sharon JD, Ward BK, et al. Aggregating the symptoms of superior semicircular canal dehiscence syndrome. *Laryngoscope.* (2018) 128:1932–8. doi: 10.1002/lary.27062

21. Remenschneider AK, Owoc M, Kozin ED, McKenna MJ, Lee DJ, Jung DH. Health utility improves after surgery for superior canal dehiscence syndrome. *Otol Neurotol.* (2015) 36:1695–701. doi: 10.1097/MAO.0000000000000886

22. Alkhafaji MS, Varma S, Pross SE, Sharon JD, Nellis JC, Santina CC, et al. Long-term patient-reported outcomes after surgery for superior canal dehiscence syndrome. *Otol Neurotol.* (2017) 38:1319–26. doi: 10.1097/MAO.0000000000001550

23. Limb CJ, Carey JP, Srireddy S, Minor LB. Auditory function in patients with surgically treated superior semicircular canal dehiscence. *Otol Neurotol.* (2006) 27:969–80. doi: 10.1097/01.mao.0000235376.70492.8e

24. Ward BK, Agrawal Y, Nguyen E, Della Santina CC, Limb CJ, Francis HW, et al. Hearing outcomes after surgical plugging of the superior semicircular canal by a middle cranial fossa approach. *Otol Neurotol.* (2012) 33:1386–91. doi: 10.1097/MAO.0b013e318268d20d

25. Ellsperman SE, Telian SA, Kileny PR, Welch CM. Auditory outcomes following transmastoid and middle cranial fossa approaches for superior semicircular canal dehiscence repair. *Otol Neurotol.* (2021) 42:1544–52. doi: 10.1097/MAO.0000000000003323

26. Lempert J. Lempert fenestra nov-ovalis for the restoration of practical unaided hearing in clinical otosclerosis; its present status. *Proc R Soc Med.* (1948) 41:617–30. doi: 10.1177/003591574804100916

27. Lempert J. Bone-dust-free Lempert fenestra nov-ovalis; a new evolutionary development of the surgical treatment of clinical otosclerosis. *Arch Otolaryngol.* (1948) 47:280–8. doi: 10.1001/archotol.1948.00690030290003

28. Shambaugh GE Jr. Julius Lempert and the fenestration operation. *Am J Otol.* (1995) 16:247–52.

29. Shea JJ Jr. A personal history of stapedectomy. *Am J Otol.* (1998) 19:S2–12.

30. Dewyer NA, Rosowski JJ, Nadol JB Jr, Quesnel AM. Otopathology findings in otosclerosis with lateral semicircular canal fenestration. *Laryngoscope Investig Otolaryngol.* (2019) 4:425–8. doi: 10.1002/lio2.286

31. Colebatch JG, Halmagyi GM, Skuse NF. Myogenic potentials generated by click-evoked vestibulocollic reflex. *J Neurol Neurosurg Psychiatry.* (1994) 57:190–7. doi: 10.1136/jnnp.57.2.190

32. Welgampola MS, Colebatch JG. Characteristics and clinical applications of vestibular-evoked myogenic potentials. *Neurology.* (2005) 64:1682–8. doi: 10.1212/01.WNL.0000161876.20552.AA

33. Curthoys IS. A critical review of the neurophysiological evidence underlying clinical vestibular testing using sound, vibration and galvanic stimuli. *Clin Neurophysiol.* (2010) 121:132–44. doi: 10.1016/j.clinph.2009.09.027

34. Maheu M, Elblidi A, Saliba I. Investigating performance of cVEMP and oVEMP in the identification of superior canal dehiscence in relation to dehiscence location and size. *Audiol Res.* (2021) 11:452–62. doi: 10.3390/audiolres11030042

35. Wackym PA, Ratigan JA, Birck JD, Johnson SH, Doornink J, Bottlang M, et al. Rapid cVEMP and oVEMP responses elicited by a novel head striker and recording device. *Otol Neurotol.* (2012) 33:1392–400. doi: 10.1097/MAO.0b013e318268d234

36. Hunter JB, Patel NS, O'Connell BP, Carlson ML, Shepard NT, McCaslin DL, et al. Cervical and ocular VEMP testing in diagnosing superior semicircular canal dehiscence. *Otolaryngol Head Neck Surg.* (2017) 156:917–23. doi: 10.1177/0194599817690720

37. Brantberg K, Bergenius J, Tribukait A. Vestibular-evoked myogenic potentials in patients with dehiscence of the superior semicircular canal. *Acta Otolaryngol.* (1999) 119:633–40. doi: 10.1080/00016489950180559

38. Streubel SO, Cremer PD, Carey JP, Weg N, Minor LB. Vestibular-evoked myogenic potentials in the diagnosis of superior canal dehiscence syndrome. *Acta Otolaryngol Suppl.* (2001) 545:41–9. doi: 10.1080/000164801750388090

39. McNerney KM, Burkard RF. The vestibular evoked myogenic potential (VEMP): air- versus bone-conducted stimuli. *Ear Hear.* (2011) 32:e6–15. doi: 10.1097/AUD.0b013e3182280299

40. Welgampola MS, Myrie OA, Minor LB, Carey JP. Vestibular-evoked myogenic potential thresholds normalize on plugging superior canal dehiscence. *Neurology.* (2008) 70:464–72. doi: 10.1212/01.wnl.0000299084.76250.4a

41. Sakakura K, Takahashi K, Takayasu Y, Chikamatsu K, Furuya N. Novel method for recording vestibular evoked myogenic potential: minimally invasive recording on neck extensor muscles. *Laryngoscope.* (2005) 115:1768–73. doi: 10.1097/01.mlg.0000173157.34039.d8

42. Gulec F, Celebisoy N, Kose T. Vestibular evoked myogenic potentials in splenius capitis muscle. *J Int Adv Otol.* (2013) 9:96–100.

43. Camp AJ, Gu C, Cushing SL, Gordon KA, Corneil BD. Splenius capitis is a reliable target for measuring cervical vestibular evoked myogenic potentials in adults. *Eur J Neurosci.* (2017) 45:1212–23. doi: 10.1111/ejn.13536

44. Ali FM, Westling M, Zhao LHL, Corneil BD, Camp AJ. Splenius capitis: sensitive target for the cVEMP in older and neurodegenerative patients. *Eur Arch Otorhinolaryngol.* (2019) 276:2991–3003. doi: 10.1007/s00405-019-05582-7

45. Yang TH, Liu SH, Young YH. A novel inner ear monitoring system for evaluating ototoxicity of gentamicin eardrops in guinea pigs. *Laryngoscope.* (2010) 120:1220–6. doi: 10.1002/lary.20923

46. Seoane A, Demmes D, Llorens J. Distal effects in a model of proximal axonopathy: 3,3'-iminodipropionitrile causes specific loss of neurofilaments in rat vestibular afferent endings. *Acta Neuropathol.* (2003) 106:458–70. doi: 10.1007/s00401-003-0744-8

47. Negishi-Oshino R, Ohgami N, He T, Ohgami K, Li X, Kato M. cVEMP correlated with imbalance in a mouse model of vestibular disorder. *Environ Health Prev Med.* (2019) 24:39. doi: 10.1186/s12199-019-0794-8

48. Shi X, Zhang Y, Li Y, Qiu S, Zhang S, Li Y, et al. Vestibular-evoked myogenic potentials in miniature pigs. *J Otol.* (2016) 11:88–93. doi: 10.1016/j.joto.2016.05.003

49. Ya L, Yan Z, ShiWei Q, Na Y, Xi S, Yuehua Q, et al. Vestibular-evoked myogenic potentials recorded from miniature pigs and rats. *J Otol.* (2016) 11:138–43. doi: 10.1016/j.joto.2016.06.004

50. Dyball AC, Govender S, Taylor RL, Young AS, Welgampola MS, Rosengren SM. Bone-conducted vestibular and stretch reflexes in human neck muscles. *Exp Brain Res.* (2020) 238:1237–48. doi: 10.1007/s00221-020-05798-8

51. Attias J, Nageris BI, Shemesh R, Shvero J, Preis M. Superior canal dehiscence effect on hearing thresholds: animal model. *Otolaryngol Head Neck Surg.* (2011) 145:648–53. doi: 10.1177/0194599811410535

52. Delsmann MM, Seist R, Stürznickel J, Schmidt FN, Mansour A, Kobelski MM, et al. Conductive hearing loss in the Hyp mouse model of X-linked hypophosphatemia is accompanied by hypomineralization of the auditory ossicles. *J Bone Miner Res.* (2021) 36:2317–28. doi: 10.1002/jbmr.4443

53. Bast TH, Anson BJ. *The Temporal Bone and the Ear*. Springfield: Charles C Thomas (1949).

54. Chole RA. Differential osteoclast activation in endochondral and intramembranous bone. *Ann Otol Rhinol Laryngol.* (1993) 102:616–9. doi: 10.1177/000348949310200809

55. Chole RA, Tinling SP. Incomplete coverage of mammalian bone matrix by lining cells. *Ann Otol Rhinol Laryngol.* (1993) 102:543–50. doi: 10.1177/000348949310200710

56. Chole RA, Tinling SP. Bone lining cells of the mammalian cochlea. *Hear Res.* (1994) 75:233–43. doi: 10.1016/0378-5955(94)90074-4

57. Nager GT. Temporal bone fractures. In: *Pathology of the Ear and Temporal Bone*. Baltimore: Williams & Wilkins (1993). p. 1247–1298.

58. Quesnel AM, Nakajima HH, Rosowski JJ, Hansen MR, Gantz BJ, Nadol JB Jr. Delayed loss of hearing after hearing preservation cochlear implantation: Human temporal bone pathology and implications for etiology. *Hear Res.* (2016) 333:225–34. doi: 10.1016/j.heares.2015.08.018

59. O'Leary SJ, Monksfield P, Kel G, Connolly T, Souter MA, Chang A, et al. Relations between cochlear histopathology and hearing loss in experimental cochlear implantation. *Hear Res.* (2013) 298:27–35. doi: 10.1016/j.heares.2013.01.012

60. Rah YC, Lee MY, Kim SH, Kim DH, Eastwood H, O'Leary SJ, et al. Extended use of systemic steroid is beneficial in preserving hearing in guinea pigs after cochlear implant. *Acta Otolaryngol.* (2016) 136:1213–9. doi: 10.1080/00016489.2016.1206965

61. Doménech J, Carulla M, Traserra J. Sensorineural high-frequency hearing loss after drill-generated acoustic trauma in tympanoplasty. *Arch Otorhinolaryngol.* (1989) 246:280–2. doi: 10.1007/BF00463575

62. Gurvich C, Maller JJ, Lithgow B, Haghgooie S, Kulkarni J. Vestibular insights into cognition and psychiatry. *Brain Res.* (2013) 1537:244–59. doi: 10.1016/j.brainres.2013.08.058

frontiers | Frontiers in Neurology

TYPE Methods
PUBLISHED 30 March 2023
DOI 10.3389/fneur.2023.1105869

OPEN ACCESS

EDITED BY
Tetsuo Ikezono,
Saitama Medical University, Japan

REVIEWED BY
Andrea Castellucci,
Azienda USL – IRCCS di Reggio Emilia, Italy
Franca Wagner,
University Hospital of Bern, Switzerland
Daisuke Yamauchi,
Tohoku University, Japan

*CORRESPONDENCE
Issam Saliba
✉ issam.saliba@umontreal.ca

†These authors have contributed equally to this work

SPECIALTY SECTION
This article was submitted to Neuro-Otology, a section of the journal Frontiers in Neurology

RECEIVED 23 November 2022
ACCEPTED 28 February 2023
PUBLISHED 30 March 2023

CITATION
Altamami N, Khoury M and Saliba I (2023) Manual neuronavigation for superior semicircular canal dehiscence surgery. *Front. Neurol.* 14:1105869. doi: 10.3389/fneur.2023.1105869

Manual neuronavigation for superior semicircular canal dehiscence surgery

Nasser Altamami[1,2†], Michel Khoury[1,2] and Issam Saliba[1,2*†]

[1]Division of Otorhinolaryngology and Head & Neck Surgery, University of Montreal, Montreal, QC, Canada, [2]Otology and Neurotology, University of Montreal Hospital Center (CHUM), Montreal, QC, Canada

Background: Intraoperative identification of a superior semicircular canal (SSC) dehiscence *via* the middle cranial fossa approach (MCFA) remains a difficult endeavor without a neuronavigation system. To address these challenges, we propose a technique to localize the SSC dehiscence intraoperatively using certain anatomical landmarks.

Method: Three anatomical landmarks should be identified on preoperative radiological images: the distance from the squamous part of the temporal bone to the dehiscent SSC, the lower limit of the craniotomy, and the exact location of the craniotomy in relation to the bony external auditory canal. The use of these landmarks intraoperatively can allow the surgeon to correctly identify the position of the SSC. Two instructional videos explaining this technique are presented.

Conclusion: The proposed manual neuronavigation technique seems to be an accurate, safe, and cost-effective alternative technique for use in SSC dehiscence surgery.

KEYWORDS

superior canal, dehiscence, SSCD, craniotomy, plugging, resurfacing, neuronavigation

Introduction

Since it was first described by Minor et al. in 1998, the presence of a pathological third window in the otic capsule has been found to manifest in a certain proportion of patients, producing severely debilitating symptoms that have a clear effect on their quality of life (1). According to the Classification Committee of the Bárány Society for vestibular disorders, a diagnosis of superior semicircular canal dehiscence (SSCD) requires the presence of four criteria related to the symptoms, clinical signs, and diagnostic tests (2). These criteria, based on the society's recommendations (2), are as follows.

1. At least one of the following symptoms consistent with the presence of a "third mobile window" in the inner ear:
    i. Bone conduction hyperacusis;
    ii. Sound-induced vertigo and/or oscillopsia time-locked to the stimulus;
    iii. Pressure-induced vertigo and/or oscillopsia time-locked to the stimulus;
    iv. Pulsatile tinnitus.

2. At least one of the following signs or diagnostic tests indicating a "third mobile window"in the inner ear:
    i. Nystagmus characteristic of excitation or inhibition of the affected superior Semicircular canal evoked by sound, or by changes in middle ear pressure or intracranial pressure;
    ii. Low-frequency negative bone conduction thresholds on pure tone audiometry;
    iii. Enhanced Vestibular evoked myogenic potential (VEMP) responses (low cervical VEMP thresholds or high ocular VEMP amplitudes).
3. High-resolution computed tomography (HRCT) imaging of the temporal bone with multiplanar reconstruction demonstrating dehiscence of the superior semicircular canal.
4. Signs and symptoms are not better accounted for by another vestibular disease or disorder (2).

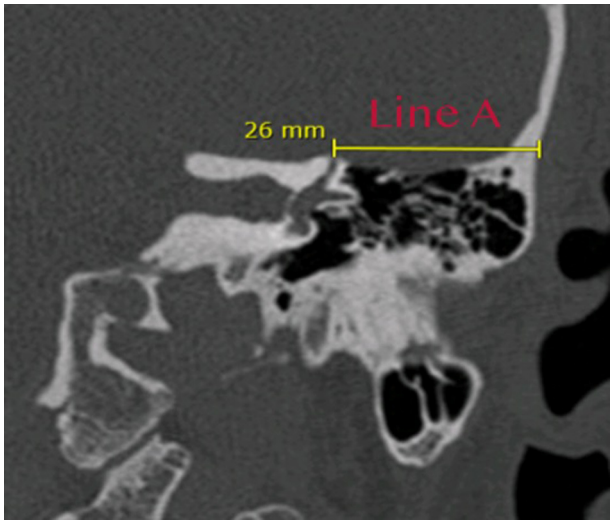

FIGURE 1
HRCT coronal view illustrating how the first measurement (line A) is taken between the center of the dehiscence medially and the most lateral part of the squamous part of the temporal bone. This line identifies the distance that will be crossed over the superior surface of the temporal bone from the craniotomy laterally to the dehiscence of the superior canal medially, 26 mm in this example.

In fact, most patients with SSCD present with tolerable symptoms and do not need any surgical treatment (3, 4). In accordance with the literature, only a minority of patients presenting with severely intolerable symptoms caused by the dehiscence are candidates for surgical plugging of the defect to improve their quality of life (3, 4). While several surgical techniques exist, our quaternary center promotes the middle cranial fossa approach (MCFA), through which the dehiscent part of the canal can be directly visualized, facilitating surgical plugging of the defect (3).

In the literature, studies have demonstrated radiologically that there is an association between SSCD and tegmen tympani dehiscence in 37%−76% of cases (5, 6). This association may lead to intraoperative confusion in identifying the SSC dehiscence rather than a tegmen tympani defect. Thus, a crucial step in this surgical technique is the correct identification of the dehiscent portion of the SSC, which can easily be mistaken for a dehiscent part of the tegmen tympani. Use of a neuronavigation system in the operating theater can facilitate this difficult step, thereby solving the problem (7). However, the accessibility of this technology remains challenging. In addition, the installation time and maintenance costs of neuronavigation systems limits their widespread use. To address these challenges, we propose a technique for intraoperative localization of the SSC using anatomical landmarks.

Methods

The patient is first subjected to a high-resolution computed tomography (HRCT) scan with a thin slice thickness of 0.6 mm.

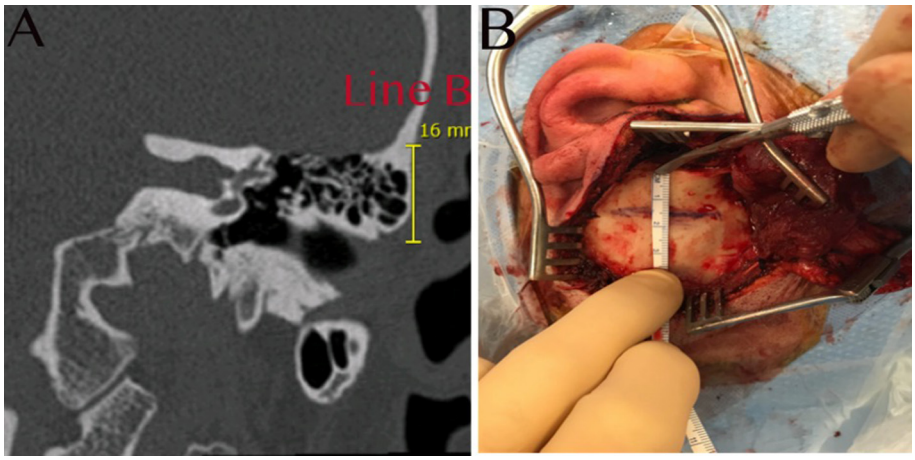

FIGURE 2
(A) HRCT coronal view illustrating how the second measurement (line B) is taken vertically; this will represent the lower limit of the craniotomy to avoid opening the air cells, 16 mm in this example. **(B)** The temporal bone is exposed, and the same measurement is demonstrated, taken from the superior part of the bony external auditory canal to the lower limit of the craniotomy.

Next, preoperative analysis of the HRCT scan using the coronal and axial views is conducted to precisely localize the dehiscence. Three landmarks are identified by the neurotologist surgeon immediately before the surgery. Finally, two measurements are noted on the coronal view.

The first measurement (Figure 1: line A) is taken by drawing a horizontal line on the coronal view HRCT scan between the center of the dehiscent segment of the SSC and the most lateral portion of the squamous part of the temporal bone. In drawing this line, the distance from the craniotomy laterally to the dehiscence of the SSC medially is measured over the temporal bone skull base. This value is important, as it represents the distance that the surgeon will measure to reach the SSC dehiscence medially while dissecting the dura of the temporal lobe.

The second measurement (Figure 2: line B) determines the height of the lower limit of the craniotomy from the superior bony part of the external auditory canal. This measurement allows the surgeon to avoid opening the pneumatized air cells during the craniotomy. A vertical line is drawn on the same coronal cut used previously, from the tegmen tympani, above the limit of the air cells, to the superior limit of the bony external auditory canal. This distance represents the minimum height for the lower line of the craniotomy to avoid opening the mastoid air cells or the epitympanic cavity and consequently creating a dehiscence of the tegmen tympani or tegmen antri.

The third measurement point in this manual neuronavigation technique is used to define the anteroposterior location of the craniotomy to position the SSC dehiscence in the middle of the operative field. This third measurement is not a calculated distance *per se*, but it serves to identify the exact position of the craniotomy in order for it to be centered on the SSCD. In the axial view, the surgeon must first identify the dehiscence with the cursor. With the cursor remaining in place, the surgeon must roll through the slices in the inferior direction until they visualize the external auditory canal. At this point, a horizontal line must be drawn from the exact position of the cursor medially to the external auditory canal laterally. This line will pass at the level of the anterior wall, at the level of the posterior wall, or between the two walls, and identifies both the center of the external auditory canal and the center of the craniotomy in the sagittal plane (Supplementary Video 1). Once these three points are radiologically defined, the surgery can begin (Figure 3).

The patient is placed in the supine position. For the patient's security, two straps keep them attached to the table. The head is turned to the opposite side of the dehiscence and the table is then turned toward the opposite side of the operated ear in order to situate the squamous part of the temporal bone in a horizontal position facing the surgeon. The surgeon then sits at the side of the patient's head.

A question mark-shaped skin incision is made starting anterior to the tragus, passing above the helix posteriorly and turning anteriorly (Figure 3). The dissection is continued above the plane of the temporalis fascia. Next, a 1 × 1 cm temporalis fascia graft is harvested for use as a cover at the end of the procedure; the bone dust is used in plugging the SSCD (Figure 4). Subsequently, careful dissection of the temporalis muscle flap pedicled anteriorly is completed to expose the squamous part of the temporal bone

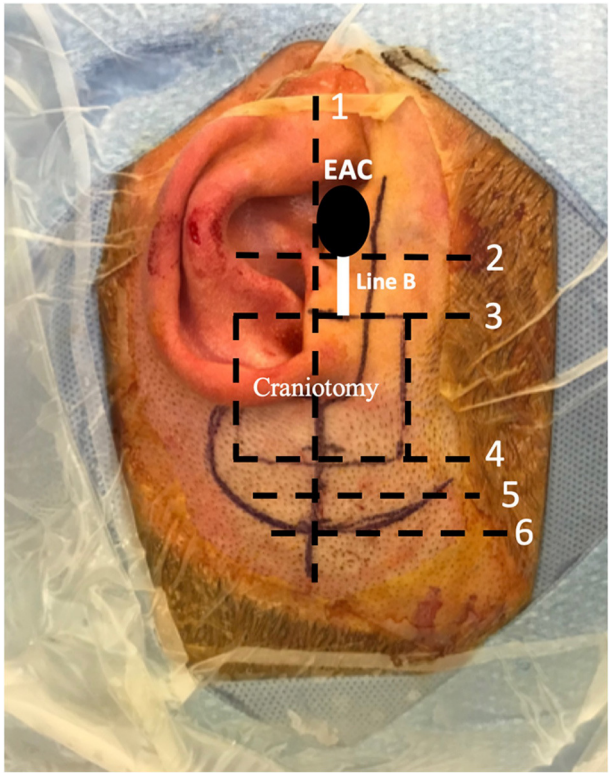

FIGURE 3
This image illustrates the surgical site and how the incision is made. The surgeon is positioned superiorly near the head of the patient. (1) An imaginary line drawn, in this case posterior to the external auditory canal (EAC), which determines the center of the craniotomy as described in Supplementary Video 1. (2) Superior limit of the bony EAC. (3) Inferior limit of the craniotomy. Line B is the height between lines 2 and 3, 16 mm in this case, as illustrated previously in Figure 2. (4) Superior limit of the craniotomy (2.5 cm × 3 cm or 3 cm × 3 cm). (5) Temporalis muscle flap incision is located 0.5 cm superior to the craniotomy. (6) Superior skin incision limit is located 0.5 cm superior to the temporalis muscle flap incision.

at the site of the craniotomy. In parallel, the superior wall of the external auditory canal should be exposed to measure the height of the inferior limit of the craniotomy (Figure 2B). Next, under a microscope and with a 2-mm cutting burr, the craniotomy (2.5 cm × 3 cm or 3 cm × 3 cm) is made. Bone dust is carefully harvested from the peripheries of the craniotomy. Hemostasis over the dura mater is performed using bipolar cautery.

The dissection of the temporal dura is continued medially toward the superior canal until visualization of the dehiscence. The surgeon should avoid applying any suction on the dehiscent part of the SSC. The middle cranial fossa retractor is used to gently retract the temporal lobe if needed in order to better expose the dehiscence. Once the dehiscence or suspected dehiscence is visualized, the surgeon confirms the dehiscence using a surgical ruler, measuring the distance between the dehiscence and the lateral part of the squamous bone as indicated by line A in the previous drawing (Figure 1). This will precisely confirm the site of the dehiscence. Once the dehiscence is confirmed, the bone dust is used to plug the superior canal and the temporalis is used to cover the bone dust

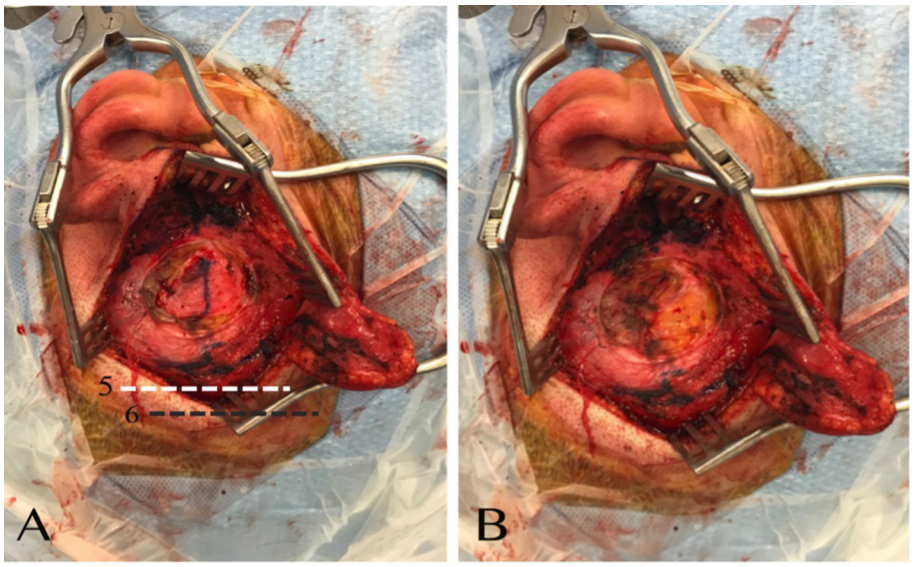

FIGURE 4
(A) The plan over the temporalis fascia is dissected, and the fascia exposed. **(B)** Temporalis fascia is harvested. (5) Demonstration of the level of the temporalis muscle flap incision. (6) Demonstration of the level of the skin incision with respect to the temporalis muscle flap incision.

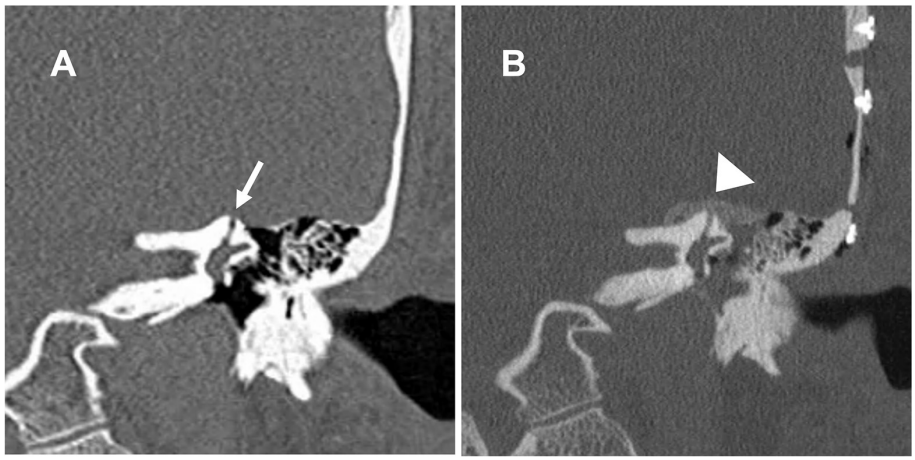

FIGURE 5
Coronal cut of a high-resolution CT scan of the left temporal bone. **(A)** The dehiscence of the left superior canal (arrow). **(B)** The bone dust plugging the dehiscence and covering the superior canal (arrowhead).

to keep it in place. The craniotomy is closed using four titanium double-Y-shaped plates (Supplementary Video 2). The temporalis muscle and the skin are approximated using absorbable sutures.

We have been using this technique to operate in cases of dehiscence of the superior semicircular canal since 2010. We have operated on 110 patients using this method. A total of 53 other patients were operated on between 2005 and 2010, before we began using this technique.

Discussion

Repairing a dehiscent SSC remains a technically challenging task, especially without neuronavigation. Given that accessibility, installation time, and maintenance remain the key factors impeding access to this technology, alternative methods are needed to overcome these limitations. To address these challenges, we propose a technique to localize the SSC intraoperatively using anatomical landmarks.

The middle cranial fossa approach is the preferred surgical technique in our center for repair of dehiscence of the SSC, given the optimal surgical exposure that it provides. Specifically, this surgical approach allows direct visualization of the dehiscent area of the canal and permits direct plugging, an option that is not possible when the transmastoid approach (TMA) is used. Through MCFA plugging, there may be a lower risk of sensorineural hearing loss to the SSC and/or vestibular function impairment in the other canals (3, 8). In addition, a recently published study by Renteria

et al. demonstrated residual SSC function 3 months postoperatively in 55.3% of patients operated on for SSC dehiscence through the MCFA (9). On the other hand, the TMA avoids craniotomy and temporal lobe retraction and remains the preferable approach for cases of medial and purely posterior dehiscence (3). A recent comparative study by Schwartz et al. comparing middle cranial fossa and transmastoid surgical techniques showed that both techniques offer symptom resolution with minimal risk (5). The round window reinforcement technique is used in some centers to counteract the third window effect. In the literature, studies of this approach have shown poor long-term results in comparison with the high success rate of dehiscence plugging; thus, it is not advisable as the first-line intervention for SSCD (3, 10–14).

In addition, the removal of the thin bone fragments at the two limits of the dehiscence should not be a problem if it is performed by an experienced surgeon. It is important that this part of the process be completed superficially, with care to avoid penetration of the membranous labyrinth. This will facilitate and ensure the correct plugging, particularly in the case of a small dehiscence.

In our quaternary center, SSCD is repaired by plugging the canal through the middle cranial fossa approach. Intraoperatively, the most difficult step is the accurate identification of the dehiscent SSC over the superior surface of the temporal bone.

As we know, the arcuate eminence reflects the superior part of the SSC, but this is not always a clear landmark. The anatomy of the superior surface of the temporal bone is variable, and the landmarks are not always consistent, particularly if the petrous bone is highly pneumatized, in which case the arcuate eminence will not always be clearly visible. In these difficult cases, the neuronavigation technique proposed here will be of great assistance. By using this method, we directly situate the canal in the middle of our operative field. Making the craniotomy in exactly the right place is extremely valuable, especially since we make a small (3 cm × 3 cm) craniotomy, which means that it is especially important to make it in the optimal position.

For procedures carried out at our center between 2005 and 2010, this manual neuronavigation technique had not yet been developed; therefore, the craniotomy for SSC surgery was sometimes positioned more anterior or posterior, or more inferior or superior, to the exact position, making the procedure more challenging. In the face of these few particular cases, we developed this manual neuronavigation technique.

A neuronavigation system is a useful tool to precisely identify SSC dehiscence. However, there are several limitations regarding the cost of such systems that prevent some centers from providing them; additional limitations are the time consumed in installation and difficulties in using the neuronavigation system when the surgeon's experience is limited. Our study proposes a simple technique that can help otologic surgeons to identify the dehiscence of the SSC precisely and efficiently. The use of line A on the HRCT axial cut, which measures the distance from the dehiscence to the lateral cortical part of the supra-auricular squamous bone, provides a precise distance that can be measured during surgery. In our institution, we perform an HRCT on day 1 postoperatively to rule out any intracranial complications such as bleeding or hematoma. In addition to this, the postoperative HRCT scan confirms the correct identification and good plugging of the SSC dehiscence (Figure 5). Another prospective study to support and validate the proposed technique is planned.

Conclusion

Although neuronavigation facilitates the surgical approach, we propose the use of surgical landmarks on a high-resolution CT scan as an alternative method to the use of a neuronavigation system. The proposed manual neuronavigation technique seems to be an accurate, safe, and cost-effective alternative technique for use in SSC dehiscence surgery. A randomized controlled trial is needed to confirm the accuracy of the proposed technique.

Data availability statement

The original contributions presented in the study are included in the article/Supplementary material, further inquiries can be directed to the corresponding author.

Ethics statement

Ethical review and approval was not required for the study on human participants in accordance with the local legislation and institutional requirements. Written informed consent for participation was not required for this study in accordance with the national legislation and the institutional requirements.

Author contributions

All authors listed have made a substantial, direct, and intellectual contribution to the work and approved it for publication.

Conflict of interest

The authors declare that the research was conducted in the absence of any commercial or financial relationships that could be construed as a potential conflict of interest.

Publisher's note

Supplementary material

The Supplementary Material for this article can be found online at: https://www.frontiersin.org/articles/10.3389/fneur.2023.1105869/full#supplementary-material

References

1. Minor LB, Solomon D, Zinreich JS, Zee DS. Sound- and/or pressure-induced vertigo due to bone dehiscence of the superior semicircular canal. *Arch Otolaryngol Head Neck Surg.* (1998) 124:249–58. doi: 10.1001/archotol.124.3.249

2. Ward BK, van de Berg R, van Rompaey V, Bisdorff A, Hullar TE, Welgampola MS, et al. Superior semicircular canal dehiscence syndrome: diagnostic criteria consensus document of the committee for the classification of vestibular disorders of the Bárány Society. *J Vestib Res.* (2021) 31:131–41. doi: 10.3233/VES-200004

3. Steenerson KK, Crane BT, Minor LB. Superior semicircular canal dehiscence syndrome. *Semin Neurol.* (2020) 40:151–9. doi: 10.1055/s-0039-3402738

4. Gioacchini FM, Alicandri-Ciufelli M, Kaleci S, Scarpa A, Cassandro E, Re M. Outcomes and complications in superior semicircular canal dehiscence surgery: a systematic review. *Laryngoscope.* (2016) 126:1218–24. doi: 10.1002/lary.25662

5. Whyte J, Cisneros AI, Garcia-Barrios A, Fraile J, Whyte A, Crovetto R, et al. Association between superior semicircular canal dehiscence and other dehiscences in temporal bone. *Folia Morphol.* (2020) 79:823–8. doi: 10.5603/FM.a2019.0138

6. Nadaraja GS, Gurgel RK, Fischbein NJ, Anglemyer A, Monfared A, Jackler RK, et al. Radiographic evaluation of the tegmen in patients with superior semicircular canal dehiscence. *Otol Neurotol.* (2012) 33:1245–50. doi: 10.1097/MAO.0b013e3182634e27

7. Zhao YC, Somers T, Dinther J. van, Vanspauwen R, Husseman J, Briggs R. Transmastoid repair of superior semicircular canal dehiscence. *J Neurol Surg B Skull Base.* (2012) 73:225–9. doi: 10.1055/s-0032-1312713

8. Carey JP, Migliaccio AA, Minor LB. Semicircular canal function before and after surgery for superior canal dehiscence. *Otol Neurotol.* (2007) 28:356–64. doi: 10.1097/01.mao.0000253284.40995.d8

9. Renteria AE, Elblidi A, Altamami N, Alhabib S, Saliba I. Video head impulse test demonstrates a residual function after plugging of dehiscent superior semicircular canal. *Otol Neurotol.* (2023) 44:252–9. doi: 10.1097/MAO.0000000000003794

10. Schwartz SR, Almosnino G, Noonan KY, Banakis Hartl RM, Zeitler DM, et al. Comparison of transmastoid and middle fossa approaches for superior canal dehiscence repair: a multi-institutional study. *Otolaryngol Head Neck Surg.* (2019) 161:130–6. doi: 10.1177/0194599819835173

11. Bunne M, Andersson H, Myhrum M. Long-term outcomes of round window reinforcement for superior semicircular canal dehiscence syndrome. *Otol Neurotol.* (2022) 43:709–16. doi: 10.1097/MAO.0000000000003561

12. Succar EF, Manickam PV, Wing S, Walter J, Greene JS, Azeredo WJ. Round window plugging in the treatment of superior semicircular canal dehiscence. *Laryngoscope.* (2018) 128:1445–52. doi: 10.1002/lary.26899

13. Chemtob RA, Noij KS, Qureshi AA, Klokker M, Nakajima HH, Lee DJ. Superior canal dehiscence surgery outcomes following failed round window surgery. *Otol Neurotol.* (2019) 40:535–42. doi: 10.1097/MAO.0000000000002185

14. Shaia WT, Diaz RC. Evolution in surgical management of superior canal dehiscence syndrome. *Curr Opin Otolaryngol Head Neck Surg.* (2013) 21:497–502. doi: 10.1097/MOO.0b013e328364b3ff

frontiers | Frontiers in Neurology

TYPE Mini Review
PUBLISHED 08 August 2023
DOI 10.3389/fneur.2023.1209567

OPEN ACCESS

EDITED BY
Carey David Balaban,
University of Pittsburgh, United States

REVIEWED BY
Bryan Kevin Ward,
Johns Hopkins University, United States
Santosh Kumar Swain,
Siksha 'O' Anusandhan University, India
Andrea Castellucci,
Azienda USL—IRCCS di Reggio Emilia, Italy

*CORRESPONDENCE
Eugen C. Ionescu
✉ eugen.ionescu@chu-lyon.fr

†These authors have contributed equally to this work and share first authorship

RECEIVED 20 April 2023
ACCEPTED 14 July 2023
PUBLISHED 08 August 2023

CITATION
Ionescu EC, Reynard P, Damien M, Ltaief-Boudrigua A, Hermann R, Gianoli GJ and Thai-Van H (2023) Why should multiple dehiscences of the otic capsule be considered before surgically treating patients with superior semicircular canal dehiscence? A radiological monocentric review and a case series. *Front. Neurol.* 14:1209567. doi: 10.3389/fneur.2023.1209567

Why should multiple dehiscences of the otic capsule be considered before surgically treating patients with superior semicircular canal dehiscence? A radiological monocentric review and a case series

Eugen C. Ionescu[1,2*†], Pierre Reynard[1,2,3†], Maxime Damien[1,2,3], Aicha Ltaief-Boudrigua[4], Ruben Hermann[5,6], Gerard J. Gianoli[7] and Hung Thai-Van[1,2,3]

[1]Department of Audiology and Otoneurological Explorations, Hospices Civils de Lyon, Lyon, France, [2]Hearing Institute, Research Center of Pasteur Institute, Team Clinical and Translational Exploration of Sensorineural Hearing Loss, Inserm, Paris, France, [3]Department of Physiology, Claude Bernard University, Lyon, France, [4]Department of Radiology, Hospices Civils de Lyon, Lyon, France, [5]Department of ENT, Cervico-Facial Surgery and Audiophonology, Hospices Civils de Lyon, Lyon, France, [6]Lyon Neuroscience Research Center, IMPACT Team, INSERM, Centre National de la Recherche Scientifique (CNRS), Lyon, France, [7]The Ear and Balance Institute, Covington, LA, United States

This review aims to draw attention to the multiple ipsilateral otic capsule dehiscences (OCDs), which may cause therapeutic failure in operated patients. A series of six severely disabled patients with symptoms and signs consistent with a superior semicircular canal dehiscence (SSCD) diagnosis, confirmed by a high-resolution CT scan, is presented here. Five of the patients underwent surgery, and in four of the cases, the postoperative results were poor and/or disappointing. The ethical principles underlying modern medicine encourage medical staff to learn from past experience even when the results are modest despite the accuracy of the treatment applied to a patient. Consequently, we reviewed the radiological records of symptomatic and asymptomatic patients diagnosed or referred to our center for confirmation over the past 5 years to determine the incidence of multiple OCD in this population. Multiple localizations of suspected OCD in the ipsilateral ear did not appear to be rare and were found in 29 of 157 patients (18.47%) in our retrospective review using high-resolution thin-sliced CT scans. The decision to perform surgery for a documented symptomatic superior SSCD should be made with caution only after ruling out concomitant lesser-known variants of OCD in the ipsilateral ear.

KEYWORDS

otic capsule dehiscence, otic capsule dehiscence syndrome, multiple otic capsule dehiscence, third window syndrome clinical-radiological correlations, third mobile window lesions diagnosis

Background

After the first description of superior semicircular canal dehiscence (SSCD) by Minor et al. (1), the understanding of this pathology generated by a third mobile window (TMW) has progressively evolved over time, while the number of reported anatomical variants has increased. Given the similarity of the auditory and/or vestibular signs specifically described in most of these variants, many authors have adopted the concept of a "spectrum of third window abnormalities" (TMWA) (2). This condition is characterized by the fact that it can mimic a considerable number of inner and/or middle ear disorders (3, 4). The recently introduced term "third mobile window syndrome" (TMWS) (5) refers to all pathologies of the TMWA spectrum whose symptoms, clinical signs, and vestibular and audiometric outcomes correspond to bony defects or otic capsule dehiscence (OCD) confirmed or not by high-resolution computed tomography (HRCT) performed according to the recommendations of the Barany Society (5–8).

The above-mentioned approach only suggests the existence of various low-impedance areas of the otic capsule but does not indicate its position or the anatomical elements involved at the dehiscence interface. Therefore, there was recently proposed a three-type anatomical–radiological classification of TMWA (Supplementary material IA), including all known OCD variants (6, 7) (Supplementary material IB). This new classification has the advantage of depicting the anatomical structures that are involved at the level of the abnormal mobile window, which can guide therapeutic management, as has been the case in some labyrinthine-vascular variants (9–12). It also indicates all the existing types of TMWA, including OCDs, multiple OCDs, and CT- or intralabyrinthine, to both ENT and radiology specialists in such a way that this pathology does not remain underdiagnosed. In fact, other OCD variants than SSCD are far from being systematically searched for in the current radiological practice, despite the obvious presence of a TMWS. This can be easily explained because most of the articles communicated or published in the past 20 years have almost exclusively focused on SSCD, although the incidence of these OCD variants is not necessarily lower (13).

Although multiple ipsilateral OCDs have been reported by several authors as case reports (14–21), information on this topic in the literature is still lacking. Only one article addresses this topic in more detail and is not just a case report (22). This article indicates that the frequency of low bone strength area or OCD associations is higher than previously thought. It reports some associations, especially between SSCD and other "classic" dehiscences (such as tegmen tympani or posterior SSCD, geniculate ganglion dehiscence, or variants involving the internal auditory canal and/or posterior semicircular canal (PSC) and the glenoid cavity of the mandible). However, lesser-known and recently described variants of OCD were not cited in this study, such as the dehiscence between the cochlea and the first facial nerve segment (cochlear-facial dehiscence [CFD]), between the lateral semicircular canal (LSC) and the tympanic segment of the facial nerve (LSC/FN) (23), or the vasculo-labyrinthine OCDs involving the internal jugular vein (IJV), the vestibular aqueduct (VA), the cochlear aqueduct (CA), or other previously reported variants (7, 8). We also reported in a recent article, a series in which 11 of 97 patients (11.3%) presented with symptoms confirming multisite OCDs (6). From our analysis of these patients, the most frequent associations appear to be between Type I and Type III OCD variants (such as SSCD and cochleo-facial or LSC/FN), followed by Type II and Type III (such as IJV/VA and CFD or LSC/FN). Previously, Wackym et al. reported a comparative percentage of double ipsilateral locations in a larger radiological study (9.18%) (24). Interestingly, the prevalence of the most frequent associations with OCD variants appears similar in both studies cited above.

We previously stated that the main challenge of multiple ipsilateral OCDs seems to be designating an appropriate treatment strategy in patients with disabling symptoms (6). This includes establishing the order in which these dehiscences should be treated and whether this should be done sequentially or simultaneously. To the best of our knowledge, no current data in the literature guide practitioners to a suitable therapeutic approach regarding multiple OCD. Therefore, the main purpose of this article is to emphasize the fact that the presence of a "classic" and large SSCD on HRCT might dissuade radiologists and neurotologists from searching for further OCDs (i.e., a "distracting lesion"), especially when the symptoms are consistent with a TMWA. Multiple OCDs might remain undiagnosed, which could lead to poor outcomes.

Methods

The investigation adhered to the principles of the World Medical Association Declaration of Helsinki.

Radiologic study

Between January 2019 and December 2022, 1,283 patients underwent HRCT of the temporal bone at our tertiary referral center. In most cases, the patients were recommended for HRCT for symptoms such as conductive or sensorineural hearing loss, including profound hearing loss, with or without vertigo or dizziness, that were found during an initial ENT consultation. HRCT records of adult candidates for cochlear implantation were therefore also considered. The files were reviewed by a neurotologist and a radiologist specializing in neurotology,

Abbreviations: CA, cochlear aqueduct; CFD, cochlear-facial dehiscence; cVEMP, cervical vestibular evoked myogenic potentials; dB, decibel; DHI, Dizziness Handicap Index; EAC, external auditory canal; FN II, second segment of facial nerve; HL, human level; HRCT, high-resolution computed tomography; IJV, internal jugular vein; LE, left ear; LSC, lateral semicircular canal; MRI, magnetic resonance imaging; OCD, otic capsule dehiscence; oVEMP, ocular vestibular evoked myogenic potentials; PSC, posterior semicircular canal; PSC, posterior semicircular canal; PTA, pure tone average audiometry; RE, right ear; SC, semicircular canal; SSC, superior semicircular canal; SSCD, superior semicircular canal dehiscence; THI, Tinnitus Handicap Index; TMW, third mobile window; TMWA, third mobile window abnormalities; TMWS, third mobile window syndrome; VA, vestibular aqueduct; VEMP, vestibular evoked myogenic potentials; VHIT, video head impulse test; VNG, videonystagmography; VOR, vestibuloocular reflex.

and the cases of suspected multiple ipsilateral localization were unanimously selected as such.

Two hundred forty-five radiologically confirmed or suspected SSCD patients were identified using targeted medical statistical research software. Patients who have undergone middle ear surgery or had chronic inflammatory, neoplastic, or degenerative inner and/or middle ear pathologies were excluded. After applying the criteria, the radiological records of 157 patients (64 men and 93 women) and 314 ears were finally included in this study.

A high-resolution CT scan (GE GSI Revolution, GE Healthcare, USA) of the temporal bone was performed in all patients. As recommended, the slices were acquired helically in the axial plane at a nominal thickness of 0.625 mm with a 50% overlap of 0.312 mm in a 60-mm field of view with a 512 matrix for an isometric voxel [1]. Images were obtained in ultrahigh resolution at 140 kV and 200 mAs/section. Primary images were reworked in the axial and coronal planes of the SSC, LSC, or PSC. Each plane was performed with a 0.2 mm thickness and a 0.2 mm increment using Advantage Workstation Server visualization software (GE Healthcare, USA). Thus, the Pöschl plane was also used to better identify SSCD variants (i.e., the superior plane of the SSC). Other thin multiplanar reconstructions (0.2 mm thickness and 0.2 mm increment) were performed to better identify OCD variants on orthogonal structures of the otic capsule suspected dehiscent. At least two orthogonal thin reconstructions were used in each case of peri-petrous OCD variants (Type III), which usually, in our experience, are not searched systematically as the other more common types of OCDs with the usual HRCT protocol (axial and coronal planes of the second turn of the cochlea of the vestibule, VA, CA). These specific planes were essential for identifying most peri-petrous Type III OCD variants (e.g., CFD and LSC/FN). Inverting the contrast in these cases could provide better recognition of these variants, even if the distinction between "real" and "near" dehiscences can sometimes be challenging (24).

Case series

The main clinical, audio-vestibular, and radiological elements are presented in this series of six patients with multiple OCD localizations. Although the Dizziness Handicap Index (DHI) and Tinnitus Handicap Inventory (THI) questionnaires were completed before and after the surgical intervention in some cases, these evaluations were not systematic.

Audio-vestibular assessment

Initial and postoperative audio-vestibular assessments were routinely performed in all patients in the case series reported here and in patients included in the Review section. The audio-vestibular postoperative evaluation was initially scheduled for 3 months, but in cases of symptom resurgence, such as intense vertigo and/or postoperative hearing loss, the patients were examined in a much shorter time interval, from 1 to 2 days up to 2 weeks after the surgery.

The protocol included clinical examinations as well as auditory and vestibular evaluation as follows: pure tone audiometry (PTA; Madsen Astera-Otometrics), middle ear reflexes (Madsen Zodiac 901 tympanometer), videonystagmography (VNG, Ulmer System®; Synapsis SA), video head impulse test (VHIT, ICS Impulse®; GN Otometrics), and cervical and ocular vestibular evoked myogenic potentials (VEMP, only in selected patients; Bio-Logic® Nav-Pro system) in air conduction (AC) stimuli with 750 Hz tone bursts.

TMWS simplified score

To identify whether a correlation existed between the level of functional impairment or symptoms and the number of documented uni- or bilateral cases of OCD in each subject, we used a simplified audio-vestibular score. This score was obtained from the medical records of the patients included in the retrospective radiological study. It assesses the most significant signs and symptoms of a TMWA as follows:

Auditory symptoms (1 point each): autophony; pulsatile tinnitus; conductive hearing loss. Vestibular symptoms (1 point each): the presence of Tullio phenomenon or pressure hypersensitivity in the external auditory canal (EAC); physically exerted vertigo or by Valsalva maneuver; permanent or episodic dizziness.

The maximum score obtained was 6, corresponding to a severely impaired patient, and the minimum score, corresponding to an asymptomatic patient, was 0.

Results

Radiologic and clinical retrospective review

Imaging records of 157 patients (64 men and 93 women), or 314 ears, were included in this study. The youngest subject at the time of the HRCT scan was a 6-year-old girl, while the oldest was an 88-year-old woman. Out of 157 patient files, we found a total of 324 OCDs. The distribution by type of OCD (6, 7) in number and affected ear was as follows (Figure 1):

Type I (*labyrinthine–meningeal*) accounted for a total of 113 dehiscences out of 324 (34.87%). Of these, 100 were SSCD [48 right ear (RE), 52 left ear (LE)], and 13 were posterior semicircular canal dehiscence (PSCD) (8 RE, 5 LE).

Type II (*labyrinthine–vascular*) accounted for 84 dehiscences out of a total of 324 (25.92%): 49 of them were variants localized between the VA and the IJV (32 RE, 17 LE); 23 variants localized between SSC/superior petrosal sinus (13 RE, 9 LE); and 1 less common variant, SSC/subarcuate vein or artery crossing SSC, was found in 1 patient (LE); 6 variants were localized between PSC/IJV (all on the RE); 4 CA/IJV (1 on RE, 3 on the LE); and 2 cochlear-carotid dehiscence variants (1 on each side in the same patient).

Type III (*labyrinthine-peripetrosal structures*) accounted for 127 dehiscences out of 324 (39.19%). LSC/FN variant was the most frequent: 69 cases (31 RE, 38 LE); 54 were CFD variants

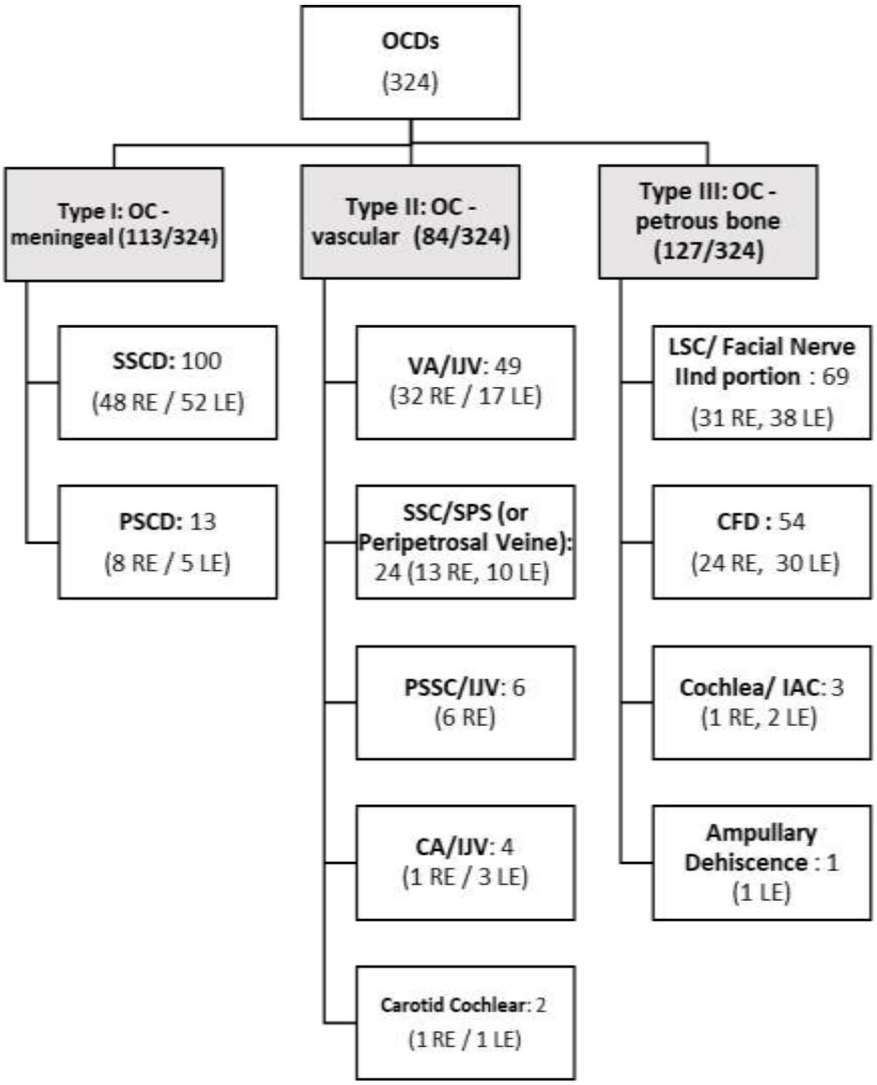

FIGURE 1
Distribution of OCD by type according to precedent classification in 324 OCDs (157 patients or 314 ears).

(24 on the RE, 30 on the LE); 3 were cochlea–internal auditory canal dehiscence variants (1 RE, 2 LE); and 1 ampullary dehiscence (LE).

Unilateral and single localizations of OCD were present in 55 out of 157 patients. Twenty patients were classified as Type I OCD (10RE, 10LE). Twenty-six were classified as Type II OCD, including 12 SSC/SPS OCDs (6RE, 6LE) and 14 VA/IJV OCDs (9RE, 4LE). Nine patients were classified as Type III OCD, including 7 patients with CFD (2RE and 5LE) and 2 patients with OCDS involving the LSC and the tympanic segment of the FN (1 RE and 1 LE).

Multiple localizations (uni- and/or bilateral) were found in 102 patients (Figure 2). There were 12 patients with unilateral double OCD and 9 with unilateral triple OCD localization. In 39 patients, we found a bilateral localization: 31 patients had a bilateral single localization, 7 patients had a bilateral double OCD, and only 1 had a bilateral triple OCD (Additional Material II). In the remaining 42 patients, we found 126 OCDs arranged in different combinations bilaterally.

Symptoms and score

Using data from clinical observations, as those patients did not complete the THI or DHI questionnaire, we retrospectively assessed the level of perceived functional hearing and vestibular impairment with a simplified assessment tool. The mean TMWS score obtained in the three groups was as follows (Table 1):

(a) TMWS score in the strictly *single* (*unilateral*) OCD localization group: 2.8 (55 patients),
(b) TMWS score in the *multiple unilateral* localization group: 3.4 (21 patients),
(c) TMWS score in the *bilateral* localization (single and/or multiple) group: 3.98 (81 patients).

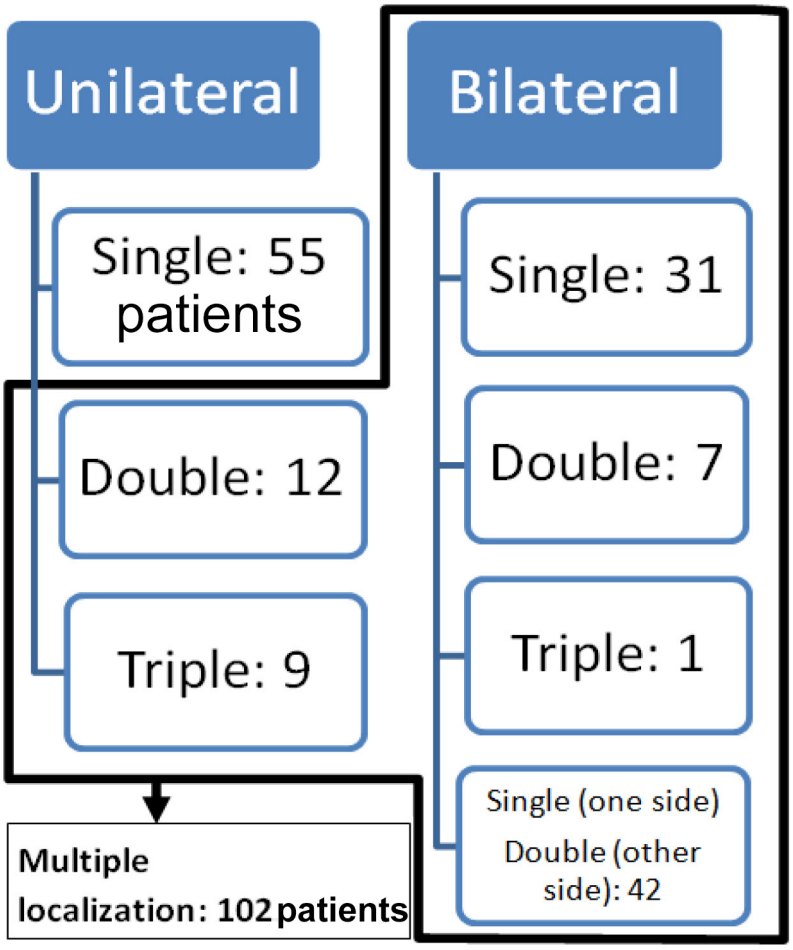

FIGURE 2
Distribution of OCD between uni- or bilateral and single or multiple OCD localizations in all 157 patients.

Case report series

A table with the essential data of these case reports can be found in Supplementary material III.

Case report 1

A 75-year-old patient was examined for hyperacusis in the left ear (LE) and sudden-onset intermittent pulsatile tinnitus. He also described rotatory vertigo triggered by loud noises. The physical examination, including otoscopy, was normal. The audiometric assessment confirmed a pure bilateral sensorineural hearing loss, more pronounced on the LE (Figure 3A). cVEMPs showed a greater response on the LE, where the thresholds were at 80 dB nHL. Caloric tests showed significant left vestibular hypofunction. VHIT gain was normal for LSC but weaker for both left vertical semicircular canals. The HRCT confirmed the presence of a left SSCD (Type I OCD; Figures 3B, C). Because of the disabling and recurrent nature of his vestibular complaints, a left SSCD plugging was performed by transmastoid approach. Unfortunately, the hearing thresholds on the operated side increased to 80 dB nHL on all frequencies after the operation and did not improve.

TABLE 1 Clinical mean score for each OCD subgroup.

	Single, unilateral OCD	Multiple, unilateral OCD	Bilateral (single or multiple) OCD
Number of patients	55	21	81
Clinical score for TMWS	2.8	3.4	3.98

10 months after surgery, after a period of improvement, the patient described a recurrence of rotatory vertigo and pulsatile tinnitus. Postoperative 3D magnetic resonance imaging (MRI) confirmed the expected absence of an endolymphatic signal, proving that the left SSC was rightly plugged (Figure 3D). When reviewing the postoperative HRCT control, two Type III OCDs could be observed: one involving the LSC and tympanic segment of the FN (LSC/FN) (Figures 3C, G), unknown in the literature at the time of the surgery, and a second dehiscence near the operated area probably due to the drilling during mastoidectomy (Figures 3D, F). The patient was lost to follow-up.

10.3389/fneur.2023.1209567

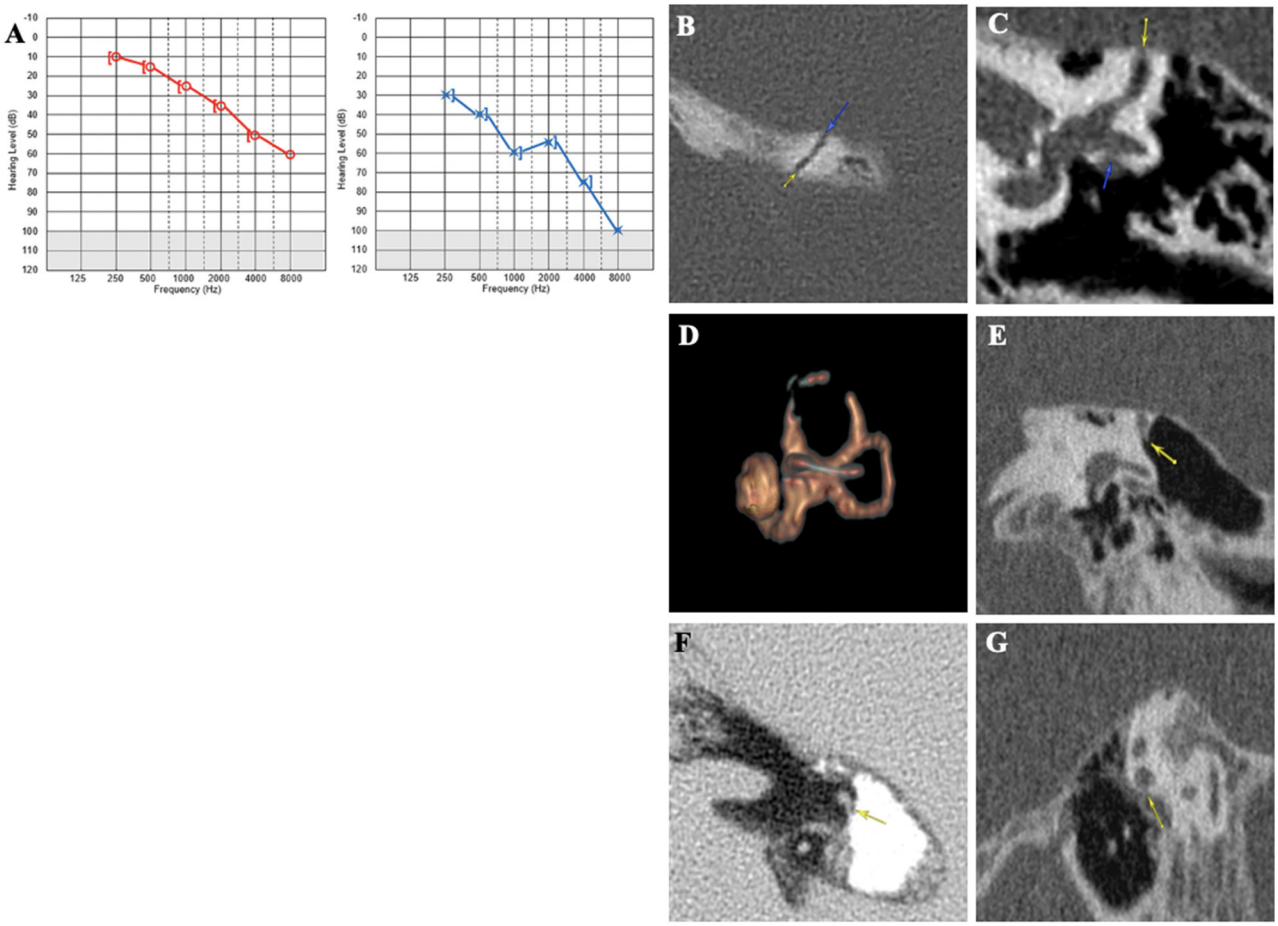

FIGURE 3
(A) Tonal audiometry showing a bilateral sensorineural hearing loss, more pronounced on the left side. **(B, C)** Left SSCD in axial **(B)** and coronal plane **(C)** and CFD (blue arrow) **(C)**. **(D)** Post-operative 3D MRI showing a correctly plugged superior canal. **(E–G)** Post-operative HRCT control showing CFD and another location of SCCD near the surgical approach (yellow arrow).

Case report 2

A 74-year-old patient presented with autophony in the RE associated with a Tullio phenomenon and effort-induced dizziness with closed glottis. The patient also complained of perceiving sounds coming from the cervical spine in the RE through neck movements. The PTA showed a bilateral sensorineural hearing loss, more pronounced on the RE, with no conductive component and very poor intelligibility (Figure 4A). cVEMPs showed very large responses, with a detection threshold of 50 dB nHL on the RE. VNG showed a slightly decreased vestibulo-ocular reflex (VOR) gain on kinetic tests and a right hypofunction on caloric testing. HRCT confirmed a right SSCD (Type I OCD; Figures 4B, C). The patient underwent an SSCD occlusion through a middle fossa approach. Within a month, he described a significant recurrence of symptoms, while audiometry showed a decrease of 30 dB in low and mid frequencies. In the third postoperative month, this PTA threshold's degradation on the operated side was doubled by major deterioration of intelligibility and autophony reappearance (Figure 4D). This subject was also lost to follow-up.

However, the HRCT image review noted two additional unidentified OCD localizations ipsilaterally: (1) a Type II labyrinthine-vascular dehiscence between the VA and the IJV (yellow arrow) (Figures 4E, F) and (2) a Type III OCD between the Lateral semicircular canal (LSC) and the tympanic segment of the Facial Nerve (FN) (Figure 4G).

Case report 3

A 70-year-old patient presented with persistent dizziness associated with hearing loss, intermittent autophony, and pulsatile tinnitus on the RE. He also complained of perceiving cervical and temporomandibular joint movements and blinking in the RE. The symptoms, which included dizziness and intense vertigo, began with a lung infection associated with coughing and intense sneezing. The vestibular symptoms seemed to be in sync with the acts of coughing and nose blowing. However, exposure to loud noises did not seem to generate the Tullio phenomenon. PTA showed mild presbycusis with a moderate conductive component at 0.25 and 0.50 kHz on the RE, with preserved bilateral intelligibility (Figure 5A). The cVEMPs showed a significant decrease in the detection threshold up to 70 dB nHL on the RE; the oVEMPs were remarkably large on the RE and absent on the LE. The caloric tests showed a slight left vestibular impairment. The HRCT scan confirmed the presence of a right SSCD (Figures 5B,

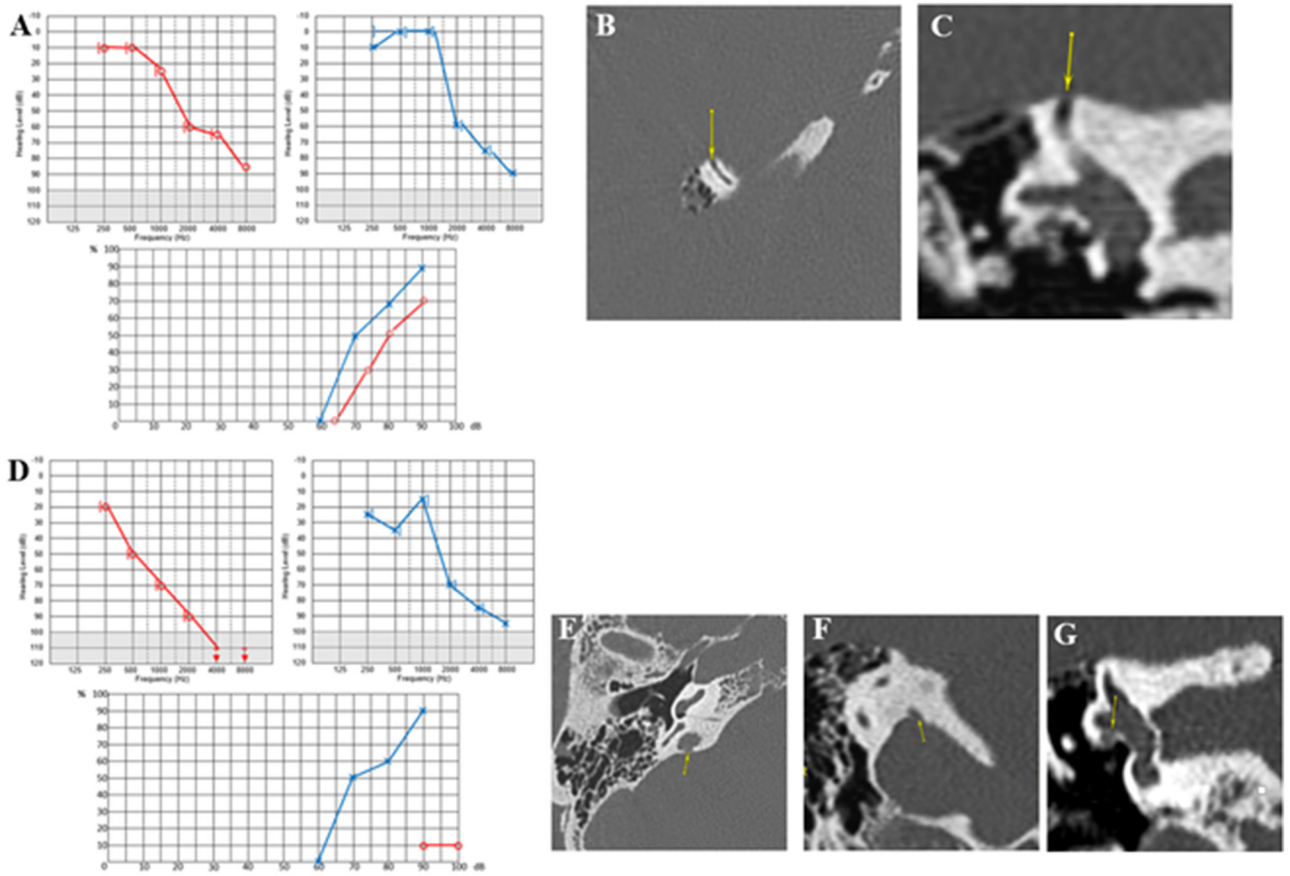

FIGURE 4
(A) Tonal and vocal audiometry showing a bilateral sensorineural hearing loss. **(B, C)** Right SSCD in axial **(B)** and coronal plane **(C)**. **(D)** Post-operative audiometry showing a major deterioration of intelligibility. **(E, F)** Right OCD involving vestibular aqueduct and intern jugular vein in axial **(E)** and coronal plane **(F)**. **(G)** Right OCD between LSC and FN (yellow arrows in **B, C, E–G** indicating various OCD).

C). Due to the severity of vertigo (DHI quoted 62/100), a right SSCD occlusion was performed using the transmastoid approach. On day 2, the patient complained of hearing loss and a stronger and more persistent resonance on the operated side than previously. Treatment with oral corticosteroids was prescribed for 10 days to protect and improve the cochlear function. Audiometry showed hearing loss on all frequencies in the RE, with a more pronounced low-frequency air-bone gap than before the surgery (Figure 5D). The vestibular assessment showed a right irritative horizontal nystagmus, inhibited by ocular fixation and unresponsive to applying 100 Hz bony vibrations. VHIT showed a normal gain for all semicircular canals. 3 weeks later, dizziness decreased during physical exertion, nose blowing, or coughing. The irritative nystagmus described earlier had disappeared. However, right hearing loss and autophony persisted. Although the PTA slightly improved compared to day 2, pulsatile tinnitus increased, and oVEMPs completely disappeared. The DHI score showed significant improvement with a score of 28/100 (compared to 60/100 before the surgery), but the THI score showed worsening of the tinnitus with a score of 50/100 (compared to 28/100 before the surgery). HRCT image reexamination noted a CFD I that was undiagnosed before surgery (Type III) (Figures 5E–G). However, MRI confirmed a good obliteration of the right SSC (Figure 5H).

At 6 months, the patient no longer had incapacitating vertigo but continued to experience very brief, non-positional vertigo intermittently. Aural fullness and autophony were less intense but still present. Audiometry showed a slight decrease in the hearing threshold with preserved intelligibility. The vestibular assessment showed no response to cVEMPs on the RE and a decreased VOR gain in the right SSC at VHIT.

Case report 4

A 32-year-old patient was referred to our department by a fellow neurologist for left pulsatile tinnitus and positional vertigo. An MRI raised the suspicion of cross-compression syndrome of the VIII cranial nerve by a vascular loop. The patient, presenting with a migraine history, also complained of persistent spontaneous dizziness or short vertigo from physical exertion. She was prescribed an anti-migraine treatment with non-steroid anti-inflammatory drugs, which, according to her, were only taken for intense headache crises. She also reported eye movement perception in the LE. Audiometry confirmed a left low-frequency conductive hearing loss (Figure 6A). Auditory brainstem responses were found to be normal. Caloric and rotatory tests were normal as well. cVEMPs showed very large responses, with a detection threshold identified at 60 dB nHL on the LE. The HRCT confirmed

10.3389/fneur.2023.1209567

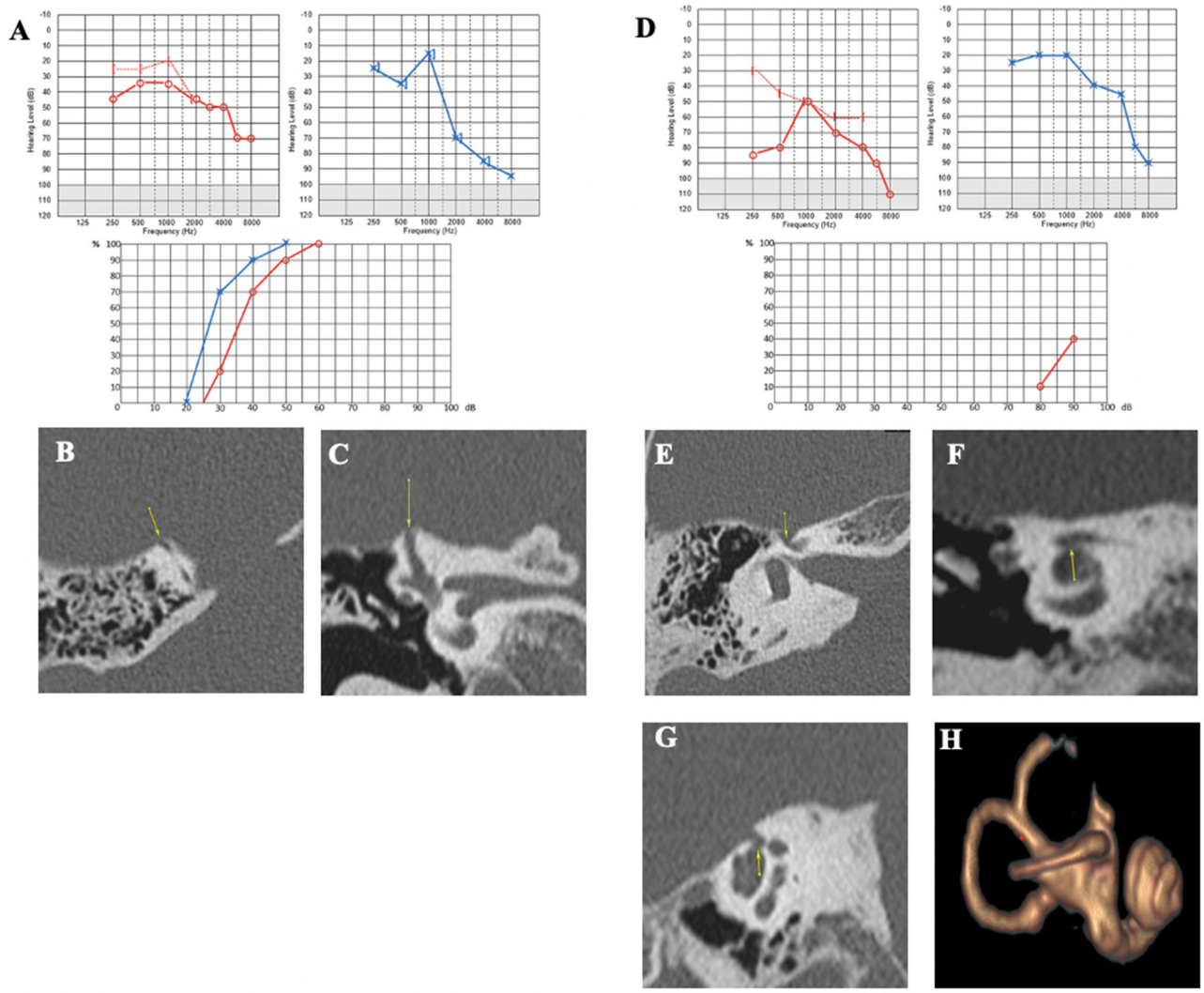

FIGURE 5
(A) Tonal and vocal audiometry showing a bilateral sensorineural hearing loss, with conductive component on the right side. **(B, C)** Right SSCD in axial **(B)** and control plane **(C)**. **(D)** Post-operative audiometry. **(E, F)** Right CFD in axial **(E)**, coronal **(F)** and sagittal plane **(G)**. **(H)** Post-operative 3D MRI showing a complete obliteration of SSCC.

a left SSCD (Figures 6B–D). On the RE, a smaller SSCD Type I was identified (Figure 6E) associated with Type II OCD (VA/IJV) (Figures 6F, G); on this side, the patient only complained of intermittent tinnitus. Given the high THI score (over 70/100), a resurfacing surgical technique of the left SSC using a transmastoid approach was decided. On day 1, an intense left horizontal nystagmus was observed. Audiometry showed a lateralized Weber test to the LE with no increased BC threshold. Postoperative HRCT on day 2 revealed air bubbles at the top of the left SSC. Dizziness gradually subsided under symptomatic treatment. For ~3 months, the patient complained of a decrease in intelligibility and fullness in the operated ear. At 4 months, she began to complain of noise reappearance in the operated ear, along with a disturbing perception of eyeball movements. Pulsatile tinnitus and vertigo sensitive to stress, fatigue, or loud noises reappeared. Audiometry revealed a deterioration of the thresholds in AC in both ears (Figure 6H). A postoperative vestibular assessment revealed normalization of the cVEMPs, thereby presenting in favor of a technically successful surgery. However, the DHI score was rated at 76/100 and the THI at 82/100, both higher scores than before the surgery. Reexamination of the HRCT showed an additional near-dehiscence Type III (between the right LSC and the tympanic segment of the FN in the LE) (Figures 6I, J). A similar localization was also identified on the RE (Figures 6K, L). The MRI showed a well-performed surgical capping technique without any complications (Figure 6M). Once again, the patient was lost to follow-up.

Case report 5

A 58-year-old patient was referred to our department for autophony and resonance in the LE (heartbeat, footsteps, and eyeball and eyelid movement perception) and left pulsatile tinnitus. Audio-vestibular assessment revealed left conductive hearing loss (Figure 7A) and cVEMP with a very large amplitude and abnormally low bilateral thresholds (70 dB nHL on the RE and

10.3389/fneur.2023.1209567

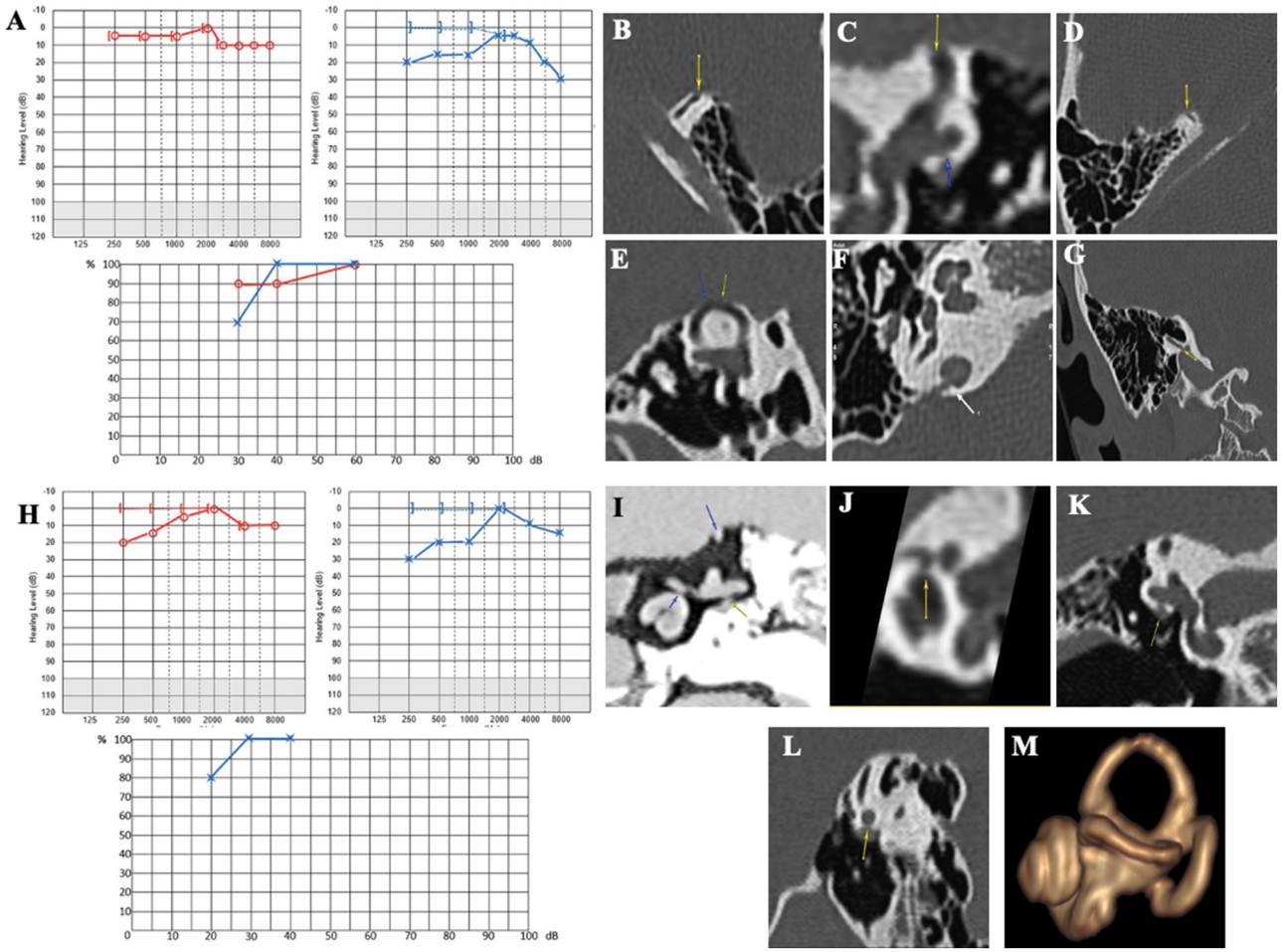

FIGURE 6
(A) Tonal and vocal audiometry showing a mild conductive hearing loss on the left side. **(B, C)** Left SDC in axial **(B)** and coronal plane **(C)**. **(D, E)** Right SDC in axial **(D)** Pöschl plane **(E)**. **(F, G)** Dehiscence between right IVJ and vestibular aqueduct in axial **(F)** and coronal plane **(G)**. **(H)** Post-operative tonal and vocal audiometry. **(I)** Coronal plane in negative contrast showing near-cochleofacial dehiscence, near-dehiscence between LSC and FN II and SSCD. **(J)** Near-cochleofacial dehiscence. **(K, L)** Near-cochleofacial between the right LSC and FN II in coronal **(K)** and sagittal plane **(L)**. **(M)** Post-operative 3D MRI showing an effective capping of SCC.

60 dB nHL on the LE). The rest of the vestibular assessment was normal. CT scan showed a bilateral SSCD (Figures 7B–E), with an additional OCD between the VA and the IJV on the right non-symptomatic ear (Figures 7F, G). An SSCD plugging was performed by the middle fossa approach.

At 4 months, the pulsatile tinnitus had disappeared. Conductive hearing loss, autophony, and resonance symptoms in the LE improved. The cVEMPs normalized on the LE. The patient reported improvement in both autophony and pulsatile tinnitus but complained of a new but less severe tinnitus, probably due to high-frequency hearing loss (Figure 7H). MRI showed that the SSCD had been properly plugged (Figure 7I).

Case report 6

In this 49-year-old patient, symptoms were triggered following acoustic trauma by exposure to a loudspeaker. Despite a 7-day course of steroid therapy, he continued to complain of bilateral pulsatile tinnitus, more pronounced on the LE, where a painful fullness and autophony were felt even with mild or medium intense sounds. There was no vertigo, just a slight but almost permanent dizziness. The clinical examination was normal. Audiometry initially revealed bilateral low- and medium-frequency conductive hearing loss (greater on the left side), with a minimally bilateral 4 kHz notch. A tinnitus assessment could not accurately indicate the characteristics of bilateral tinnitus (Figure 8A). HRCT showed SSCD (Type I OCD) on the LE (Figures 8B–D) and a very thin bony covering on the RE, suggesting a "near" SSCD. THI was rated at 90/100. After 3 months of follow-up, audiometric tests showed that the conductive hearing loss had disappeared on the RE and diminished on the LE. Cervical and ocular VEMPs were consistent with an SSCD on the LE. The patient still did not complain of vestibular symptoms, and the chronic dizziness gradually disappeared. HRCT images showed a second OCD (a CFD variant) (Figures 8E, F) on the LE. We also noticed that the SSCD on the LE was located on the anterior slope (arrows) and not "typically" placed on the convexity of the bony SSC (Figure 8G). Considering the experience from similar Case 3, the

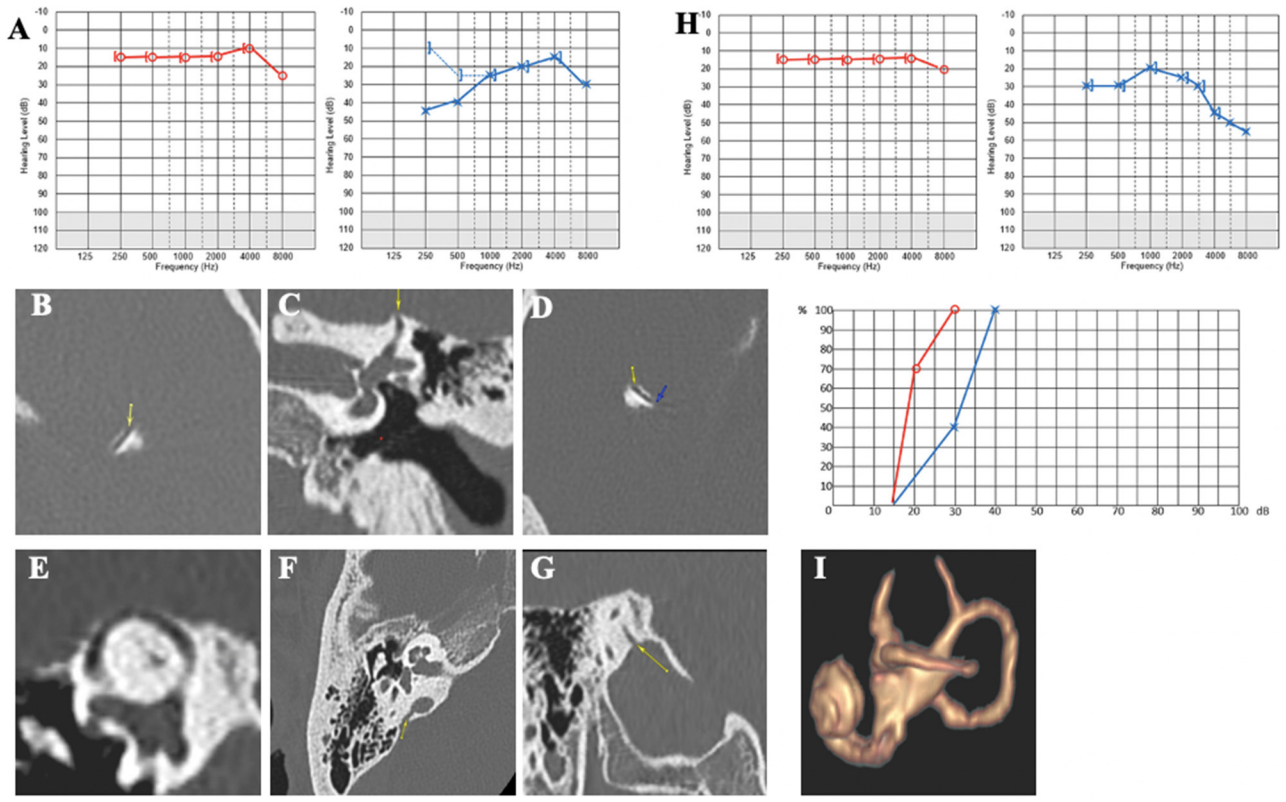

FIGURE 7
(A) Tonal and vocal audiometry showing a mild conductive hearing loss on the left side. **(B, C)** left SDC in axial **(B)** and coronal plane **(C)**. **(D, E)** Right SDC in axial **(D)** Pöschl plane **(E)**. **(F, G)** Dehiscence between right IVJ and vestibular aqueduct in axial **(F)** and coronal plane **(G)**. **(H)** Post-operative tonal and vocal audiometry. **(I)** Post-operative 3D MRI showing an effective plugging of SCC.

patient followed our advice and did not undergo surgery, tinnitus being the dominant symptom in his case. A hearing aid was fitted to the left ear combined with an ipsilateral white noise tinnitus masking. This resulted in progressive improvement in symptoms. After 6 months, the THI fell to 60/100, and the patient no longer used anxiolytics or other medication to fall asleep.

Discussion

Retrospective review

After analysis of various medical records, since THI or DHI questionnaires were not available, we retrospectively rated the severity of auditory and/or vestibular symptoms with a simplified assessment tool (Table 1). When combining the higher incidence of multiple localizations and the higher audio-vestibular discomfort score in multiple OCDs, it appears that the higher the score (in a severely impaired patient), the greater the likelihood of finding multiple dehiscences. Further studies targeting patients operated on with a poor or disappointing postoperative result could support these observations.

The reason behind such a difference between the number of diagnosed SSCDs and the total (much larger) number of OCDs observed after systematic radiological reexamination is that many otologists and radiologists seem to mainly focus on the most common variants of otic dehiscence (e.g., SSCD or PSCD) and ignore or be unaware of the existence of other lesser-known variants. Therefore, radiologists trained in otology should be informed and aware of possible multiple locations, but they should also be more familiar with the recently described variants of OCD. Likewise, otologic surgeons should consider the possibility of multiple OCDs before proposing a surgical approach for what initially looks like a typical SSCD. For multiple dehiscences that can be accommodated, such as a combined SSCD and PSCD, concomitant surgical repair may be considered. For many of the lesser-known OCDs, such as CFD and horizontal semicircular canal-FN dehiscence, there is no direct surgical repair of the dehiscence at present. However, the identification of these lesions preoperatively notifies the surgeon of the possible use of window reinforcement during surgery (24).

In a general way, all ENTs should be informed that OCD is not as rare as it was believed a few years ago. The John Hopkins histological study carried out on more than 1,000 temporal bones shows that 1.5% of specimens have extreme bony thinning (25). Furthermore, SSCD and CFD, defined together with "near" variants, accounted for 6.5% of the general population (26). It could be added that many of the SSCD cases are probably not diagnosed because the ENT, in the absence of conductive hearing loss, as one can observe in some TMWA, only obtains an MRI for the patient who complains of autophony and dizziness, but not an HRCT. Thus, the diagnosis can be missed, especially in cases of

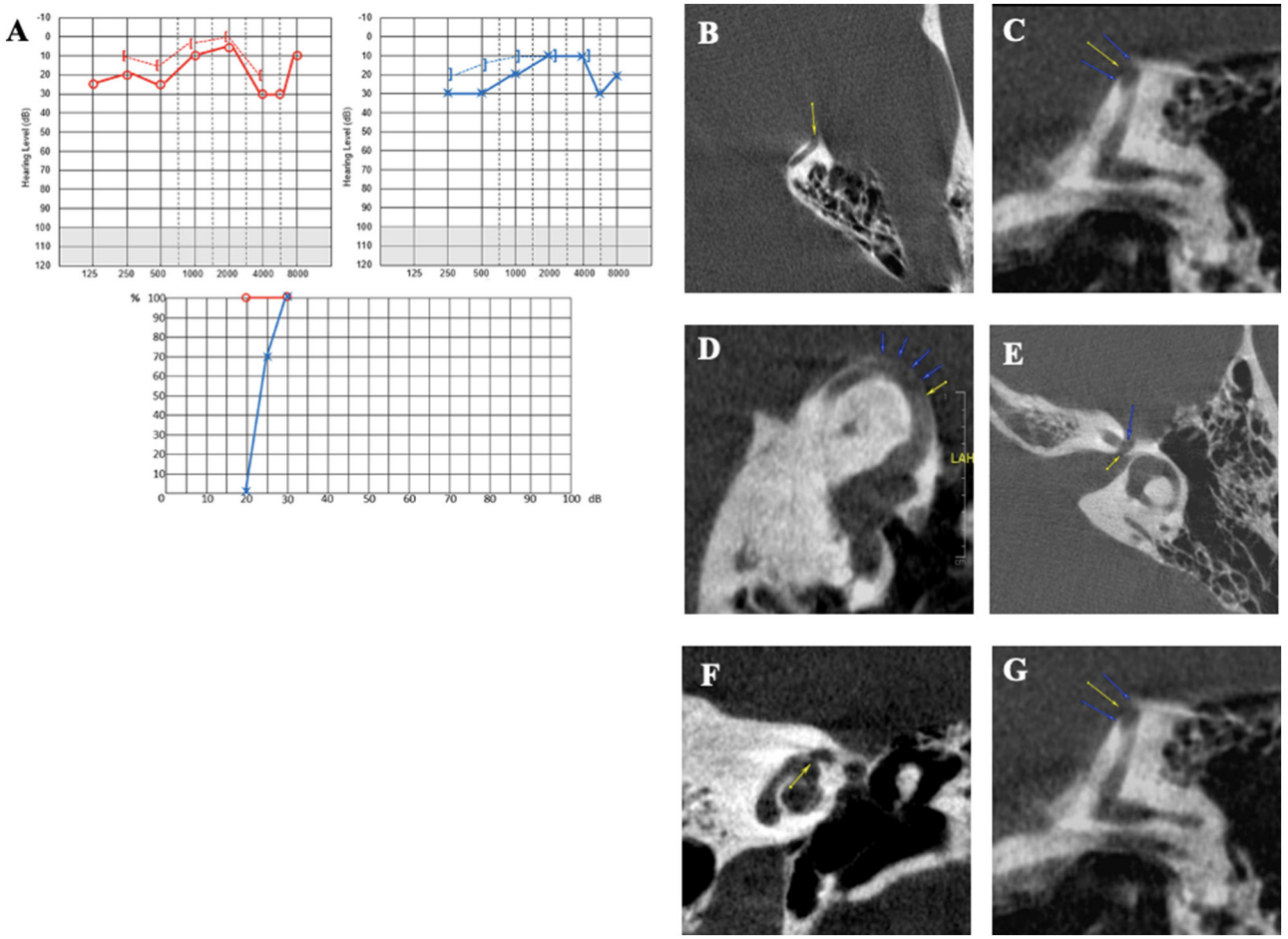

FIGURE 8
(A) Tonal and vocal audiometry showing a slight bilateral conductive hearing loss. **(B–D)** Left SSCD in axial **(B)**, coronal **(C)** and Pöschl plane **(D)**. **(E, F)** Left cochleofacial dehiscence in axial **(E)**, and coronal plane **(F)**. **(G)** Left SSCD in a control plane.

lesser-known OCD variants. That is to say that a normal audiogram is not sensitive to TMWS, and consequently, it is not a good enough screening test to exclude TMWS. Another possible cause of underdiagnosis or misdiagnosis of OCDs is that many audiologist technicians or even ENT specialists do not insist enough on looking for the real auditory thresholds in bone conduction (BC). This is even more true when the air conduction and the tympanogram with the study of middle ear reflexes are normal. Thus, it is possible to pass along and not detect a supra-normal auditory threshold in bone conduction, which can indicate a TMW lesion.

Case series

We presented a series of six patients with symptomatic SSCD. Five of them underwent surgery, while in one patient we advised against the originally planned surgery. In four of the five operated patients, the postoperative results were considered unfavorable or disappointing. After reviewing the radiological and clinical files, we can speculate that the treatment failure in these patients may be due not only to surgical technique errors, as can be discussed in Case 1, but also possibly and very likely to the simultaneous presence of other OCDs in the treated ear that had not been diagnosed before surgery.

This is also the reason why the sixth patient, initially scheduled for a plugging operation, did not undergo surgery because the reexamination of the HRCT images revealed the presence of an ipsilateral CFD in addition to the previously diagnosed SSCD.

This finding led us to analyze additional records, thus completing the initial objective of this article. Therefore, all radiological records of patients diagnosed with SSCD in our center during the last 5 years were reviewed. The results, including all types of otic dehiscence known at the time of submission, were reported in the order of their incidence and according to their type, following the classification of Reynard et al. (6).

In patients 1 and 2, no typical conductive hearing loss was found (Figures 2A, 3A), as may be expected in symptomatic SSCD. Patient 1 presented a profound postsurgical neurosensorial hearing loss, despite what would appear to be a well-performed left SSC plugging on the postoperative MRI (Figure 3D). However, fullness and vertigo triggered by loud sounds reappeared in the operated LE. After analysis of the postoperative radiological images, the existence of a second dehiscence (or near dehiscence) between the left LSC and the FN in its second segment (LSC/FN) was

suspected (Figure 3C – blue arrow and G – yellow arrow). A third OCD was also observed on the same LE, which was probably iatrogenic and mainly contributed to the symptom's reappearance (Figures 3E, F). Although postoperative pure-tone hearing loss did not occur in patient 2, speech audiometry dramatically decreased after SSCD plugging (Figure 4D). As in Case 1, when the radiological records were reexamined after the surgery, an additional OCD was diagnosed on the operated ear (Figures 4E–G). A possible explanation of the postsurgical hearing loss observed in these two cases could be that the SSCD plugging reduced the volume of the endolymphatic space, generating a hyper-pressure in the membranous cochlear canal and, thus, a significant auditory transduction disruption. This assumption is in accordance with the results of experimental animal models of hydrops (27, 28). Moreover, the apparition of hyper-pressure in the endolymphatic system that seemed to manifest itself immediately after plugging is also supported by the two following cases in which signs of vestibular hydrops were evident.

Patient 3 presented with postoperative irritative nystagmus, significant hearing loss, and other clinical signs suggestive of induced endolymphatic hydrops (EH) persisting for several weeks. An ipsilateral CFD II (Figures 5E–G) was diagnosed after surgery, while a 3D labyrinthine MRI confirmed a well-performed SSCD plugging (Figure 5H).

Patient 4 presented the same clinical signs of secondary hydrops on day 1 after surgery. However, the technique, in this case, was a capping type (Figure 5M), and the Type III additional OCD (LSC/FN) was rather "near" dehiscence (Figures 5K, L). Therefore, it is difficult in this case to attribute the appearance of clinical signs of hydrops to a reduction in the volume of the endolymphatic system that would be minimal with this surgical technique. However, the phenomenon could be partially explained by the local pressure change at the LSC/FN dehiscence level once the impedance at the SSCD interface has been normalized by confinement. On the other hand, the gradual onset of vertigo after surgery could also be due to right-sided OCDs that could have started to manifest themselves clinically. Indeed, the follow-up audiometry showed a right-sided conductive hearing loss, initially absent.

Patient 5 only complained of a transient increase in tinnitus on the LE after surgery. This can also be explained by the appearance of hydrops induced by the SSCD plugging, which was well performed according to the control labyrinthine MRI (Figure 7I). However, in this case, the evolution was good after a few weeks, with a significant improvement in symptoms. In patient 6, who also presented with clinical signs of SSCD, the discovery of additional ipsilateral dehiscence justified the cancellation of the proposed surgical intervention since the main complaints were only tinnitus and ear fullness. In this case, plugging or resurfacing would probably have led, as in Cases 1, 2, 3, and 4, to the exacerbation of symptoms through the expected secondary hydrops. Furthermore, the dehiscence occurred very anteriorly. Therefore, any temporal lobe descent into the membranous SSC would be limited by the bony overhang of the semicircular canal (Figure 8C). This fact, combined with a thicker folded expansion of the dura mater at the interface of the SSC window, would limit its lack of resistance, thus explaining the lack of impairing vestibular symptoms. 3D labyrinthine MRI performed to exclude SSCD autoplugging or other membranous labyrinthine deformations was normal. This patient finally benefited from a medical treatment conducted by a psychologist by combining a tinnitus masker and tinnitus retraining therapy, which has led to the improvement of the patient's symptoms. What also contributed to our recommendations against surgery was that only a very small and transient conductive hearing loss was observed with the PTA, while the cervical and ocular cVEMP thresholds were very low, as in the case of the first two patients in this series. In a recent study, Noij et al. (29) pointed out that the coherence between the bone and air conduction gap at PTA and the cVEMSs threshold is a very useful tool for confirming the diagnosis of symptomatic SSCD. This was verified in patients 1, 2, and 6, in whom the bone gap was initially insignificant (6) or completely absent (as in Cases 1 and 2), as "the indicator of a symptomatic SSCD" was negative. The rest of the audiometric or vestibular examinations (VHIT and VNG) obtained before surgery seem to be of no use to indicate the presence of multiple OCDs in the same ear. These observations suggest that in the absence of the Tullio phenomenon or equivalent vestibular signs or symptoms, together with the absence of conductive hearing loss, but with cVEMPs or oVEMPs indicating a TMWA, the otologist should consider that another variant of OCD on the same ear may be present, apart from an easily noticeable SSCD. On the other hand, the skull vibration test, easy and quick to perform in daily practice under the mask of videonystagmoscopy, can indicate the appearance of a characteristic nystagmus as previously shown (30), thus drawing the attention of the examiner that an OCD may be present. This can be more useful as the rest of the vestibular evaluation through VNG and VHIT returns to normal quite frequently.

Regarding the surgical approach, our team generally preferred the transmastoid route because we consider it more convenient for moderate or small-sized dehiscence. Instead, in Cases 2 and 5, a middle fossa approach (Additional Material III) was used because the SSCD dimensions were larger than in the other three cases and it was considered that a wider approach would ensure better-quality plugging and/or capping.

A required systematic radiological protocol

In case of clinical and audiological signs or symptoms suggestive of TMWA, the HRCT radiological protocol should first include a careful search for all known variants of OCD (Types 1 and 2). Special attention should be paid to peri-petrous variants of OCD (Type 3) because their size is smaller and, in case of association with a prominent SSCD (or another better-known variant), there is a risk of overlooking or failing to diagnose dual or multiple ipsilateral OCDs. Careful investigation of these variants is also very important, as their incidence appears to be higher than that of other variants (39.07% in this study). These might be harder to find and be considered "symptomatic" because their size is much smaller than the "classic" variants. The grayscale inversion function is especially valuable when small OCD variants (or Type III peri-petrous) are suspected. As for "classic" OCDs, it can be hypothesized that if

a special HRCT technique is not applied with slices smaller than 0.6 mm or even 0.5 mm, there is a risk of underdiagnosis of small dehiscences, or, in the opposite sense, overestimating their clinical importance. Presently, in our knowledge of TMW pathology, it is not possible to understand with the currently accepted mechanism models how these small subvariants of OCDs can disturb the cochlear micromechanics, a fact that is frequently observed in these cases (4, 5, 23, 24).

Although there are currently standard criteria in the literature to differentiate a "near" SSCD from a "real" one (31, 32), this is not yet the case for newer and "smaller" variants of OCD. However, we do know that a near SSCD can present clinical and audio-vestibular features of TMWS (32) and that performing surgery in some of these cases could improve them (33). It is also worth noting that positive radiological diagnosis can be negatively impacted by HRCT techniques that often use a 0.6 mm slide, which may be too large for visualizing these smaller variants of OCD. The use of procedures such as cone-beam CT (34) or photon-counting CT, which should improve the contrast-to-noise ratio and spatial resolution (35), would probably be an option in future for better recognition of these variants.

Therapeutic challenge

Although we currently have guidelines for the diagnosis of SSCD (8), there are no published studies on the criteria for selecting a candidate for surgical intervention (36). Thus, in the case of very symptomatic and disabled patients in everyday life, the expected benefit/risk ratio must be discussed and very well-explained to avoid postoperative disappointments. Although the strength of this study is limited by the analysis of records from a single center and the fact that the number of patients reported is not large enough to support a comparative statistical study, we think that the essential emerging message is still clear. Surgeons should be aware that a cause of surgical failure in a patient with SSCD may be the unnoticed presence of another OCD, even of minimal or "atypical" size. Considering the consistently poor postoperative results in this series of patients with multiple OCDs who underwent technically successful surgeries, it is justified to question whether the currently accepted third window techniques and mechanisms for (single) SSCD (36, 37) also apply to multiple OCDs. It is reasonable to believe the opposite since in the case of several abnormal areas of low impedance at the level of the otic capsule, the dispersion of acoustic energy would be logically greater and more diffuse than in the case of a "single" TMW. This fact could have negative consequences for the normal transmission of acoustic energy, or "traveling waves" (38, 39), to the basilar membrane of the cochlear canal. Because in this case the rigidity of the endolymphatic system is presumably altered, local acoustic phenomena — as for example standing waves or the phenomena of abnormal local resonance (40) — may appear with negative consequences on auditory transduction process. These could therefore generate not only the "classic conductive hearing loss" involving the inner ear but also a potential decrease in intelligibility or auditory distortions, as we have observed in some of our patients with multiple OCDs (Supplementary material II). From a practical point of view, it means that in very symptomatic and disabled patients, the therapeutic decision to perform an SSC plugging should be taken only after the exclusion of another associated OCD. Thus, in the case of ignored multiple OCDs, performing surgery for an SSCD in a patient without clear and specific vestibular symptoms evocative of TMWS (e.g., Tullio phenomenon or pressure sensitivity in the EAC) could worsen the postoperative clinical status of an undiagnosed OCD. This seems obvious because the volume of the endolymphatic system after a plugging procedure is diminished by the surgical procedure, favoring the appearance or persistence of concomitant EH (41). Regarding the EH associated with OCD, it should be added that some authors have reported this entanglement between two apparently distinct pathologies (41–43). Future studies should verify whether the simultaneous presence of a an EH (confirmed by electrocochleography and dedicated imaging), it does not constitute a risk factor for the postoperative results in case of SSCD plugging-type surgery. This appears as obvious, since the physical stress generated by the decrease of the volume of the endolymphatic space after the respective surgical intervention, would logically lead to a additional increase in pressure in the endolymphatic space. In light of clinical symptoms and initial and postoperative vestibular assessments, it is possible that we are talking about just such a subject in the first two case reports of the present series.

To solve all these theoretical and therapeutic dilemmas, future studies should be carried out not only on numerical or animal models but also on physical models of semicircular canals that would allow the simulation of this complex pathology. However, in our opinion, it should be expected in the case of multiple ipsilateral OCDs that the treatment be addressed simultaneously for all OCDs by micro-invasive methods—or at least for those more surgically accessible. An essential role would be the precise identification of the bone defect location as well as its geometry and dimensions. Three-dimensional bone printers would therefore play an important role in future (44). While waiting for a more adapted therapeutic solution, a more aggressive medical treatment, including anti-hydrops drugs, can be tried in very symptomatic patients (avoiding the trigger factors, prescribing diuretics, and/or anti-migraine drugs) (45).

Limitations of the study

The authors chose to limit the radiological study only to patients with "spontaneous" OCDs. Therefore, patients who underwent previous otological surgery and those suspected of having ear malformations in relation to neoplastic, infectious, or degenerative pathological conditions were excluded. Another limitation is the fact that the total number of surgically treated patients in our center did not allow for a comparison between the postoperative results of the group of patients reported here whose multiple OCDs were undiagnosed before the surgery and the postoperative results of a comparable group of patients who underwent surgery for a certain SSCD diagnosis. The cause is that in our center, the number of SSCD surgeries is still small. Obviously, this should ideally be carried out multicentrically in the future. The purpose of this study is to

sensitize fellow neurotologists since multiple OCDs associated with different types of variants are not as rare as one might think. We also must add that the voxels were anisotropic for the HRCT technique, so there may be limitations due to partial volume averaging that could overemphasize the presence of anatomic dehiscence.

Conclusion

The otologist should rule out any suspicion of multiple localizations of abnormal mobile windows in the same ear, especially when the clinical presentations appear "atypical" before performing plugging-type surgery. Awareness of the existence of new OCD variants must be systematically raised among all ENT specialists, especially radiologists, but also among audiology professionals. They also need to be aware of possible multiple localizations of OCDs in cases of "atypical" clinical presentations. Future studies and modeling should allow the development of therapeutic strategies to be adopted in cases of multiple OCDs. The acoustic energy shunt known in the classic pathomechanism model of TMWA applied in SSCD could be different and, therefore, not applicable in the case of multiple OCDs. In this case, the dispersion or depredation of acoustic energy is more likely to be diffuse.

Author contributions

EI and PR have equal contributions in writing the manuscript. EI literature research and multiple OCDs localizations concept. GG and HT-V supervison and analysis. AL-B and EI imaging review. MD and RH analysis and interpretation. GG and RH critical review. All authors contributed to the article and approved the submitted version.

Acknowledgments

The authors thank Ruxandra Ionescu for editing the article and Eric Truy and Stéphane Tringali for the data supply.

Conflict of interest

The authors declare that the research was conducted in the absence of any commercial or financial relationships that could be construed as a potential conflict of interest.

Publisher's note

All claims expressed in this article are solely those of the authors and do not necessarily represent those of their affiliated organizations, or those of the publisher, the editors and the reviewers. Any product that may be evaluated in this article, or claim that may be made by its manufacturer, is not guaranteed or endorsed by the publisher.

Supplementary material

The Supplementary Material for this article can be found online at: https://www.frontiersin.org/articles/10.3389/fneur.2023.1209567/full#supplementary-material

References

1. Minor LB, Solomon D, Zinreich JS, Zee DS. Sound- and/or pressure-induced vertigo due to bone dehiscence of the superior semicircular canal. *Arch Otolaryngol-Head Neck Surg.* (1998) 124:249–58. doi: 10.1001/archotol.124.3.249

2. Ho ML, Moonis G, Halpin CF, Curtin HD. Spectrum of third window abnormalities: semicircular canal dehiscence and beyond. *Am J Neuroradiol.* (2017) 38:2–9. doi: 10.3174/ajnr.A4922

3. Merchant SN, Rosowski JJ. Conductive hearing loss caused by third-window lesions of the inner ear. *Otol Neurotol.* (2008) 29:282–9. doi: 10.1097/MAO.0b013e318161ab24

4. Wackym PA, Balaban CD, Mowery TM. History and Overview of Third Mobile Window Syndrome. In: Gianoli, GJ, Thomson, P (eds) *Third Mobile Window Syndrome of the Inner Ear.* Springer, Cham. (2023). doi: 10.1007/978-3-031-16586-3_1

5. Wackym PA, Wood SJ, Siker DA, et al. Otic capsule dehiscence syndrome: superior semicircular canal dehiscence syndrome with no radiographically visible dehiscence. *Ear Nose Throat J.* (2015) 94:E8–EE24. doi: 10.1177/014556131509400802

6. Reynard P, Idriss S, Ltaief-Boudrigua A, Bertholon P, Pirvan A, Truy E, et al. Proposal for a unitary anatomo-clinical and radiological classification of third mobile window abnormalities. *Front Neurol.* (2022) 12:792545. doi: 10.3389/fneur.2021.792545

7. Ionescu E, Gianoli GJ, Wackym PA. Classification of Third Mobile Window Anomalies. In: Gianoli, G.J., Thomson, P. (eds) *Third Mobile Window Syndrome of the Inner Ear*. Springer, Cham. (2022) doi: 10.1007/978-3-031-16586-3_4

8. Ward BK, van de Berg R, van Rompaey V, Bisdorff A, Hullar TE, Welgampola MS, et al. Superior semicircular canal dehiscence syndrome: diagnostic criteria consensus document of the committee for the classification of vestibular disorders of the Bárány Society. *J Vestib Res.* (2021) 31:131–41. doi: 10.3233/VES-200004

9. Thénint MA, Barbier C, Hitier M, Patron V, Saleme S, Courthéoux P. Endovascular treatment of symptomatic vestibular aqueduct dehiscence as a result of jugular bulb abnormalities. *J Vasc Interv Radiol.* (2014) 25:1816–20. doi: 10.1016/j.jvir.2014.07.013

10. Ionescu EC, Coudert A, Reynard P, Truy E, Thai-Van H, Ltaief-Boudrigua A, et al. Stenting the superior petrosal sinus in a patient with symptomatic superior semicircular canal dehiscence. *Front Neurol.* (2018) 9:689. doi: 10.3389/fneur.2018.00689

11. Aw GE, Parker GD, Halmagyi GM, Saxby AJ. Pulsatile tinnitus in superior semicircular canal dehiscence cured by endovascular coil occlusion of the superior petrosal sinus. *Otol Neurotol.* (2021) 42:e629–630. doi: 10.1097/MAO.0000000000003012

12. Reynard P, Ionescu E, Hitier M, Barbier C, Turjman F. Endovascular therapy for third mobile window syndrome. In: Gianoli, G.J., Thomson, P. (eds) *Third Mobile Window Syndrome of the Inner Ear*. Springer, Cham. (2022) doi: 10.1007/978-3-031-16586-3_16

13. Motasaddi Zarandy M, Kouhi A, Emami H, Amirzargar B, Kazemi MA. Prevalence of otic capsule dehiscence in temporal bone computed tomography scan. *Eur Arch Otorhinolaryngol.* (2023) 280:125–30. doi: 10.1007/s00405-022-07464-x

14. Zhou G, Poe DS. Multiple semicircular canals with dehiscence. *Otol Neurotol.* (2009) 30:241–2. doi: 10.1097/MAO.0b013e3181662cd4

15. Manzari L, Modugno GC. Bilateral dehiscence of both superior and posterior semicircular canals. *Otol Neurotol.* (2009) 30:423–5. doi: 10.1097/MAO.0b013e3181684048

16. Manzari L. Multiple dehiscences of bony labyrinthine capsule. A rare case report and review of the literature. *Acta Otorhinolaryngol Ital.* (2010) 30:317–20.

17. Meehan T, Nogueira C, Rajenderkumar D, Shah J, Stephens D, Dyer K. Dehiscence of the posterior and superior semicircular canal presenting in pregnancy. *B-ENT.* (2013) 9:165–8.

18. Manzari L, Scagnelli P. Large bilateral internal auditory meatus associated with bilateral superior semicircular canal dehiscence. *Ear, Nose Throat J.* (2013) 92:25–33. doi: 10.1177/014556131309200109

19. Dang PT, Kennedy TA, Gubbels SP. Simultaneous, unilateral plugging of superior and posterior semicircular canal dehiscences to treat debilitating hyperacusis. *J Laryngol Otol.* (2014) 128:174–8. doi: 10.1017/S0022215113003605

20. Kundaragi NG, Mudali S, Karpagam B, Priya R. Intracranially protruded bilateral posterior and superior SCCs with multiple dehiscences in a patient with positional vertigo: CT and MR imaging findings and review of literature. *Indian J Radiol Imaging.* (2014) 24:406–9. doi: 10.4103/0971-3026.143904

21. Bijou W, El Krimi Z, Abdulhakeem B, Oukessou Y, Mahtar M. Asymptomatic multiple semicircular canal dehiscence: a rare entity. *Oxf Med Case Reports.* (2022) 26:omab125. doi: 10.1093/omcr/omab125

22. Whyte J, Cisneros AI, Garcia-Barrios A, Fraile J, Whyte A, Crovetto R, et al. Association between superior semicircular canal dehiscence and other dehiscences in temporal bone. *Folia Morphol.* (2020) 79:823–28. doi: 10.5603/FM.a2019.0138

23. Gianoli G, Soileau J, Shore B. Description of a new labyrinthine dehiscence: horizontal semicircular canal dehiscence at the tympanic segment of the facial nerve. *Front Neurol.* (2022) 13:879149. doi: 10.3389/fneur.2022.879149

24. Wackym PA, Balaban CD, Zhang P, Siker DA, Hundal JS. Third window syndrome: surgical management of cochlea-facial nerve dehiscence. *Front Neurol.* (2019) 10:1281. doi: 10.3389/fneur.2019.01281

25. Fang CH, Chung SY, Blake DM, Vazquez A, Li C, Carey JP, et al. Prevalence of cochlear-facial dehiscence in a study of 1,020 temporal bone specimens. *Otol Neurotol.* (2016) 37:967–72. doi: 10.1097/MAO.0000000000001057

26. Carey JP, Minor LB, Nager GT. Dehiscence or thinning of bone overlying the superior semicircular canal in a temporal bone survey. *Arch Otolaryngol Head Neck Surg.* (2000) 126:137–47. doi: 10.1001/archotol.126.2.137

27. Ding CR, Xu XD, Wang XW, Jia XH, Cheng X, Liu X, et al. Effect of endolymphatic hydrops on sound transmission in live guinea pigs measured with a laser doppler vibrometer. *Neural Plast.* (2016) 2016:8648297. doi: 10.1155/2016/8648297

28. Wang SQ Li CL, Xu JQ, Chen LL, Xie YZ Dai PD, Ren LJ, Yao WJ, et al. The effect of endolymphatic hydrops and mannitol dehydration treatment on guinea pigs. *Front Cell Neurosci.* (2022) 16:836093. doi: 10.3389/fncel.2022.836093

29. Noij KS, Duarte MJ, Wong K, Cheng YS, Masud S, Herrmann BS, et al. Toward optimizing cervical vestibular evoked myogenic potentials (cVEMP): combining air-bone gap and cVEMP thresholds to improve diagnosis of superior canal dehiscence. *Otol Neurotol.* (2018) 39:212–20. doi: 10.1097/MAO.0000000000001655

30. Aw ST, Aw GE, Todd MJ, Bradshaw AP, Halmagyi GM. Three-dimensional vibration-induced vestibulo-ocular reflex identifies vertical semicircular canal dehiscence. *J Assoc Res Otolaryngol.* (2011) 12:549–58. doi: 10.1007/s10162-011-0274-3

31. Baxter M, McCorkle C, Trevino Guajardo C, Zuniga MG, Carter AM, Della Santina CC, et al. Clinical and physiologic predictors and post-operative outcomes of near dehiscence syndrome. *Otol Neurotol.* (2019) 40:204–12. doi: 10.1097/MAO.0000000000002077

32. Ward BK, Wenzel A, Ritzl EK, Gutierrez-Hernandez S, Della Santina CC, Minor LB, et al. Near-dehiscence: clinical findings in patients with thin bone over the superior semicircular canal. *Otol Neurotol.* (2013) 34:1421–8. doi: 10.1097/MAO.0b013e318287efe6

33. Hong M, Mozaffari K, Uy B, Kim WJ, Umesh A, Chandla A, et al. Post-operative outcomes of patients with thin bone overlying the superior semicircular canal: a single institution's experience. *World Neurosurg.* (2022) 166:e93–8. doi: 10.1016/j.wneu.2022.06.118

34. Sepúlveda I, Schmidt T, Platín E. Use of cone beam computed tomography in the diagnosis of superior semicircular canal dehiscence. *J Clin Imaging Sci.* (2014) 4:49. doi: 10.4103/2156-7514.141554

35. Willemink MJ, Persson M, Pourmorteza A, Pelc NJ, Fleischmann D. Photon-counting CT: technical principles and clinical prospects. *Radiol.* (2018) 289:293–312. doi: 10.1148/radiol.2018172656

36. Gianoli GJ. Surgery, Complication, Revisions. In: Gianoli, GJ, Thomson, P (eds) *Third Mobile Window Syndrome of the Inner Ear*. Springer Cham. (2022). doi: 10.1007/978-3-031-16586-3_15

37. Grieser BJ, Kleiser L, Obrist D. Identifying mechanisms behind the tullio phenomenon: a computational study based on first principles. *J Assoc Res Otolaryngol.* (2016) 17:103–18. doi: 10.1007/s10162-016-0553-0

38. Iversen MM, Rabbitt RD. Biomechanics of Third Window Syndrome. *Front Neurol.* (2020) 11:891. doi: 10.3389/fneur.2020.00891

39. Ruggero MA. Cochlear delays and traveling waves: comments on 'Experimental look at cochlear mechanics'. *Audiol.* (1994) 33:131–42. doi: 10.3109/00206099409071874

40. De Boer E. Auditory physics. Physical principles in hearing theory III. *Physics Reports.* (1991) 203:125–231. doi: 10.1016/0370-1573(91)90068-W

41. Johanis M, De Jong R, Miao T, Hwang L, Lum M, Kaur T, et al. Concurrent superior semicircular canal dehiscence and endolymphatic hydrops: a novel case series. *Int J Surg Case Rep.* (2021) 78:382–6. doi: 10.1016/j.ijscr.2020.12.074

42. Arts HA, Adams ME, Telian SA, El-Kashlan H, Kileny PR. Reversible electrocochleographic abnormalities in superior canal dehiscence. *Otol Neurotol.* (2009) 30:79–86. doi: 10.1097/MAO.0b013e31818d1b51

43. Sone M, Yoshida T, Morimoto K, Teranishi M, Nakashima T, Naganawa S. Endolymphatic hydrops in superior canal dehiscence and large vestibular aqueduct syndromes. *Laryngoscope.* (2016) 126:1446–50. doi: 10.1002/lary.25747

44. Kozin ED, Remenschneider AK, Cheng S, Nakajima HH, Lee DJ. Three-dimensional printed prosthesis for repair of superior canal dehiscence. *Otolaryngol Head Neck Surg.* (2015) 153:616–9. doi: 10.1177/0194599815592602

45. Gianoli GJ, Soileau JS. Medical therapy. In: Gianoli, GJ, Thomson, P (eds) *Third Mobile Window Syndrome of the Inner Ear*. Springer, Cham. (2022). doi: 10.1007/978-3-031-16586-3_13

frontiers | Frontiers in Neurology

TYPE Case Report
PUBLISHED 28 September 2023
DOI 10.3389/fneur.2023.1281023

OPEN ACCESS

EDITED BY
P. Ashley Wackym,
Rutgers, The State University of New Jersey, United States

REVIEWED BY
Jeremy Hornibrook,
University of Canterbury, New Zealand
Takeshi Tsutsumi,
Tokyo Medical and Dental University, Japan

*CORRESPONDENCE
Toru Seo
✉ tseo@marianna-u.ac.jp

RECEIVED 21 August 2023
ACCEPTED 15 September 2023
PUBLISHED 28 September 2023

CITATION
Seo T, Kemmochi A, Koike Y, Aomi M, Shinohe T and Komori M (2023) Case report: Perilymphatic fistula from a round window microfissure.
Front. Neurol. 14:1281023.
doi: 10.3389/fneur.2023.1281023

Case report: Perilymphatic fistula from a round window microfissure

Toru Seo[1]*, Arata Kemmochi[1], Yosuke Koike[1], Mizuho Aomi[1], Tatsuya Shinohe[1] and Manabu Komori[2]

[1]Department of Otolaryngology, Yokohama Seibu Hospital, St. Marianna University School of Medicine, Yokohama, Japan, [2]Department of Otolaryngology, St. Marianna University School of Medicine, Kawasaki, Japan

A microfissure near the round window niche is an anatomical structure that communicates between middle ear and the ampulla of the posterior semicircular canal. It has been suggested that the microfissure can cause inner ear symptoms; however, the etiology has not yet been confirmed clinically. We report, to our knowledge, the first case of microfissure with complaint of hearing loss and vertigo and improvement in hearing after surgical sealing of the microfissure. A 50-year-old man complained of hearing disturbance, tinnitus with flowing-water sound in the left ear, and a floating sensation upon pushing the left tragus. He had moderate sensorineural hearing loss (43.3dB) in the left ear for 3days. His hearing worsened and he complained of severe vertigo. An exploratory tympanotomy was performed 8days after onset. A microfissure and accumulation of clear fluid in the floor of the round window niche were detected, and leakage point was packed with connective tissue. One month after surgery, his hearing (20.0dB) and disequilibrium had improved. The inner ear symptoms improved after the surgery in this case, suggesting that the microfissure might have caused the symptoms.

KEYWORDS

microfissure, round window niche, hearing loss, exploratory tympanotomy, perilymphatic fistula

Introduction

Perilymphatic fistula (PLF) is a distinctive otological disorder. It involves an abnormal opening between the inner ear and the external surface of the labyrinthine capsule, allowing perilymph to leak and causing specific disruptions in hearing, balance, or both (1–3). There are various causes for PLF. Japanese researchers have categorized it into four main categories (4): Category 1: Linked to trauma, middle and inner ear disease, middle and/or inner ear surgery. Category 2: Linked to barotrauma caused by antecedent events of external origin (such as flying or driving). Category 3: Linked to barotrauma caused by antecedent events of internal origin (such as straining, sneezing, or coughing). Category 4: Has no apparent antecedent event. Among these categories, Category 4, idiopathic, remains a subject of controversy.

The two recognized sites for PLFs from anatomical microfissure are the fissula ante fenestram at the oval window (5), the usual site of origin of otosclerosis, and a fissure in the round window niche (2, 3). A round window fissure communicates with the posterior semicircular canal (6, 7). Kohut et al. (8) claimed a relationship between the fissure and hearing and vestibular symptoms, but Shazly et al. (9) could not find a relationship between the fissure and sudden sensorineural hearing loss in 34 temporal bones (9). To

our knowledge only three cases with hearing disturbances have been surgically as having a round window fissure (10, 11). In these, the fluid leakage was sealed. However, the patients did not have any measurable improvement in their hearing, so a cause and effect was not established. In this paper we present a novel case of a surgically repaired round window fissure resulting in a significant postoperative improvement in hearing.

Case report

A 50-year-old man presented to our clinic with a 3-day history of hearing disturbance and tinnitus with flowing-water sounds in the left ear. The symptoms did not have an instantaneous onset, but were slowly progressive. He did not remember any antecedent event related to barotrauma. He had no history of trauma, ear disease or ear surgery. Additionally, he described a feeling of floating when he pressed the tragus of his left ear. An audiogram showed moderate sensorineural hearing loss (43.3 dB) in the left ear (Figure 1). He did not have any gaze, spontaneous, or positional nystagmus. Caloric testing did not show any unilateral vestibular weakness. We strongly suspected the presence of a PLF and instructed the patient to maintain a head-up position of 30° and intravenous administration of prednisolone of 60 mg per day was initiated. Despite of these treatment, his hearing worsened (Figure 1) and he experienced vertigo with rightward beating nystagmus on lying in the left-side down position. An exploratory tympanotomy was performed on the 8 days after onset. A small fissure with accumulating clear fluid at the floor of the round window niche was observed (Figure 2). Although the fluid was absorbed carefully using a micro cotton ball, it reappeared within minutes. No fluid was observed leaking from any visible area, including near the oval window. The leakage point was packed with small pieces of connective tissue and fixed using fibrin glue. Postoperatively, his hearing (20.0 dB at 1 month after surgery) and disequilibrium improved (Figure 3).

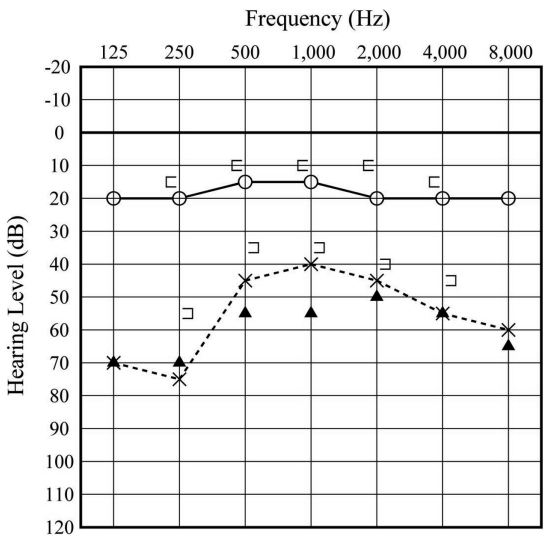

FIGURE 1
Preoperative audiogram. The open circles and x-marks indicate audiograms of the right and left ear, respectively, at first visit. Filled triangles indicate the audiogram of the left ear acquired 4 days later.

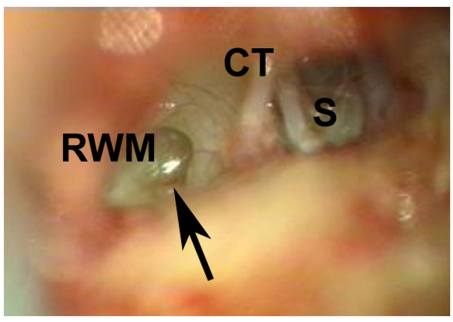

FIGURE 2
Surgical view. A small fissure (arrow) is seen in the floor of the round window niche, and clear fluid is seen leaking. CT, chorda tympani; RWM, round window membrane; S, stapes.

Discussion

In regard to the pathogenesis of the round window fissure, Okano et al. (6) found it in 100% of human temporal bones after the age of 6 years, and regarded it as a normal anatomical structure. After studying 1,000 temporal bones, Moreano et al. (7) suggested the fissure could allow bacteria and ototoxic drops to enter the inner ear, and acknowledged it had been postulated as being a potential route for a perilymph leak. Kohut et.al (8) conducted a single-blind study of 65 temporal bones to explore the connection between microfissure patency and hearing and/or balance symptoms. 86% of symptomatic patients had a patent microfissure, and 94% without symptoms had a closed microfissure. Seo et al.

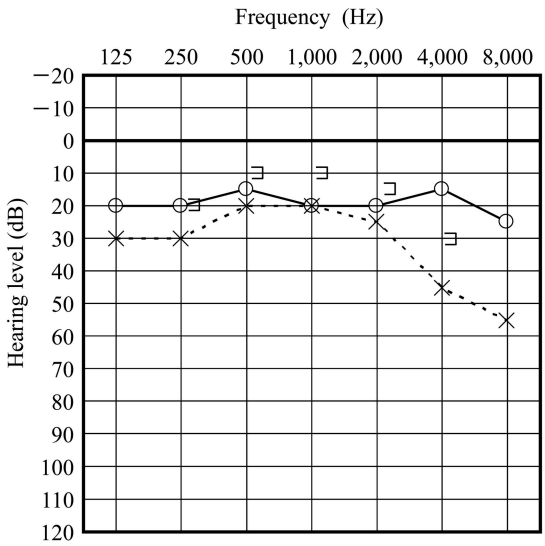

FIGURE 3
Audiogram acquired 1 month postoperatively. Hearing acuity of the left ear is improved.

(12) has suggested that hearing and balance symptoms from a microfissure could be related to reduced patency of the cochlear aqueduct. Although a round window microfissure seems to be a normal anatomical structure it can be symptomatic in certain specific circumstances.

As shown in Figure 2, a microfissure was located in the floor of the round window niche in our case. Although a three-dimensional reconstruction of temporal bone study by Sato et al. (13) showed most round window microfissures are posteromediosuperior of round window niche they can be inferior as in our case.

During surgery it was challenging to determine whether the fluid observed was perilymph or exudate. Because the fluid was not tested for cochlin tomoprotein (14), we cannot directly prove that the fluid identified intraoperatively is perilymph. However, the postoperative improvement in the patient's vestibular symptoms and recovery of hearing confirms that the symptoms were caused by the fissure. Therefore, it can be strongly inferred that the fluid was perilymph.

PLF commonly links trauma, barotrauma, ear disease or ear surgery (3, 4). The existence of cases without a history of disease, i.e., idiopathic PLF, had been controversial. In a Japan nationwide study, 19% of cases with no antecedent cause were positive cochlin tomoprotein (4), so idiopathic PLF does exist. So, what is the cause of perilymph leakage in such cases? Terayama suggests that patients with idiopathic PLF may not be aware of the cause (15). Straining, sneezing, or coughing, which trigger the onset of PLF, are events that often occur in daily life, so if the slowly progressive cases like in our case, the patient may not remember them.

Data availability statement

The original contributions presented in the study are included in the article/supplementary material, further inquiries can be directed to the corresponding author.

Ethics statement

Written informed consent was obtained from the individual(s) for the publication of any potentially identifiable images or data included in this article.

Author contributions

TSe: Conceptualization, Data curation, Writing – original draft. AK: Data curation, Writing – original draft. YK: Data curation, Writing – original draft. MA: Data curation, Writing – original draft. TSh: Writing – review & editing. MK: Writing – review & editing.

Funding

The author(s) declare that no financial support was received for the research, authorship, and/or publication of this article.

Conflict of interest

The authors declare that the research was conducted in the absence of any commercial or financial relationships that could be construed as a potential conflict of interest.

Publisher's note

All claims expressed in this article are solely those of the authors and do not necessarily represent those of their affiliated organizations, or those of the publisher, the editors and the reviewers. Any product that may be evaluated in this article, or claim that may be made by its manufacturer, is not guaranteed or endorsed by the publisher.

References

1. Bojrab DI, Bhansali SA, Battista RA. Perilymph fistula –peripheral vestibular disorders In: RK Jackler and DE Brackmann, editors. *Neurotology*. St. Louis: Mosby (1994). 640–2.

2. Kohut RI. Perilymph fistulas. *Arch Otolaryngol Head Neck Surg*. (1992) 118:687–92. doi: 10.1001/archotol.1992.01880070017003

3. Sarna B, Abouzari M, Merna C, Jamshidi S, Saber T, Djalilian HR. Perilymphatic fistula: a review of classification, etiology, diagnosis, and treatment. *Front Neurol*. (2020) 11:1046. doi: 10.3389/fneur.2020.01046

4. Matsuda H, Sakamoto K, Matsumura T, Saito S, Shindo S, Fukushima K, et al. A nationwide multicenter study of the cochlin Tomo-protein detection test: clinical characteristics of perilymphatic fistula cases. *Acta Otolaryngol*. (2017) 137:S53–9. doi: 10.1080/00016489.2017.1300940

5. Kohut RA, Hinojosa R, Thompsom N, Ryu JH. Idiotpathic perilymph fistulae: a temporal bone histopathlogical study: clinical, surgical, and histopathological correlations. *Acta Otolaryngol (Stock)*. (1995) 115:225–34. doi: 10.3109/00016489509125235

6. Okano Y, Myers EN, Dickson DR. Microfissure between the round window niche and posterior canal ampulla. *Ann Otol Rhinol Laryngol*. (1977) 86:49–57. doi: 10.1177/000348947708600108

7. Moreano EH, Paparella MM, Zelterman D, Goycoolea MV. Prevalence of microfissure in the human temporal bone: a report of 1000 temporal bones. *Laryngoscope*. (1994) 104:741–6. doi: 10.1288/00005537-199406000-00015

8. Kohut RI, Hinojosa R, Ryu JH. Perilymphatic fistulae: a single-blind clinical histopathological study. *Adv Oto-Rhino-Laryng*. (1988) 42:148–52. doi: 10.1159/000416095

9. Shazly EI, Linthicum FH. Microfissure of the temporal bone: do they have any clinical significance? *Am J Otol*. (1991) 12:169–71.

10. Kamere DB, Sando I, Hirsch B, Takagi A. Perilymph fistula resulting from microfissures. *Am J Otol*. (1987) 8:489–94.

11. Kohut RI, Hinojosa R, Thompson JN, Ryu JH. Idiopathic perilymphatic fistulas, a temporal bone histopathologic study with clinical, surgical, and histopathologic correlations. *Arch Otolaryngol*. (1995) 121:412–20. doi: 10.1001/archotol.1995.01890040036006

12. Seo T, Sakagami M, Ryu JH, Kohut RI. Relationship between perilymphatic fistula due to microfissure and the cochlear aqueduct -human histopathological study [Japanese]. *Equilibrium Res*. (1998) 57:64–8. doi: 10.3757/jser.57.64

13. Sato H, Takahashi H, Sando I. Computer-aided three dimensional reconstruction and measurement of microfissures. *Am J Otol*. (1992) 13:141–5.

14. Ikezono T, Matsumura T, Matsuda H, Shikaze S, Saitoh S, Shindo S, et al. The diagnostic performance of a novel ELISA for human CTP (Cochlintomoprotein) to detect perilymph leakage. *PLoS One*. (2018) 13:e0191498. doi: 10.1371/journal.pone.0191498

15. Terayama Y. Etiology of perilymphatic fistula. [Japanese]. *JOHNS*. (1994) 10:895–900.

frontiers | Frontiers in Neurology

TYPE Original Research
PUBLISHED 12 October 2023
DOI 10.3389/fneur.2023.1269298

OPEN ACCESS

EDITED BY
Takao Imai,
Bell Land General Hospital, Japan

REVIEWED BY
Richard D. Rabbitt,
The University of Utah, United States
Ingo Todt,
Bielefeld University, Germany
Gerard Joseph Gianoli,
The Ear and Balance Institute, United States
Richard Charles Dowell,
The University of Melbourne, Australia

*CORRESPONDENCE
Tetsuo Ikezono
✉ ikezono.tetsuo@1972.saitama-med.ac.jp

RECEIVED 29 July 2023
ACCEPTED 19 September 2023
PUBLISHED 12 October 2023

CITATION
Matsuda H, Hornibrook J and Ikezono T (2023) Assessing the efficacy of perilymphatic fistula repair surgery in alleviating vestibular symptoms and associated auditory impairments.
Front. Neurol. 14:1269298.
doi: 10.3389/fneur.2023.1269298

Assessing the efficacy of perilymphatic fistula repair surgery in alleviating vestibular symptoms and associated auditory impairments

Han Matsuda[1], Jeremy Hornibrook[2] and Tetsuo Ikezono[1]*

[1]Department of Otorhinolaryngology, Faculty of Medicine, Saitama Medical University, Saitama, Japan, [2]Department of Otolaryngology-Head and Neck Surgery and Audiology, Christchurch Hospital, Christchurch, New Zealand

Perilymph Fistula (PLF), abnormal communication between the fluid-filled space of the inner ear and the air-filled space of the middle ear, is a significant cause of vestibular and auditory symptoms. This is a retrospective study of 22 cases treated with PLF repair surgery, selected based on our surgical indication. We analyzed the characteristics of these 22 cases and evaluated the efficacy of PLF repair surgery in treating vestibular and auditory symptoms. Cases with antecedent events had significantly shorter intervals before surgery. The postoperative recovery from vestibular symptoms following PLF repair surgery was strikingly rapid, with 82% of cases demonstrating marked improvement within a week, even in chronic cases. Despite the notable absence of a control group in the study, the marked improvements in vestibular symptoms and substantial reductions in Dizziness Handicap Inventory (DHI) scores suggest that the observed benefits are attributable to the surgical intervention. Further, timely surgery showed improvements in hearing, with some benefits also seen in late-stage surgeries. Using the perilymph-specific protein Cochlin-tomoprotein (CTP) as a diagnostic biomarker, we could prove that PLF could be responsible for disequilibrium and related auditory disturbances in these patients. A new hypothesis is proposed that the chronic disequilibrium experienced by many PLF patients is due to enhanced mobility of the utricle and not to endolymphatic hydrops. Further research is needed to fully elucidate PLF's symptoms and treatment efficacy using the surgical indication we developed.

KEYWORDS

dizziness, vertigo, disequilibrium, postural instability, unsteadiness, PLF repair surgery, CTP, Cochlin-tomoprotein

Introduction

Perilymph fistula (PLF) is an abnormal communication between the fluid (perilymph)-filled inner ear and the air-filled space of the middle ear and mastoid, or cranial spaces. PLF is a well-known cause of vestibular and auditory symptoms, and there are many reports on treatment outcomes, and a high cure rate has been reported, especially for the vestibular symptoms (1, 2). We have noted that patients presenting with suspected PLF-induced disequilibrium, even those with longstanding intractable chronic disequilibrium, often demonstrate significant and rapid

improvements following PLF repair surgery. This observation has been recurrently emphasized in academic discussions among specialists.

Despite those previous experiences, this fact has yet to be fully documented in scientific literature. There needs to be a standardized, established treatment for vestibular symptoms of PLF. One reason for this unfortunate situation is that there was no definitive diagnostic method to identify the perilymph leakage (3, 4). We have identified an isoform of Cochlin, Cochlin-tomoprotein (CTP), as a perilymph-specific protein that is not expressed in the blood, CSF, or saliva (5). We have reported the specificity and sensitivity of the CTP test (6) and the clinical characteristics, epidemiology, and anatomic leakage routes of PLF diagnosed with the CTP test (7, 8). The Japanese FDA approved this test, which became eligible for national insurance coverage in Japan in 2022. The advent of the CTP test has enabled a scientific appraisal of this condition, long dubbed as controversial.

The principal objectives of this investigation are threefold. First, we aim to understand the features of cases selected based on our surgical indication. Second, our focus shifts to evaluating the outcomes of cases post-PLF repair surgery. This includes examining the duration until noticeable improvement in disequilibrium issues is observed and significant changes in the Dizziness Handicap Inventory (DHI) before and after the procedure. Within this context, we are also keen on assessing the degree of auditory enhancement and identifying specific characteristics of cases that show notable progress. Lastly, we intend to introduce and gauge the efficacy of our recently developed, highly specific CTP detection test designed to pinpoint perilymph leakage.

Materials and methods

This study involves a retrospective review of patient records of individuals who underwent PLF repair surgery between July 2011 and May 2019 at our tertiary referral hospital. All the cases were checked by CT scan by 2 certified radiologists, and none of them showed any evidence of otic capsule dehiscence. Of the 37 cases that underwent surgery during this timeframe, we excluded 4 cases involving direct stapes injury and 11 presenting solely cochlear symptoms. The study concentrates on analyzing the remaining 22 cases exhibiting vestibular symptoms. To evaluate subjective vestibular symptoms, we conducted interviews with the patients. These interviews aimed to ascertain whether patients experienced rotational vertigo or other symptoms, such as disequilibrium, postural instability, and unsteadiness. DHI was also utilized. Furthermore, the study examined the duration of symptoms from onset until surgery, evaluated the presence of nystagmus through positional and positioning nystagmus tests using an infrared camera, determined auditory thresholds using the pure tone average (PTA), the arithmetic mean of five frequencies (0.25, 0.5, 1, 2, and 4 kHz) from audiometric testing and utilized a CTP detection test (explained below). vHIT (head impulse test) and VEMP (Vestibular Evoked Myogenic Potential) were performed on some patients but not all; hence, we excluded those results from the whole group analysis.

We categorized the cases into four groups based on antecedent events and underlying causes, following the criteria formulated by a Japanese study group (Table 1) (7). Category 1 is limited to cases linked with a history of head trauma from traffic accidents. While the original category encompassed direct trauma to the inner/middle ear and middle/inner ear diseases and surgeries, these cases are beyond the purview of this study and are therefore excluded. Category 2 comprised cases with barotraumas stemming from external factors, including activities such as flying and diving. Category 3 encompassed cases with barotraumas linked to internal factors, such as nose-blowing and straining. Category 4 was designated for idiopathic cases, which lacked any discernible antecedent events. A comprehensive interview was conducted to chronicle the patient's medical history, with particular attention to events preceding the onset of symptoms. Pre-operative care included conservative treatment employing standard methodologies. A combination of corticosteroids, isosorbide, vitamin B12, and adenosine triphosphate was administered for cases of hearing loss. We instruct patients to avoid the following activities: external barotraumatic events, which typically include hyperbaric oxygen therapy, flying, diving, and rapid altitude changes; and internal barotraumatic events, which include lifting heavy objects, blowing their nose strongly, straining during constipation (for which they should take prescribed pills), solid coughing, engaging in sexual activity, and performing intense physical exercise. We recommend that they remain in bed at a 30° elevated position for 1 week if possible. For cases exhibiting vestibular symptoms, betahistine and diphenidol were prescribed. All patients with a history of symptoms lasting longer than 3 months were advised to undertake a home-based vestibular rehabilitation program (9).

TABLE 1 Categorization of PLF cases formulated by a Japanese study group.

■ Category 1
Linked to trauma, middle, and/or inner ear diseases, surgeries
1) a Direct labyrinthine trauma (stapes luxation, otic capsule fracture, etc.)
b Other trauma (head injury, body contusion, etc.)
2) a Middle or inner ear diseases (cholesteatoma, tumor, anomaly, dehiscence, etc.)
b Iatrogenic (ear surgeries, medical treatments, etc.)
■ Category 2
Linked to barotrauma caused by antecedent events of external origin (such as flying or diving)
■ Category 3
Linked to barotrauma caused by antecedent events of internal origin (such as straining, sneezing, or coughing)
■ Category 4
Has no apparent antecedent event (idiopathic)

"Spontaneous" should not be used.

Our indication for PLF repair surgery to address vestibular symptoms were as follows (Table 2A): (1) the patient having a history of traumatic or barotraumatic events before the onset of vestibular symptoms, and (2) In idiopathic patients whose chief complaint is sustained disequilibrium, the onset or exacerbation of vestibular symptoms were accompanied by sudden, fluctuating (both improvement and deterioration of more than 10 dB in PTA), and progressive (deterioration of more than 10 dB) hearing loss. The sustained vestibular symptoms are disequilibrium, unsteadiness, and postural instability, swaying, all henceforth referred to as disequilibrium. The surgery was conducted under general anesthesia,

TABLE 2 Surgical indication (A) and the number of cases in each characteristic (B).

(A)
1. Group1: cases in Category 1, 2, and 3 • Having a history of traumatic or barotraumatic events before the onset of vestibular symptoms. 2. Group 2: cases in category 4 (idiopathic) • Having sustained vestibular symptoms (disequilibrium, unsteadiness, postural instability, and swaying) • The onset or exacerbation of vestibular symptoms was accompanied by sudden, fluctuating, and progressive hearing loss.

(B)		
Group 1: cases in category 1, 2, and 3		
1A	Sudden hearing loss	4 cases
1B	Progressive/fluctuating hearing loss	9 cases
1C	without hearing loss	2 cases
Group 2: cases in category 4 (idiopathic)		
2A	Sudden hearing loss	4 cases
2B	Progressive/fluctuating hearing loss	3 cases

Group 1, which encompasses Categories 1, 2, and 3, and Group 2, which includes Category 4 cases. Subgroup A encompassed cases exhibiting sudden hearing loss, Subgroup B included cases with progressive or fluctuating hearing loss, whereas Subgroup C consisted of cases without hearing loss.

utilizing a transcanal approach with the elevation of the tympanomeatal flap, facilitating the visualization of the middle ear. Connective tissue and fibrin glue were used to seal the round and oval windows, microfissures around windows (10), and the fissula ante fenestram. Thin aural cartilage was placed over the round window to stabilize the connective tissue. Throughout the surgical procedure, meticulous examination was conducted to ascertain the presence or absence of a fistula and any perilymph leakage.

After the PLF repair surgery, improvement in vestibular symptoms was assessed through patient interviews, and the results were binarily categorized as either unchanged/progressing or demonstrating marked improvement compared to the pre-surgery state. Evaluations of vestibular symptoms and nystagmus were systematically conducted at 1 week, 1 month, 3 months, and 6 months after the surgery. The moment when vestibular symptoms noticeably decrease and patients report symptom relief is identified as the point of marked improvement. The time frame in which patients experienced marked symptom improvement and resolution of nystagmus was classified as follows: A—within 1 week postoperatively, B—within 1 month postoperatively, C—within 3 months postoperatively, D–within 6 months postoperatively, E—no observable improvement in vestibular symptoms or resolution of nystagmus. DHI score was evaluated prior to surgery and either at the resolution of vestibular symptoms or at a six-month post-operative period, whichever came first. Of the 22 cases, DHI assessment was executed in 12 cases that underwent surgery post-September 2015. Although the video head impulse test and vestibular evoked myogenic potentials were performed, these tests were not conducted in all cases; therefore, the data gathered from these tests were not incorporated into the analysis. PTA was evaluated once auditory stability was achieved, defined by a constant PTA that did not exhibit variations beyond a 10 dB threshold. The evaluation of auditory recovery followed the criteria established by the Acute Severe Hearing Loss Study Group, which are as follows: "Complete recovery" signifies recovery to a hearing level within 20 dB at PTA or to the same hearing level as the unaffected side. "Marked recovery" refers to more than 30 dB recovery in PTA. "Slight recovery" is a recovery of 10–29 dB, and "No response" corresponds to a recovery of less than 10 dB (11). A binary statistical analysis was executed to classify treatment responses as either positive (improvement exceeding 10 dB) or negative (improvement of less than 10 dB or a decline) in PTA.

The CTP detection test was conducted as previously detailed (7). Briefly, following myringotomy or during surgery, the middle ear was irrigated with 0.3 mL of saline and the fluid retrieved was termed Middle Ear Lavage (MEL). The MEL was frozen, sent to the central pathology lab (SRL Inc.), then subjected to analysis using the ELISA method with polyclonal antibodies (6). CTP concentrations equal to or greater than 0.8 ng/mL were deemed positive; values between 0.4 and 0.8 ng/mL were considered intermediate, and levels below 0.4 ng/mL were classified as negative. A positive CTP level led to the definitive diagnosis of PLF.

Patient data was thoroughly analyzed, and follow-ups were conducted until the resolution of vestibular symptoms or at a six-month post-operative period, whichever came first. Statistical analysis was performed using JMP Pro 16 software. The Wilcoxon test was employed to compare pre-and post-operative DHI scores. At the same time, Spearman's rank correlation coefficient was utilized to analyze the relationship between hearing improvement and the number of days. A value of p less than 0.05 was taken as indicative of statistical significance. The Institutional Review Board (IRB) of Saitama Medical University Hospital approved this study (approval number 13-086).

Results

Based on the established categorization criteria (as shown in Table 1) and a comprehensive interview and exclusion process, 22 patients were included in this study, diagnosed as suspected cases of PLF, and considered for surgical intervention. As detailed in the Materials and Methods section and Table 2A, our surgical indication is based on the sustained vestibular symptom, antecedent traumatic events, and/or associated hearing loss (sudden, progressive, or fluctuating). Table 2B summarizes the number of cases in each characteristic. Given the limited number of patients, we conducted a bifurcated analysis by Group 1 (Category 1, 2, 3; Table 3A) and Group 2 (Category 4; Table 3B). The demographics were summarized in Table 4, and detailed patient numbers in groups 1 and 2 are summarized in Supplementary Table.

Among the studied population, preceding incidents were head injury due to a traffic accident (Category 1), airplane flying, descent from a high-altitude mountain, insufflation (Category 2), nose-blowing, blowing the whistle, sexual intercourse, and vomiting (Category 3). Table 3 systematically organizes the patients in descending order according to the period from the onset of symptoms

TABLE 3 Clinical features of cases in Group 1 (A) and Group 2 (B).

(A)																
No.	Age	Gender	Category	Event	Days from onset to surgery	CTP test	Vestibular symptom	Improvement in vestibular symptom	Resolution of nystagmus	Hearing type	Preop DHI	Postop DHI	Preop PTA	Postop PTA	Hearing recovery	Follow-up period	Surgical indication
1	49	F	3	Nose blowing	5	I	D	A	C	-	16	0	NOR	NOR	-	13	1C
2	64	F	2	Airplane	8	N	R-D	A	A	S	NA	NA	111	111	NR	6	1A
3	46	M	3	Blow the whistle	11	N	D	A	B	P	62	0	104	67	MR	3	1B
4	33	M	2	Airplane	12	N	R-D	C	A	P	NA	NA	89	49	MR	11	1B
5	13	M	3	Nose blowing	14	N	D	A	A	P	20	0	101	72	SR	23	1B
6	32	F	3	Nose blowing	18	P	R-D	A	A	F	96	0	74	58	SR	9	1B
7	65	F	3	Airplane	27	N	D	A	A	P	76	2	110	87	SR	14	1B
8	52	M	2	Descent from high altitude	35	P	R-D	A	B	F	58	10	101	86	SR	17	1B
9	32	F	3	Sexual intercourse	69	I	D	A	-	P	NA	NA	98	92	NR	53	1B
10	47	F	1	Traffic accident	102	N	D	A	C	S	NA	NA	37	22	SR	15	1A
11	39	F	2	Airplane	136	P	D	A	-	-	NA	NA	NOR	NOR	-	2	1C
12	66	M	2	Insufflation	150	I	D	A	A	F	NA	NA	31	35	NR	36	1B
13	67	M	3	Vomit	167	N	D	E	E	S	78	48	68	78	NR	12	1A
14	45	F	3	Nose blowing	179	N	R-D	A	A	S	NA	NA	58	60	NR	3	1A
15	62	M	1	Traffic accident	190	I	D	A	-	P	NA	NA	53	36	SR	1	1B

(Continued)

10.3389/fneur.2023.1269298

TABLE 3 (Continued)

(B)															
No.	Age	Gender	Days from onset to surgery	CTP test	Vestibular symptom	Improvement in vestibular symptom	Resolution of nystagmus	Preop DHI	Postop DHI	Hearing type	Preop HL	Postop HL	Hearing recovery	Follow-up period	Surgical indication
16	39	M	41	N	R-D	B	D	NA	NA	S	111	70	MR	46	2B
17	44	F	77	N	D	A	A	62	0	P	111	111	NR	30	2B
18	48	M	122	N	R-D	A	D	44	0	P	56	48	NR	6	2B
19	74	F	215	N	D	E	E	54	42	S	82	89	NR	11	2A
20	47	F	290	N	D	A	-	80	0	S	60	64	NR	14	2A
21	55	M	390	N	D	A	-	NA	NA	S	59	62	NR	1	2A
22	47	M	1,500	P	R-D	A	-	92	68	S	98	104	NR	9	2A

The cases were numbered in order of the duration from onset to surgery. The patients were categorized into four groups based on antecedent events and underlying causes (Category, Event). The Days represent the number of days from onset to surgery. CTP examination results were indicated as positive (P), intermediate (I), or negative (N). Vestibular symptoms were classified as follows: cases initially complained of rotatory vertigo and turned into disequilibrium (R-D), and cases originally presented as disequilibrium (D). The time frame in which patients experienced marked symptom improvement and resolution of nystagmus was classified as follows: A—within 1 week postoperatively, B—within 1 month postoperatively, C—within 3 months postoperatively, D—within 6 months postoperatively, E—no observable improvement in vestibular symptoms or nystagmus persisted. A minus sign (–) was recorded in the nystagmus column for cases without preoperative nystagmus. The hearing type was classified as sudden (S), progressive (P), or fluctuating (F). Preoperative and postoperative PTA were measured as the average air conduction thresholds at 0.25 to 4kHz frequencies. NOR indicates normal hearing. Hearing recovery was classified as marked recovery (MR), slight recovery (SR), and no response (NR). The follow-up period represents the duration of postoperative follow-up (months). Surgical indications were documented based on (Table 2B). Group 1; Among the 15 cases, marked improvement of vestibular symptoms within 1 week was observed in 13 cases. Group 2; Among the 7 cases, marked improvement of vestibular symptoms was observed within 1 week in 5 cases. A statistically significant shorter interval before surgery was observed in Group 1 than in Group 2.

to the surgical intervention. The duration varied from 5 days to approximately 4 years, with a median of 89.5 days. A statistically significant shorter interval before surgery was observed in Group 1 ($p < 0.05$, Wilcoxon test). Five patients underwent surgery during the acute phase (within 2 weeks post-symptom onset). Ten patients experienced a chronic phase of vestibular symptoms lasting 90 days or longer.

CTP test outcomes varied across the patient population: 4 patients had positive results, 4 had intermediate results, and 14 demonstrated negative results. Only one instance (case 6) (8) showed a visible intraoperative fistula due to a malformed stapes footplate and minimal perilymph leakage. In contrast, in the remaining 21 cases, neither fistula nor microfissure was detected, nor was any noticeable perilymph leakage observed intraoperatively. Eight patients initially experienced rotatory vertigo, subsequently evolving into disequilibrium within a 1 to 7-day timeframe. In contrast, 14 patients did not experience initial rotatory vertigo, presenting with disequilibrium at onset. MRI findings in the affected ear revealed an inner ear hemorrhage in case 13 and fibrosis in the posterior semicircular canal in case 19. These 2 cases were intractable in several measures, subjective vestibular symptom, DHI, nystagmus and hearing, as explained below. Within a week post-surgery, 18 out of the 22 patients (82%) demonstrated marked improvements in vestibular symptoms (Table 5). Among the remaining 4 patients, one experienced marked improvement a month after surgery, while another observed this change 3 months post-surgery. Two patients (cases 13 and 19) failed to achieve marked improvement 6 months after the surgical intervention. Peripheral nystagmus was observed in 16 of the 22 patients before surgery. All cases displayed unidirectional rotatory-horizontal nystagmus during the positioning nystagmus test.

TABLE 4 Demographics of the enrolled patients.

	Overall (22 cases)	Group 1 (Table 3A)	Group 2 (Table 3B)
Gender	11 males, 11 females	7 males, 8 females	4 males, 3 females
Age range	13 to 74 years	13 to 67 years	39 to 74 years
Median age	47 years	47 years	47 years
Duration from Symptom onset to surgery*	5 days to ~4 years, Median: 89.5 days	5 to 190 days, Median: 35 days*	41 days to ~4 years, Median: 215 days

*Statistical significance. Shorter interval before surgery ($p < 0.05$, Wilcoxon test).

TABLE 5 The interval from surgery to the point of marked improvement in vestibular symptoms.

Point of resolution	The number of cases
Within 1 W	18
1 M	1
3 M	1
No change	2

Within a week post-surgery, 18 out of the 22 patients (82%) demonstrated marked improvements in vestibular symptoms. Among the remaining four patients, one experienced marked improvement a month after surgery, while another observed this change 3 months post-surgery. Notably, two patients (13 and 19) failed to achieve marked improvement 6 months after the surgical intervention.

Additionally, Case 13 exhibited down-beating rotatory nystagmus in the Dix-Hallpike test at the onset. Postoperatively, nystagmus subsided in 8 patients after 1 week, 2 patients after 1 month, 2 patients after 3 months, and 2 patients after 6 months. However, 2 patients (cases 13, 19) continued to exhibit nystagmus 6 months after surgery. DHI scores varied between 16 and 96 preoperatively and 0–68 postoperatively, showing a statistically significant improvement post-surgery ($p < 0.05$, Wilcoxon test), as depicted in Figure 1.

Excluding two cases with normal hearing (cases 1 and 11), hearing loss was identified in 20 patients. Nine patients experienced sudden onset, 3 had fluctuating hearing loss, and 8 had progressive hearing loss. Postoperative hearing improvements ranged from a decrease of 10 dB to an increase of 41 dB, with a median improvement of 7 dB. The only case where hearing deteriorated by more than 10 dB was Case 13, which had inner ear hemorrhage. There were no instances of complete recovery. However, marked recovery was observed in 3 cases, slight recovery in 6 cases, and no recovery was found in 11 cases. Patients who demonstrated a postoperative response to the treatment, reflected by a hearing improvement of 10 dB or more (either marked or slight recovery), had a statistically significantly shorter interval from symptom onset to surgery (median 27 days) compared to those who exhibited no response (median 167 days; $p < 0.05$ Spearman's rank correlation coefficient).

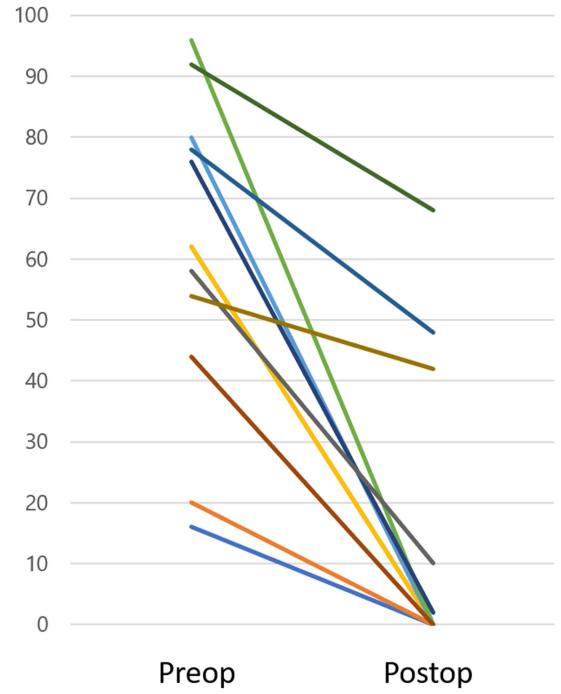

FIGURE 1
DHI score. Preoperative DHI scores ranged from 16 to 96, while postoperative scores were between 0 and 68, demonstrating a significant improvement after surgery ($p < 0.05$). Three cases (Case 13, 19, and 22) sustained a DHI score over 10 (48, 42, 68, respectively) within the observation period.

Discussion

Drawing from our experiences, we have established indication for PLF repair surgery to address vestibular symptoms. The indication are: (1) the patient has a history of traumatic or barotraumatic events preceding the onset of vestibular symptoms, and (2) vestibular symptoms are accompanied by sudden, fluctuating, or progressive hearing loss, as explained in the method section (Table 2). In Group 1, the patients exhibited specific antecedent events that are characteristic indicators for PLF. Given these clinical histories, the likelihood of diagnosing PLF becomes comparatively more straightforward. Our study found a statistically significant shorter interval before surgery in Group 1 patients, compared to Group 2 patients without a history of antecedent events. This is reasonable because Group 2 patients were referred to our clinic for sustained disequilibrium. In Group 1, 20% of the cases (3 out of 15) tested positive for CTP, aligning with the positive rate discovered in our prior nationwide study. That study reported positive rates of 32% for Category 1, 11% for Category 2, and 24% for Category 3 cases, all of which led to a confirmed diagnosis of PLF. Most cases (13 out of 15) had an abrupt onset of vestibular and auditory symptoms following these events, excluding two cases with normal hearing (cases 1 and 11). PLF repair surgery was chosen due to the apparent relationship between the event and onset in case 1, the preoperative positive CTP test result in case 11. In Group 2, comprising idiopathic cases, only one case (1/7, 14%) tested positive for CTP. Although this category of PLF is a matter of ongoing debate, our previous nationwide study confirmed its existence, with 18% of CTP-positive cases being verified as PLF in Category 4, idiopathic. The hearing progression in patients with PLF can present with various types of hearing impairment, including sudden or progressive/fluctuating sensorineural hearing loss. The presence of these auditory symptoms, together with vestibular disturbances, could serve as an indicator for clinicians to suspect PLF (7). Hence, diagnosing PLF without cochlear signs or a traumatic history can be challenging. Our study did not include such isolated cases.

Determining how to include PLF-suspected cases based on specific vestibular/cochlear symptoms is paramount. To date, the classic symptoms and signs that conclusively link to a PLF diagnosis remain unidentified. In our research, 8 patients initially exhibited rotatory vertigo, which later transitioned into disequilibrium. Meanwhile, the other 14 cases did not have initial rotatory vertigo but presented with disequilibrium from the onset. Hearing loss patterns varied, ranging from sudden onset to fluctuating and progressive patterns. Thus, during patient interviews, the pivotal question is: "Do you recall any preceding traumatic or barotraumatic events that could correlate with the commencement of your current vestibular/cochlear symptoms?" For idiopathic patients whose chief complaint is sustained disequilibrium, the central focus is determining if the onset or exacerbation of vestibular symptoms is aligned with acute hearing loss or with progressive/fluctuating hearing loss. In our analysis, 5 out of the 7 idiopathic cases experienced acute hearing loss just before symptom onset, while the remaining 2 reported progressive or fluctuating hearing loss.

A prior animal study provides potential explanations for those variable vestibular symptoms, highlighting diverse pathologies in the membranous labyrinth (12). For example, experimental fistulae in guinea pigs led to the collapse of the semicircular canal ampullae, potentially causing rotatory vertigo, and hydrops or collapse of the otolithic organs. As such, PLF patients may exhibit a spectrum of symptoms due to these varied inner ear conditions.

The postoperative recovery from vestibular symptoms following PLF repair surgery was strikingly rapid, with 82% of cases demonstrating marked improvement within a week (87% in Group 1, 71%in Group 2). All eight patients with positive or intermediate CTP and 10 out of 14 with negative CTP exhibited significant improvement within a week. It is essential to understand that improving CTP-negative patients post-PLF repair surgery does not negate the possibility of perilymph leakage. This is attributed to the potential limitations of the CTP test, which may produce negative results in scenarios of sporadic leakage or minimal perilymph presence in the middle ear during the test. Therefore, due to the test's constraints, these instances could represent either genuine PLF-negative cases or undiagnosed PLF cases. This insight is vital when analyzing CTP test results within the framework of our research. Most importantly, despite a low positivity rate, it suggests the detectability of perilymph leakage in this cohort. This evidence supports the hypothesis that PLF could be responsible for disequilibrium and related auditory disturbances in these patients.

The immediate relief of vestibular symptoms following PLF repair surgery has not been extensively documented in existing medical literature. However, our observations have been corroborated by neuro-otologists worldwide who specialize in performing this surgery. The underlying pathomechanisms are hypothesized based on detailed anatomical studies. Smith and colleagues have provided a comprehensive description of the intricate structure of the membranous labyrinth in their 2021 study (13). The utricular macula is attached to the bony labyrinth by a perforated membrane, the membrana limitans, giving it some mobility. It is plausible that abnormal endolymph flow due to a window leak may magnify utricular mobility, leading to aberrant vestibulospinal signals that result in unilateral postural instability (14, 15). The fact that repair of the leak ameliorates this symptom aligns with this proposed mechanism and thus should not be surprising. There is a prevalent theory that the vestibular symptoms associated with PLF are due to endolymphatic hydrops (EH) (16), and our current data does not completely deny this theory. However, in a recent Gd-enhanced MRI study showed EH is not a rare finding in the inner ear and is not related to vestibular symptoms. Laine et al. described a 3% incidence of EH in otosclerosis patients and there was no correlation with vestibular symptoms (17). Yoshida et al. reported an incidence of EH in a control group consisting of patients with parotid gland tumors, laryngeal diseases, and sinusitis, who did not exhibit vestibular and cochlear symptoms. EH was identified in 16 out of 42 ears (38%), with significant hydrops observed in 4 out of 42 ears (10%) (18). In addition, the hydrops theory fails to account for the rapid improvement of a patient's vestibular symptoms after repair of a perilymph leak. The vestibular symptoms from a superior canal dehiscence can be treatable in some cases by "reinforcing" the oval and round windows. However, we do not believe otic capsule dehiscence cases were mistakenly included in the present study. As explained in the methods section, before enrolling patients, we evaluated CT scans to exclude any instances of otic capsule dehiscence. Additionally, VEMPs were tested in 10 of the current cases, revealing hypofunction in the affected ear; none exhibited hyperreactivity.

Two of the 22 cases displayed persistent vestibular and cochlear symptoms and failed to achieve "marked improvement" within the 6-month observation period. Case 13 presented with an episode of vomiting, followed by the onset of vestibular symptoms and auditory impairment. Suspecting an inner ear hemorrhage based on the patient's MRI findings and ongoing anticoagulant therapy due to a previous myocardial infarction, it was anticipated that the PLF repair surgery would not result in symptom improvements. The link between poor prognosis and sudden sensorineural hearing loss associated with inner ear hemorrhage has been previously documented (19). Case 19's MRI detected fibrosis in the affected side's posterior semicircular canal, corroborated by a vHIT revealing impaired functionality. Autoimmune diseases or infarctions within the inner ear can cause inner ear fibrosis (20, 21), but the cause of fibrosis in this case remains unclear. In both 2 cases (13 and 19), vHIT showed a reduction in VOR gain on the affected side, and the compensation process still may need time to heal. The DHI evaluated vestibular symptoms, revealing a statistically significant post-surgical improvement (Figure 1). Three cases sustained a DHI score over 10 within the observation period. Cases 13 and 19, as described above, showed pathologies on the MRI that aligned with their DHI scores of 48 and 42, respectively. Case 22, with a positive CTP test, reported marked improvement within a week following surgery. However, 6 months post-operation, a high DHI score of 68 persisted. The patient was diagnosed with Persistent Postural-Perceptual Dizziness (PPPD) and is presently engaged in cognitive behavioral therapy as part of the treatment protocol (22). The surgical indication for PLF employed in this study were indirectly supported by the positive postoperative outcomes, except for three cases diagnosed with apparent comorbidities, suggesting their overall effectiveness.

The timing of receiving CTP test results is an essential factor when deciding to perform PLF repair surgery. Under the current CTP test architecture covered by the Japanese national health insurance, it typically takes 1 to 3 weeks to receive the results from the central pathology lab. This delay means that decisions about surgery are often made based on other factors, such as the patient's history, symptoms, and physiological test results. Only 2 cases in this study (cases 11 and 22) had CTP test results available before surgery, as these patients requested to know the results before deciding to undergo surgery. A new point-of-care immunochromatography test to detect CTP is currently under development, which could provide faster and on-site test results. The availability of such a test could lead to more rational surgical indications for PLF repair surgery.

With regard to auditory recovery, cases displaying an improvement of 10 dB or more had a significantly shorter period between onset and surgery compared to those with no response. This aligns with existing literature underscoring the importance of prompt PLF repair surgery (23, 24). In our study, two instances (Case 10 and Case 15) where surgery was conducted more than 3 months post-onset, achieved a postoperative hearing improvement of over 10 dB. In both scenarios, despite a lack of progress with conservative treatment, auditory function improved following surgery. This suggests that auditory improvement is likely attributable to the PLF repair surgery. In situations with a known cause of onset, anticipated severe hearing loss with a poor prognosis, or worsening or fluctuating auditory function, the potential therapeutic benefits of PLF repair surgery should be articulated to the patient, and the appropriateness of surgery should be carefully evaluated.

This study carries several weaknesses. The present study is limited by the absence of a control group, either non-surgical or receiving sham surgery, which introduces the potential for a placebo effect on subjective vestibular symptoms. Regardless, our findings demonstrated that even among the 11 cases presenting chronic phase vestibular symptoms (cases 10 through 15, and 18 through 22, each persisting beyond 3 months), 9 cases (or 82%) exhibited marked improvement

within one-week post-surgery. This supports the inference that the observed gains are likely attributable to the surgical intervention.

Conclusion

From our current study, we observed rapid and marked improvements in vestibular symptoms and significant reductions in DHI scores after PLF repair surgery. These results highlight the high efficacy of this procedure in treating PLF, provided that patients are appropriately selected based on clinical findings. Additionally, when the surgery was performed early, we noticed improvements in hearing. Out of our sample, the CTP test was positive in four cases and intermediate in another four. Although the positivity rate was low, it indicates that perilymph leakage is detectable in this population. This evidence supports the hypothesis that PLF could be responsible for disequilibrium and related auditory disturbances in these patients.

The effectiveness of PLF repair surgery for PLF can be influenced by factors such as the size of the fistula, the extent of perilymph leakage, the number of days to surgery, and the severity of inner ear damage at the onset. Conducting a prospective study using our developed surgical indication will further elucidate PLF's symptoms and treatment efficacy.

Data availability statement

The raw data supporting the conclusions of this article will be made available by the authors, without undue reservation.

Ethics statement

The studies involving humans were approved by Institutional Review Board of Saitama Medical University Hospital. The studies were conducted in accordance with the local legislation and institutional requirements. Written informed consent for participation in this study was provided by the participants' legal guardians/next of kin.

Author contributions

HM: Writing – original draft. JH: Writing – review & editing. TI: Conceptualization, Writing – original draft.

Funding

The author (s) declare financial support was received for the research, authorship, and/or publication of this article. This work was supported by the Ministry of Health and Welfare, Japan (H29-Nanchitou(Nan)-Ippan-031) (http://www.mhlw.go.jp/english/).

Acknowledgments

The authors have appreciated conversations with Ian Curthoys (University of Sydney) and Christopher Smith (Icahn School of Medicine at Mount Sinai), who concur with the hypothesis that the chronic disequilibrium experienced by many PLF patients might be explained by an enhanced mobility of the utricle on its membrana limitans. We thank Tomohiro Matsumura (Nippon Medical School), Shiho Saitoh and Koichi Toyoda (Saitama Medical University) for their generous contribution to establishing the CTP detection test. We also thank Ryuichiro Araki (Saitama Medical University), a certified statistician, for his advice on medical statistics and Iichiro Osawa, a certified radiologist, for reviewing the imaging study.

Conflict of interest

Saitama Medical University, where HM and TI are affiliated, holds the patents for the hCTP ELISA test. This fact did not influence the results of the study. The remaining author has no commercial or financial relationships that could be perceived as potential conflicts of interest.

Publisher's note

Supplementary material

The Supplementary material for this article can be found online at: https://www.frontiersin.org/articles/10.3389/fneur.2023.1269298/full#supplementary-material

References

1. Black FO, Pesznecker S, Norton T, Fowler L, Lilly DJ, Shupert C, et al. Surgical management of perilymphatic fistulas: a Portland experience. *Am J Otol.* (1992) 13:254–62.

2. Choi JE, Moon IJ, Kim H, Lee K, Cho YS, Chung WH. Diagnostic criteria of barotraumatic perilymph fistula based on clinical manifestations. *Acta Otolaryngol.* (2017) 137:16–22. doi: 10.1080/00016489.2016.1213419

3. Hornibrook J. Perilymph fistula: fifty years of controversy. *ISRN Otolaryngol.* (2012) 2012:281248:1–9. doi: 10.5402/2012/281248

4. Deveze A, Matsuda H, Elziere M, Ikezono T. Diagnosis and treatment of Perilymphatic fistula. *Adv Otorhinolaryngol.* (2018) 81:133–45. doi: 10.1159/000485579

5. Ikezono T, Shindo S, Sekiguchi S, Hanprasertpong C, Li L, Pawankar R, et al. Cochlin-tomoprotein: a novel perilymph-specific protein and a potential marker for the diagnosis of perilymphatic fistula. *Audiol Neurootol.* (2009) 14:338–44. doi: 10.1159/000212113

6. Ikezono T, Matsumura T, Matsuda H, Shikaze S, Saitoh S, Shindo S, et al. The diagnostic performance of a novel ELISA for human CTP (Cochlin-tomoprotein) to detect perilymph leakage. *PLoS One.* (2018) 13:e0191498. doi: 10.1371/journal.pone.0191498

7. Matsuda H, Sakamoto K, Matsumura T, Saito S, Shindo S, Fukushima K, et al. A nationwide multicenter study of the Cochlin Tomo-protein detection test: clinical characteristics of perilymphatic fistula cases. *Acta Otolaryngol.* (2017) 137:S53–9. doi: 10.1080/00016489.2017.1300940

8. Matsuda H, Tanzawa Y, Sekine T, Matsumura T, Saito S, Shindo S, et al. Congenital membranous stapes footplate producing episodic pressure-induced Perilymphatic fistula symptoms. *Front Neurol*. (2020) 11:747. doi: 10.3389/fneur.2020.585747

9. Dix MR. The rationale and technique of head exercises in the treatment of vertigo. *Acta Otorhinolaryngol Belg*. (1979) 33:370–84.

10. Sato H, Takahashi H, Sando I. Computer-aided three-dimensional reconstruction and measurement of microfissures. *Am J Otol*. (1992) 13:141–5.

11. Kanzaki J, Inoue Y, Ogawa K, Fukuda S, Fukushima K, Gyo K, et al. Effect of single-drug treatment on idiopathic sudden sensorineural hearing loss. *Auris Nasus Larynx*. (2003) 30:123–7. doi: 10.1016/S0385-8146(03)00009-9

12. Nomura Y, Hara M. Experimental perilymphatic fistula. *Am J Otolaryngol*. (1986) 7:267–75. doi: 10.1016/S0196-0709(86)80049-7

13. Smith CM, Curthoys IS, Mukherjee P, Wong C, Laitman JT. Three-dimensional visualization of the human membranous labyrinth: the membrana limitans and its role in vestibular form. *Anat Rec*. (2022) 305:1037–50. doi: 10.1002/ar.24675

14. Hornibrook J. The postural and cognitive Disabilites of chronic perilymph fistula (PLF) after mild head trauma. *Annals Clin Case Rep*. (2018) 3:1514. doi: 10.25107/2474-1655.1514

15. Pelosi S, Schuster D, Jacobson GP, Carlson ML, Haynes DS, Bennett ML, et al. Clinical characteristics associated with isolated unilateral utricular dysfunction. *Am J Otolaryngol*. (2013) 34:490–5. doi: 10.1016/j.amjoto.2013.04.008

16. Harrison WH, Shambaugh GE Jr, Derlacki EL, Clemis JD. Perilymph fistula in stapes surgery. *Laryngoscope*. (1967) 77:836–49. doi: 10.1288/00005537-196705000-00011

17. Laine J, Hautefort C, Attye A, Guichard JP, Herman P, Houdart E, et al. MRI evaluation of the endolymphatic space in otosclerosis and correlation with clinical findings. *Diagn Interv Imaging*. (2020) 101:537–45. doi: 10.1016/j.diii.2020.03.009

18. Yoshida T, Sugimoto S, Teranishi M, Otake H, Yamazaki M, Naganawa S, et al. Imaging of the endolymphatic space in patients with Ménière's disease. *Auris Nasus Larynx*. (2018) 45:33–8. doi: 10.1016/j.anl.2017.02.002

19. Wei FQ, Wen L, Chen K, Liu M, Wu X. Different prognoses in patients with profound sudden sensorineural hearing loss. *Acta Otolaryngol*. (2019) 139:598–603. doi: 10.1080/00016489.2019.1605195

20. Joglekar S, Deroee AF, Morita N, Cureoglu S, Schachern PA, Paparella M. Polyarteritis nodosa: a human temporal bone study. *Am J Otolaryngol*. (2010) 31:221–5. doi: 10.1016/j.amjoto.2009.02.006

21. Castellucci A, Pepponi E, Bertellini A, Senesi C, Bettini M, Botti C, et al. Case report: filling defect in posterior Semicircular Canal on MRI with balanced steady-state gradient-Echo sequences after labyrinthine ischemia in the common Cochlear artery territory as an early sign of fibrosis. *Front Neurol*. (2020) 11:608838. doi: 10.3389/fneur.2020.608838

22. Waterston J, Chen L, Mahony K, Gencarelli J, Stuart G. Persistent postural-perceptual dizziness: precipitating conditions, co-morbidities and treatment with cognitive behavioral therapy. *Front Neurol*. (2021) 12:795516. doi: 10.3389/fneur.2021.795516

23. Komori M, Yamamoto Y, Yaguchi Y, Ikezono T, Kojima H. Cochlin-tomoprotein test and hearing outcomes in surgically treated true idiopathic perilymph fistula. *Acta Otolaryngol*. (2016) 136:901–4. doi: 10.3109/00016489.2016.1165861

24. Prenzler NK, Schwab B, Kaplan DM, El-Saied S. The role of explorative tympanotomy in patients with sudden sensorineural hearing loss with and without perilymphatic fistula. *Am J Otolaryngol*. (2018) 39:46–9. doi: 10.1016/j.amjoto.2017.10.006

frontiers | Frontiers in Neurology

TYPE Original Research
PUBLISHED 12 October 2023
DOI 10.3389/fneur.2023.1259030

OPEN ACCESS

EDITED BY
Rick Friedman,
University of California, San Diego,
United States

REVIEWED BY
Gerard Joseph Gianoli,
The Ear and Balance Institute, United States
Quinton Gopen,
University of California, Los Angeles,
United States

*CORRESPONDENCE
Todd M. Mowery
✉ tm692@rwjms.rutgers.edu

RECEIVED 14 July 2023
ACCEPTED 14 September 2023
PUBLISHED 12 October 2023

CITATION
Mowery TM, Wackym PA, Nacipucha J, Dangcil E, Stadler RD, Tucker A, Carayannopoulos NL, Beshy MA, Hong SS and Yao JD (2023) Superior semicircular canal dehiscence and subsequent closure induces reversible impaired decision-making. *Front. Neurol.* 14:1259030. doi: 10.3389/fneur.2023.1259030

Superior semicircular canal dehiscence and subsequent closure induces reversible impaired decision-making

Todd M. Mowery[1,2]*, P. Ashley Wackym[1,2], Jacqueline Nacipucha[1], Evelynne Dangcil[1], Ryan D. Stadler[1], Aaron Tucker[1], Nicolas L. Carayannopoulos[1], Mina A. Beshy[1], Sean S. Hong[1] and Justin D. Yao[1,2]

[1]Department of Otolaryngology – Head and Neck Surgery, Rutgers Robert Wood Johnson Medical School, New Brunswick, NJ, United States, [2]Rutgers Brain Health Institute, New Brunswick, NJ, United States

Background: Vestibular loss and dysfunction has been associated with cognitive deficits, decreased spatial navigation, spatial memory, visuospatial ability, attention, executive function, and processing speed among others. Superior semicircular canal dehiscence (SSCD) is a vestibular-cochlear disorder in humans in which a pathological third mobile window of the otic capsule creates changes to the flow of sound pressure energy through the perilymph/endolymph. The primary symptoms include sound-induced dizziness/vertigo, inner ear conductive hearing loss, autophony, headaches, and visual problems; however, individuals also experience measurable deficits in basic decision-making, short-term memory, concentration, spatial cognition, and depression. These suggest central mechanisms of impairment are associated with vestibular disorders; therefore, we directly tested this hypothesis using both an auditory and visual decision-making task of varying difficulty levels in our model of SSCD.

Methods: Adult Mongolian gerbils (n = 33) were trained on one of four versions of a Go-NoGo stimulus presentation rate discrimination task that included standard ("easy") or more difficult ("hard") auditory and visual stimuli. After 10 days of training, preoperative ABR and c+VEMP testing was followed by a surgical fenestration of the left superior semicircular canal. Animals with persistent circling or head tilt were excluded to minimize effects from acute vestibular injury. Testing recommenced at postoperative day 5 and continued through postoperative day 15 at which point final ABR and c+VEMP testing was carried out.

Results: Behavioral data (d-primes) were compared between preoperative performance (training day 8–10) and postoperative days 6–8 and 13–15. Behavioral performance was measured during the peak of SSCD induced ABR and c+VEMP impairment and the return towards baseline as the dehiscence began to resurface by osteoneogenesis. There were significant differences in behavioral performance (d-prime) and its behavioral components (Hits, Misses, False Alarms, and Correct Rejections). These changes were highly correlated with persistent deficits in c+VEMPs at the end of training (postoperative day 15). The controls demonstrated additional learning post procedure that was absent in the SSCD group.

Conclusion: These results suggest that aberrant asymmetric vestibular output results in decision-making impairments in these discrimination tasks and could

be associated with the other cognitive impairments resulting from vestibular dysfunction.

KEYWORDS

cognitive dysfunction, decision-making, dizziness, headache, migraine, superior semicircular canal dehiscence, vestibular

Introduction

In adults, vestibular loss and dysfunction has been associated with cognitive deficits. Specifically, vestibular loss in adults is associated with decreased spatial navigation (1), spatial memory (2), visuospatial ability (3–6), attention (7, 8), executive function (5, 9), and processing speed (5), among others. In addition, individuals with chronic vestibular disorders have been reported to have accompanying cognitive dysfunction (9–13). These cognitive impairments can be observed in patients within a group of vestibular-cochlear disorders referred to as "Third Window Syndrome." In this disorder a pathological third mobile window of the otic capsule creates changes to the flow of sound pressure energy between the oval and round window (see review 14). The nature and location of this third mobile window can occur at many different sites (or multiple sites); however, the most common third mobile window is superior semicircular canal dehiscence (SSCD), (9, 13, 15–18). The primary physiological symptoms include sound-induced dizziness/vertigo, inner ear/otic capsule conductive hearing loss, autophony (hearing internal sounds abnormally well [one-third can hear their eyes move or blink]), headaches, and visual problems (convergence disorders, skew deviation, nystagmus, oscillopsia). However, individuals also experience measurable deficits in basic decision-making, short-term memory, concentration, spatial cognition, and depression (9, 13). This can lead to significant decreases in quality of life, lower academic performance in children, and decreased job performance in adults. Even with surgical treatment (dehiscence plugging/resurfacing) these chronic symptoms can be persistent, and recovery can be prolonged. This suggests that central networks undergo maladaptive neural plasticity; however, there has been limited investigation into the vast vestibular projections that integrate with virtually every major cognitive behavioral and sensory system of the brain.

It has been suggested that the vestibular system can be considered a potential window for exploring brain function beyond that of maintenance of balance, and into areas of cognitive, affective and psychiatric symptomology (19). It is known that normal vestibular activity is important for accurate sound localization (20) and higher-order sensorimotor integration at the level of the cortex (21). Indeed, emerging research is also demonstrating that disruption of vestibular input can cause deficits to visuospatial processing, memory, navigation, attention, and executive function (7). To this end, neuropsychology studies before and after surgical management of third window syndrome, including SSCD, have shown that cognitive dysfunction can occur and improve over time (9). We have developed a gerbil model that is accompanied by peripheral measures of impairment (elevated ABR thresholds, increased c+VEMPs amplitudes) that manifest and then resolve as the surgically created SSCD closes by spontaneous osteoneogenesis; resulting in resurfacing of the canal (22). The current study's scientific premise is that by utilizing this experimental model of SSCD we can design experiments that directly investigate the SSCD-induced changes to central plasticity along vestibular and auditory circuits that are associated with cognitive impairments, which then resolve after natural bone regrowth. This approach will allow us to explore the interactions between the vestibular nucleus and the vast integration of their long-range projections to the auditory system through neural recordings taken during behavioral paradigms that test higher order cognition such as decision-making. We found that animals were impaired on both an auditory and visual decision-making task shortly after SSCD, which corresponded with the peak of peripheral impairment that we previously reported (22). As these physiological symptoms return towards baseline, we find a reduction in the impairment; however, inter-animal variability in recovery rates shows that the vestibular component (c+VEMP amplitude) is directly correlated with behavioral impairment and recovery to preoperative levels. Together these results show that our model allows a unique timeline to investigate central cognitive components of vestibular induced impairment and recovery.

Materials and methods

Animals

A total of (33) adult male and female Mongolian gerbils *Meriones unguiculatus* met the inclusion criteria and were used in this study. All animals were housed in the same vivarium facility under a 12/12 dark cycle with *ad libitum* access to food and water. Surgical creation of a 1.5 mm fenestration of the superior (anterior) semicircular canal produced the SSCD. The details of this procedure have been published previously (22). Exclusion criteria included removing any animals with persistent circling or head tilt present at post SSCD day 3 from the study protocol. The Rutgers University IACUC reviewed and approved this research protocol (PROTO202000179).

Auditory brainstem response testing

Animals were anesthetized with isoflurane (1.0%) and placed in a small sound chamber (IAC, Sound Room Solutions, Inc., Glen Cove, NY). Auditory brainstem response (ABR) recordings were made by inserting pin electrodes subcutaneously at the vertex of the skull and just caudal to the right pinna; the ground electrode was inserted into the base of the tail. BioSigRZ software and the TDT ABR system (Tucker-Davis Technologies, Alachua, FL, United States) were used to collect ABR data. A 10-cm tube (closed field) was inserted into the ear

and placed at the opening of the ear canal. The left ear of the animal was stimulated *via* multi-field speaker (MF1, Tucker-Davis Technologies) at 1, 2, 4, 8, and 16 kHz tones (90 to 20 dB SPL [10 dB steps]), 5 ms, 2 ms linear ramp rise-fall times at 25 Hz. Traces were averaged across 500 (threshold) sweeps. Thresholds for each frequency were measured as the last dB SPL, i.e., 10 dB SPL resolution stimulus level, that elicited a tone-induced ABR.

Sound-induced cervical positive potential vestibular evoked myogenic potentials

Sound-induced otolithic stimulation and evoked intramuscular excitatory potential recordings were made by inserting pin electrodes into the neck extensor muscles (splenius capitus m.) and the reference electrode in the vertex of the skull measured (positive cervical vestibular evoked potential [c+VEMP]). BioSigRZ software and the TDT ABR system were used to collect c+VEMP data. A 10-cm tube capable of delivering 100 dB SPL (see TDT specs, Closed Field) was inserted into the ear and placed at the opening of the ear canal. The left ear of the animal was stimulated via multi-field speaker (MF1, Tucker-Davis Technologies) at 2 kHz (100 to 80 dB SPL [5 dB steps], 5 ms, 2 ms linear ramp rise-fall times sampled at 25 kHz). Traces were averaged across 500 (threshold) sweeps. The c+VEMPs were recorded under low-isoflurane anesthesia (<1.5%), near conditions of wakefulness. The c+VEMP was measured when it appeared under the condition of stimulation of air-conducted sound at 2 kHz and 100 dB. Peak amplitudes were measured by subtracting the peak of the negative N1 wave (in μV) from the later positive P1 wave.

Auditory discrimination task

We assessed auditory perceptual skill in gerbils with a positive reinforcement "Go-NoGo" appetitive conditioning paradigm. Briefly, gerbils were placed on controlled access to food and trained to discriminate between amplitude-modulated (AM) broadband noise presented at 4 versus 12 Hz. Gerbils were placed in a behavioral arena test cage housed in a sound attenuation chamber (Med Associates, Inc., Fairfax, VT) and observed via a closed-circuit monitor. Auditory stimuli were presented from a calibrated multifield speaker (MF1, Tucker-Davis Technologies, Alachua, FL, United States) positioned 15 inches above the test cage floor. Sound calibration measurements were made with a 1/4-inch free-field condenser recording microphone (Brüel & Kjær, Nærum, Denmark). A modular pellet dispenser (Med Associates, Inc., [20 mg]) was connected to a trough type pellet receptacle (Med Associates, Inc.) placed within the test cage, and a cylindrical nose port with a 1-inch diameter hole (Med Associates, Inc.) was placed on the opposite side. Sensitive infrared sensors bisected the nose port and pellet receptacles to detect gerbil nose and head entry, respectively. Stimuli, food reward delivery, and behavioral data acquisition were controlled by an iPac computer system running iCon behavioral interfaces (Tucker-Davis Technologies). Gerbils self-initiated trials by placing their nose in the noseport. On each trial, one of two stimulus types were presented. The "Go" stimulus consisted of AM broadband noise (25 dB roll-off at 3.5 and 20 kHz) with a modulation rate of 4 Hz and a modulation depth of 100%. The "NoGo" stimulus for the less difficult ("easy") auditory discrimination task consisted of AM broadband noise presented at a modulation rate of 12 Hz at 100% modulation depth. The NoGo stimulus for the more difficult ("hard") auditory discrimination task consisted of AM broadband noise presented at a modulation rate of 6 Hz at 100% modulation depth. All stimuli were presented at a sound level of 70 dB SPL and was recalibrated daily with a sound level meter. Gerbils were shaped to approach the food troughs upon presentation of the Go stimulus, and received a 20-mg pellet reward. Once gerbils reached a criterion of three consecutive days of 100 trials with >90% Hit (correctly approaching the food trough during a Go trial), they were then trained to repoke upon presentation of the NoGo stimulus. During this phase, NoGo trials (20% probability) were randomly interleaved with Go trials. Gerbils performed the task for at least 120 trials per day, or until over 20 NoGo trials occurred. Typically, a session lasted 45 min to 1 h. This training continued for 10 days.

Trials were scored as Hit, Miss (failing to approach the food trough and repoking during a Go trial), Correct Reject (CR; correctly repoking during a NoGo trial), or False Alarm (FA; incorrectly approaching the food trough on a NoGo trial). Hit and FA rates were constrained to floor (0.05) and ceiling (0.95) values. A performance metric, d-prime was calculated for each session by performing a z-transform of both hit rate and false alarm rate: d-prime = z (Hit rate) − z (FA rate). Criterion was set at d-primes of 1.5. It typically took normal hearing animals 3–4 days to achieve the criterion of d-prime 1.5 when performing the easy auditory discrimination task. It typically takes normal hearing animals 5–6 days to achieve the criterion of d-prime 1.5 when performing the hard auditory discrimination ask.

Visual discrimination task

Visual perceptual skill was assessed with positive reinforcement "Go-NoGo" appetitive conditioning paradigm, similar to that as described for the AM rate auditory discrimination task above. In contrast to the AM rate auditory discrimination task, visual stimuli were delivered from a light-emitting diode (LED; Med Associates, Inc.). The Go stimulus consisted of a flashing LED presented at 4 Hz. The NoGo stimulus for the less difficult ("easy") visual discrimination task consisted of a flashing LED presented at 24 Hz. The NoGo stimulus for the more difficult ("hard") visual discrimination task consisted of a flashing LED presented at 12 Hz. Go and NoGo training were identical to the procedures described for the AM rate auditory discrimination task.

Control (sham surgery) experiments

Control (sham surgery) SSCD animals (n = 4, easy auditory discrimination task; n = 4, easy visual discrimination task) were anesthetized with isoflurane (1.0%) and prepared for stereotaxic surgery. An incision was made over the nuchal muscles on the left side of the head just posterior to the ear. Once exposed the nuchal muscles were sharply and then bluntly dissected to expose the left superior bulla. A 5.0 mm opening was made with a 1.5 mm diamond bur. The intact superior (anterior) semicircular canal was directly visualized but was not fenestrated. The open bulla was then sealed/partitioned with Sterile Silastic (Dow Chemical Company, Midland, MI) to

partition the air-filled bulla from the overlying neck muscles thereby restoring the normal air-filled middle ear and avoiding a true conductive hearing loss. Condensation on the interior surface of the Silastic seal was deemed indicative of this restoration of function. Finally, the reattached muscles were glued to the skull with Medbond tissue glue (Stoelting Co., Wood Dale, IL) which allowed c+VEMP testing after the control (sham surgery) procedure. The incision was closed with a running locked 4-0 Vicryl suture (Ethicon US, LLC, New Brunswick, NJ) and topical antibiotic was applied to the wound. Preoperative c+VEMPs and ABRs were performed and repeated at post day 15. Behavioral training for the easy auditory and visual tasks was completed as described above. The easy auditory discrimination task and visual discrimination task was carried out for the same timeline as the SSCD group (post day 6–15).

Results

In this study we collected behavioral, ABR, and c+VEMP data from 33 male and female Mongolian gerbils. An auditory discrimination task and visual discrimination task was used, and each had two difficulty levels (easy auditory [$n = 7$], hard auditory [$n = 8$], easy visual [$n = 11$], hard visual [$n = 7$]). Of those animals included in this study, 85% ($n = 28$) had no head tilt or circling after surgical creation of the SSCD and 15% ($n = 8$) had head tilt that resolved by post day 3 and before electrophysiologic and behavioral testing beginning on post day 7.

In humans, mild cognitive impairments have been associated with third window syndrome including SSCD prior to surgical treatment. These impairments have been shown to improve after surgery repair. In our recent gerbil SSCD model publication we showed that the site of dehiscence was spontaneously resurfaced *via* osteoneogenesis in the weeks following fenestration which is accompanied by a peak in c+VEMP amplitude and ABR threshold shift at post day 7 that progressively returned towards baseline between post days 14 and 21 (22). The duration required for resurfacing was a function of fenestration size. Therefore, we tracked the relationship between behavioral performance, and physiological measures associated with SSCD diagnostic findings (ABRs, c+VEMPs), and recovery as the SSCD spontaneously resurfaced.

SSCD induced cognitive impairments in an auditory and visual Go-NoGo task

Because there is a mild hearing impairment associated with SSCD we ran an auditory and visual version of the discrimination task to test for modality specific effects on behavioral performance. For each modality (auditory/visual) a hard and easy version of the task was used to identify if task difficulty was a factor in SSCD cognitive impairment. Figure 1 shows the learning curves for both tasks and the behavioral impairments associated with the peak of the ABR threshold shift and c+VEMP amplitude increase (post day 6, 7, 8) and the progressive shift towards baseline as the dehiscence undergoes resurfacing (post day 13, 14, 15). Figure 1A shows the learning curves over 10 days of behavioral testing for both versions and difficulty levels of the task. Criterion was set at a d-prime of 1.5, thus both the easy auditory discrimination task and easy visual discrimination task were learned at the same rate, with a similar delay in learning the more difficult task.

There was no significant difference between the learning rate for the easy auditory discrimination task and easy visual discrimination task [$F(1,16) = 0.57$, $p = 0.45$] or the hard auditory discrimination task and the hard visual discrimination task [$F(1,13) = 0.16$, $p = 0.68$]. Within each task there was a significant difference in the learning rate between the easy and hard task (auditory, [$F(1,13) = 9.43$, $p = 0.0089$]; [$F(1,16) = 5.06$, $p = 0.0389$]). After 10 days of the testing the animals were given surgical fenestrations of the superior (anterior) semicircular canal and allowed to recover for 5 days prior to being returned to the behavioral paradigm. The animals then received 10 more days of testing to create statistical comparisons at the peak of the physiological impairment (post day 7) and during the recovery process (post day 14). Comparing preoperative d-prime performance (training day 8–10) to post day 7 (post days 6–8) and post day 14 performance (post days 13–15) showed a significant main effect of SSCD on behavior [$F(2,294) = 42.28$, $p < 0.0001$] with significant decreases at post day 7 (preoperative 2.77 ± 0.085 vs. post day 7, 1.83 ± 0.074, [$p < 0.0001$]) and post day 14 (preoperative 2.77 ± 0.085 vs. post day 14, 2.5 ± 0.048, [$p = 0.0431$]). When compared by task difficulty the significant decrease at post day 7 remained (easy: preoperative 2.99 ± 0.095 vs. post day 7, 2.15 ± 0.093, [$p < 0.0001$]; hard, preoperative 2.50 ± 0.105 vs. post day 7, 1.44 ± 0.109, [$p < 0.0001$]), while the main effect at post 14 was no longer significant (easy: preoperative 2.99 ± 0.095 vs. post day 14, 2.68 ± 0.094, [$p = 0.059$]; hard, preoperative 2.50 ± 0.105 vs. post day 14, 2.32 ± 0.104, [$p = 0.453$]). We next divided the data by task modality and difficulty for individual comparisons. Figures 1A–D shows the behavioral impairment associated with SSCD for the easy auditory discrimination task, hard auditory discrimination task, easy visual discrimination task, and hard visual discrimination task. There were significant differences between the preoperative behavior and postop day 7 for both tasks and difficulties (easy auditory, preoperative 2.96 ± 0.115 vs. post day 7, 2.45 ± 0.131, [$p = 0.0049$]; hard auditory, preoperative 2.40 ± 0.108 vs. post day 7, 1.41 ± 0.103, [$p < 0.0001$]; easy visual, preoperative 3.01 ± 0.132 vs. post day 7, 1.96 ± 0.123, [$p < 0.0001$]; hard visual, preoperative 2.60 ± 0.190 vs. post day 7, 1.47 ± 0.181, [$p = 0.0003$]). By post day 14 these impairments had largely resolved (easy auditory, preoperative 2.96 ± 0.115 vs. post day 14, 2.63 ± 0.111, [$p = 0.098$]; hard auditory, preoperative 2.40 ± 0.108 vs. post day 14, 2.17 ± 0.103, [$p = 0.297$]; easy visual, preoperative 3.01 ± 0.132 vs. post day 14, 2.72 ± 0.133, [$p = 0.274$]; hard visual, preoperative 2.60 ± 0.190 vs. post day 14, 2.45 ± 0.32, [$p = 0.831$]).

Behavioral metrics associated with cognitive impairments

As previously reported, there are individual variances associated with each animal concerning magnitude of the ABR threshold shifts and changes to c+VEMP amplitudes as the dehiscence is resurfaced *via* spontaneous osteoneogenesis. Therefore, we wanted to see if changes in ABR and c+VEMP properties were correlated with behavioral performance at post day 14. The behavioral measure d-prime is an expression of the ratio of the Hit rate to the FA rate. There are two main factors that can increase or decrease d-prime. Figure 2 shows the factors in this study that contributed to the impairments we report at

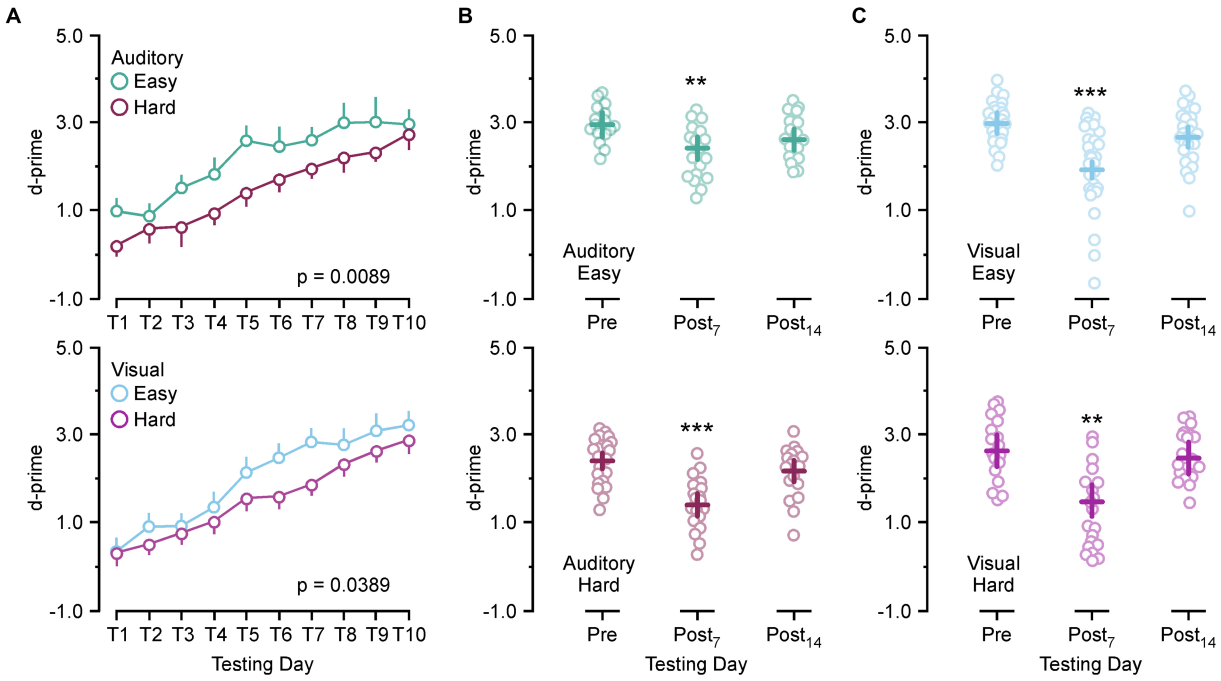

FIGURE 1
Behavioral impairments associated with postoperative days. **(A)** Line plot showing the group learning rates for the easy auditory discrimination task (green) and hard auditory discrimination task (purple) (top) and the easy visual discrimination task (blue) and hard visual discrimination task (purple) (bottom). **(B)** Scatter diagram showing comparisons between preoperative performance and postoperative day 7 ($Postop_7$) and postoperative day 14 ($Postop_{14}$) for the easy auditory discrimination task (green) (top) and hard auditory discrimination task (purple) (bottom). **(C)** Scatter diagram showing comparisons between preoperative performance and postoperative day 7 ($Postop_7$) and postoperative day 14 ($Postop_{14}$) for the easy visual discrimination task (blue) (top) and hard visual discrimination task (purple) (bottom). $^{**}p \leq 0.001$, $^{***}p \leq 0.0001$.

post day 7 and the return towards terminal behavior scores at post day 14. Our results showed d-prime naturally increases for both the easy and hard task as the animals learn to respond correctly [$F(1,35) = 14.72$, $p = 0.0006$] (Figure 2A). A significantly smaller number of trials occurred in the harder task [$F(1,35) = 14.85$, $p = 0.0005$] (Figure 2B). Figure 2C shows that this leads to a smaller Hit rate in the harder task [$F(1,35) = 10.05$, $p = 0.0032$], but similarly decreasing FA rates [$F(1,35) = 0.157$, $p = 0.693$] (Figure 2D).

Figure 3 compares the number of trials performed, Hit rate, and FA rate between preoperative behavior, post day 7, and post day 14 for the easy and hard versions of the auditory discrimination task and the visual discrimination task. In Figure 3A both the easy and the hard auditory discrimination task and the visual discrimination task show a significant reduction in overall trial number at post day 7 (easy, preoperative 202.3 ± 8.2 vs. post day 7, 133.2 ± 7.2, [$p < 0.0001$]; hard, preoperative 136.8 ± 7.53 vs. post day 7, 105.5 ± 5.77, [$p = 0.0109$]) that returned towards baseline at post day 14 (easy, preoperative 202.3 ± 8.2 vs. post day 14, 173.8 ± 8.30, [$p = 0.054$]; hard, preoperative 136.8 ± 7.53 vs. post day 14, 128.8 ± 8.35, [$p = 0.735$]). The same effect is present for the Hit rate in Figure 3B (easy, preoperative 0.97 ± 0.012 vs. post day 7, 0.91 ± 0.075, [$p = 0.0015$]; hard, preoperative 0.96 ± 0.013 vs. post day 7, 0.89 ± 0.035, [$p = 0.0007$]; easy, preoperative 0.97 ± 0.012 vs. post day 14, 0.94 ± 0.011, [$p = 0.126$]; hard, preoperative 0.96 ± 0.013 vs. post day 14, 0.93 ± 0.031, [$p = 0.258$]), and FA rate in Figure 3C (easy, preoperative 0.27 ± 0.019 vs. post day 7, 0.37 ± 0.061, [$p = 0.0303$]; hard, preoperative 0.36 ± 0.031 vs. post day 7, 0.49 ± 0.091, [$p = 0.0141$]; easy, preoperative 0.27 ± 0.012 vs. post day 14, 0.30 ± 0.018, [$p = 0.720$]; hard, preoperative 0.36 ± 0.031 vs. post day 14, 0.33 ± 0.027, [$p = 0.847$]). Overall, the SSCD lowered the number of trials, decreased the Hit rate, and increased the FA rate, suggesting that there was not a single factor driving the impairment.

SSCD induced physiological factors associated with cognitive impairments

Due to the recovery phase of the animals after SSCD and from being food deprived, we did not collect ABR or c+VEMP data at post day 7; however, we did take final recordings at post day 15. Therefore, we tested whether there were specific correlations between ABR thresholds, c+VEMP amplitudes, Hit rates, or FA rates and the last few days of behavioral performance. Figure 4 shows the correlations for the behavioral data at post day 14. Figure 4A illustrates the correlation between ABR thresholds (top) c+VEMP amplitudes (bottom) and d-prime for the auditory and visual discrimination tasks. There was not a significant effect of threshold shift on performance (ABR Threshold [dB] = 0.39–0.05 * behavior (d-prime), adjusted $R^2 = 0.03$, $p = 0.146$); however, there was a significant correlation of c+VEMP amplitude on behavior (c+VEMP amplitude [μV] = 0.75–0.20 * behavior [d-prime], adjusted $R^2 = 0.35$, $p \leq 0.0001$). Despite not having a straightforward group deficit at post day 14, individual differences in animals showed that higher c+VEMP amplitudes at post day 14 were associated with lower performance. Figure 4B shows the correlation between ABR thresholds (top), c+VEMP amplitudes

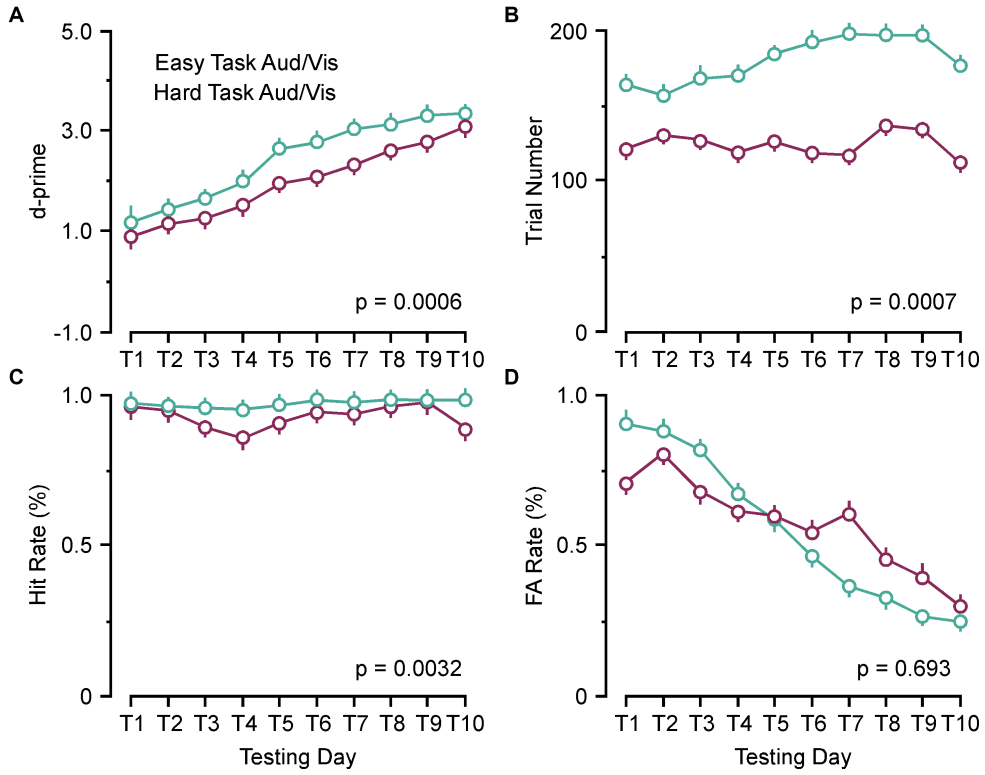

FIGURE 2
Behavioral parameters associated with performance (d-prime). **(A)** Line plots comparing the group learning rates for the pooled easy auditory and visual discrimination tasks (green) and hard auditory and visual discrimination (purple) tasks. **(B)** Line plot comparing the group trial numbers for the pooled easy auditory and visual discrimination tasks (green) and hard auditory and visual discrimination (purple) tasks. **(C)** Line plot comparing the group hit rates for the pooled easy auditory and visual discrimination tasks (green) and hard auditory and visual discrimination (purple) tasks. **(D)** Line plot comparing the group false alarm (FA) rates (%) for the pooled easy auditory and visual discrimination tasks (green) and hard auditory and visual discrimination (purple) tasks. Aud, auditory discrimination task; Vis, visual discrimination task.

(bottom) and Hit rate for the auditory and visual tasks. It should be noted that Hit rate was not affected by either threshold shifts (ABR Threshold [dB] = 0.40–0.146 * Hit Rate [%], adjusted $R^2 = -0.017$, $p = 0.513$) or c+VEMP amplitudes (c+VEMP amplitude [μV] = 0.75–0.52 * Hit rate (%), adjusted $R^2 = 0.033$, $p = 0.156$). However, FA rate was significantly affected by both the threshold shift (ABR Threshold [dB] = 0.182 + 0.287 * FA rate (%), adjusted $R^2 = 0.16$, $p = 0.011$) and the c+VEMP amplitudes (c+VEMP amplitude [μV] = 0.068 + 0.610 * FA rate (%), adjusted $R^2 = 0.28$, $p = 0.0009$; Figure 4C). This suggests that interactions between vestibular dysfunction associated with increased c+VEMP amplitudes can lead to behavioral impairments by influencing FA rates.

Control (sham surgery) experiments

The results of the control (sham surgery) experiments are shown in Table 1; Figure 5. For these analyses we compared data from control (sham surgery) animals ($n = 8$) to SSCD animals at post day 7 (post days 6–8) and post day 14 (post days 13–15) that had completed 10 days of training followed by 10 days of postoperative training in the easy auditory task ($n = 4$) and the easy visual task ($n = 4$; Table 1; Figure 5). There was an additional learning phase in the sham group that led to a significant difference between the sham control and SSCD animals for both the easy discrimination auditory task [$F(1,9) = 18.79$, $p = 0.0019$] and the easy visual discrimination task [$F(1,13) = 4.99$, $p = 0.0436$]. This could suggest that even though the SSCD animals' behavioral performance returns to preoperative levels, that the vestibular impairment might have delayed or possibly prevented the additional learning phase. This additional learning was more prominent in the easy auditory discrimination task compared to the easy visual discrimination task. Further evidence is presented in the statistical comparisons of the behavioral metrics and peripheral ear physiology at post day 7 and post day 14 (Table 1; Figure 5).

For the animals that were run through the easy auditory discrimination task there were highly significant differences in the behavioral metrics at post day 7 and post day 14 when compared to SSCD animals. Sham animals ran significantly more trials at both post day 7 (sham post day 7, 208 ± 15 vs. SSCD post day 7, 143 ± 9 [$p = 0.0007$]) and post day 14 (sham post day 14, 307 ± 24 vs. SSCD post day 14, 155 ± 15 [$p < 0.0001$]). Their d-primes were significantly higher as well at both time points (sham post day 7, 3.04 ± 0.18 vs. SSCD post day 7, 2.42 ± 0.11 [$p = 0.0060$]; sham post day 14, 3.79 ± 0.21 vs. SSCD post day 14, 2.31 ± 0.13 [$p < 0.0001$]). This was driven by significant differences in the FA rates (sham post day 7, 13.3 ± 0.04 vs. SSCD post day 7, 37.8 ± 0.03 [$p < 0.0001$]; sham post day 14, 7.6 ± 0.19 vs. SSCD post day 14, 22.3 ± 0.02 [$p = 0.0022$]) as opposed to the differences in Hit rates (sham post day 7, 94.4 ± 0.04 vs. SSCD post day 7, 91.1 ± 0.02 [$p = 0.489$]; sham post day 14, 91.99 ± 0.008 vs. SSCD post day 14, 96.5 ± 0.005 [$p = 0.021$]), which were only different at post day 14.

10.3389/fneur.2023.1259030

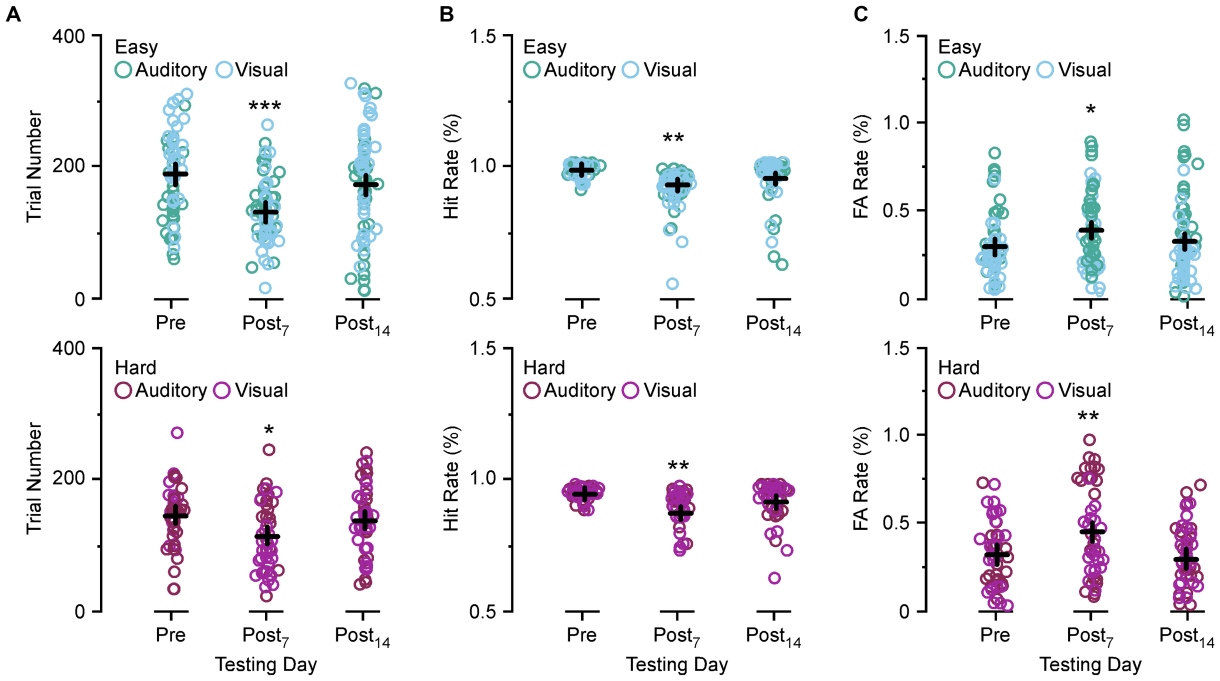

FIGURE 3
Comparison of the trial numbers performed, Hit rate, and false alarm (FA) rate between preoperative and postoperative days. **(A)** Scatter diagram showing group comparisons of average trial numbers performed between preoperative testing and postoperative day 7 and 14 for the easy auditory discrimination task (green) and easy visual discrimination task (blue) (top) and hard auditory discrimination task (red) and hard visual discrimination task (purple) (bottom). **(B)** Scatter diagram showing group comparisons of Hit rate between preoperative testing and postoperative day 7 ($Postop_7$) and postoperative day 14 ($Postop_{14}$) for the easy auditory discrimination task (green) and easy visual discrimination task (blue) (top) and hard visual discrimination task (purple) (bottom). **(C)** Scatter diagram showing group comparisons of average FA rate between preoperative testing and postoperative day 7 ($Postop_7$) and postoperative day 14 ($Postop_{14}$) for the easy auditory discrimination task (green) and easy visual discrimination task (blue) (top) and hard visual discrimination task (purple) (bottom). *$p \leq 0.01$, **$p \leq 0.001$, ***$p \leq 0.0001$.

Performance in the easy visual discrimination task was also better in the sham group; however, the results were not as robust. These sham animals did not run more trials than the SSCD animals at either post day 7 (sham post day 7, 132 ± 17 vs. SSCD post day 7, 122 ± 10 [$p = 0.617$]) or post day 14 (sham post day 14, 192 ± 13 vs. SSCD post day 14, 178 ± 22 [$p = 0.613$]). There were slightly significant increases in d-primes at post day 7 (sham post day 7, 2.43 ± 0.25 vs. SSCD post day 7, 1.96 ± 0.15 [$p = 0.0452$]) and post day 14 (sham post day 14, 3.32 ± 0.20 vs. SSCD post day 14, 2.72 ± 0.12 [$p = 0.018$]), but not nearly as robustly significant as the easy auditory task sham animal d-primes. This was accompanied by slightly significant increases in Hit rate (sham post day 7, 97.3 ± 0.004 vs. SSCD post day 7, 95.2 ± 0.007 [$p = 0.0226$]; sham post day 14, 98.01 ± 0.03 vs. SSCD post day 14, 87.9 ± 0.02 [$p = 0.022$]) and lower FA rates (sham post day 7, 23.9 ± 0.02 vs. SSCD post day 7, 37.3 ± 0.04 [$p = 0.0182$]; sham post day 14, 14.7 ± 0.07 vs. SSCD post day 14, 49.0 ± 0.04 [$p = 0.0005$]) at both postoperative points.

Finally, significant increases in ABR thresholds remained in the SSCD group for both tasks, whereas sham animals showed no real changes from baseline at post day 14 (easy auditory discrimination task; sham post day 14, 3.3 ± 0.02 vs. SSCD post day 14, 31.0 ± 0.01 [$p < 0.0001$]; easy visual discrimination task; sham post day 14, 1.1 ± 0.03 vs. SSCD post day 14, 19.3 ± 0.02 [$p < 0.0001$]). The same trend was present for c+VEMP amplitude measurements (easy auditory task; sham post day 14, 1.1 ± 0.03 vs. SSCD post day 14, 19.3 ± 0.02 [$p < 0.0001$]; easy visual task; sham post day 14, −1.9 ± 0.05 vs. SSCD post day 14, 12.9 ± 0.03 [$p < 0.0001$]). As expected, this suggests that the sham surgery does not impose a change to cochlear or vestibular function.

Discussion

Vestibular function plays a crucial role in decision-making, as it provides ongoing real time feedback about body position, balance, and motion that integrates with auditory, visual, and somatosensory inputs (23–27) to make precise judgements regarding our orientation, velocity, and acceleration in relation to our head/world position in space (28). Together the integration of vestibular information across the central nervous system culminates in the emergence of cognitive processing (29). Conversely, dysfunction of the vestibular system leads to cognitive impairments (30). In this study we used a form of vestibular injury, i.e., SSCD, to ask how decision-making in an associative conditioning task is affected by aberrant asymmetric vestibular output. We found decreases in decision-making performance that were highly correlated with the peak and return towards baseline of ABR and c+VEMP measurements that we previously reported (22) and observed in the current study. The c+VEMP amplitude was specifically and highly correlated with variable recovery and lingering decision-making performance deficits. These were consistent across both a visual and auditory task of varying difficulty.

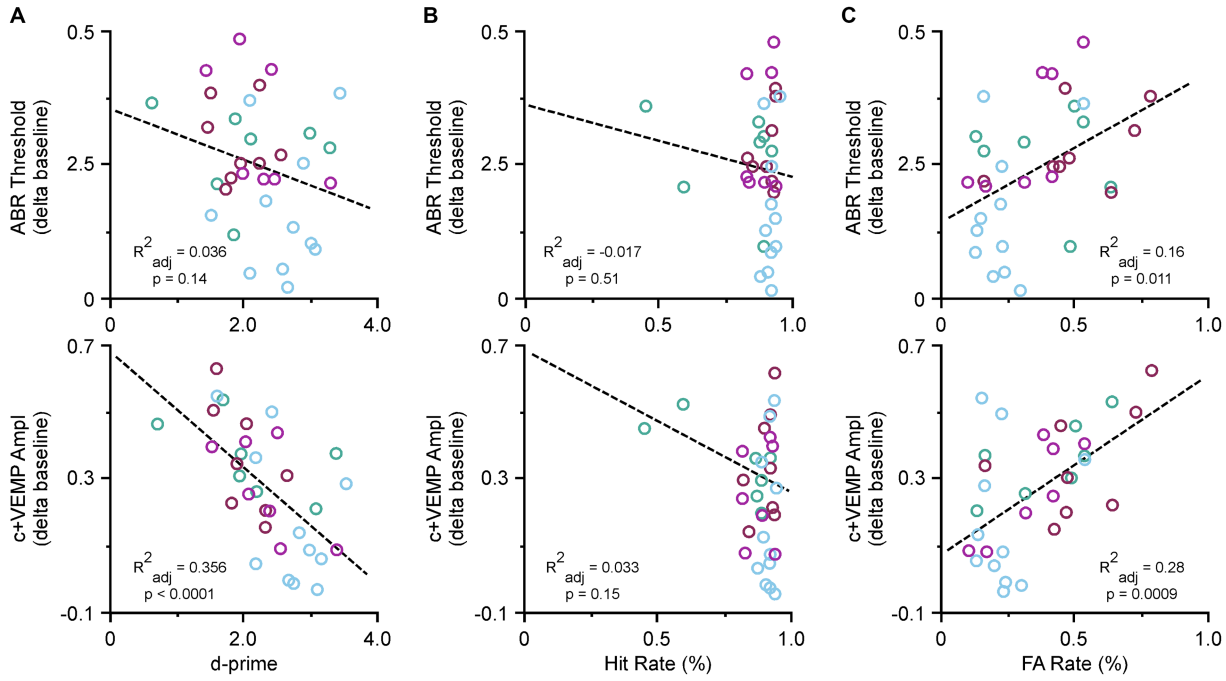

FIGURE 4
Correlations between ABR thresholds, c+VEMP amplitudes, d-primes, hit rates and false alarm (FA) rates. **(A)** Scatter plot showing correlations across all tasks for ABR thresholds and d-primes (easy auditory discrimination task [green] and easy visual discrimination task [blue], and hard auditory discrimination task [red] and hard visual discrimination task [purple]) (top) and c+VEMP amplitudes and d-primes (easy auditory discrimination task [green] and easy visual discrimination task [blue], and hard auditory discrimination task [red] and hard visual discrimination task [purple]) (bottom). **(B)** Scatter plot showing correlations across all tasks for ABR thresholds and hit rates (top) and c+VEMP amplitudes and hit rates (bottom). **(C)** Scatter plot showing correlations across all tasks for ABR thresholds and false alarm (FA) rates (%) (easy auditory discrimination task [green] and easy visual discrimination task [blue], and hard auditory discrimination task [red] and hard visual discrimination task [purple]) (top) and c+VEMP amplitudes and FA rates (easy auditory discrimination task [green] and easy visual discrimination task [blue], and hard auditory discrimination task [red] and hard visual discrimination task [purple]) (bottom).

TABLE 1 **Statistical comparisons between SSCD and sham controls for easy auditory task and easy visual task behavioral metrics and physiology.**

	Easy auditory task post day 7	Easy auditory task post day 14	Easy visual task post day 7	Easy visual task post day 14
d-primes	$p = 0.0060$*	$p < 0.0001$***	$p = 0.0452$*	$p = 0.018$*
Trial number	$p = 0.0007$**	$p \leq 0.0001$***	$p = 0.617$ n.s.	$p = 0.613$ n.s.
Hit rates	$p = 0.489$ n.s.	$p = 0.021$*	$p = 0.0226$*	$p = 0.022$*
False Alarm rates	$p < 0.0001$***	$p = 0.0022$**	$p = 0.0182$*	$p = 0.0005$**
ABR thresholds	NA	$p < 0.0001$***	NA	$p < 0.0001$***
c+VEMP amplitudes	NA	$p < 0.0001$***	NA	$p < 0.0001$***

*$p < 0.05$; **$p < 0.01$; ***$p < 0.001$. ABR, auditory brainstem response; c+VEMP, positive cervical vestibular evoked myogenic potential; NA, not applicable; n.s., not statistically significant; Post, postoperative.

Human cognitive impairment in SSCD and third window syndrome

Previously, there has been controversy over whether there is a direct link between vestibular disorders and certain forms of cognitive impairment (31). However, recent research has shown that the relationship between vestibular function and cognition is incredibly intricate (32, 33), with a high incidence of some form of impairment present in patients with third window syndrome (13, 17, 34–44). In this context, the term "cognitive dysfunction" is being used broadly to refer to characteristics that are not directly influenced by vestibular sensorimotor coupling.

In patients with third window syndrome, including SSCD, cognitive dysfunction is almost always present due to otolithic asymmetry. This is not typically seen in disorders such as benign positional vertigo, vestibular neuronitis, or other rotational receptor dysfunctions (45). Patients with third window syndrome often report cognitive difficulties such as poor memory and concentration, trouble reading, forgetting words, and difficulty expressing themselves. To understand the intricate relationship between vestibular dysfunction and cognitive impairment, we must examine behavioral and anatomical studies in animals. Hitier et al. provide an excellent review of the neuroanatomical pathways from the vestibule to the central nervous system in rodents, cats, and non-human primates (29). Hitier et al. described five major pathways

10.3389/fneur.2023.1259030

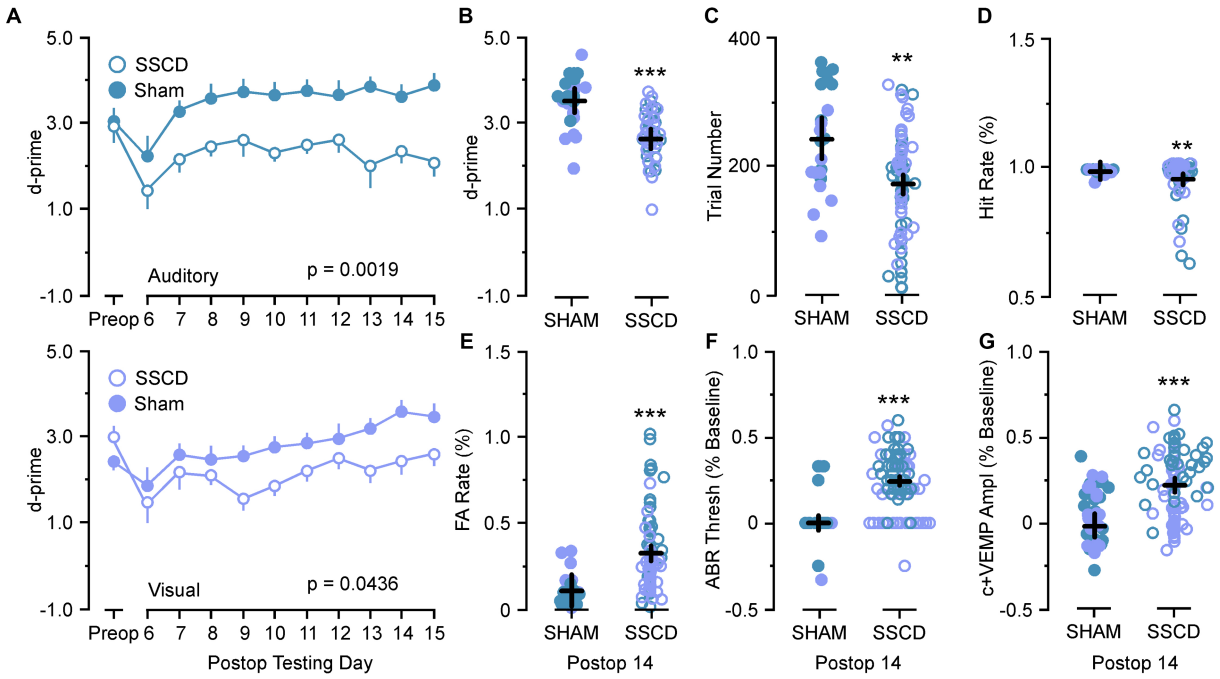

FIGURE 5
Statistical comparisons between SSCD and SSCD sham control animals. **(A)** Line graph comparing behavioral performance (d-prime) between SSCD (open blue) group and control (sham surgery) (solid blue) group for the easy auditory discrimination task across testing days (top). Line graph showing comparing behavioral performance (d-prime) between SSCD (open lavender) and control (sham surgery) (solid lavender) animals for the easy visual discrimination task across testing days (bottom). **(B)** Scatter plot showing the significant increase in d-primes in the control (sham surgery) group (solid colors) over the SSCD group (open colors) at postoperative day 14 (postoperative days 13–15) for both the easy auditory discrimination task (blue) and easy visual discrimination task (lavender). **(C)** Scatter plot showing that the control (sham surgery) group (solid colors) ran consistently more trials in both easy auditory discrimination task (blue) and easy visual discrimination task (lavender) compared to the SSCD group (open colors) at postoperative day 14. **(D)** Scatter plot showing the persistent slight decrease in Hit Rate for the SSCD group (open colors) compared to the control (sham surgery) group (solid colors) for both the easy auditory discrimination task (blue) and the easy visual discrimination task (lavender) at postoperative day 14. **(E)** Scatter plot showing the persistent elevation of false alarm (FA) rates on both the easy auditory discrimination task (blue) and the easy visual discrimination task (lavender) for the SSCD group (open colors) compared to the control (sham surgery) group (solid colors). **(F)** Scatter plot showing the persistent elevation of ABR thresholds for some SSCD animals (open colors) in both the easy auditory discrimination task (blue) and the easy visual discrimination task (lavender) at postoperative day 14 compared to the control (sham surgery) animals (solid colors). **(G)** Scatter plot showing the persistent elevation of c+VEMP amplitudes for some SSCD animals (open colors) in both the easy auditory discrimination task (blue) and the easy visual discrimination task (lavender) at postoperative day 14 compared to the control (sham surgery) animals (solid colors). ABR, auditory brainstem response; c+VEMP, positive cervical vestibular evoked myogenic potential; FA, false alarm; Postop, postoperative; Preop, preoperative; SHAM, control (sham surgery); SSCD, superior semicircular canal dehiscence. $^{**}p < 0.01$, $^{***}p < 0.001$.

that integrate vestibular information throughout the brain, each with a specific function related to spatial learning and memory (29). These include: "(1) a vestibulo-thalamic-cortical pathway for environmental spatial integration, (2) a tegmental-thalamic-entorhinal pathway for calculating head direction, (3) a reticularis pontis oralis-supramammillary-septal pathway to the hippocampus involved with spatial memory and object recognition, (4) a cerebellar-thalamic-cortical pathway that supports spatial learning, and (5) a vestibular-thalamic-striatal pathway that supports spatial learning and memory." The detailed anatomical pathways are beyond the scope of this discussion, but it is clear that vestibular dysfunctions, such as those seen in third window syndrome, will affect normal activity along these pathways, resulting in cognitive impairments. The complexity of the vestibular system's non-classical sensory function has led to debates about the relationship between vestibular function and cognition. In contrast to classic sensory systems like vision, which have modal-specific inputs with straightforward pathways to the cortex *via* the thalamus, the vestibular system's sensory inputs are more complex. The brain regions contain stable receptive fields where sensory stimuli are represented by external maps. These maps are retinotopic, tonotopic, and somatotopic, representing the peripheral receptors of the retina, cochlea, and skin throughout each modality specific neuraxis. Vestibular pathways heavily integrate with these modalities through direct vestibular nucleus projections and multisynaptic pathways to higher-order brain regions in the midbrain and thalamus. The core regions integrate environmental spatial auditory and visual information, proprioceptive somatotopic information, and vestibular information about head direction, angular velocity, and momentum. Vestibular information is continually updated and lacks a classical central topographical map, making it difficult to interpret and study. Although animal research investigating this topic is limited, human data offer interesting clues as to how vestibular dysfunction can cause cognitive impairment.

Behavioral features associated with vestibular function/dysfunction and cognitive impairment

To ask questions about cognition in lower animals such as rodents we turn to behavioral paradigms. Many previous animal

studies have used unilateral labyrinthectomy and other forms of vestibular stimulation to probe the effect of vestibular dysfunction on various behaviors. The effects of vestibular manipulation on simple behaviors such as open field exploration suggest a definite role is spatial exploratory behavior (46, 47), while spatial navigation in the Morris water maze requires vestibular dependent cues (48). Reference memory in a radial arm maze task is significantly impaired by loss of vestibular information (49–51). Vestibular information even seems to be important for non-spatial processes such as object recognition (52). Studies using non-spatial associative conditioning have not been previously used to examine the effect of vestibular dysfunction on decision-making despite large input to the associative conditioning centers of the striatum (53–55). In this study we used a behavioral task with a decision-making component to ask whether superior semicircular canal dehiscence will produce measurable performance deficits. We found that at a postoperative timepoint associated with the peak of the auditory and vestibular physiological disruption (22), 7 days after SSCD, showed significant behavioral impairments to decision-making. Hit rates were lowered, misses were increased, FAs increased, and correct rejections decreased, leading to overall lowering of d-prime performance measures. These results were consistent across task modality (auditory/visual) and difficulty (easy/hard) suggesting a conserved source for the impairment. It further suggests that the raised auditory thresholds in the left ear were not the causative factor in the auditory task impairments. Observation of the animals showed that they were often confused and would go to an adjacent non-used food trough (misses) or would pause and then continue to the correct food trough (FA, NoGo trial). The increased FA rate was specifically correlated with the presence of a lingering increase in c+VEMP amplitude, which were also significantly correlated with lowered d-primes. Animals that had more recovery towards baseline, had lower c+VEMP amplitudes compared to baseline, lower FA rates, and thus higher d-primes. This suggests a clear connection between the decision-making errors which result in false alarms and the asymmetric vestibular dysfunction. This associative conditioning task has cortical dependent properties to it (56) that could suggest that errors in the decision-making could be due to cortical processing errors that are passed down to the striatum. There could also be hippocampal dependent components associated with spatial reference and navigation to the correct food trough, of which vestibular dysfunction disrupts the allocentric and egocentric reference required to navigate the behavioral arena (49, 50). Along these lines, there could be cerebellar aspects to the impairments, as this structure governs features of vestibular mediated spatial navigation (57).

Control (sham surgery) experiments

There was an additional learning phase in the control (sham surgery) group that led to a significant difference between the control (sham surgery) and SSCD groups for both the easy auditory discrimination task and the easy visual discrimination task. This could suggest that even though the SSCD animals' behavioral performance returns to preoperative levels, the vestibular impairment might have delayed or possibly prevented the additional learning phase. This additional learning was more prominent in the easy auditory discrimination task compared to the easy visual discrimination task. Further evidence was presented in the statistical comparisons of the behavioral metrics at post day 7 and post day 14 and the peripheral ear physiology at post day 14 (Table 1; Figure 5). For the control (sham surgery) group that completed the easy auditory discrimination task there were highly significant differences in the behavioral metrics at post day 7 and post day 14 when compared to the SSCD group. Their d-primes were significantly higher as well at both time points (Table 1). This was driven by significant differences in the FA rates as opposed to the differences in Hit rates, which were only different at post day 14. Performance in the easy visual discrimination task was also better in the sham group; however, the results were not as robust. Finally, despite the lack of significance when comparing preoperative to post 14 ABR thresholds, and c+VEMPs in the SSCD animals as a group, the comparisons to control (sham surgery) animals revealed that peripheral physiology was still recovering in the SSCD group.

Gerbils as an ideal model to study SSCD central impairments

Altogether, this model of SSCD induced impairment in gerbils adds a powerful new scientific tool to study the effects of vestibular dysfunction on central circuits involved with learning, memory, behavior, and cognition. There is extensive literature that characterizes gerbil visual and auditory function. The gerbil is a diurnal rodent possessing a retina and cone density that is more similar to humans than those of mice and rats (58), providing excellent motion and depth perception (58–60). For auditory function, gerbils possess robust low frequency hearing, and its audiogram overlaps with the human audiogram (61). This contrasts with more standard rodent models, such as mice and rats, as they possess greater sensitivity over very high frequencies and are limited at low frequencies (62, 63). The gerbil also possesses robust auditory perceptual skill (56, 64–81) that is vulnerable to hearing impairment (71, 75, 76, 82–85). Furthermore, previous work in gerbils also demonstrated that cognitive variables, such as the ability to generalize a learned rule, are vulnerable to hearing loss (86). More recently, the gerbil has been utilized as a model to assess temporal integration, a hallmark of cognitive function, during auditory decision-making (80, 84, 87). Thus, the gerbil is a suitable animal model for assessing cognitive function, particularly across visual and auditory domains.

An important issue with this animal model, in the context of measuring cognitive dysfunction/impaired decision-making, is the question of when the acute vestibular injury induced by surgically creating the SSCD becomes a chronic intermittent vestibular asymmetry. With acquired SSCD in patients, at some point the dehiscence is an acute change and because of the longstanding presence of the dehiscence, patients experience a chronic intermittent vestibular asymmetry. While the timeline for transition from acute injury to chronic condition in our gerbil model that parallels the human experience is unknown, in general rodent timelines are more rapid than in humans, as is the development milestones, aging and shorter life expectancy. We do not know the how the gerbil development timeline maps to that of humans; however, we do know that in adult rats, every day of the animal is approximately equivalent to 34.8 human days (88). It is known that in gerbils with unilateral

labyrinthectomy (a more severe acute vestibular injury), vestibular compensation with vision shows improved vestibulo-ocular reflex (VOR) just 24 h after labyrinthectomy (89). Thus, we expect that any acute vestibular injury had resolved by post day 7. To minimize effects due to acute vestibular injury, our exclusion criteria included removing animals from the protocol that had persistent circling or head tilt present at post SSCD day 3. Of those animals included in this study ($n = 33$), 85% ($n = 28$) had no head tilt or circling after surgical creation of the SSCD and 15% ($n = 8$) had head tilt that resolved by post day 3 and before electrophysiologic and behavioral testing beginning on post day 7. We know from previous studies that the surgically created SSCD resurfaces *via* spontaneous osteoneogenesis by post day 14 (22), and our electrophysiologic and behavioral results in this study suggest that the SSCD also closed by post day 14.

To enhance our comprehension of the effects of the vestibular system on behavior, cognition, and symptomatology in central brain processes, it is essential to systematically investigate analogous animal models of vestibular dysfunction. This approach will allow us to create experiments that reproduce the peripheral causes of vestibular dysfunction and explore central alterations along the five pathways outlined earlier (29). Recently, our team has developed a gerbil model of third window syndrome that will serve as a foundation for a thorough examination of the symptomatology patients with SSCD experience (22). This model involves creating a fenestration in the superior semicircular canal that produces an inner ear/otic capsule-conductive hearing loss and sound-evoked changes in vestibular evoked myogenic potentials (c+VEMPs) similar to what is seen in humans with third window syndrome due to SSCD. As reported herein, this model also displays substantial reversible impairments in decision-making, which we can use to investigate the maladaptive central plasticity resulting from vestibular injury that leads to cognitive dysfunction. This eliminates the need for a second surgical intervention to plug the SSCD, offering us an experimental window to carry out electrophysiological and behavioral studies to evaluate decision-making as a proxy for cognitive dysfunction. This model will also aid in determining the precise vestibular contributions of the five primary neuroanatomical pathways described earlier (29) and assist in understanding the central plasticity resulting from SSCD. Advanced tools such as adeno-associated viruses (e.g., optogenetics; ChR2, DREADDs; HM4Di), along with improvements in awake behaving neurophysiology and *in vitro* whole-cell recording, can be employed to isolate and manipulate specific brain circuits selectively. This will allow us to pose highly informative questions about the effect of vestibular function on physiology (e.g., balance), emotional states (e.g., anxiety, fear), and cognitive-behavioral processes. By unraveling the intricacies of vestibular influence on central brain function, we should obtain new insights into the etiology of symptomatology in humans that will hopefully result in new treatment approaches for chronic third window syndrome symptoms and other vestibular-related conditions in the years ahead.

Conclusion

Vestibular dysfunction in humans is associated with cognitive deficits that can lead to greatly reduced quality of life. Fortunately, treatments do exist for disorders such as SSCD, that involve surgical plugging or resurfacing the site of dehiscence. To enhance our understanding of how vestibular function affects behavior, cognition, and the central brain processes, it is necessary to systematically investigate vestibular disorders in animal models that are analogous to humans. Unlike humans who require surgical intervention, a particularly novel aspect of this SSCD model is the fenestration self-closure of the surgically created SSCD through spontaneous osteoneogenesis (22). This allows us the unique opportunity to study both impairment and recovery. We can also exploit this feature of the model to determine if there are persistent changes to central plasticity after recovery from injury. Herein, we report for the first-time, higher order associative decision-making impairments related to aberrant asymmetric vestibular output in an animal model of SSCD. These impairments resolve as the bone resurfaces *via* spontaneous osteoneogenesis; providing a unique window to study decision-making errors and their resolution. We can exploit this timeframe to design experiments that replicate the peripheral causes of vestibular dysfunction in SSCD and examine the central changes that underlie this dysfunction along many different brain circuits that receive vestibular inputs. We hope to expand these results in future experiments that study many of the circuits along which auditory, visual, and vestibular pathways integrate to drive learning, behavior, and higher-order cognition.

Data availability statement

The raw data supporting the conclusions of this article will be made available by the authors, without undue reservation.

Ethics statement

The animal study was approved by the Rutgers University IACUC reviewed and approved this research protocol (PROTO202000179). The study was conducted in accordance with the local legislation and institutional requirements.

Author contributions

TMM: Conceptualization, Data curation, Formal analysis, Funding acquisition, Investigation, Methodology, Project administration, Resources, Software, Supervision, Validation, Visualization, Writing – original draft, Writing – review & editing. PAW: Conceptualization, Data curation, Formal analysis, Funding acquisition, Investigation, Methodology, Project administration, Resources, Software, Supervision, Validation, Visualization, Writing – original draft, Writing – review & editing. JN: Data curation, Formal analysis, Writing – review & editing. ED: Data curation, Formal analysis, Writing – review & editing. RDS: Data curation, Formal analysis, Writing – review & editing. AT: Data curation, Formal analysis, Writing – review & editing. NLC: Data curation, Formal analysis, Writing – review & editing. MAB: Data curation, Formal analysis, Writing – review & editing. SSH: Writing – review & editing, Data curation, Formal analysis. JDY: Formal analysis, Validation, Writing – original draft, Writing – review & editing.

Funding

The author(s) declare financial support was received for the research, authorship, and/or publication of this article. The Rutgers Biomedical Health Sciences Chancellor Scholar Award to PAW provided funding to help support this work.

Conflict of interest

The authors declare that the research was conducted in the absence of any commercial or financial relationships that could be construed as a potential conflict of interest.

The author(s) declared that they were an editorial board member of Frontiers, at the time of submission. This had no impact on the peer review process and the final decision.

Publisher's note

References

1. Xie Y, Bigelow RT, Frankenthaler SF, Studenski SA, Moffat SD, Agrawal Y. Vestibular loss in older adults associated with impaired spatial navigation: data from the triangle completion task. *Front Neurol.* (2017) 8:173. doi: 10.3389/fneur.2017.00173

2. Kremmyda O, Hüfner K, Flanagin VL, Hamilton DA, Linn J, Strupp M. Beyond dizziness: virtual navigation, spatial anxiety and hippocampal volume in bilateral vestibulopathy. *Front Hum Neurosci.* (2016) 10:139. doi: 10.3389/fnhum.2016.00139

3. Guidetti G, Guidetti R, Manfredi M, Manfredi M. Vestibular pathology and spatial working memory. *Acta Otorhinolaryngol Ital.* (2020) 40:72–8. doi: 10.14639/0392-100X-2189

4. Smith L, Wilkinson D, Bodani M, Bicknell R, Surenthiran SS. Short-term memory impairment in vestibular patients can arise independently of psychiatric impairment, fatigue, and sleeplessness. *J Neuropsychol.* (2019) 13:417–31. doi: 10.1111/jnp.12157

5. Popp P, Wulff M, Finke K, Rühl M, Brandt T, Dieterich M. Cognitive deficits in patients with a chronic vestibular failure. *J Neurol.* (2017) 264:554–63. doi: 10.1007/s00415-016-8386-7

6. Ayar DA, Kumral E, Celebisoy N. Cognitive functions in acute unilateral vestibular loss. *J Neurol.* (2020) 267:153–9. doi: 10.1007/s00415-020-09829-w

7. Bigelow RT, Semenov YR, Trevino C, Ferrucci L, Resnick SM, Simonsick EM, et al. Association between visuospatial ability and vestibular function in the Baltimore longitudinal study of aging. *J Am Geriatr Soc.* (2015) 63:1837–44. doi: 10.1111/jgs.13609

8. Dobbels B, Mertens G, Gilles A, Claes A, Moyaert J, van de Berg R, et al. Cognitive function in acquired bilateral vestibulopathy: a cross-sectional study on cognition, hearing, and vestibular loss. *Front Neurosci.* (2019) 13:340. doi: 10.3389/fnins.2019.00340

9. Wackym PA, Balaban CD, Mackay HT, Wood SJ, Lundell CJ, Carter DM, et al. Longitudinal cognitive and neurobehavioral functional outcomes after repairing otic capsule dehiscence. *Otol Neurotol.* (2016) 37:70–82. doi: 10.1097/MAO.0000000000000928

10. Chari DA, Liu YH, Chung JJ, Rauch SD. Subjective cognitive symptoms and dizziness handicap inventory (DHI) performance in patients with vestibular migraine and Menière's disease. *Otol Neurotol.* (2021) 42:883–9. doi: 10.1097/MAO.0000000000003081

11. Liu YF, Locklear TD, Sharon JD, Lacroix E, Nguyen SA, Rizk HG. Quantification of cognitive dysfunction in dizzy patients using the neuropsychological vertigo inventory. *Otol Neurotol.* (2019) 40:e723–31. doi: 10.1097/MAO.0000000000002311

12. Eraslan Boz H, Kırkım G, Koçoğlu K, Çakır Çetin A, Akkoyun M, Güneri EA, et al. Cognitive function in Meniere's disease. *Psychol Health Med.* (2023) 28:1076–86. doi: 10.1080/13548506.2022.2144637

13. Wackym PA, Balaban CD, Zhang P, Siker DA, Hundal JS. Third window syndrome: surgical management of cochlea-facial dehiscence. *Front Neurol.* (2019) 10:1281. doi: 10.3389/fneur.2019.01281

14. Iversen MM, Rabbitt RD. Biomechanics of third window syndrome. *Front Neurol.* (2020) 11:891. doi: 10.3389/fneur.2020.00891

15. Carey JP, Minor LB, Nager GT. Dehiscence or thinning of bone overlying the superior semicircular canal in a temporal bone survey. *Arch Otolaryngol Head Neck Surg.* (2000) 26:137–47. doi: 10.1001/archotol.126.2.137

16. Minor LB. Clinical manifestations of superior semicircular canal dehiscence. *Laryngoscope.* (2005) 115:1717–27. doi: 10.1097/01.mlg.0000178324.55729.b7

17. Ward BK, Carey JP, Minor LB. Superior canal dehiscence syndrome: lessons from the first 20 years. *Front Neurol.* (2017) 8:177. doi: 10.3389/fneur.2017.00177

18. Wackym PA, Agrawal Y, Ikezono T, Balaban CD. Editorial: third window syndrome. *Front Neurol.* (2021) 12:704095. doi: 10.3389/fneur.2021.704095

19. Gurvich C, Maller JJ, Lithgow B, Haghgooie S, Kulkarni J. Vestibular insights into cognition and psychiatry. *Brain Res.* (2013) 1537:244–59. doi: 10.1016/j.brainres.2013.08.058

20. Lewald J, Karnath HO. Vestibular influence on human auditory space perception. *J Neurophysiol.* (2000) 84:1107–11. doi: 10.1152/jn.2000.84.2.1107

21. Oh S-Y, Boegle R, Ertl M, Stephan T, Dieterich M. Multisensory vestibular, vestibular-auditory, and auditory network effects revealed by parametric sound pressure stimulation. *NeuroImage.* (2018) 1:354–63. doi: 10.1016/j.neuroimage.2018.04.057

22. Wackym PA, Balaban CD, Van Osch OJ, Morris BT, Tamakloe M-A, Salvatore VL, et al. New model of superior semicircular canal dehiscence with reversible diagnostic findings characteristic of patients with the disorder. *Front Neurol.* (2023) 13:1035478. doi: 10.3389/fneur.2022.1035478

23. Bakker RS, Selen LPJ, Medendorp WP. Transformation of vestibular signals for the decisions of hand choice during whole body motion. *J Neurophysiol.* (2019) 121:2392–400. doi: 10.1152/jn.00470.2018

24. Genzel D, Firzlaff U, Wiegrebe L, Mac Neilage PR. Dependence of auditory spatial updating on vestibular, proprioceptive, and efference copy signals. *J Neurophysiol.* (2016) 116:765–75. doi: 10.1152/jn.00052.2016

25. Rincon-Gonzalez L, Selen LP, Halfwerk K, Koppen M, Corneil BD, Medendorp WP. Decisions in motion: vestibular contributions to saccadic target selection. *J Neurophysiol.* (2016) 116:977–85. doi: 10.1152/jn.01071.2015

26. Gao W, Lin Y, Shen J, Han J, Song X, Lu Y, et al. Diverse effects of gaze direction on heading perception in humans. *Cereb Cortex.* (2023) 2:bhac 541. doi: 10.1093/cercor/bhac541

27. Goel R, De Dios YE, Gadd NE, Caldwell EE, Peters BT, Reschke MF, et al. Assessing somatosensory utilization during unipedal postural control. *Front Syst Neurosci.* (2017) 11:21. doi: 10.3389/fnsys.2017.00021

28. Mac Neilage PR, Banks MS, DeAngelis GC, Angelaki DE. Vestibular heading discrimination and sensitivity to linear acceleration in head and world coordinates. *J Neurosci.* (2010) 30:9084–94. doi: 10.1523/JNEUROSCI.1304-10.2010

29. Hitier M, Besnard S, Smith PF. Vestibular pathways involved in cognition. *Front Integr Neurosci.* (2014) 8:59. doi: 10.3389/fnint.2014.00059

30. Chari DA, Madhani A, Sharon JD, Lewis RF. Evidence for cognitive impairment in patients with vestibular disorders. *J Neurol.* (2022) 269:5831–42. doi: 10.1007/s00415-022-11289-3

31. Gizzi M, Zlotnick M, Cicerone K, Riley E. Vestibular disease and cognitive dysfunction: no evidence for a causal connection. *J Head Trauma Rehabil.* (2003) 18:398–407. doi: 10.1097/00001199-200309000-00002

32. Ferrè ER, Haggard P. Vestibular cognition: state-of-the-art and future directions. *Cogn Neuropsychol.* (2020) 37:413–20. doi: 10.1080/02643294.2020.1736018

33. Smith PF. The vestibular system and cognition. *Curr Opin Neurol.* (2017) 30:84–9. doi: 10.1097/WCO.0000000000000403

34. Wackym PA. Right Perilymph Fistula Not Superior Canal Dehiscence. Patient Video Describing Symptoms Before and After Surgical Repair; (2023). Available at: https://www.youtube.com/watch?v=bDph0B0uLbg. (Accessed September 15, 2023)

35. Wackym PA. Right Cochlea-Facial Nerve Dehiscence: 16 Year Old Thought to Have Conversion Disorder; (2019). Available at: https://youtu.be/fTjsnnUALBw. (Accessed September 15, 2023)

36. Wackym PA. Perilymph Fistula; (2012). Available at: https://www.youtube.com/watch?v=jSAM6h-7Mwc. (Accessed September 15, 2023)

37. Wackym PA. Right Superior Semicircular Canal Dehiscence Repair: Symptoms and Recovery; (2017). Available at: https://youtu.be/er4k8NZrG2I. (Accessed September 15, 2023)

38. Wackym PA. Recurrent Third Window Syndrome Co-Morbidity: Functional Neurological Symptom Disorder; (2017). Available at: https://youtu.be/AgUy07QxTxo. (Accessed September 15, 2023)

39. Wackym PA. Otic Capsule Dehiscence Syndrome in One Ear After a Car Accident; (2015). Available at: https://www.youtube.com/watch?v=1Nl9T6etxqM. (Accessed September 15, 2023)

40. Wackym PA. Cochlea-Facial Nerve Dehiscence: Traumatic Third Window Syndrome After a Snowboarding Accident; (2019). Available at: https://youtu.be/NCDMD5FGf-w. (Accessed September 15, 2023)

41. Wackym PA. Surgery for Cochlea-Facial Nerve Dehiscence: Symptoms and Tuning Fork Testing; (2019). Available at: https://youtu.be/lFR-zdYlIsY. (Accessed September 15, 2023)

42. Wackym PA. Tuning Fork Testing in Otic Capsule Dehiscence Syndrome; (2015). Available at: https://www.youtube.com/watch?v=Szp_kO8oVos. (Accessed September 15, 2023)

43. Wackym PA. Tuning Fork Testing Before and After Repair of Two Types of Otic Capsule Dehiscence; (2015). Available at: https://www.youtube.com/watch?v=NIauJPbvSpA. (Accessed September 15, 2023)

44. Wackym PA. Vestibular Migraine. Patient Video Describing Symptoms Before and After Treatment with Topamax; (2012). https://www.youtube.com/watch?v=Zy7YjCDnLYM. (Accessed September 15, 2023)

45. Demirhan MA, Celebisoy N. Cognitive functions in episodic vestibular disorders: Meniere's disease and vestibular migraine. *J Vestib Res*. (2023) 33:63–70. doi: 10.3233/VES-220025

46. Porter JD, Pellis SM, Meyer ME. An open-field activity analysis of labyrinthectomized rats. *Physiol Behav*. (1990) 48:27–30. doi: 10.1016/0031-9384(90)90255-3

47. Banovetz MT, Lake RI, Blackwell AA, Oltmanns JR, Schaeffer EA, Yoder RM, et al. Effects of acquired vestibular pathology on the organization of mouse exploratory behavior. *Exp Brain Res*. (2021) 239:1125–39. doi: 10.1007/s00221-020-06032-1

48. Clark BJ, Hong NS, Bettenson DJ, Woolford J, Horwood L, McDonald RJ. Maintained directional navigation across environments in the Morris water task is dependent on vestibular cues. *J Exp Psychol Anim Learn Cogn*. (2015) 41:301–8. doi: 10.1037/xan0000066

49. Russell NA, Horii A, Smith PF, Darlington CL, Bilkey DK. Bilateral peripheral vestibular lesions produce long-term changes in spatial learning in the rat. *J Vestib Res*. (2003) 13:9–16. doi: 10.3233/VES-2003-13102

50. Russell NA, Horii A, Smith PF, Darlington CL, Bilkey DK. Long-term effects of permanent vestibular lesions on hippocampal spatial firing. *J Neurosci*. (2003) 23:6490–8. doi: 10.1523/JNEUROSCI.23-16-06490.2003

51. Ossenkopp KP, Hargreaves EL. Spatial learning in an enclosed eight-arm radial maze in rats with sodium arsanilate-induced labyrinthectomies. *Behav Neural Biol*. (1993) 59:253–7. doi: 10.1016/0163-1047(93)91034-k

52. Zheng Y, Darlington CL, Smith PF. Bilateral labyrinthectomy causes long-term deficit in object recognition in rat. *Neuroreport*. (2004) 15:1913–6. doi: 10.1097/00001756-200408260-00016

53. Kato S, Nishizawa K, Kobayashi K. Thalamostriatal system controls the acquisition, performance, and flexibility of learning behavior. *Front Syst Neurosci*. (2021) 15:729389. doi: 10.3389/fnsys.2021.729389

54. Stiles L, Smith PF. The vestibular–basal ganglia connection: balancing motor control. *Brain Res*. (2015) 1597:180–8. doi: 10.1016/j.brainres.2014.11.063

55. Sabzevar FT, Vautrelle N, Zheng Y, Smith PF. Vestibular modulation of the tail of the rat striatum. *Sci Reports*. (2023) 13:4443. doi: 10.1038/s41598-023-31289-1

56. Paraouty N, Mowery TM. Early sensory deprivation leads to differential inhibitory changes in the striatum during learning. *Front Neural Circuits*. (2021) 15:670858. doi: 10.3389/fncir.2021.670858

57. Zachou A, Bronstein AM. Vestibulo-spatial navigation: pathways and sense of direction. *J Neurophysiol*. (2023) 129:672–84. doi: 10.1152/jn.00422.2022

58. Yang S, Luo X, Xiong G, So KF, Yang H, Xu Y. The electroretinogram of Mongolian gerbil (*Meriones unguiculatus*): comparison to mouse. *Neurosci Lett*. (2015) 589:7–12. doi: 10.1016/j.neulet.2015.01.018

59. Baker AG, Emerson VF. Grating acuity of the Mongolian gerbil (*Meriones unguiculatus*). *Behav Brain Res*. (1983) 8:195–209. doi: 10.1016/0166-4328(83)90054-2

60. Jacobs GH, Deegan JF 2nd. Sensitivity to ultraviolet light in the gerbil (*Meriones unguiculatus*): characteristics and mechanisms. *Vis Res*. (1994) 34:1433–41. doi: 10.1016/0042-6989(94)90144-9

61. Garbers C, Henke J, Leibold C, Wachtler T, Thurley K. Contextual processing of brightness and color in Mongolian gerbils. *J Vis*. (2015) 15:13–4. doi: 10.1167/15.1.13

62. Kelly JB, Masterton B. Auditory sensitivity of the albino rat. *J Comp Psychol (Baltim)*. (1977) 91:930–6. doi: 10.1037/h0077356

63. Radziwon KE, June KM, Stolzberg DJ, Xu-Friedman MA, Salvi RJ, Dent ML. Behaviorally measured audiograms and gap detection thresholds in CBA/CaJ mice. *J Comp Physiol*. (2009) 195:961–9. doi: 10.1007/s00359-009-0472-1

64. Ohl FW, Wetzel W, Wagner T, Rech A, Scheich H. Bilateral ablation of auditory cortex in Mongolian gerbil affects discrimination of frequency modulated tones but not of pure tones. *Learning Memory*. (1999) 6:347–62. doi: 10.1101/lm.6.4.347

65. Ohl FW, Scheich H, Freeman WJ. Change in pattern of ongoing cortical activity with auditory category learning. *Nature*. (2001) 412:733–6. doi: 10.1038/35089076

66. Wagner E, Klump GM, Hamann I. Gap detection in Mongolian gerbils (*Meriones unguiculatus*). *Hear Res*. (2003) 176:11–6. doi: 10.1016/S0378-5955(02)00643-3

67. Hamann I, Gleich O, Klump GM, Kittel MC, Strutz J. Age-dependent changes of gap detection in the Mongolian gerbil (*Meriones unguiculatus*). *J Assoc Res Otolaryngol*. (2004) 5:49–57. doi: 10.1007/s10162-003-3041-2

68. Maier JK, Klump GM. Resolution in azimuth sound localization in the Mongolian gerbil (*Meriones unguiculatus*). *J Acoust Soc Am*. (2006) 119:1029–36. doi: 10.1121/1.2159429

69. Gleich O, Hamann I, Kittel MC, Klump GM, Strutz J. A quantitative analysis of psychometric functions for different auditory tasks in gerbils. *Hear Res*. (2006) 220:27–37. doi: 10.1016/j.heares.2006.06.014

70. Wetzel W, Ohl FW, Scheich H. Global versus local processing of frequency-modulated tones in gerbils: an animal model of lateralized auditory cortex functions. *Proc Natl Acad Sci U S A*. (2008) 105:6753–8. doi: 10.1073/pnas.0707844105

71. Buran BN, von Trapp G, Sanes DH. Behaviorally gated reduction of spontaneous discharge can improve detection thresholds in auditory cortex. *J Neurosci*. (2014) 34:4076–81. doi: 10.1523/JNEUROSCI.4825-13.2014

72. Buran BN, Sarro EC, Manno FA, Kang R, Caras ML, Sanes DH. A sensitive period for the impact of hearing loss on auditory perception. *J Neurosci*. (2014) 34:2276–84. doi: 10.1523/JNEUROSCI.0647-13.2014

73. Sarro EC, von Trapp G, Mowery TM, Kotak VC, Sanes DH. Cortical synaptic inhibition declines during auditory learning. *J Neurosci*. (2015) 35:6318–25. doi: 10.1523/JNEUROSCI.4051-14.2015

74. von Trapp G, Buran BN, Sen K, Semple MN, Sanes DH. A decline in response variability improves neural signal detection during auditory task performance. *J Neurosci*. (2016) 36:11097–106. doi: 10.1523/JNEUROSCI.1302-16.2016

75. Caras ML, Sanes DH. Top-down modulation of sensory cortex gates perceptual learning. *Proc Natl Acad Sci U S A*. (2017) 114:9972–7. doi: 10.1073/pnas.1712305114

76. Caras ML, Sanes DH. Neural variability limits adolescent skill learning. *J Neurosci*. (2019) 39:2889–902. doi: 10.1523/JNEUROSCI.2878-18.2019

77. Tolnai S, Beutelmann R, Klump GM. Exploring binaural hearing in gerbils (*Meriones unguiculatus*) using virtual headphones. *PLoS One*. (2017) 12:e0175142. doi: 10.1371/journal.pone.0175142

78. Mowery TM, Caras ML, Hassan SI, Wang DJ, Dimidschstein J, Fishell G, et al. Preserving inhibition during developmental hearing loss rescues auditory learning and perception. *J Neurosci*. (2019) 39:8347–61. doi: 10.1523/JNEUROSCI.0749-19.2019

79. Eipert L, Klump GM. Uncertainty-based informational masking in a vowel discrimination task for young and old Mongolian gerbils. *Hear Res*. (2020) 392:107959. doi: 10.1016/j.heares.2020.107959

80. Yao JD, Sanes DH. Temporal encoding is required for categorization, but not discrimination. *Cereb Cortex*. (2021) 31:2886–97. doi: 10.1093/cercor/bhaa396

81. Jüchter C, Beutelmann R, Klump GM. Speech sound discrimination by Mongolian gerbils. *Hear Res*. (2022) 418:108472. doi: 10.1016/j.heares.2022.108472

82. Rosen MJ, Sarro EC, Kelly JB, Sanes DH. Diminished behavioral and neural sensitivity to sound modulation is associated with moderate developmental hearing loss. *PLoS One*. (2012) 7:e41514. doi: 10.1371/journal.pone.0041514

83. Ihlefeld A, Chen YW, Sanes DH. Developmental conductive hearing loss reduces modulation masking release. *Trends Hear*. (2016) 20:2331216516676255. doi: 10.1177/2331216516676255

84. Yao JD, Sanes DH. Developmental deprivation-induced perceptual and cortical processing deficits in awake-behaving animals. *elife*. (2018) 7:e33891. doi: 10.7554/eLife.33891

85. Anbuhl KL, Yao JD, Hotz RA, Mowery TM, Sanes DH. Auditory processing remains sensitive to environmental experience during adolescence in a rodent model. *Nat Commun*. (2022) 13:2872. doi: 10.1038/s41467-022-30455-9

86. von Trapp G, Aloni I, Young S, Semple MN, Sanes DH. Developmental hearing loss impedes auditory task learning and performance in gerbils. *Hear Res*. (2017) 347:3–10. doi: 10.1016/j.heares.2016.07.020

87. Yao JD, Zemlianova KO, Hocker DL, Savin C, Constantinople CM, Chung S, et al. Transformation of acoustic information to sensory decision variables in the parietal cortex. *Proc Natl Acad Sci U S A*. (2023) 120:e2212120120. doi: 10.1073/pnas.2212120120

88. Sengupta P. The laboratory rat: relating its age with human's. *Int J Prev Med*. (2013) 4:624–30.

89. Shinder ME, Perachio AA, Kaufman GD. VOR and Fos response during acute vestibular compensation in the Mongolian gerbil in darkness and in light. *Brain Res*. (2005) 1038:183–97. doi: 10.1016/j.brainres.2005.01.043

frontiers | Frontiers in Neurology

TYPE Case Report
PUBLISHED 19 October 2023
DOI 10.3389/fneur.2023.1276991

OPEN ACCESS

EDITED BY
Todd Mowery,
The State University of New Jersey,
United States

REVIEWED BY
Francesco Comacchio,
University Hospital Sant'Antonio, Italy
Han Matsuda,
Saitama Medical University, Japan

*CORRESPONDENCE
Yusuke Ito
ito_yusuke0728@yahoo.co.jp

RECEIVED 13 August 2023
ACCEPTED 02 October 2023
PUBLISHED 19 October 2023

CITATION
Ito Y, Seo T, Sasano Y, Mochizuki F and Koizuka I (2023) Perilymphatic fistula with characteristic findings of the inner ear by contrast-enhanced magnetic resonance imaging: a case report.
Front. Neurol. 14:1276991.
doi: 10.3389/fneur.2023.1276991

Perilymphatic fistula with characteristic findings of the inner ear by contrast-enhanced magnetic resonance imaging: a case report

Yusuke Ito[1]*, Toru Seo[2], Yoshiyuki Sasano[1], Fumihiro Mochizuki[1,3] and Izumi Koizuka[1]

[1]Department of Otolaryngology, St. Marianna University School of Medicine, Kawasaki, Japan,
[2]Department of Otolaryngology, St. Marianna University Yokohama Seibu Hospital, Yokohama, Japan,
[3]Department of Otolaryngology, University of Miami Miller School of Medicine, Miami, FL, United States

A perilymphatic fistula (PLF) presents with abnormal traffic in the otic capsule, causing cochlear and vestibular symptoms. However, the mechanisms underlying symptom recurrence remain controversial. Herein, we report the case of a 27-year-old female who complained of hearing disturbance in her right ear and recurrent vertigo after sudden onset of hearing loss with vertigo. The caloric test revealed unilateral weakness in the right ear, and the video head impulse test (vHIT) showed decreased vestibulo-ocular reflex (VOR) gain. Contrast-enhanced magnetic resonance imaging (MRI) using hybrid of reversed image of positive endolymph signal and negative image of perilymph signal (HYDROPS) indicated a collapsed endolymphatic space. As the vestibular symptoms did not improve, an exploratory tympanotomy was performed on the right ear. Although perilymph leakage was not noted in the oval or round windows, both windows were sealed with connective tissue. The patient's vestibular symptoms rapidly improved after surgery, and postoperative contrast-enhanced MRI showed improvement in the collapsed endolymphatic space. Although the caloric test revealed unilateral weakness, the VOR gain on the vHIT improved to normal on the right side. Thus, these findings indicated that recurrent symptoms caused by PLF are associated with a collapsed endolymphatic space. We speculate that the collapsed endolymphatic space was due to a ruptured Reissner's membrane. We hypothesized that sealing the fistula would promote normalization of perilymph pressure. The ruptured Reissner's membrane may have been gradually repaired as vestibular symptoms improved. This case adds to the existing literature on the occurrence of the "double-membrane break syndrome". Collapse of the endolymph due to a ruptured Reissner's membrane may be the cause of PLF symptoms.

KEYWORDS

perilymphatic fistula, magnetic resonance imaging, HYDROPS, vHIT, Reissner's membrane, vestibular atelectasis

1. Introduction

A perilymphatic fistula (PLF) presents with abnormal traffic in the otic capsule, causing cochlear and vestibular symptoms. PLFs can be classified as those with and without identifiable causes. PLFs are more likely to be diagnosed after middle or inner ear surgery, such as stapes surgery, or trauma. However, it is often difficult to identify the cause of PLFs in the absence of prior surgery or trauma. In Japan, PLFs are classified into four categories according to the cause and diagnosed based on clinical symptoms, microscopic or endoscopic examination of the fistula between the middle and inner ears, or detection of a perilymph-specific protein in the middle ear (Table 1) (1, 2). Sarna et al. proposed similar diagnostic criteria (3). However, the mechanisms underlying symptom recurrence remain controversial. One of the most common signs is pneumolabyrinth, which aids in the diagnosis of Category 1 cases. But, this is not a common finding in cases of Categories 2, 3, and 4 (4). We report a case of PLF that caused hearing loss and vertigo in a young female patient. In this case, we gained insight into the pathogenesis of PLF by performing preoperative and postoperative vestibular function tests and contrast-enhanced magnetic resonance imaging (MRI) using hybrid of reversed image of positive endolymph signal and negative image of perilymph signal (HYDROPS) to identify endolymphatic hydrops in Meniere's disease (MD).

2. Case report

A 27-year-old female complained of hearing disturbance in her right ear and recurrent vertigo after sudden onset of hearing loss with vertigo. She had no history of trauma or headaches. At the age of 15 years, she began to experience vertigo preceded by right ear blockage without any trigger. Vertigo was induced by blowing the nose. At the age of 19 years, her symptoms worsened further, and the frequency of vertigo increased; therefore, she visited a local Ear, Nose and Throat (ENT) clinic, but no hearing loss was noted and no apparent abnormality was found. At the age of 26 years, she suddenly developed hearing loss in her right ear and severe vertigo, which she had never experienced before, and visited another ENT hospital. The mean pure-tone air conduction threshold at 500 Hz, 1,000 Hz, and 2,000 Hz was 70.0 dB. An A-B gap was present at low frequencies (Figure 1A). The spontaneous nystagmus turned leftward, especially in the right lateral recumbent position. She was diagnosed with sudden onset hearing loss with vertigo and was treated with prednisolone (60 mg/day tapered for 1 week). However, the patient's hearing did not improve. Variations in low frequencies of 5–10 dB were observed during the monthly audiometric testing. Thereafter, 2–3 times in a month, she experienced recurrent vertigo lasting several hours, with hearing loss, tinnitus, and a blocked sensation in the right ear. During the interictal period, she had gait instability, especially deviating to the right, and dizziness in the right lateral recumbent position.

TABLE 1 PLF categorization.

Category 1: linked to trauma, middle and inner ear diseases, middle and/or inner ear surgeries
Category 2: linked to barotrauma caused by antecedent events of external origin (such as flying or diving)
Category 3: linked to barotrauma caused by antecedent events of internal origin (such as straining, sneezing or coughing)
Category 4: has no apparent antecedent event

One year later, she returned to the hospital with hearing loss and severe vertigo, and her right hearing had deteriorated and scaled out (Figure 1B). The patient was again treated with prednisolone (60 mg/day tapered for 1 week), but she experienced no improvement. She was referred to our hospital to investigate the cause and received treatment for hearing loss and vertigo. At the time of the initial visit to our clinic, spontaneous nystagmus was not present. However, the head-shaking test showed constant directional nystagmus to the left. Moreover, during her vertigo attacks, as in the previous case, constant directional nystagmus to the left was observed regardless of the head position and was especially enhanced in the right lateral recumbent position. The fistula test results were negative. High-resolution computed tomography of the temporal bone revealed no pneumolabyrinths, fractures, malformations, or findings suggestive of superior canal dehiscence. Brain MRI revealed no abnormalities. Initially, we suspected MD because of the recurrent attacks of vertigo with hearing loss, tinnitus, and blocked sensation in the right ear. Contrast-enhanced MRI using HYDROPS did not show endolymphatic hydrops in the affected inner ear, which is characteristic of MD; rather, a few contrast-deficient images indicated the endolymph (Figure 2A). MD often shows a decreased response in the caloric test, which is normal in the video head impulse test (vHIT). However, in this case, the caloric test results revealed unilateral weakness in the right ear (canal paresis, CP = 50%), and the vHIT showed decreased vestibulo-ocular reflex (VOR) gain in the lateral semicircular canal (Figure 3A). She had repeated attacks of vertigo, and we considered the possibility that the PLF had progressed. Therefore, we performed an exploratory tympanotomy 4 months after her arrival at our hospital. A transcanal approach with tympanomeatal flap elevation revealed no perilymph leakage from the round window niche or surrounding footplate of the stapes. Leakages that were not visible were repaired, the mucosa was dissected, a round window was placed above and behind the footplate of the stapes, and the fissula ante fenestram was sealed with connective tissue. Middle ear lavage was collected intraoperatively andacochlin tomoprotein (CTP) detection test by monoclonal antibodies based ELISA (SRL Inc., Tokyo, Japan) revealed 30.2 ng/ml which means positive (the cutoff criteria, 30.0 ng/ml) (5). Postoperatively, the presence of PLF was confirmed. The patient's vestibular symptoms rapidly improved and nystagmus disappeared the day after surgery. Her hearing loss persisted, with no improvement. Five months postoperatively, the CP% was 52.4%, which was unchanged from the preoperative level; however, the VOR gain in the lateral semicircular canal improved in the vHIT group (Figure 3B). Six months postoperatively, contrast-enhanced MRI using HYDROPS revealed a contrast defect in the endolymph on the affected side, which was rarely observed preoperatively (Figure 2B).

10.3389/fneur.2023.1276991

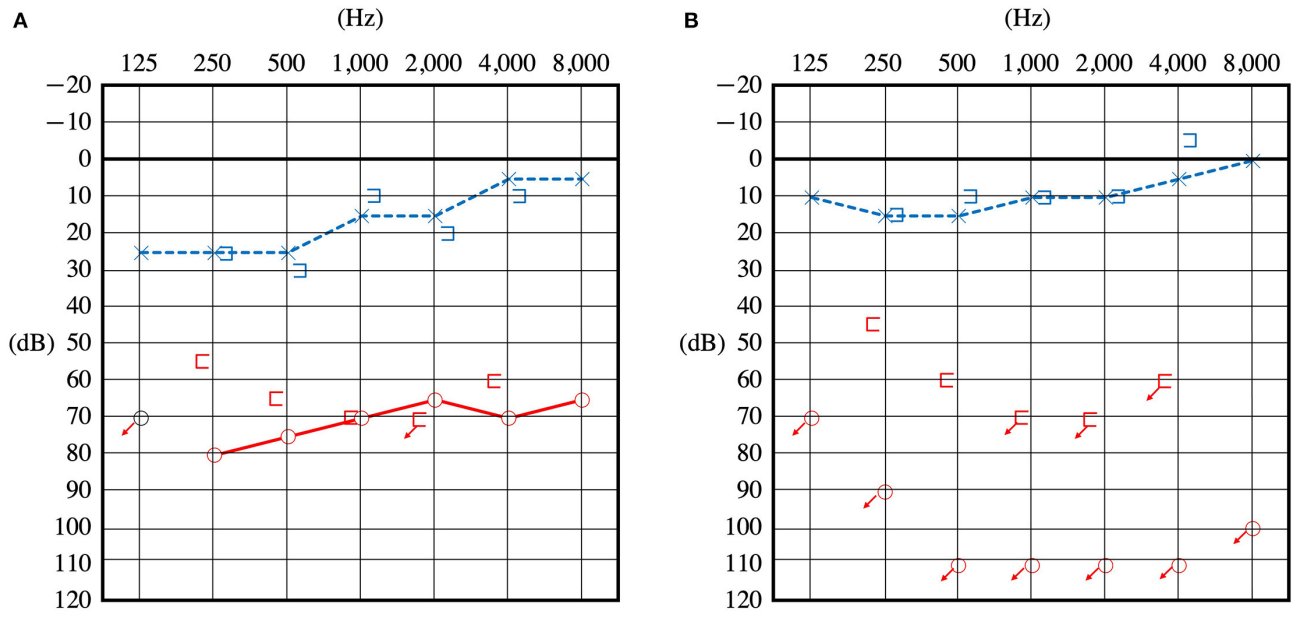

FIGURE 1
Pure tone audiometry before surgery. Audiometry of the patient upon presentation of sudden hearing loss **(A)** and 1 year later showing a reduction in hearing **(B)**.

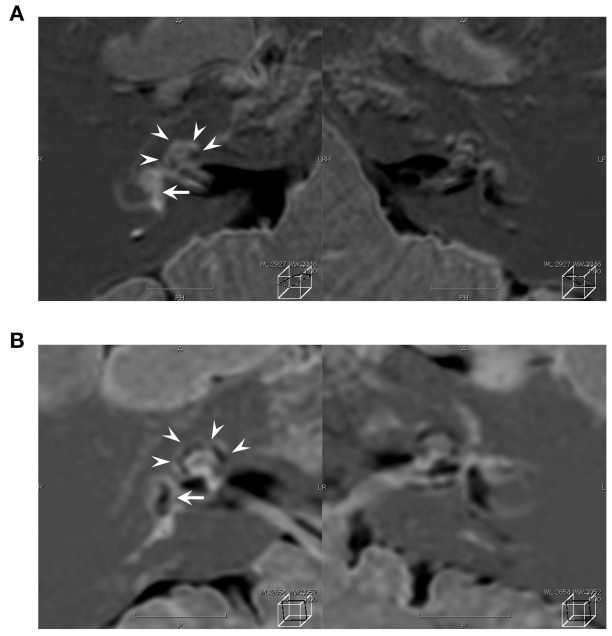

FIGURE 2
Contrast-enhanced MRI images using HYDROPS. The arrow heads and long arrows indicate the enlarged cochlea vestibule, respectively. Contrast-deficient images (black areas) indicate the presence of endolymph. A contrast-enhanced deficient image of the endolymph of the right ear was rarely observed preoperatively **(A)** but is observed postoperatively **(B)**.

3. Discussion

Since vertigo was induced by blowing the nose, this case was classified as Category 3 according to the Japanese PLF categorization, and the positive CTP result confirmed the diagnosis (Table 1) (1, 2). Contrast-enhanced MRI using HYDROPS showed few or no contrast deficit in the vestibule and cochlea on the affected side (Figure 2A). The mechanism of this defect is assumed to be the collapse of the endolymphatic space due to endolymph leakage at the onset of perilymph leakage and rupture of Reissner's membrane. The possibility that the rupture of Reissner's membrane in combination with PLF can cause severe hearing loss was first reported in the 1970s by Simmons as "double-membrane break syndrome" (6). Our case supports this view. The perilymphatic space is covered by a bony labyrinth that preserves the lumen even if the perilymph leaks. The perilymphatic space tends to be enlarged by the collapse of the endolymphatic space, and the contrast-enhanced perilymphatic space appears to be highlighted. After surgery, a contrast-enhanced defect on MRI revealed an endolymphatic space, which was rarely observed before surgery. The ruptured Reissner's membrane repairs itself over time, and we hypothesized that the cessation of perilymph leakage into the middle ear maintains perilymph homeostasis, resulting in gradual repair of the ruptured area (Figure 2B).

PLFs generally present with an acute onset of auditory symptoms, vestibular symptoms, or both. Sometimes, vestibular symptoms occur with fluctuating or progressive hearing loss, and as in this case, they are differentiated from MD. Therefore, in

10.3389/fneur.2023.1276991

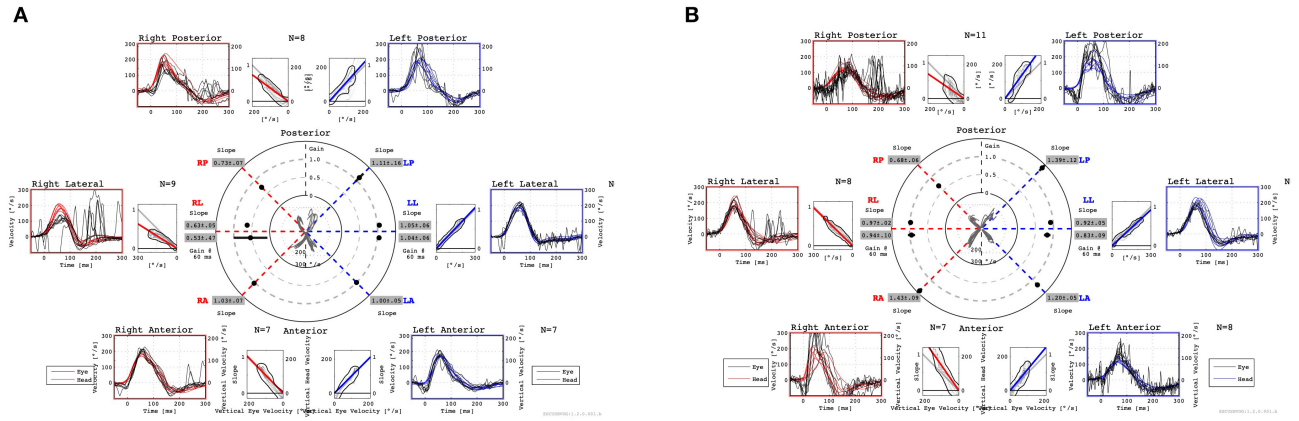

FIGURE 3
Preoperative vHIT shows a decreased VOR gain in the right LSC and PSC **(A)**. Postoperative vHIT shows that the decrease in VOR gain in the right PSC remained unchanged, but the decrease in VOR gain in the right LSC improved **(B)**. Both preoperatively and postoperatively, vHIT shows normal VOR gain in the right ASC with no change **(A, B)**. vHIT, video head impulse test; VOR, vestibulo-ocular reflex; LSC, lateral semicircular canal; PSC, posterior semicircular canal; ASC, anterior semicircular canal.

previous reports, MD and PLF were closely related, and PLF is thought to be complicated by endolymphatic hydrops, similar to MD (3, 7–9). Cerebrospinal fluid (CSF) fistula is a vestibular disorder that involves fistula as well as PLF. CSF fistula also presents with hearing loss and vestibular symptoms, similar to MD. The perilymph communicates with the CSF via the cochlear aqueduct and the CSF fistula is considered to be perilymph depletion with endolymphatic hydrop (10–13). In this case, contrast-enhanced MRI of the inner ear showed the opposite result; therefore, the fluctuating and progressive hearing loss and intermittent vestibular symptoms may be solely due to PLF.

Merchant and Schuknecht first described a histopathological entity called vestibular atelectasis, which shows the collapse of the ampulla and utricle walls (14). Eliezer et al. clinically confirmed endolymph collapse, defined as failure to visualize the utricle and at least two ampullas using delayed contrast-enhanced MRI (15). The present case had similar imaging findings and was considered to have an endolymph collapse with rupture of the Reissner's membrane. The postoperative improvement in vestibular symptoms and positive CTP suggested that there was preoperative traffic between the perilymph space and the middle ear space. In other words, preoperatively, she was thought to have a "double membrane rupture syndrome" as proposed by Simmons, in which perilymph leakage combined with rupture of Reissner's membrane causes severe hearing loss. In support of this, animal models of PLF have reported that rupture of round window alone results in mild hearing loss, but that hearing loss becomes severe when accompanied by a rupture of Reissner's membrane as well (16–19). The patient had recurrent attacks of vertigo from the age of 15 until surgery, each time the fistula was thought to have repeatedly opened and spontaneously closed. However, at age 26 and 1 year later, the patient had hearing loss along with vertigo attacks, suggesting that the Reissner's membrane had ruptured.

The patient's symptoms improved postoperatively. Even if the traffic between the perilymph space and middle ear space were surgically blocked, the rupture of Reissner's membrane would have remained. We hypothesized that the rupture of Reissner's membrane would have spontaneously repaired after surgery and that the endolymphatic collapse would have improved on imaging. Rupture and spontaneous repair of Reissner's membrane was considered the mechanism of vertigo attacks and their recovery in MD. However, this has been debated in recent years because it is not accompanied by significant hearing loss during vertigo attacks (20, 21). In fact, spontaneous repair of Reissner's membrane has not been pathologically confirmed, making this hypothesis controversial.

The patient had vestibular disorders, as determined in both the preoperative caloric test and the vHIT. Although both tests are functional tests of semicircular canals, they differ in stimulation frequency; the caloric test uses low-frequency stimulation, whereas the vHIT uses high-frequency stimulation (22, 23). Merchant and Schuknecht reported a remarkable decrease in hair cells in the vestibular atelectasis (14). Since type I hair cells are thought to be associated with high-frequency stimulation and type II hair cells with low-frequency stimulation (24), it is possible that both were disordered. Postoperatively, there was a decrease in the response to the caloric test, but the vHIT improved. This suggests that type II hair cells remained impaired, whereas type I hair cells may have been repaired. Endolymph collapse should be considered a cause of PLF symptoms.

4. Conclusions

The mechanisms by which PLFs cause vestibular symptoms and hearing loss remain unclear. However, in the present case, endolymph collapse on the affected side was noted on cochlear contrast-enhanced MRI. Endolymph collapse due to rupture of the Reissner's membrane may be the cause of these symptoms.

Data availability statement

The original contributions presented in the study are included in the article/supplementary material, further inquiries can be directed to the corresponding author.

Ethics statement

Ethical review and approval was not required for the study on human participants in accordance with the local legislation and institutional requirements. The participants provided their written informed consent to participate in this study. Written informed consent was obtained from the individual(s) for the publication of any potentially identifiable images or data included in this article.

Author contributions

YI: Writing—original draft, Writing—review and editing. TS: Writing—review and editing. YS: Writing—review and editing. FM: Writing—review and editing. IK: Writing—review and editing.

Funding

The author(s) declare that no financial support was received for the research, authorship, and/or publication of this article.

Conflict of interest

The authors declare that the research was conducted in the absence of any commercial or financial relationships that could be construed as a potential conflict of interest.

Publisher's note

All claims expressed in this article are solely those of the authors and do not necessarily represent those of their affiliated organizations, or those of the publisher, the editors and the reviewers. Any product that may be evaluated in this article, or claim that may be made by its manufacturer, is not guaranteed or endorsed by the publisher.

References

1. Kanzaki J. Diagnostic criteria for acute profound deafness. *Acta Otolaryngol.* (1994) 514:7–8. doi: 10.3109/00016489409127548

2. Matsuda H, Sakamoto K, Matsumura T, Saito S, Shindo S, Fukushima K, et al. A nationwide multicenter study of the cochlin tomoprotein detection test: clinical characteristics of perilymphatic fistula cases. *Acta Otolaryngol.* (2017) 137:S53–9. doi: 10.1080/00016489.2017.1300940

3. Sarna B, Abouzari M, Merna C, Jamshidi S, Saber T, Djalilian HR. Perilymphatic Fistula: a review of classification, etiology, diagnosis, and treatment. *Front Neurol.* (2020) 11:1046. doi: 10.3389/fneur.2020.01046

4. Hidaka H, Miyazaki M, Kawase T, Kobayashi T. Traumatic pneumolabyrinth: air location and hearing outcome. *Otol Neurotol.* (2012) 33:123–31. doi: 10.1097/MAO.0b013e318241bc91

5. Matsuda H, Ikezono T. [Cochlin tomoprotein (CTP): World's first diagnostic marker for perilymphatic fistula] Rinnsyoukennsa update cochlin tomoprotein (CTP) sekaihatu no gairinnpa rousyutu sinndann marker ni tuite (in Japanese). *Modern Media.* (2023) 69:102–6.

6. Simmons FB. The double-membrane break syndrome in sudden hearing loss. *Laryngoscope.* (1979) 89:59–64. doi: 10.1288/00005537-197901000-00006

7. Potter CR, Conner GH. Hydrops following perilymph fistula repair. *Laryngoscope.* (1983) 93:810–2. doi: 10.1288/00005537-198306000-00022

8. Fitzgerald DC. Perilymphatic fistula and Meniere's disease. Clinical series and literature review. *Ann Otol Rhinol Laryngol.* (2001) 110:430–6. doi: 10.1177/000348940111000507

9. House HP. The fistula problem in otosclerosis surgery. *Laryngoscope.* (1967) 77:1410–26. doi: 10.1288/00005537-196708000-00015

10. Walsted A. Effects of cerebrospinal fluid loss on hearing. *Acta Otolaryngol.* (2000) 120:95–8. doi: 10.1080/000164800454099

11. Walsted A. Effects of cerebrospinal fluid loss on the auditory system. Clinical and experimental investigations. *Dan Med Bull.* (1998) 45:268–81.

12. Walsted A, Garbarsch C, Michaels L. Effect of craniotomy and cerebrospinal fluid loss on inner ear. An experimental study. *Acta Otolaryngol.* (1994) 114:626–31. doi: 10.3109/00016489409126116

13. Walsted A, Nilsson P, Gerlif J. Cerebrospinal fluid loss and threshold changes. 2. Electrocochlegraphic changes of the compound action potential after CSF aspiration: an experimental study. *Audiol Neurootol.* (1996) 1:256–64. doi: 10.1159/000259209

14. Merchant SN, Schuknecht HF. Vestibular atelectasis. *Ann Otol Rhinol Laryngol.* (1988) 97:565–76. doi: 10.1177/000348948809700601

15. Eliezer M, Attyé A, Guichard J-P, Vitaux H, Guillonnet A, Toupet M, et al. Vestibular atelectasis: myth or reality? *Laryngoscope.* (2019) 129:1689–95. doi: 10.1002/lary.27793

16. Kobayashi T, Gyo K, Yanagihara N. Combined rupture of Reissner's membrane and round window: an experimental study in guinea pigs: experimental double-membrane rupture. *Am J Otolaryngol.* (1999) 20:179–82.

17. Oshiro EM, Shelton C, Lusted HS. Role of perilymphatic fistula in sudden hearing loss: an animal model. *Ann Otol Rhinol Laryngol.* (1989) 98:491–5. doi: 10.1177/000348948909800701

18. Funai H, Hara M, Nomura Y. An electrophysiologic study of experimental perilymphatic fistula. *Am J Otolaryngol.* (1988) 9:244–55. doi: 10.1016/S0196-0709(88)80034-6

19. Nomura Y, Okuno T, Hara M, Young YH. "Floating" labyrinth. Pathophysiology and treatment of perilymph fistula. *Acta Otolaryngol.* (1992) 112:186–91. doi: 10.1080/00016489.1992.11665401

20. McNeill C, Cohen MA, Gibson WP. Changes in audiometric thresholds before, during and after attacks of vertigo associated with Meniere's syndrome. *Acta Otolaryngol.* (2009) 129:1404–7. doi: 10.3109/00016480902751672

21. Gibson WP. Hypothetical mechanism for vertigo in Meniere's disease. *Otolaryngol Clin North Am.* (2010) 43:1019–27. doi: 10.1016/j.otc.2010.05.013

22. McGarvie LA, Curthoys IS, McDougall HG, Halmagyi GM. What does the dissociation between the results of video head impulse versus caloric testing reveal about the vestibular dysfunction in Ménière's disease? *Acta Otolaryngol.* (2015) 135:859–65. doi: 10.3109/00016489.2015.1015606

23. Maire R, Van Melle G. Vestibulo-ocular reflex characteristics in patients with unilateral Ménière's disease. *Otol Neurotol.* (2008) 29:693–8. doi: 10.1097/MAO.0b013e3181776703

24. Shugyo M, Ito T, Shiozaki T, Nishikawa D, Ohyama H, Fujita H, et al. Comparison of the video head impulse test results with caloric test in patients with Meniere's disease and other vestibular disorders. *Acta Otolaryngol.* (2020) 140:728–35. doi: 10.1080/00016489.2020.1766700

frontiers | Frontiers in Neurology

TYPE Original Research
PUBLISHED 04 January 2024
DOI 10.3389/fneur.2023.1263513

OPEN ACCESS

EDITED BY
P. Ashley Wackym,
The State University of New Jersey,
United States

REVIEWED BY
Takefumi Kamakura,
Osaka University, Japan
Krzysztof Morawski,
University of Opole, Poland

*CORRESPONDENCE
Paul R. Kileny
✉ pkileny@med.umich.edu
Megan M. Cherry
✉ mcherry@med.umich.edu

RECEIVED 19 July 2023
ACCEPTED 12 December 2023
PUBLISHED 04 January 2024

CITATION
Kileny PR, Cherry MM and McCaslin DL (2024) Electrocochleography in the diagnosis of third window conditions.
Front. Neurol. 14:1263513.
doi: 10.3389/fneur.2023.1263513

Electrocochleography in the diagnosis of third window conditions

Paul R. Kileny*, Megan M. Cherry*and Devin L. McCaslin

Michigan Medicine, Department of Otolaryngology, Head and Neck Surgery, Division of Audiology, University of Michigan, Ann Arbor, MI, United States

Introduction: Superior semicircular canal dehiscence (SSCD) is the best-known and most common presentation of so-called "third window conditions." There are a variety of diagnostic measures and tests for this condition in the current literature, including air-bone gap, vestibular-evoked myogenic potentials, and electrocochleography (EcochG). The purpose of this study was to investigate the diagnostic utility of EcochG and its relationship to air-bone gap in a cohort of patients with confirmed SSCD.

Methods: We reviewed data from 20 patients (11 female and 9 male subjects, age ranging 21–78 years), with confirmed unilateral or bilateral superior canal dehiscence. In total, 11 patients had unilateral SSCD and 9 patients had bilateral SSCD as determined by high-resolution CT scan. This resulted in the inclusion of twenty-nine ears with superior canal dehiscence and 11 normal ears.

Results: Our results indicated that all confirmed SSCD ears presented with an abnormal EcochG SP/AP value and that there was a statistically significant difference between normal and dehiscent ears. There was no statistically significant relationship between air-bone gap and SP/AP ratio in the ears diagnosed with SSCD nor was there a significant difference between dehiscent and normal ears in terms of air-bone gap at three frequencies.

Discussion: These results are consistent with previous studies showing the diagnostic utility of EcochG for this condition and the variability of air-bone gap. While an unexpected air-bone gap continues to be a red flag for SSCD, its absence along with the presence of subjective symptoms is a reasonable indicator for further clinical investigation to include EcochG.

KEYWORDS

electrocochleography, SSCD = superior semicircular canal dehiscence, air-bone gap, SP/AP ratio, autophony, bone conduction hypersensitivity, diagnosis, EcochG

Introduction

Superior semicircular canal dehiscence (SSCD) is the best-known and most common presentation of so-called "third window conditions" and was first described by Minor et al. (1). A normal inner ear has two openings or "windows" in the otic capsule (i.e., round and oval windows). This condition is characterized by a combination of auditory and vestibular symptoms resulting from this super numerary opening into the otic capsule caused by the absence of bone overlying the superior semicircular canal and, at times, less frequently, other canals such as the posterior canal. Among auditory phenomena, there can be autophony, pulsatile tinnitus, aural fullness, and air-bone gaps in the absence of middle ear pathology. This air-bone gap is typically caused by what is referred to as "bone conduction hyperacusis," that is, sub-zero dB bone conduction thresholds. When bone-conducted stimuli are used, the third

window changes the acoustic impedance on the vestibular side of the cochlear partition resulting in increased auditory sensitivity or lower bone conduction thresholds than would be expected (2). The low-to-mid-frequency air-bone gap is considered to be caused by the dissipation of acoustic energy through the abnormal, supernumerary third window which falsely elevates the air conduction thresholds, and this is added to the bone conduction hyperacusis characterized by unusually low bone conduction thresholds.

Vestibular symptoms may include sound and pressure-induced vertigo, disequilibrium, and, at times, oscillopsia.

The clinical utility of vestibular-evoked myogenic potentials (VEMPs) in identifying and documenting whether dehiscence is "active" has been well documented. The two most commonly described VEMPs are the cervical VEMP (i.e., cVEMP) and the ocular VEMP (i.e., oVEMP). The primary generator of the cVEMP is the saccule, and it is most commonly recorded from the sternocleidomastoid muscle. The oVEMP response is generated by the utricular macula and recorded, most robustly, from the contralateral extraocular muscles (i.e., inferior oblique). Overall, it has been reported that cVEMPs and oVEMPs have a high sensitivity and specificity for identifying SSCD. Hunter et al. reported that when using a criterion of a cVEMP being present at <70-dB nHL threshold, the sensitivity was 73% and the specificity was 94%. The sensitivity was 78.6% for oVEMP amplitudes, exceeding 12 μV, and the specificity was 81.7% (3).

The diagnostic test largely considered the gold standard for identifying SSCD is high-resolution CT. Although it is convenient to think of the bony defect as always occurring at the arcuate eminence, there are data showing that there is substantial variability in where the dehiscence is located (4). The bony defect can occur on the medial descending limb, lateral ascending limb, and the descending limb close to the superior petrosal sinus. Although CT is considered the most sensitive and specific approach to identifying dehiscence, it is not perfect. This is due to the fact that anatomical variations such as a thinning of the bone over the canal can be read as a positive result.

In addition to air and bone conduction audiological testing, computed tomography (CT) of the temporal bone, vestibular-evoked myogenic potentials (VEMP), and electrocochleography (EcochG) have been determined to be diagnostically and interventionally useful and informative for SSCD. Our group was the first one to recognize the utility of EcochG and its contribution to the diagnostic study of superior semicircular canal dehiscence (5).

EcochG is defined as the recording of cochlear potentials such as the cochlear-microphonic (CM) and the summating potential (SP) and the whole nerve action potential (AP) generated by the cochlear nerve. These components of the auditory evoked response are obtained by applying recording techniques that emphasize these particular components. Briefly, EcochG is the measurement of the above defined combination of inner ear and cochlear nerve-generated potentials elicited by a transient acoustic stimulus, i.e., in our case, a click. Responses are recorded using the hydrogel-tipped recording electrode in contact with the lateral surface of the tympanic membrane, introduced with microscopic visualization of the ear canal and the tympanic membrane. Depending upon the polarity configuration of the transient acoustic stimulus, one can record the cochlear microphonic if using constant polarity or the summating potential if using alternating polarity transient stimuli such as clicks. This is followed by the cochlear nerve action potential also referred to as N1 or AP. The summating potential is essentially a direct current potential that follows the stimulus envelope and would be superimposed upon the cochlear microphonic baseline shift when using tone bursts as stimuli. With a click, it is a relatively brief peak or shoulder-like manifestation preceding the cochlear nerve action potential (AP). The summating potential rises from direct current intracellular potentials and is generated predominantly by inner hair cells with some contribution from the outer hairs. The SP is related to a rectified and smooth version of the basilar membrane's displacement (6). When using a transient stimulus like a click, elicited by alternating polarity stimulation, the summating potential is a short-duration peak preceding the action potential by up to 1 millisecond, and at times, it can blend into the leading edge of the action potential. The action potential (AP) is the cochlear nerve compound action potential and is in fact the manifestation of wave I of the auditory brain stem response. There has been extensive literature regarding the utility of EcochG in the diagnosis of Meniere's disease for diagnostic purposes and in monitoring the effects of treatment. Based on a previous study by Davis et al. in the 1950s, the position of the basilar membrane that would be displaced when endolymphatic hydrops are present does have an effect on the amplitude of the SP by enhancing it. When the basilar membrane is statically displaced toward the scala of tympani, this results in an increase of the SP/AP ratio due to an increase in the absolute amplitude of the SP, and this has been used in assisting with the diagnosis of Meniere's disease (7).

In 2009, our team was the first one to identify the presence of an abnormal, elevated SP/AP ratio in patients with confirmed SSCD (5). In this initial report, we presented seven adult patients with unilateral SSCD and four adult patients with bilateral SSCD. All of these patients underwent tympanic electrocochleography. They also underwent air and bone conduction audiology testing, vestibular-evoked myogenic potential testing (VEMP) as well as high-resolution temporal bone computer tomography which was reformatted to optimize the resolution of the superior semicircular canal. At the time, 5 patients of the total 11 patients underwent superior canal occlusion. We also obtained postoperative EcochG from four patients at the time of publication. Additionally, EcochG was monitored continuously during the surgical repair. Of a total of 15 ears with confirmed SSCD using high-resolution CT, 14 were found to have an elevated SP/AP ratio exceeding a value of 0.4, which was the clinical normative limit that has been used in our clinic for the past 3 decades. The mean SP/AP ratio for the affected ears was 0.73, with a standard deviation of 0.29, and for the unaffected ears, it was 0.27, with a standard deviation of 0.14. In terms of audiometry, the air-bone gap was typically the largest at the lowest frequencies in the affected ears, and the mean air conduction threshold was elevated across the frequency range in the affected ears. In the next publication by our group, we reported on 33 patients (45 ears) with clinical symptoms and CT evidence of SSCD. All patients underwent electrocochleography and 8 patients underwent intraoperative electrocochleography during superior canal occlusion as well. Nine patients also underwent postoperative EcochG after occlusion surgery. Overall, electrocochleography was associated with 89% sensitivity and 70% specificity relative to SSCD based on the computer tomography gold standard. The mean SP/AP ratio among affected ears was significantly higher than among unaffected ears: 0.62 vs. 0.29 mean values. This difference was statistically significant. During surgery, the SP/AP ratio increased upon the exposure of the canal lumen, and after completion of occlusion, the SP/AP ratio was

reduced to values below the intraoperative baseline with a mean change of 0.23 (standard deviation of plus or minus 0.5). In all patients who underwent postoperative electrocochleography between 1 and 3 months following SSCD repair, the SP/AP ratio was well within normal limits, under the value of 0.4. This was represented by the 9 patients who underwent postoperative outpatient EcochG at the time of that publication (8).

These two early reports convinced us of the diagnostic utility of EcochG in patients suspected of SSCD. Additionally, these early clinical studies also demonstrated the intraoperative monitoring utility of electrocochleography during SSCD repair. Therefore, we adopted EcochG as a clinical diagnostic standard in patients suspected of SSCD and in intraoperative monitoring standards in patients undergoing SSCD repair. More recently, our team demonstrated the strong correlation between EcochG SP/AP ratio normalization and symptom improvement in patients undergoing SSCD repair (9). This study included 46 patients who underwent SSCD repair (14 were unilateral and 6 were bilateral), with 24 who underwent the middle cranial fossa approach and 28 who underwent the transmastoid approach. There were no differences between the surgical groups in terms of preoperative, intraoperative, or postoperative EcochG SP/AP ratio. All patients, regardless of surgical approach, demonstrated subjective improvement in the vestibular symptoms in both groups. Vestibular symptoms persisted more often in patients with concomitant migraine and in a few patients with persistently abnormal EcochG measures postoperatively. Overall, the normalization of the preoperative EcochG values postoperatively correlated with patients experiencing symptom improvement after SSCD repair.

The purpose of the present study was to further explore whether the size of the air-bone gap is associated with EcochG SP/AP ratio values in ears with confirmed SSCD.

Methods

EcochG was performed by positioning a hydrogel-tipped electrode onto the lateral surface of the tympanic membrane. This was accomplished by direct visualization of the ear canal and tympanic membrane with an oto-microscope. The tympanic membrane electrode was stabilized by the foam tip of the insert audio transducer. Alternating polarity clicks of 100 ms duration presented at 85 to 95 dB nHL were used as stimuli. This range was used subject to magnitude of hearing loss in an effort to obtain clear, repeatable, and interpretable records. Typically, two replications of averaged responses elicited by 1,000 to 2,000 clicks at a rate of 9 to 11.7 per second were obtained and grand averaged. Responses were band-passed filtered (20–1,500 Hz) and averaged, and the SP/AP ratio was calculated (10, 11). As previously mentioned, an SP/AP ratio of greater than 0.4 was considered to be abnormal for the purpose of this study, based on our clinical norms that we have used for approximately 3 decades. All subjects underwent audiological testing consisting of air and bone conduction audiometry, word recognition scores, and speech reception threshold. The speech audiometry results were irrelevant for this patient population, and for the purposes of this study, therefore those results were not included in the data analysis. Every effort was made to determine the presence of sub-zero dBHL bone conduction thresholds. The air-bone gap was evaluated at 250, 500, and 1,000 Hz for each patient to capture this predominantly low-to-mid-frequency phenomenon.

Subjects

For the purpose of this study, we reviewed data from 20 patients (11 female and 9 male patients) with confirmed unilateral or bilateral superior canal dehiscence. The age range was 21 to 78 years.

Twenty-nine ears with superior canal dehiscence and 11 normal ears were included in the study. In total, 11 participants had unilateral SSCD and 9 patients had bilateral SSCD as determined by high-resolution CT scan. The degree of hearing loss for ears with SSCD ranged from normal hearing thresholds to moderate hearing loss.

Table 1 is a summary of subjects and affected ears. Table 2 lists the participants with age range, gender, air-bone gap values at three frequencies, and EcochG SP/AP values of the affected ears. Table 3 provides a description of normal contralateral ears from our sample.

Statistical analysis

Continuous variables were presented with means, standard deviations (SD), and ranges; categorical variables were summarized with percentages and frequency counts. Comparisons of variables between ears with and without SSCD were evaluated using Mann–Whitney U tests and linear mixed effects model analysis. All tests were two-sided, and p-values of <0.05 were considered statistically significant. Associations of SP/AP ratios with ABGs at 250, 500, and 1,000 Hz were evaluated using Pearson product–moment correlation coefficients. Results were considered significant at the $p < 0.05$ level. Statistical analyses were performed using IBM SPSS Statistics version 29.

Results

Associations of conductive hearing loss at three frequencies and their average as well as measurements of SP/AP ratios derived from the EcochG among all 29 abnormal ears and 11 normal ears are summarized in Tables 2, 3. In six of the nine patients with bilateral

TABLE 1 Subject demographic information.

	n	%
Total participants	20	
Female	11	55%
Male	9	45%
Unilateral	11	55%
Bilateral	9	45%
Total ears	29	
Right ears	13	45%
Left ears	16	55%
Unilateral	11	38%
Bilateral	18	62%

TABLE 2 Individual clinical data used in data analysis.

Participant number	Gender	Age range	ABG 250	ABG 500	ABG 1000	SP/AP	Ear
1	M	40–49	15	5	5	0.5	R^N
			10	5	5	0.57	L^N
2	F	40-49	0	0	5	0.61	R
			35	20	25	0.83	L^T
3	M	50–59	25	15	20	0.6	R
			25	20	15	0.8	L^{AT}
4	F	50–59	5	5	15	0.61	R
			5	5	15	0.68	L^A
5	M	60-69	40	35	35	0.53	R
			20	0	15	0.53	L^{AT}
6	M	40–49	10	0	5	0.646	R^N
			10	0	10	0.525	L^N
7	F	40-49	5	10	0	0.51	R^A
			0	10	0	0.44	L
8	F	50–59	35	15	20	0.51	R^T
			15	10	10	0.55	L
9	F	60–69	45	20	20	0.45	R^T
			15	0	10	0.5	L^A
10	F	70–79	5	10	5	0.47	L
11	F	40–49	10	15	5	0.54	L
12	F	30–39	10	10	10	0.66	L
13	M	60–69	10	5	5	0.61	R
14	M	20–29	5	5	10	0.65	L
15	F	40–49	10	5	20	0.41	R
16	M	20–29	10	0	5	0.53	R
17	M	50–59	15	5	15	0.5	L
18	F	30–39	15	5	15	0.596	L
19	F	40–49	5	0	5	0.62	L
20	M	60–69	0	10	10	0.55	R

ABG = Air-Bone Gap; SP/AP – SP/AP Ratio; R = Right; L = Left. ^{A} = Stronger side for autophony. ^{T} = Stronger side for tinnitus/muffled hearing. ^{N} = No lateralizing symptoms.

SSCD, the symptoms lateralized to one side. In two of these six patients, tinnitus was the only lateralizing symptom. In an additional two of these six patients, autophony was the only lateralizing symptom. Two patients noted both tinnitus and autophony lateralizing to the same side. Additionally, there was one patient who noted tinnitus lateralized to one side (right) and autophony lateralized to the other side (left). Of the six patients who had lateralizing symptoms, the side with the stronger symptoms had the higher SP/AP ratio for four of the six patients. One patient had equally elevated SP/AP ratios bilaterally. Interestingly, the patient with stronger autophony in the right and stronger tinnitus in the left had a slightly higher SP/AP ratio in the left ear although these values (0.47 and 0.50, respectively) were not significantly different. For the two patients without lateralizing symptoms, the SP/AP ratios differed by 0.07 for one patient and 0.121 for the other patient.

We conducted a linear mixed effects analysis with SP/AP amplitude ratio as the dependent variable. The fixed effect of interest was ears with SSCD and healthy ears and the random effect included subjects. There was a significant main effect of SSCD on SP/AP amplitude ratio ($p < 0.001$). The 29 ears with SSCD ($M = 0.57$, SE = 0.15) had larger SP/AP ratios than the ears with no SSCD from patients with unilateral SSCD ($M = 0.34$, SE = 0.23) indicating a significant increase in the SP/AP ratio in ears with radiologically confirmed SSCD. There was no observed significant correlation between SP/AP amplitude ratio and air-bone gap at any of the tested frequencies. There was no significant difference between SSCD and healthy ears for air-bone gap at any of the frequencies tested. Finally, there was no evidence to suggest that there was a significant positive or negative association of SP/AP amplitude ratio with ABG (Figures 1–3).

Case study

The purpose of this case study is to illustrate our standard protocol for patients with SSCD, including our EcochG technique, and to

TABLE 3 Data from contralateral ears (normal).

Participant number	Gender	Age range	ABG 250	ABG 500	ABG 1000	SP/AP	Ear
2	F	70–79	15	20	0	0.35	R
3	F	40–49	0	10	15	0.42	R
6	F	30–39	15	5	5	0.53	R
7	M	60–69	10	5	5	0.27	L
8	M	20–29	5	5	10	0.33	R
11	F	40–49	15	10	15	0.22	L
12	M	20–29	5	0	5	0.24	L
13	M	50–59	10	5	10	0.5	R
16	F	40–49	15	0	10	0.22	R
17	F	40–49	5	0	5	0.31	R
19	M	60–69	−5	10	0	0.35	L

ABG, Air-Bone Gap; SP/AP – SP/AP Ratio; R = Right L = Left.

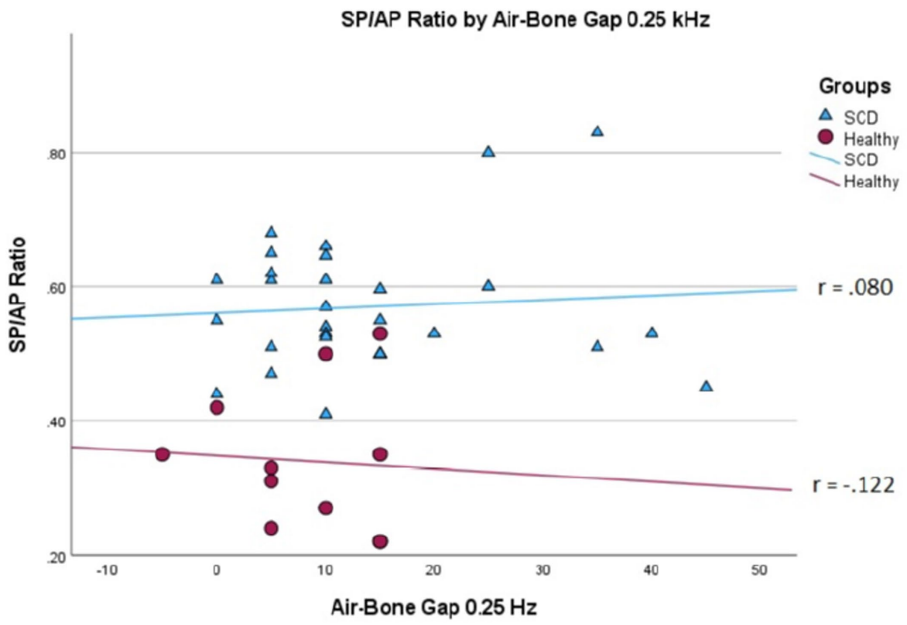

FIGURE 1
Correlations of ABG at 250 Hz and SP/AP ratio in healthy (Pearson $r = -0.122$, $p = 0.720$) and SSCD (Pearson $r = -0.080$, $p = 0.678$) ears.

provide an example of EcochG waveforms obtained. This is the case of a male (Case 14, in Table 2) with left ear symptoms that were first noted approximately 10 months prior to our consultation. These consisted of hearing his eyes move in his head in his left ear in quiet as well as left-sided pulsatile tinnitus when his head was on the pillow left eat down, left ear autophony, and sound sensitivity. The patient denied diminished hearing in both ears, otalgia, discharge, vertigo, noise exposure, prior ear surgery, prior ear infections, and prior ototoxic medications.

The review of his audiogram (Figure 4) demonstrated normal hearing on the right with bone conduction hypersensitivity at 1000 Hz; in the left ear, there was mild conductive hearing loss with bone conduction hypersensitivity with negative thresholds at 250 and 500 Hz. Speech reception threshold on the right was 10 dB with a word recognition score of 100%, and speech reception threshold on the left was 10 dB with a word recognition score of 100%. Tympanograms were type A bilaterally, and acoustic reflexes were present in all conditions.

Electrocochleography (Figure 5) was carried out using a set of surface electrodes along with a hydrogel tympanic membrane electrode introduced under microscopic visualization of the ear canals and tympanic membranes, as previously described. Clicks were used as stimuli.

With right ear stimulation, the summating potential to action potential ratio was within normal limits with a value of 0.33. The auditory brainstem response I-V interpeak latency, also available in such recording was also evaluated, and was within normal limits with a value of 3.94 ms.

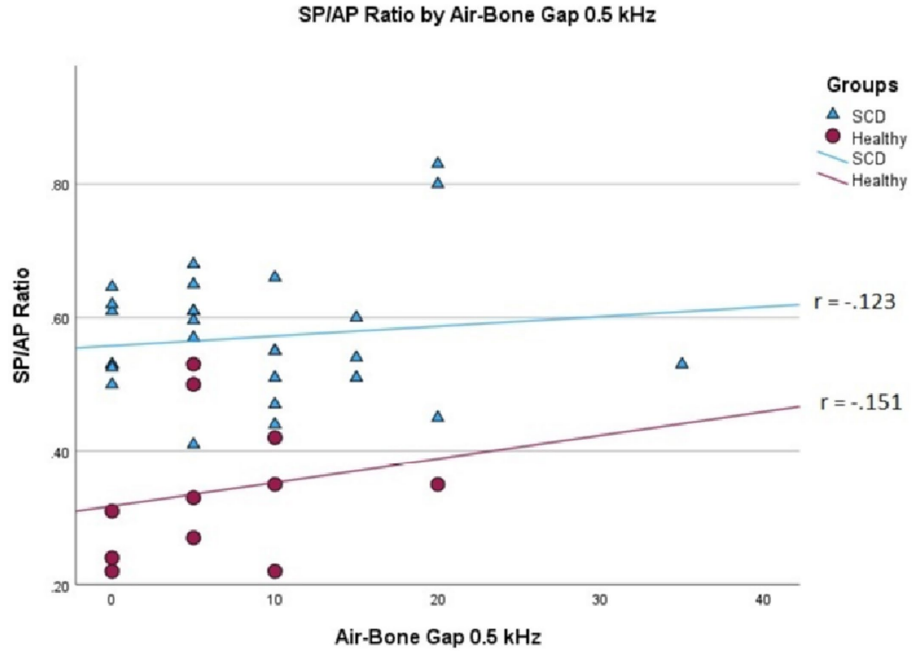

FIGURE 2
Correlations of ABG at 500 Hz and SP/AP ratio in healthy (Pearson $r = -0.151$, $p = 0.658$) and SSCD (Pearson r = −0.123, $p = 0.524$) ears.

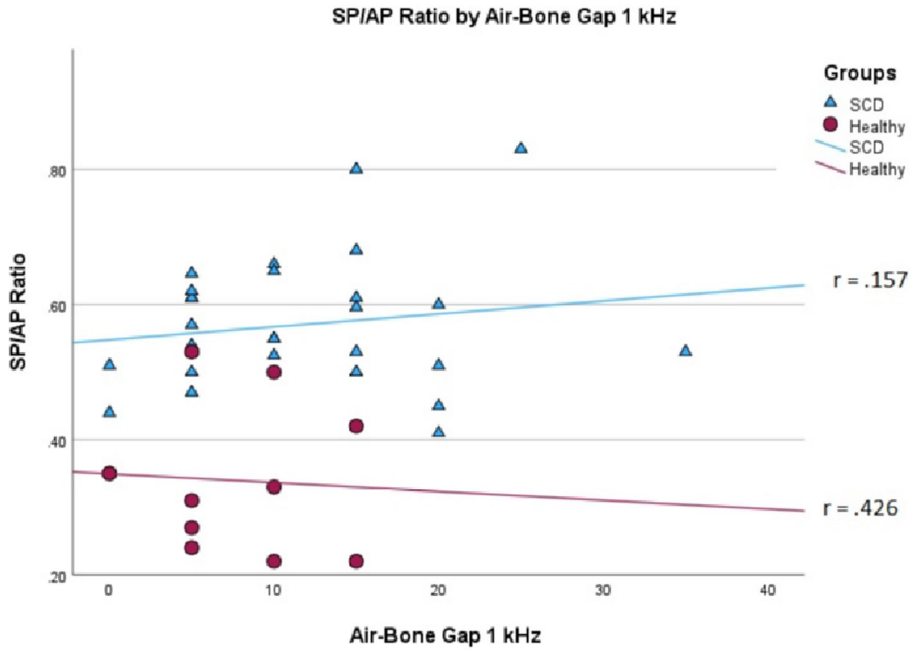

FIGURE 3
Correlations of ABG at 1000 Hz and SP/AP ratio in healthy (Pearson $r = -0.426$, $p = 0.192$) and SSCD (Pearson $r = -0.157$, $p = 0.415$) ears.

With left ear stimulation, the summating potential to action potential ratio was elevated with an abnormal value of 0.65. We also evaluated the auditory brainstem response I-V interpeak latency, which was within normal limits with a value of 4.02 ms.

A CT scan was obtained subsequently and demonstrated a bony dehiscence involving the left superior semicircular canal, and relative thinning involving the bony plate of the right superior semicircular canal but no dehiscence (Figure 6).

In summary, this patient presented with predominantly left ear symptoms that raised the suspicion of left superior semicircular canal dehiscence. CT imaging confirmed the presence of dehiscence of the left superior canal. He subsequently underwent surgical

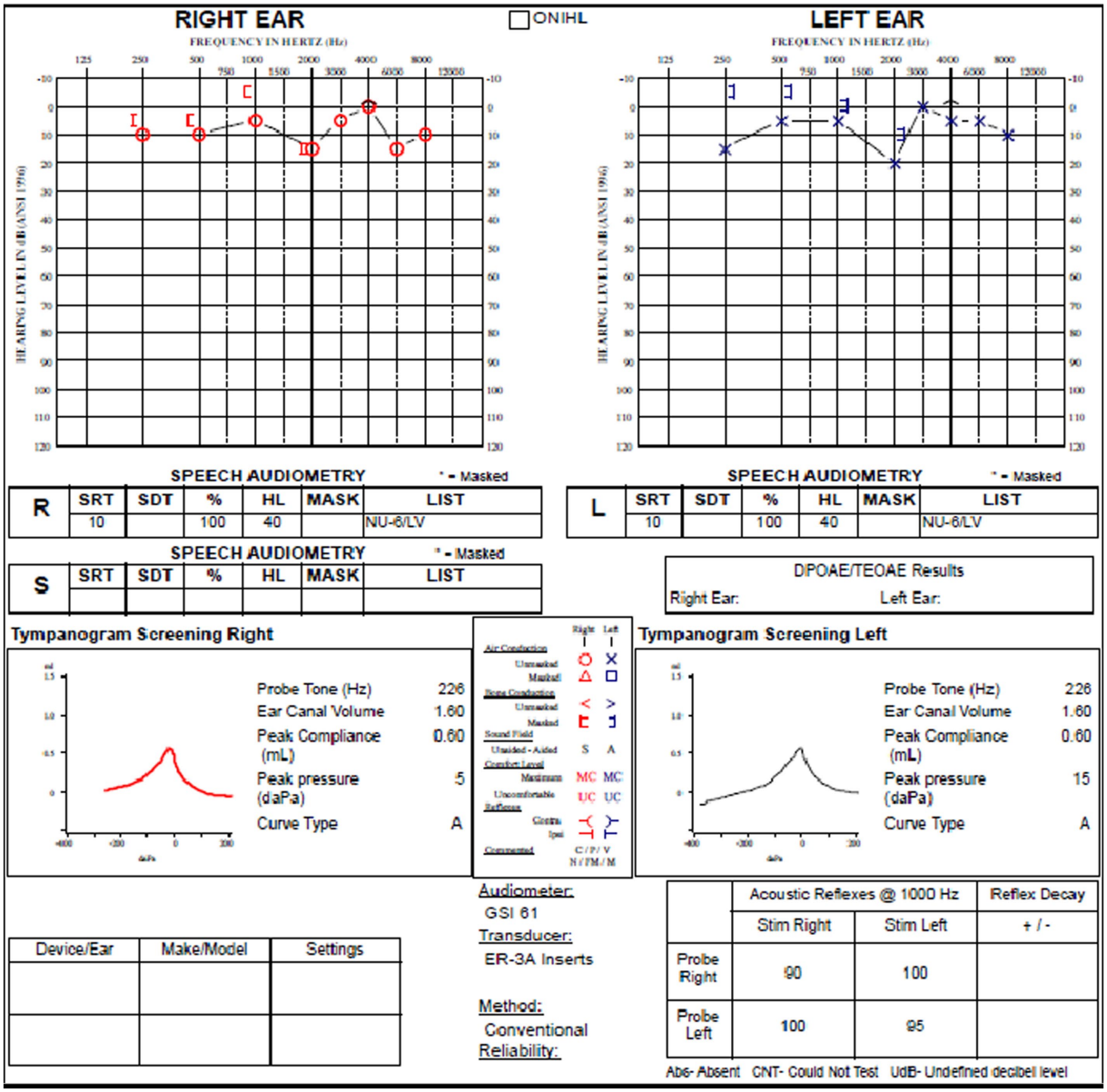

FIGURE 4
Audiogram of subject with left SSCD demonstrates relatively modest air-bone gap in the left ear.

repair to plug the left superior semicircular canal. He did well post-operatively, and his disturbing autophony and other symptoms resolved immediately. Follow-up testing within 1 year of surgery demonstrated intact hearing in the left, operated ear, and a normal SP/AP value in the operated ear.

Discussion and conclusion

The results of this report demonstrated that the EcochG SP/AP ratio was abnormal in the dehiscent ear of all of the patients with bilateral or unilateral SSCD. When the findings were examined for patients with bilateral SSCD in which symptoms localized to one ear, the SP/AP ratio trended toward being higher for that ear. This physiological change in the EcochG SP/AP ratio was observed to normalize in real time during the surgical procedure, intraoperatively, as previously reported by our group (5, 8, 9). This study did not address intraoperative and postoperative changes in SP/AP values in patients with SSCD as the purpose was to determine the diagnostic utility of EcochG and its relationship with air-bone gap in patients with this condition. One of the limitations of the current study is that it is a retrospective study without a corresponding control group for our experimental group. However, it is of note that 11 normal ears from 11 out of 20 subjects with unilateral SSCD were included in the data analysis. Additionally, the use of a multiplanar reformatted CT has been shown in previous studies to have a negative predictive value of 100%. Accordingly, the chance that the ears assigned as "negative" in our study have an undiagnosed SSCD is extremely low.

The EcochG is a response recorded from the tympanic membrane that represents the evoked responses from both the cochlea and the

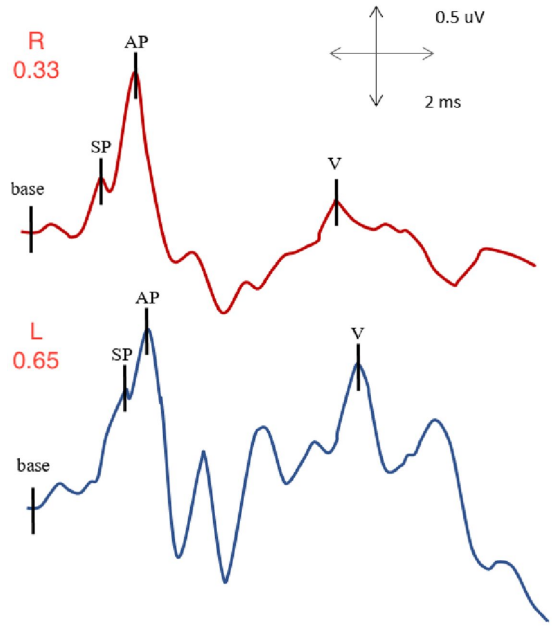

FIGURE 5
EcochG from right and left ears of subject with left SSCD: normal SP/AP value for the right ear (0.33) and elevated SP/AP value for the left, involved ear (0.65).

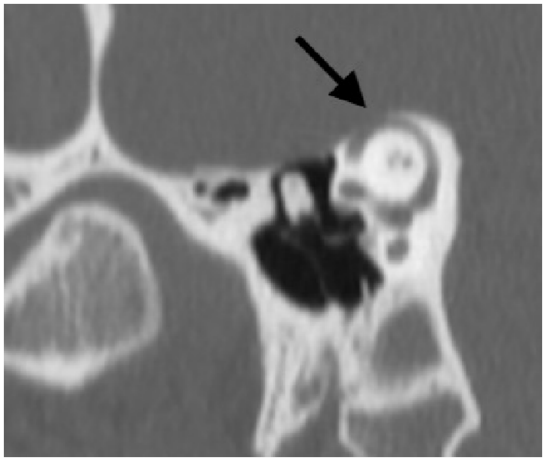

FIGURE 6
Poschl view of left SSCD shows clear absence of bone over the left superior semicircular canal.

auditory nerve in response to an auditory stimulus. The response occurs in approximately the first 3 ms following the presentation of the stimulus. Although the mode of stimulation and recording parameters can vary the response, it is typically composed of the peripheral end-organ responses that are the cochlear microphonic and summating potential and neural response referred to as the compound action potential of the cochlear nerve. In the current study, the EcochG was recorded using a commercially available tympanic membrane electrode.

The response properties of the SP are that it is a direct current response, can be represented as a positive or negative shift in polarity when measured from the pre-stimulus baseline, and can occur simultaneously with the cochlear microphonic. The response is often recorded using an alternating polarity to cancel out the CM. The origin of the SP is believed to be derived from both the inner and outer hair cells and represents the non-linear mechanical properties of the cochlea. For a brief, transient stimulus, the SP waveform will typically occur immediately before the AP. The AP is commonly displayed as a negative deflection and represents the simultaneous activation of the auditory nerve fibers. This response, although opposite in polarity, is the Wave I observed during an auditory brainstem response recording.

The SP response can vary significantly in amplitude, and an increase in amplitude as measured against the AP amplitude has been suggested as an indication of endolymphatic hydrops commonly associated with the disorder referred to as Meniere's disease (MD). This increase in amplitude of the SP has been set forth as being due to increased static displacement of the basilar membrane toward the scala tympani in the cochlear. The underlying mechanism for this increased movement has been reported to be due to an increase in the hydrostatic pressure above the basilar membrane in the cochlea. This phenomenon presents clinically when the SP and AP are recorded in patients with active MD. As many as two-thirds of patients with MD have been suggested to generate abnormal SP/AP ratios. This has also been shown in animal models that reported significant hydromechanical alterations in the scala media and subsequently explained the enhanced SP relative to the AP (12). Interestingly, the SP/AP ratio could be returned to normal by removing perilymph using suction through a fistula created surgically in the cochlea (13). A third window condition such as SSCD has been shown to mimic the enhanced SP/AP ratio observed in endolymphatic hydrops by altering the hydrostatic properties of the cochlea. The physiological mechanism for this effect of a third window on the SP/AP ratio may be that the pressure in the scala tympani and scala vestibuli is reduced creating an endolymphatic differential pressure. During surgical exposure and drilling of the dehiscence to access the perilymph compartment, a significant drop in perilymph pressure was observed. The physiological response from this introduction of a third window to the cochlear system was explained as causing a reduction in the perilymphatic pressure and a corresponding increase in the endolymphatic pressure. The effect of this change in pressure would push the basilar membrane toward the scala tympani and would result in an enhanced SP when EcochG techniques were used for recording. This is a common observation during EcochG intraoperative monitoring of the dehiscence repair. Effective plugging of the dehiscence is more often than not associated with the immediate reduction of the SP/AP ratio that brings it into the normal range (5, 8). All ears with CT-confirmed SSCD in this cohort generated elevated SP/AP ratios exceeding our stated normal of 0.4. None of the ears with intact (even thinning) bony covering exhibited increased SP/AP values above 0.4. It is of note, that some of the ears with thin, but intact bone, and negative (normal) SP/AP ratio, were associated with abnormal C-VEMP results, further supporting the superiority of the EcochG as a diagnostic tool for SSCD. According to these findings, we set forth that SSCD should be strongly considered as being in the differential diagnosis when there is an observed enhanced SP/AP ratio and symptoms that would suggest a third window disorder (e.g., Tullio's phenomenon).

Our results presented in this study continue to illustrate how the EcochG has a high sensitivity for detecting SSCD independent of the necessity of active patient participation, that may be challenging to some,

as is the case with the cVEMP. Tympanic EcochG is not associated with the anxiety and discomfort of a transtympanic needle, and it provides excellent response resolution. As a result, a much wider proportion of the patient population is appropriate for this diagnostic test, if necessary. This is not to be confused with the so-called Tip-trode, ear canal EcochG measurement which has a much poorer resolution and tends to be very inconsistent. The EcochG offers a number of advantages over the VEMP for identifying active SSCD. This includes not requiring EMG monitoring, patient fatigue associated with activating the sternocleidomastoid muscle, and a significant absence of responses in patients over 65 years. Our institutional experience has evaluated and diagnosed with EcochG approximately 3,000 patients. Our EcochG procedures have been shown to be well tolerated by older pediatric patients and can be done in the outpatient setting and inpatient setting alike. As such, the EcochG has a great clinical utility in the operating room for patients with SSCD. While VEMP cannot be performed under general anesthesia, the EcochG has no such limitation. In the operating room setting during an SSCD repair, the EcochG can document immediate changes in the SP/AP ratio and confirm that the plugging or resurfacing of the dehiscence is successful.

This report adds new information to what we have learned till now using the EcochG technique to assess and manage patients with SSCD. As previously noted, although there was a positive trend in frequency and audiometric ABGs, our results failed to reach significance. Furthermore, the non-significant *p*-values for the correlations between ABG and SP/AP ratios in ears with confirmed SSCD suggests that the association of ABGs is similar for ears with and without SSCD. It is possible that where the sample is larger, there is a significant effect. The determination of ABG is a purely subjective measure as opposed to the SP/AP ratio derived from appropriately carried out EcochG. The advantages of the EcochG over tests such as audiometry and VEMP are that it is a purely objective measure and not dependent upon the patients' level of focus and overall participation.

Data availability statement

The original contributions presented in the study are included in the article/supplementary material, further inquiries can be directed to the corresponding authors.

Ethics statement

Ethical approval was not required for the study involving humans in accordance with the local legislation and institutional requirements. Written informed consent to participate in this study was not required from the participants or the participants' legal guardians/next of kin in accordance with the national legislation and the institutional requirements.

Author contributions

PK: Conceptualization, Investigation, Methodology, Supervision, Writing – original draft, Writing – review & editing. MC: Data curation, Formal analysis, Investigation, Writing – original draft, Writing – review & editing. DM: Data curation, Investigation, Writing – review & editing.

Funding

The author(s) declare that no financial support was received for the research, authorship, and/or publication of this article.

Conflict of interest

The authors declare that the research was conducted in the absence of any commercial or financial relationships that could be construed as a potential conflict of interest.

Publisher's note

References

1. Minor LB, Solomon D, Zinreich JS, Zee DS. Sound- and/or pressure-induced vertigo due to bone dehiscence of the superior semicircular canal. *Arch Otolaryngol Head Neck Surg*. (1998) 124:249. doi: 10.1001/archotol.124.3.249

2. Rosowski JJ, Songer JE, Nakajima HH, Brinsko KM, Merchant SN. Clinical, experimental, and theoretical investigations of the effect of superior semicircular canal dehiscence on hearing mechanisms. *Otol Neurotol*. (2004) 25:323–32. doi: 10.1097/00129492-200405000-00021

3. Hunter JB, Patel NS, O'Connell BP, Carlson ML, Shepard NT, McCaslin DL, et al. Cervical and ocular VEMP testing in diagnosing superior semicircular canal dehiscence. *Otolaryngol Head Neck Surg*. (2017) 156:917–23. doi: 10.1177/0194599817690720

4. Lookabaugh S, Kelly HR, Carter MS, Niesten MEF, McKenna MJ, Curtin H, et al. Radiologic classification of Superior Canal dehiscence. *Otol Neurotol*. (2015) 36:118–25. doi: 10.1097/mao.0000000000000523

5. Arts HA, Adams ME, Telian SA, El-Kashlan H, Kileny PR. Reversible electrocochleographic abnormalities in Superior Canal dehiscence. *Otol Neurotol*. (2009) 30:79–86. doi: 10.1097/mao.0b013e31818d1b51

6. Smith CA, Vernon JA. *Handbook of auditory and vestibular research methods*. Springfield, IL: C.C. Thomas (1976).

7. Davis H, Deatherage BH, Eldredge DH, Smith CA. Summating potentials of the cochlea. *Am J Physiol*. (1958) 195:251–61. doi: 10.1152/ajplegacy.1958.195.2.251

8. Adams ME, Kileny PR, Telian SA, El-Kashlan HK, Heidenreich KD, Mannarelli GR, et al. Electrocochleography as a diagnostic and intraoperative adjunct in superior semicircular canal dehiscence syndrome. *Otol Neurotol*. (2011) 32:1506–12. doi: 10.1097/mao.0b013e3182382a7c

9. Ellsperman SE, Telian SA, Kileny PR, Welch CM. Intraoperative electrocochleography correlates to outcomes in transmastoid and middle cranial fossa superior semicircular canal dehiscence repair. *Otol Neurotol*. (2021) 43:120–7. doi: 10.1097/mao.0000000000003350

10. Kileny PR, McCaslin DL. Electrocochleography (EcochG) In: G Jacobson, editor. *Balance function assessment and management*. San Diego, CA, USA: Plural Publishing Inc. (2021)

11. Ferraro JA, Kileny PR, Grasel SS. Electrocochleography: new uses for an old test and normative values. *Am J Audiol*. (2019) 28:783–95. doi: 10.1044/2019_aja-heal18-18-0190

12. Jin XM, Guo YQ, Huangfu MS. Electrocochleography in an experimental animal model of acute endolymphatic hydrops. *Acta Otolaryngol*. (1990) 110:334–41. doi: 10.3109/00016489009107452

13. Campbell KC, Savage MM. Electrocochleographic recordings in acute and healed perilymphatic fistula. *Arch Otolaryngol Head Neck Surg*. (1992) 118:301–4. doi: 10.1001/archotol.1992.01880030089018

frontiers | Frontiers in Neurology

TYPE Original Research
PUBLISHED 26 February 2024
DOI 10.3389/fneur.2024.1336627

OPEN ACCESS

EDITED BY
Todd Mowery,
Rutgers, The State University of New Jersey, United States

REVIEWED BY
Nicolas Perez-Fernandez,
University Clinic of Navarra, Spain
Nils Guinand,
Hôpitaux Universitaires de Genève (HUG), Switzerland

*CORRESPONDENCE
Daniel J. Lee
djlee1@mgh.harvard.edu

†These authors have contributed equally to this work

RECEIVED 11 November 2023
ACCEPTED 06 February 2024
PUBLISHED 26 February 2024

CITATION
Benchetrit L, Shave S, Garcia A, Chung JJ, Suresh K and Lee DJ (2024) Predictors of non-primary auditory and vestibular symptom persistence following surgical repair of superior canal dehiscence syndrome. *Front. Neurol.* 15:1336627. doi: 10.3389/fneur.2024.1336627

Predictors of non-primary auditory and vestibular symptom persistence following surgical repair of superior canal dehiscence syndrome

Liliya Benchetrit[1,2†], Samantha Shave[1,3†], Alejandro Garcia[1,4], Janice J. Chung[1], Krish Suresh[1] and Daniel J. Lee[1*]

[1]Department of Otolaryngology–Head and Neck Surgery, Massachusetts Eye and Ear and Harvard Medical School, Boston, MA, United States, [2]Department of Otolaryngology–Head, and Neck Surgery, Boston University, Boston, MA, United States, [3]Rutgers Robert Wood Johnson Medical School, New Brunswick, NJ, United States, [4]Department of Otolaryngology–Head, and Neck Surgery, University of Iowa, Iowa City, IA, United States

Objective: Patients with superior canal dehiscence syndrome (SCDS) can present with a plethora of auditory and/or vestibular symptoms associated with a bony defect of the superior semicircular canal. While surgical repair is a reasonable option for patients with significant localizing symptoms, the degree of clinical improvement will vary among patients and poses challenges in outcome prediction. This study aims to assess the relationship between preoperative and postoperative symptoms and identify predictors of symptom persistence following repair.

Study design: Retrospective chart review.

Setting: Tertiary neurotology single-institution care center.

Main outcome measures: The primary outcome was to determine the proportion of resolved and persistent primary (most bothersome) and non-primary audiologic and vestibular symptoms following SCD repair. Secondary outcomes included comparison of patient, operative and radiologic characteristics between patients with resolved vs. persistent symptoms. Standardized patient questionnaires including 11 auditory and 8 vestibular symptoms were administered to patients at their preoperative and follow-up visits. Patient pre- vs. postoperative survey results, demographic and clinical characteristics, operative characteristics, audiometric data and cervical vestibular evoked myogenic potential (cVEMP) thresholds were compared via univariate χ^2 and multivariate binary logistic regression analyses between those patients reporting full postoperative resolution of symptoms and persistence of one or more symptoms. Radiologic computed tomography (CT) measurements of superior canal dehiscence (SCD) defect size, location, and laterality were also compared between these two groups.

Results: Of 126 patients (132 ears) included in our study, 119 patients (90.2%) reported postoperative resolution ($n = 82$, 62.1%) or improvement ($n = 37$, 28.0%) of primary (most bothersome) symptoms, while 13 patients (9.8%) reported persistence of primary symptoms. The median (interquartile range) and range between surgery and questionnaire completion were 9 (4–28), 1–124 months, respectively. Analyzing all symptoms (primary and non-primary) 69 (52.3%) and 68 (51.1%) patients reported complete postoperative auditory and vestibular symptom resolution, respectively. The most likely persistent symptoms included

imbalance (33/65/67, 50.8%), positional dizziness (7/20, 35.0%) and oscillopsia (44/15, 26.7%). Factors associated with persistent auditory symptoms included history of seizures (0% vs. 7.6%, $p = 0.023$), auditory chief complaint (50.0% vs. 70.5%), higher PTA (mean 19.6 vs. 25.1 dB, $p = 0.043$) and higher cervical vestibular evoked myogenic potential (cVEMP) thresholds at 1000 Hz (mean 66.5 vs. 71.4, $p = 0.033$). A migraine diagnosis (14.0% vs. 41.9% $p < 0.010$), bilateral radiologic SCD (17.5% vs. 38.1%, $p = 0.034$) and revision cases (0.0% vs. 14.0%, $p = 0.002$) were associated with persistent vestibular symptoms. Neither SCD defect size nor location were significantly associated with symptom persistence ($P > 0.05$).

Conclusions: Surgical repair for SCDS offers meaningful reduction in the majority of auditory and vestibular symptoms. However, the persistence of certain, mostly non-primary, symptoms and the identification of potential associated factors including migraines, PTA thresholds, cVEMP threshold, bilateral SCD, and revision cases emphasize the importance of individualized patient counseling and management strategies.

KEYWORDS

superior canal dehiscence syndrome, cVEMP, vestibular evoked myogenic potential, third window, surgery, middle fossa craniotomy, transmastoid, mastoidectomy

Introduction

Third window syndrome encompasses a set of vestibular and auditory signs and symptoms that arise when a pathological third mobile window is present in the bony labyrinth of the inner ear. One of the most thoroughly studied conditions within this category is known as superior canal dehiscence syndrome (SCDS). This syndrome is due to a bony defect of the superior semicircular canal (SSC). This "third window" disrupts the bony barrier between the SSC and middle cranial fossa, most commonly at the arcuate eminence and, in rare cases, between the descending limb of the SSC and superior petrosal sinus (1, 2). The morphology of this bony defect, clinical presentation, and diagnostic indicators varies widely across patients. This has presented many challenges in terms of both diagnosis and clinical decision making. Some SCDS patients present with severe vestibular and/or auditory symptoms while others are minimally symptomatic. Patients experiencing unremitting localizing symptoms are possible candidates for surgical repair while the majority of SCDS patients can be observed.

There are currently no known medical therapies that are suitable for SCDS aside from avoidance or reduction of triggers. Surgery is a safe and reasonable management option, but there is a lack of consensus on which technique is the most effective. There are three main surgical approaches for the repair of SCD described in the literature - middle cranial fossa (MCF) approach, transmastoid approach (TM) and, round window reinforcement or plugging through a transcanal approach. The MCF approach has been the predominant technique for surgical repair, but there has been recent debate on the efficacy of the TM approach compared to MCF approach. The MCF approach provides better visualization; however, it carries an increased risk for morbidity of craniotomy with brain retraction (3, 4). In comparison, where TM approach lacks in direct visualization of the defect, it does avoid the morbidity of a craniotomy (4, 5). Of note, a recent literature review demonstrated that the MCF approach for the repair of SCD is associated with greater symptom resolution when compared to the TM approach (6). The primary goal of surgical repair is to create a watertight seal at the site of the defect. This is often described in the literature as gentle "plugging" or sealing of the dehiscence, where a variety of different materials have been described to achieve a watertight repair with no clear consensus among studies regarding specific technique. In contrast, attempts to "resurface" the bony defect are associated with higher rates of symptom recurrence compared to plugging or sealing of the SCD (7). In addition, the rate and durability of symptom resolution is highly variable, making clinical counseling challenging (5, 8–15).

Although many studies show clinical improvement in most surgical patients, a formal analysis on persistent symptoms following operative repair is limited (16–19). Some research has suggested that mechanically induced symptoms (i.e., low-frequency conductive hearing loss, autophony, pulsatile tinnitus, and sound- and pressure-induced vertigo) tend to resolve more readily compared to headaches, chronic disequilibrium, and brain fog. An analysis of three studies that included 124 patients reported postoperative resolution of symptoms of autophony, pulsatile tinnitus and sound- and pressure-induced vertigo in the range of 73%−100%, compared to 63%−95% for general disequilibrium and aural fullness. What is not well understood are the preoperative variables that predict postoperative clinical outcomes (5, 16, 20–22).

Theories to explain residual symptoms include "unmasking" of the contralateral ear in patients with bilateral dehiscence, iatrogenic alteration of the vestibular system or comorbid pathologies, and limitations of modern surgical repair techniques. Several studies have shown worse outcomes in patients with bilateral disease compared to those with unilateral disease, and it has come into question whether patients with bilateral defects receive bilateral repair or only unilateral repair (19, 21, 23–26). In addition,

our group identified that in female patients, three factors were associated with prolonged recovery: (1) a history of migraines, bilateral SCD, and a larger dehiscence. In the same study, we observed a predominance residual vestibular symptom compared to auditory symptoms, with ∼37% of patients experiencing continued balance issues postoperatively (16). Migraines are an important comorbid condition associated with ongoing vestibular issues after repair (16, 27).

We will extend our prior observations to identify clinical features of SCD patients that report symptom persistence following operative repair and evaluate the relationship between preoperative diagnostic indicators and clinical outcomes to improve patient counseling and surgical decision making.

Materials and methods

This retrospective cohort study comprised a review of patients diagnosed with SCDS for which they underwent a surgical repair at our institution between 2002 and 2021. This study was approved by the Institutional Review Board (IRB) at Massachusetts General Brigham under protocol number (2021P001712).

Subjects, survey instruments, and surgical intervention

Patient data were obtained retrospectively from the electronic medical records (EMR) and managed using REDCap electronic data capture tools hosted at Massachusetts Eye and Ear Infirmary (28, 29). Patient (sex, age, past medical history, comorbid otologic/vestibular conditions, symptom duration) and surgical (radiologic laterality, surgical approach, endoscope use, and primary or revision case) characteristics were recorded.

Responses on a standardized symptomatology questionnaire collected from patients at their preoperative and postoperative visits were recorded. This questionnaire has been previously used successfully for research by our group (19, 30, 31). Briefly, the questionnaire asked patients to identify if their most bothersome complaint is hearing-related (auditory chief complaint) or balance-related (vestibular chief complaint). Binary replies (yes/no) were then recorded for the subjective experience of 11 auditory symptoms (hearing loss, aural fullness, pulsatile tinnitus, non-pulsatile tinnitus, autophony (hearing your voice too loudly), hyperacusis, hearing your voice echo, hearing your footsteps, hearing your eyeballs moving or hearing hair brushing or shaving sounds too loudly) and 8 vestibular symptoms (general dizziness, sense of imbalance, Tullio phenomenon, straining causing dizziness, physical activity causing dizziness, blowing your nose/sneezing/coughing causing dizziness, oscillopsia and positional dizziness). Information regarding postoperative resolution of primary (most bothersome) symptom complaint was obtained from the EMR and stratified to resolved, improved and persisted according to recorded patient description of symptoms.

Plugging of the SCD was performed through an MFC or TM approach. These surgical techniques have been described throughout the literature (2, 32). In summary, in the MFC approach the defect was plugged with bone wax, and then, any associated tegmen defects were repaired with temporalis fascia and split calvarial bone graft. When the TM approach was used, both limbs of the superior semicircular canal were plugged after labyrinthotomies were made on either side of the dehiscence with no direct contact with the defect (16). We excluded patients whose dehiscence was a result of tumor (cholesteatoma, epidermoid) extension given difficulty in ascertaining etiology of reported symptoms.

Audiometric and VEMP data

Audiometric measurements were recorded from audiologic and vestibular testing during pre- and postoperative visits. Audiogram data included air- and bone- conduction thresholds. The bone conduction (BC) threshold was collected at 250, 500, 1, 000, 2000, and 4000 Hz pre- and postoperatively. The air-bone gap (ABG) was calculated at each tested frequency by subtracting the bone conduction threshold from the air conduction threshold. We collected ABG values at 250, 500, 1, 000, 2000, and 4000 Hz. Pure tone average (PTA) calculated by averaging air conduction thresholds at 500, 1000, and 2000 Hz were recorded. Lastly, cervical vestibular evoked myogenic potential (cVEMP) thresholds were obtained during sternocleidomastoid (SCM) contraction via four surface electromyography (EMG) electrodes.

Tone bursts were presented monaurally at a repetition rate of 13 bursts/second. To determine cVEMP thresholds responses were first obtained at 123 dB peSPL (equivalent to 90 dB HL) after which the sound level was decreased in 10 dB steps until no response could be distinguished from residual noise. To determine threshold, sound levels were then raised by 5 dB. Threshold was defined as the lowest sound level at which a cVEMP was present as determined by the audiologist performing the cVEMP. If no response was identified at the highest possible stimulus intensity (133 dB peSPL) cVEMP threshold was defined as 10 dB higher than our equipment limit, for this would have been the next sound level used. cVEMP thresholds at 500, 750, and 1000 Hz were collected and analyzed. This method has previously been used and described by our institution (33).

Superior canal dehiscence defect size and location

Two independent author raters (AG and JC) measured the size of the defect on pre-operative computed tomography (CT) using the same methods. The Pöschl view, which is perpendicular to the long axis of the temporal bone and parallel to the SSC plane, was analyzed for two measurements: chord length (linear distance between the two ends of the SCD) and arc length (two equal radii were measured from the center – approximated by the arcuate artery – to the two defect ends) (Figure 1). SCD location was described according to our institution's radiologic classification study and include: dehiscence of the lateral upslope (ascending limb of SCC), arcuate eminence, medial downslope (descending limb

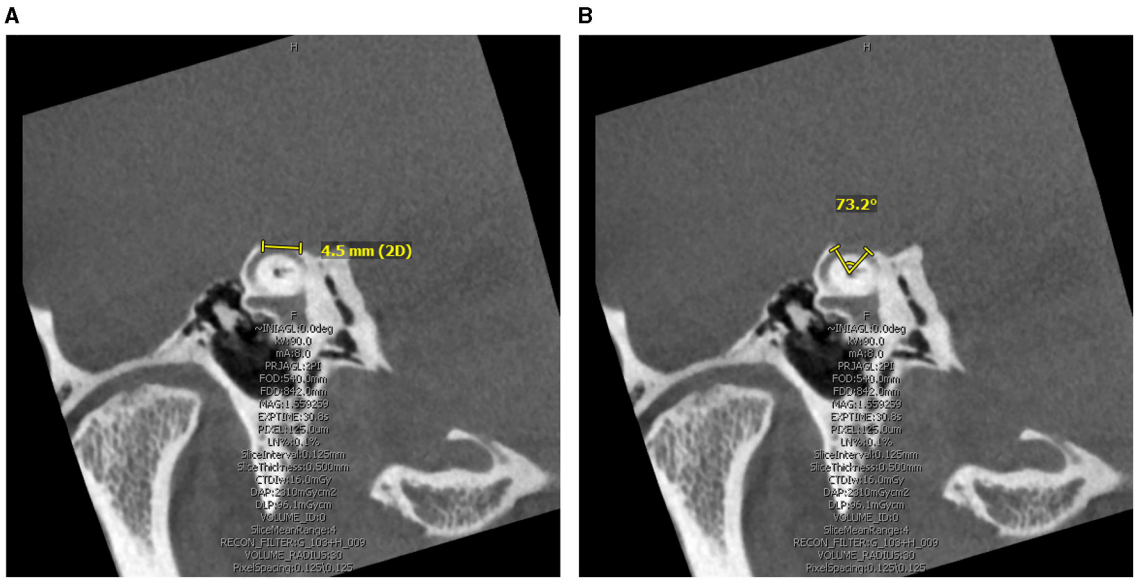

FIGURE 1
Computed Tomography superior canal dehiscence (SCD) measurement in the Pöschl view. **(A)** Linear length measurement obtained as the linear distance between the two ends of the SCD. **(B)** Arc length measurement obtained by radii and angle measure approximating defect center by the arcuate artery.

of SSC), proximity to superior petrosal sinus (SPS), and combined arcuate eminence and SPS defects, as shown in Figure 2 (34).

Our cohort had six patients who underwent bilateral sequential SCD repair surgery. We included each case separately with symptom questionnaire and objective testing obtained before and after each operated ear case.

Statistical analysis

Baseline cohort characteristics were summarized as proportions. Continuous variables were reported by median and interquartile range (IQR) or mean and standard deviation (SD). Each patient's symptom response on the survey was analyzed pre- and postoperatively and classified postoperatively into (1) resolved (if patient endorsed the symptom preoperatively and denied it postoperatively), (2) persistent (if patient endorsed the symptom pre and post operatively), or (3) new symptom (if patient denied the symptom preoperatively but endorsed it post operatively). Primary (most bothersome) symptom status was classified into resolved, improved, and persisted. The McNemar's test for paired nominal data was used to compare the proportions of resolved and persistent symptoms as recorded from survey responses, and resolved, improved and persistent primary symptoms as recorded from the EMR. We evaluated the association between patient, audiometric/vestibular results and surgical/SCD characteristics with auditory and vestibular symptom status (resolved vs. persistent – persistent status was defined as at least one persistent symptom, regardless of whether reported as primary symptom or not) using univariate χ^2 and Fisher exact (in cases of <10 cases) test for categorical variables. An independent *t* test and the Mann–Whitney *U*-test were used to compare means of continuous variables with normal and non-normal distribution, respectively. Factors identified significant on univariate analyses were associated with auditory and vestibular symptom persistence status via multivariate binary logistic regression. Regression models were assessed for multicollinearity and variables with variance inflation factors >4 were removed (35). A Pearson correlation was used to evaluate the relationship between the mean number of symptoms a patient reported (stratified by auditory and vestibular) with SCD defect size and audiometric and vestibular test results, both pre- and post- operatively. Missing values were excluded. All data analyses were performed using SPSS version 29.0 (SPSS, Inc). Significance was determined at the $P < 0.05$ level.

Results

Patient characteristics and presenting signs and symptoms

Our institution manages a database of almost 800 pediatric and adult patients with SCD. We identified a total of 126 patients (132 ears) who had underwent surgical repair for SCDS and met inclusion criteria for this study. The median (IQR) age of patients at the time of surgery was 50.6 (16.7) years. Most of the patients were female (55.6%). The median (IQR) length of follow-up from surgery to time of postoperative questionnaire administration was 9.0 (24.0) months. Thirty-five (27.8%) patients had radiologic evidence of bilateral SCD. The mean (SD) arc and linear SCD length were 4.2 (1.9) mm and 3.9 (1.5) mm, respectively. Middle fossa craniotomy was performed in the majority (92.4%) of cases. The remainder of baseline characteristics is shown in Table 1. All patients underwent canal plugging. The number of audiologic and vestibular symptoms, ABG at 250 Hz, 500 Hz and 1000 Hz

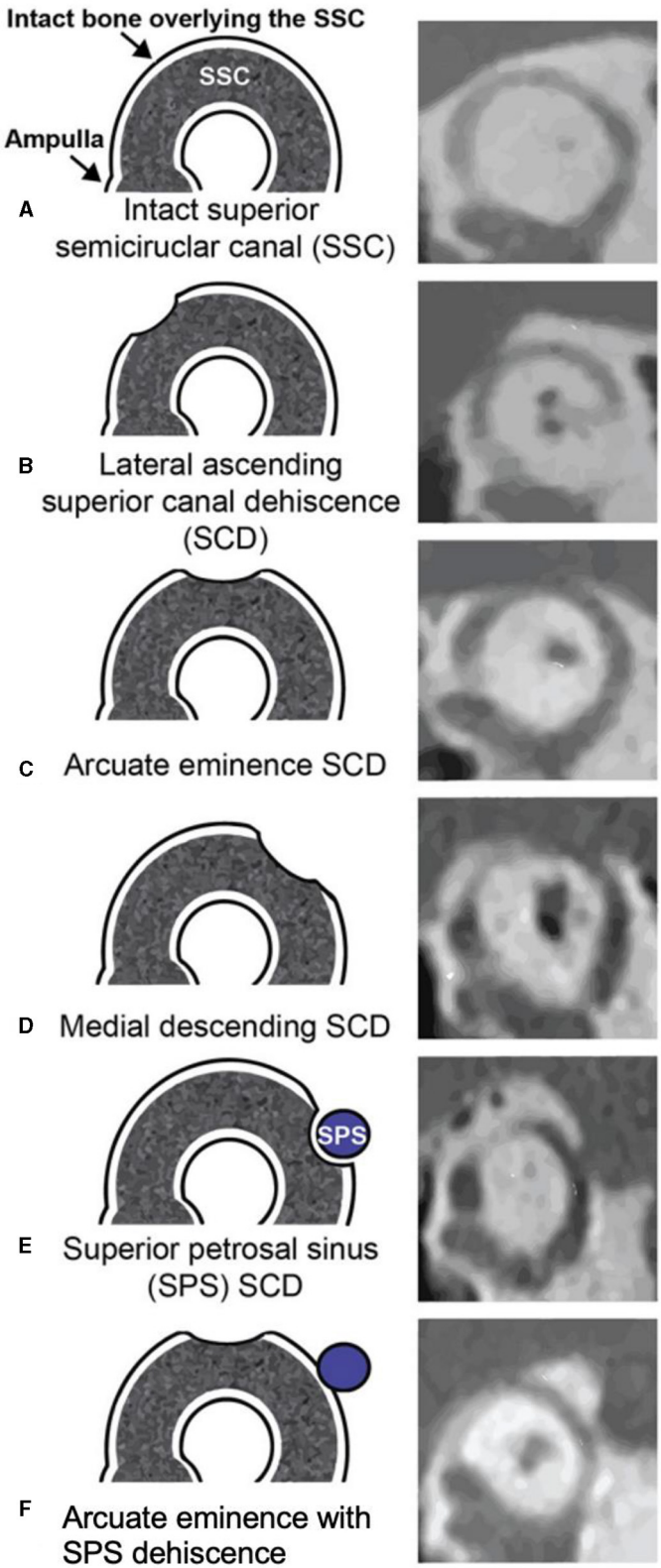

FIGURE 2
Obtained with permission from Lookabaugh et al. (34). Classification of superior canal dehiscence (SCD) based on location. Left column, diagram of defect location; right column, computed tomography images of corresponding defect location. **(A)** Intact superior semicircular canal (SSC), **(B)** Dehiscence on the lateral SSC upslope, **(C)** Dehiscence of the arcuate eminence, **(D)** Dehiscence on the medial SSC downslope, **(E)** Superior petrosal sinus-associated SCD (SPS-SCD), **(F)** Arcuate eminence and SPS dehiscence.

TABLE 1 Baseline cohort characteristics.

Patient characteristics	All $N = 132$ cases (100%)	*P*-value*
Sex		0.076
Male	56 (44.4%)	
Female	70 (55.6%)	
Age at surgery, median (IQR), y	50.6 (41.1–57.8)	
PMH DM	10 (7.9%)	<0.001
PMH HTN	43 (34.1%)	<0.001
PMH obesity (BMI > 30)	22 (17.4%)	<0.001
BMI (kg/m^2), median (IQR)	27.6 (24.9–31.7)	
PMH seizures	5 (4.0%)	<0.001
Migraine diagnosis	40 (27.5%)	<0.001
Prior ear surgery or infection	13 (10.6%)	<0.001
Head Trauma	23 (18.3%)	<0.001
Brain fog	13 (10.3%)	<0.001
Symptom duration prior to SCD diagnosis, median (IQR), m	24.0 (8.8–60.0)	
Follow-up duration (surgery to questionnaire), median (IQR), range, m	10.0 (4.0–28.0), 1.0–124.0	
Chief complaint		
Auditory	76 (59.8%)	0.002
Vestibular	51 (40.2%)	
SCD/operative characteristics		
Radiologic laterality		0.025
Right	39 (30.9%)	
Left	52 (41.3%)	
Bilateral	35 (27.8%)	
SCD location		<0.001
Lateral upslope	30 (22.7%)	
Arcuate eminence	79 (59.8%)	
Medial downslope	17 (12.9%)	
SPS	3 (2.3%)	
Arcuate + SPS	1 (0.8%)	
SCD arc length (mean, SD), mm	4.2 (1.9)	
SCD linear length (mean, SD), mm	3.9 (1.5)	
Surgical Approach		<0.001
Middle fossa craniotomy	122 (92.4%)	
Transmastoid	10 (7.6%)	
Endoscope		<0.001
Used	40 (30.3%)	
Not used	89 (67.4%)	
OSH revision case	8 (6.1%)	<0.001
Underwent revision post index case	19 (14.4%)	<0.001

*P-value represents comparison of proportions within each category via the χ^2 or Fisher exact test (if n < 10). Categories with percentages not adding to 100% are due to unknown/missing information. Categories with only one measured group correlates to those with the disease/symptoms. y, years; m, months; IQR, interquartile range; DM, diabetes mellitus; HTN, hypertension; MBI, body mass index; SCD, superior canal dehiscence; SD, standard deviation; SPS, superior petrosal sinus; OSH, outside hospital.

and all tested cVEMP thresholds showed significant postoperative improvement ($p < 0.001$) (Table 2). There was no significant difference in pre (22.2 dB) - vs. postoperative (21.5 dB) PTA ($p = 0.726$). However, BC thresholds increased significantly among all tested frequencies other than 2000 Hz (Table 2).

Postoperative symptoms

In this cohort, 119 patients (90.2%) reported postoperative resolution ($n = 82$, 62.1%) or improvement ($n = 37$, 28.0%) of primary symptoms, while 13 patients (9.8%) reported persistence of primary symptoms ($p < 0.001$ between persistent and non-persistent symptomatology). Of these 13 patients, 10 (76.9%) reported an auditory chief complaint and 3 (23.1%) patients reported a vestibular chief complaint, $p = 0.007$ (Figure 3). Analyzing all symptoms (primary and secondary), 63 (47.7%) and 64 (48.5%) patients reported persistence of at least one auditory symptom and one vestibular symptom, respectively. All auditory symptoms showed a statistically significant difference between proportion resolution and persistence ($p < 0.001$ for all) (Figure 4A, Supplementary Table 1). Persistent vestibular symptoms included a sense of imbalance (24.2% resolved vs. 25.0% persistent, $p = 0.880$), positional dizziness (9.8% resolved vs. 5.3% persistent, $p = 0.167$) and oscillopsia (8.3% resolved vs. 3.0% persistent, $p = 0.063$) (Figure 4B, Supplementary Table 1).

Factors associated with persistent auditory symptoms included history of seizures (0% vs. 7.9%, $p = 0.023$), auditory chief complaint (50.0% vs. 75.0%), greater number of pre-operative auditory symptoms (3.1 vs. 4.7, $p < 0.001$), higher preoperative PTA threshold (19.6 vs. 25.1 dB, $p = 0.043$) and higher preoperative cVEMP thresholds at 1000Hz (66.5 vs. 71.4 dB HL, $p = 0.033$). Patients with persistent auditory symptoms were more likely to undergo revision surgery (7.4% vs. 22.2%) (Table 3, Figure 5). Factors associated with persistent vestibular symptoms included a migraine diagnosis (20.6% vs. 41.3% $p < 0.001$), number of pre-operative auditory (3.4 vs. 4.3, $p = 0.040$) and vestibular (2.6 vs. 3.3, $p = 0.011$) symptoms, bilateral radiologic SCD (17.5% vs. 38.1%, $p = 0.034$) and patients presenting for a revision case from an outside hospital (0.0% vs. 14.0%, $p = 0.002$) (Table 4). Neither SCD defect size nor location significantly associated with audiologic (Table 3) or vestibular (Table 4) symptom persistence ($p > 0.05$).

TABLE 2 Symptom audiometric and cVEMP results pre- and post- operatively.

	Preoperative	Postoperative	*P*-value*
Symptoms (mean, SD)			
Number of auditory symptoms	3.8 (2.3)	1.2 (1.5)	**<0.001**
Number of vestibular symptoms	2.9 (1.6)	1.2 (1.2)	**<0.001**
Audiometric and cVEMP testing (mean, SD)			
ABG 250 Hz (dB)	23.8 (15.9)	9.1 (12.0)	**<0.001**
ABG 500 Hz (dB)	16.1 (13.3)	6.8 (9.8)	**<0.001**
ABG 1000 Hz (dB)	13.1 (11.6)	6.6 (8.7)	**<0.001**
ABG 2000 Hz (dB)	3.9 (7.6)	2.8 (5.2)	0.181
ABG 4000 Hz (dB)	5.2 (8.1)	5.5 (7.5)	0.761
PTA dB	22.2 (14.9)	21.5 (16.7)	0.726
Bone conduction 250 Hz (dB)	2.9 (12.8)	10.2 (12.5)	**<0.001**
Bone conduction 500 Hz (dB)	8.6 (12.8)	15.6 (13.5)	**<0.001**
Bone conduction 1000 Hz (dB)	7.2 (12.9)	13.1 (14.1)	**<0.001**
Bone conduction 2000 Hz (dB)	18.9 (15.9)	19.8 (18.1)	0.151
Bone conduction 4000 Hz (dB)	22.2 (19.4)	27.2 (20.3)	**<0.001**
cVEMP 500 Hz (dB HL)	65.9 (12.3)	86.9 (10.6)	**<0.001**
cVEMP 750 Hz (dB HL)	66.5 (12.1)	87.8 (10.6)	**<0.001**
cVEMP 1000 Hz (dB HL)	68.9 (11.4)	89.1 (9.9)	**<0.001**

*P-value for comparison of pre and post- operative means via two sample t-test. Bolded values with an * indicate a statistically significant result.

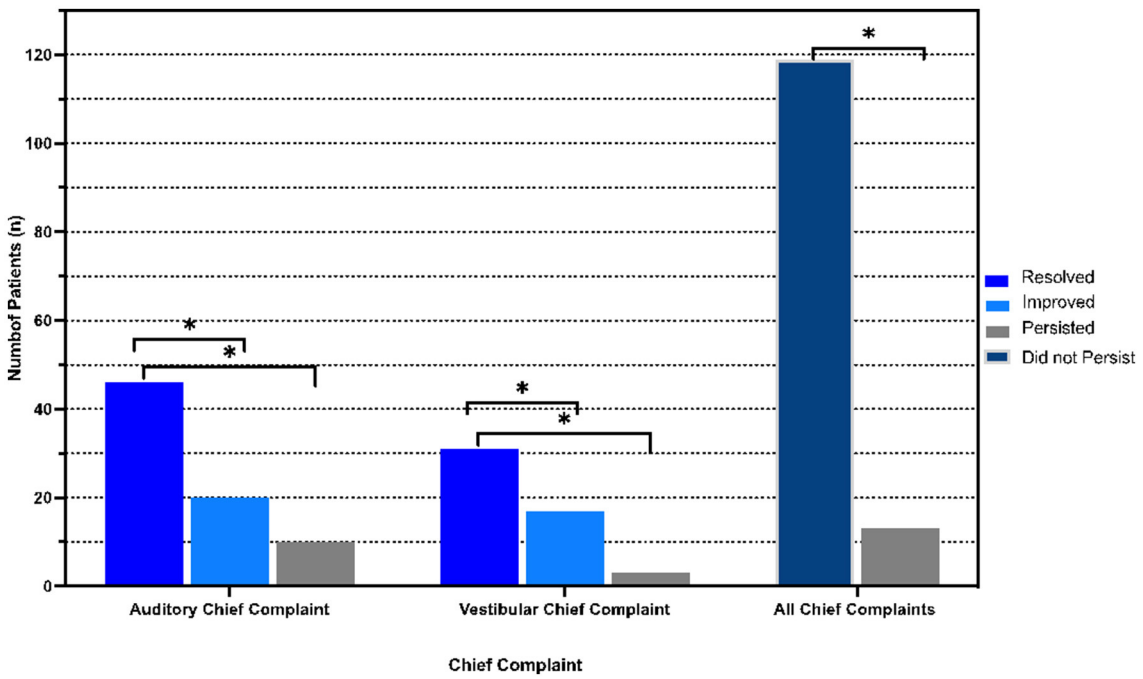

FIGURE 3
Postoperative distribution of primary symptoms. Resolved, improved, persistent and non-persistent (combination of resolved and improved) symptom distribution stratified by primary symptom (chief complaint). *$p < 0.05$ indicates statistical significance.

On multivariate binary logistic regression analysis evaluating the factors found significant on univariate analysis (excluding number of pre-operative auditory symptoms due to multicollinearity) and clinically deemed relevant factors, higher preoperative cVEMP thresholds at 1000 Hz were associated with a higher risk of auditory symptom persistence [Odds Ratio (OR):

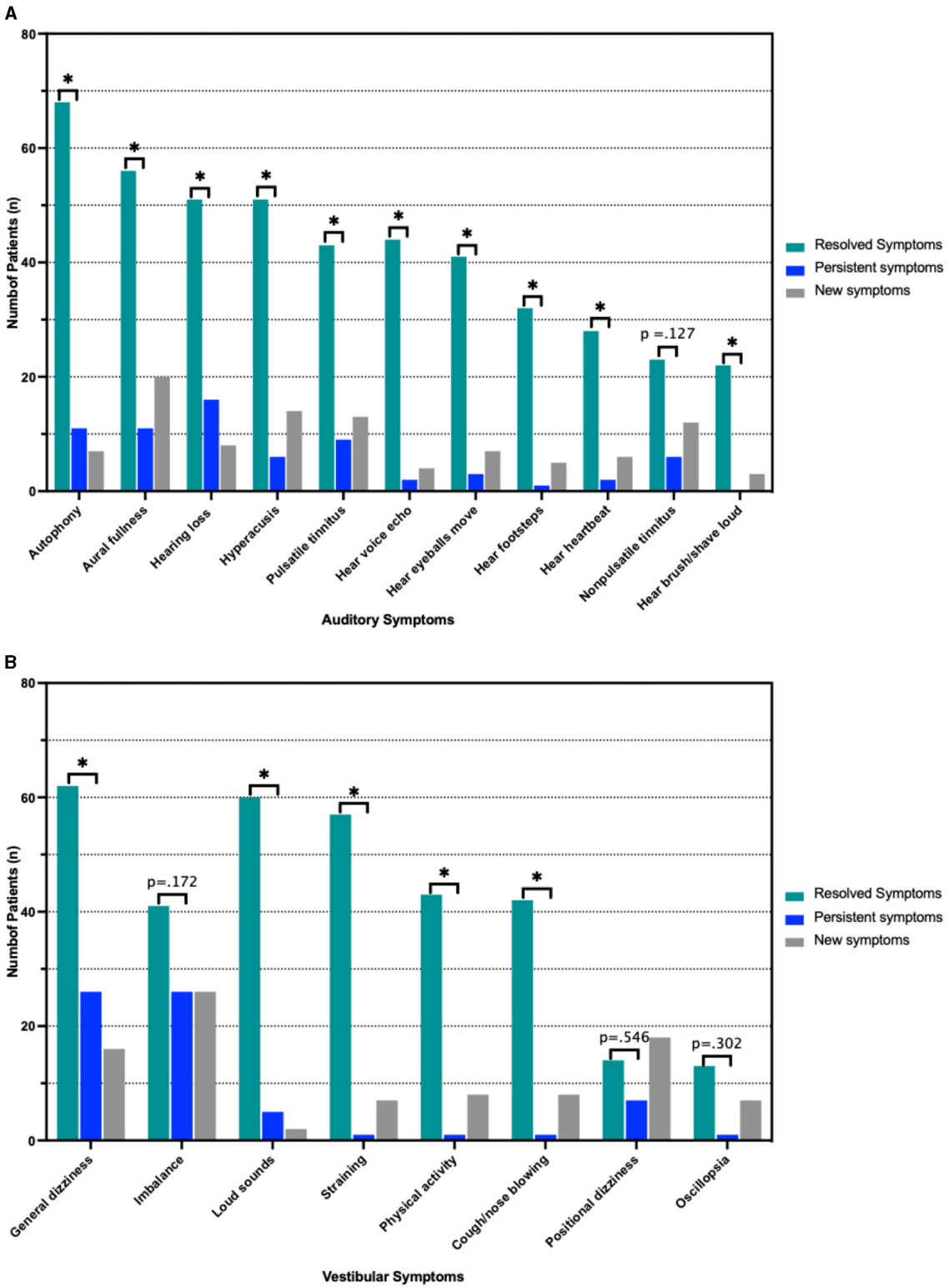

FIGURE 4
Pre- and Postoperative symptoms. **(A)** Resolved, persistent and new auditory symptoms according to number of patients reporting them. **(B)** Frequency of vestibular symptoms stratified as above. *$p < 0.05$ indicated statistical significance comparing resolved and persistent symptoms. Actual p-value is shown in cases with no statistically significant difference between resolved and persistent symptoms.

1.05, 95% Confidence Interval (CI): 1.01–1.10] (Table 5). For vestibular symptoms, multivariate analysis (excluding number of preoperative vestibular symptoms variable due to multicollinearity) showed association of migraines (OR: 2.5, 95% CI: 1.19–7.96) and bilateral radiologic SCD (OR: 3.08, 95% CI: 1.24–7.65) with risk of symptom persistence (Table 6).

TABLE 3 Clinical and demographic characteristics by postoperative auditory symptom status.

	Postoperative auditory symptom status		*P*-value
	Resolved $N = 69$ (52.3%)	Persistent (at least 1) $N = 63$ (47.7%)	0.456
Patient characteristics			
Sex			0.294
Male	33 (47.8%)	24 (38.1%)	
Female	36 (52.2%)	39 (61.9%)	
Age at surgery, median (y)	48.9 (36.8–58.2)	52.6 (46.4–57.8)	0.101
PMH DM	3 (4.3%)	7 (11.1%)	0.193
PMH HTN	24 (34.8%)	19 (30.2%)	0.583
PMH obesity	8 (11.6%)	14 (22.2%)	0.110
PMH seizures	0 (0.0%)	5 (7.9%)	**0.023***
Migraine diagnosis	19 (27.5%)	21 (33.9%)	0.432
Prior ear surgery or infection	4 (6.3%)	9 (14.5%)	0.152
Head Trauma	12 (19.0%)	11 (20.0%)	896
Brain fog	6 (9.4%)	7 (12.1%)	1.000
Symptom duration prior to SCD diagnosis (mean, SD), months	39.1 (51.9)	38.7 (40.9)	0.274
Duration of follow up (mean, SD), months	12.3 (97.7)	23.4 (29.2)	0.416
Chief complaint			**0.19**
Auditory	33 (50.0%)	43 (70.51%)	
Vestibular	23 (50.0%)	18 (29.5%)	
Number of preoperative auditory symptoms (mean, SD)	3.1 (2.2)	4.7 (2.1)	**<0.001***
Number of preoperative vestibular symptoms (mean, SD)	2.8 (1.5)	3.1 (1.7)	0.322
Audiologic characteristics (mean, SD)			
Pre-op ABG 250 Hz (dB)	21.9 (14.6)	25.9 (17.0)	0.160
Pre-op ABG 500 Hz (dB)	16.4 (14.4)	15.8 (12.3)	0.810
Pre-op ABG 1000 Hz (dB)	12.6 (11.6)	13.5 (11.8)	0.669
Pre-op ABG 2000 Hz (dB)	3.8 (775)	4.1 (7.6)	0.804
Pre-op ABG 4000 Hz (dB)	5.4 (7.9)	5.2 (8.2)	0.569
Pre-op PTA dB	19.6 (12.8)	25.1 (16.7)	**0.043***
Pre-op cVEMP 500 Hz (dB HL)	65.0 (0.4)	66.8 (13.9)	0.487
Pre-op cVEMP 750 Hz (dB HL)	64.2 (10.7)	68.3 (12.9)	0.093
Pre-op cVEMP 1000 Hz (dB HL)	66.5 (9.8)	71.4 (12.5)	**0.033***
SCD/operative characteristics			
Radiologic Laterality			0.490
Right	22 (32.8%)	16 (27.1%)	
Left	29 (43.2%)	23 (39.0%)	
Bilateral	16 (23.8%)	20 (33.9%)	
SCD Location			0.226
Lateral upslope	14 (20.6%)	16 (25.8%)	
Arcuate eminence	42 (61.8%)	37 (59.7%)	

(Continued)

TABLE 3 (Continued)

	Postoperative auditory symptom status		*P*-value
	Resolved $N = 69$ (52.3%)	Persistent (at least 1) $N = 63$ (47.7%)	
Medial downslope	11 (16.2%)	6 (9.7%)	
SPS	0 (0.0%)	3 (4.8%)	
Arcuate + SPS	1 (1.5%)	0 (0.0%)	
SCD arc length, mean (SD)	4.0 (1.9)	4.4 (1.9)	0.293
SCD linear length, mean (SD)	3.7 (1.6)	4.0 (1.5)	0.319
Surgical approach			0.193
Middle fossa craniotomy	66 (95.7%)	56 (88.9%)	
Transmastoid	3 (4.3%)	7 (22.2%)	
OSH Revision case	3 (4.6%)	5 (8.5%)	0.476
Underwent revision post index case	5 (7.4%)	14 (22.2%)	**0.024***

Bolded values with an * indicate a statistically significant result.

Interestingly, postoperative audiometric testing results were not significantly associated with risk of audiologic or vestibular symptom persistence ($p > 0.05$ for all) (Supplementary Table 2). Similarly, the number of vestibular and audiologic symptoms did not show significant correlation with audiometric testing, neither pre- nor postoperatively ($p > 0.05$ for all) (Supplementary Table 3).

Discussion

Our study demonstrates significant improvement and resolution in the most bothersome SCDS symptoms as determined from record review and an overall significant reduction of both auditory and vestibular symptoms following surgical repair. We used a standardized questionnaire evaluating 11 auditory and 8 vestibular symptoms. A handful of persistent (majorly non-primary) symptoms and several associated preoperative factors such as migraines, PTA thresholds, cVEMP thresholds, bilateral SCD and revision cases were also identified. These findings highlight the nuances in the variable symptomatology and offer potential insight to preoperative counseling and postoperative recovery management. There are several proposed theories for why symptoms persist for patients following surgical repair. Many explanations include iatrogenic alteration of the vestibular system, psychosocial discrepancy in distinguishing prolonged recovery from persistent and/or new symptoms, the heightening of symptoms in the contralateral ear in cases of bilateral defects, etc. The vestibular system is part of a multisensory system structure, and direct surgical repair by "plugging" or resurfacing" can influence underlying function. Some studies suggest that plugging of the superior canal can lead to long-term deficits of the vestibulo-ocular reflex in response to head impulses (17, 36, 37). However, a recent study found that in response to the Subjective Visual Vertical test was not sensitive for identifying pathology after SCDS repair. This finding suggests that function may be well preserved following surgical plugging, supported by lowered, but still existent, VEMP responses in most patients (38). It is possible that patients may confuse prolonged surgical recovery with persistent or new symptoms related to their condition. The differentiation between symptom persistence and prolonged postoperative recovery is unclear, with no definitive time frame criteria or symptom severity criteria to distinguish between the two. One study with a cohort of 33 patients described clinical factors that are associated with prolonged recovery (average follow-up of 28.7 months) and reported that patients with bilateral SCD, a history of migraines, and larger defects may be at risk of prolonged recovery, however, this study was limited due to its small sample size (16). Our study had a median follow-up time of 9 months (IQR 9–28), range 1–124 months but with a notably larger cohort of 126 patients. This study thus aims to expand our understanding of the factors associated with symptom persistence using a much larger cohort in an effort to (1) improve clinical counseling and patient expectations following surgical repair (2) potentially define the difference between persistent symptoms and prolonged recovery, and (3) emphasize the importance of developing standardized methods for monitoring patient disease and outcomes using audiometric data, cVEMP testing, radiologic measurements, and a validated patient survey.

Persistent and new postoperative symptoms

With regards to persistent auditory symptoms, our cohort followed a different pattern of audiometric findings compared to previous studies that describe persistent hearing loss postoperatively (11, 12, 39). Persistent mild SNHL following primary surgical repair of dehiscence, often in the form of high frequency hearing loss, is not uncommon (9, 40). In our study, there was a significant improvement in ABG at 250 Hz, 500 Hz, and 1000 Hz with no significant changes in the higher frequencies and there was significant resolution of all 11 subjective auditory

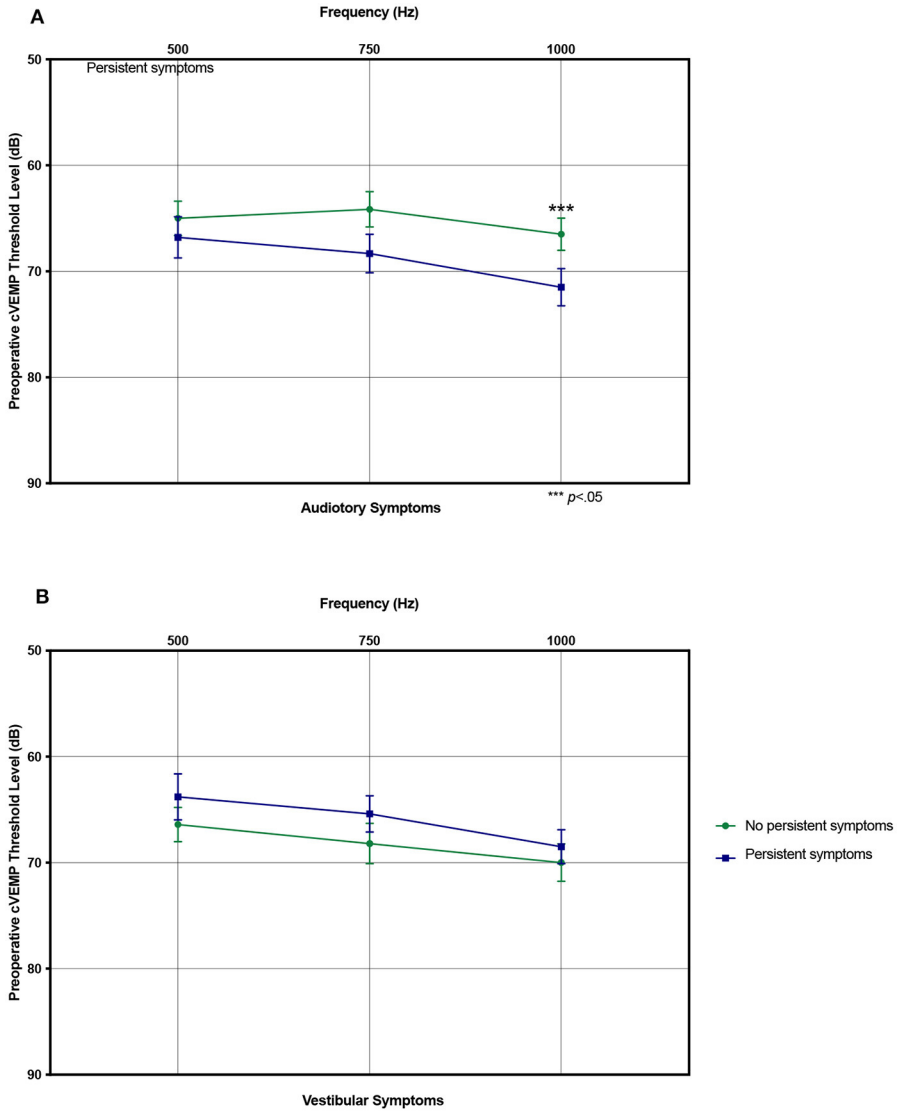

FIGURE 5
Preoperative cervical vestibular evoked myogenic potential (cVEMP) thresholds. **(A)** Mean preoperative cVEMP thresholds stratified by resolved and persistent postoperative auditory symptoms. **(B)** Same showing for vestibular symptoms. ***$p < 0.05$ indicating statistical significance comparing resolved and persistent symptoms. Error bars denote standard error.

symptoms, perhaps pointing to the comprehensive nature of the used survey.

Acute vestibular postoperative impairment is frequently reported in the literature. However, long-term persistence of this group of symptoms is limited. Additionally, acute vestibular impairment can occur after SCD repair, but most patients are able to compensate within several months (38, 41). This is consistent with vestibular impairment in the acute postoperative setting. Reduced SSC function alone can likely not explain cases of prolonged vestibular impairment. In our study patients with persistent vestibular symptoms after surgery presented mostly with a sense of imbalance, positional dizziness and oscillopsia with a prevalence below 20 %. For instance, prolonged vestibular impairment is common among patients with a concomitant migraine diagnosis or with bilateral SCDS, likely due to the more generalized vestibular impairment prior to surgery and a reduced ability of central compensation (16, 27). Previous studies have shown that patients with concurrent SCDS and migraine may have prolonged recovery after surgery (16, 27). The finding of bilateral radiologic dehiscence showing more persistent symptoms following a unilateral repair also supports the theory of "unmasking" by which symptoms might become more noticeable or be perceived as originating more clearly from the unoperated ear (8, 42). Bilateral dehiscence is an important finding in the preoperative workup, and it is critical that patients be counseled that they may be at higher risk for persistent, new, or heightened symptoms following surgery. Our findings demonstrated that patients with persistent vestibular symptoms presented with higher prevalence of vestibular migraine, bilateral radiologic superior canal dehiscence

and were more likely to have been revision cases from other institutions.

Size and defect location

There have been several studies that relate size and location of the bony defect with clinical presentation, disease severity, and audiometric data, but with no clear consensus (43, 44). Defect size is an important factor for surgical repair, as there may be a relationship between dehiscence size with hearing thresholds and symptom presentation (43). A variety of methods have been used to measure the size of the defect including three-dimensional curved reconstruction, measurement of the bone density profile, linear distance between identified ends of the defect, intraoperative manual measurements, and using number of radial sections in which the dehiscence was found to calculate the area of the defect (21, 34). The cohort described in this study demonstrated no association between defect size and location with persistence of symptoms, which is consistent with some studies but inconsistent with others. Our study was limited by a less comprehensive analysis of defect size, and further studies should aim to standardize defect measurement to best correlate this with patient presentation and surgical recovery.

Body mass index and superior canal dehiscence syndrome

Due to prior research we were interested in the evaluation of persistent SCDS symptomatology with elevated BMI; however an association was not identified in our study (45, 46). Prior research has generally shown association of elevated BMI with sensorineural hearing loss (SNHL), and in the context of skull base defects, elevated BMI has been used as a surrogate indicator of elevated intracranial pressure (47, 48). The research regarding the relationship between obesity and SCDS is conflicting and still underway. One study found an increased incidence of obesity among patients with SCDS within a cohort of 31 patients; however, obesity was also found to not be related with symptomatic SCD (45, 49). This study also found no difference in incidence of BMI between surgical and non-surgical SCDS cases, and size of dehiscence poorly correlated with BMI. Theories regarding obesity and SCDS described that obesity has been shown to relate to increased intracranial pressure, thought to be due to increased intrathoracic pressure as a result of increased abdominal girth, thereby restricting cerebral venous drainage (50). The increased intracranial hypertension is hypothesized to lead to erosion of the skull base from direct repeated pulsations of the dura over time (51). With regards to SCDS, this erosion may thin the bone over the superior canal, thereby causing symptoms related to SCDS (46). While our study did not identify a significant difference, we had a relatively small cohort of patients with elevated BMI (17.5%, $n = 22$), and further research will assist to confirm or dispute the association in order to improve patient counseling.

Audiometric and cVEMP data

Pure tone air and bone conduction threshold (including supranormal thresholds at −5 and −10 db) testing is routinely used for diagnosis as well as to monitor postoperative hearing. Primarily low frequency ABG is typically seen on diagnosis and postoperative closure of this gap indicates adequate SCD repair. Resolution of reduced hearing symptom has also been well associated with postoperative closure of the ABG (39). Some studies also describe that a larger ABG is associated with a larger defect, making audiometric data an important diagnostic tool in congruence with radiologic testing (43). In our study, ABG magnitude was not associated with postoperative auditory or vestibular symptom persistence (Tables 3, 4) and was also not associated with the number of presenting symptoms (Supplementary Table 2). Prior studies showed similar findings (31). These further highlight the discrepancy between diagnostic SCD testing and subjective patient experience. While the low-frequency ABG decreased significantly postoperatively, PTA thresholds remained stable. These findings were elucidated by bone conduction thresholds increasing significantly in the postoperative period. Given the paradoxical reduction in BC thresholds among patients with SCD, explained by hypersensitivity to vibrations (such as the stimulus used for BC) transmitted in the body, the corresponding increase in BC thresholds postoperatively is an additional indication of adequate SCD repair (52–54).

The mean PTA however, was significantly higher among patients with persistent auditory symptoms (19.6 dB) compared to those with resolved auditory symptoms (25.1 dB). While statistically significant, these PTA values may not represent true clinical significance given the overall small difference. Nevertheless, higher preoperative PTA values, measuring air conduction, may indicate an overall worse SCD-associated hearing loss. PTA has been associated with dehiscence size and postoperative speech discrimination scores, but these results are often not significant (55, 56). Clinically, PTA is a frequently used diagnostic tool for SCDS. Research is limited with regards to analyzing the relationship between persistent auditory symptoms and pre-operative PTA; therefore, future studies should investigate this variable.

VEMP testing is an important diagnostic indicator the evaluation of patients whom SCDS is suspected. Compared with healthy subjects, SCDS patients typically show lower cVEMP thresholds, higher cVEMP amplitudes, and air-bone gaps (ABG) (8, 57–62). Incongruously, our results showed higher (more normal) cVEMP thresholds at 1000Hz were associated with persistence of auditory symptoms. Hypothesizing that perhaps patients with more normal cVEMP thresholds were more likely to reports a primary auditory vs. vestibular chief complaint and as such symptom severity was not correlated with cVEMP thresholds, a sub-group analysis was conducted, but refuted this hypothesis (pre-operative cVEMP 1000 Hz thresholds mean of 67.2 dB HL for patients with auditory chief complaint vs. 72.3 dB HL with vestibular chief complaint, $p = 0.069$). Another explanation to this counterintuitive finding is that patients with higher cVEMP thresholds might have less severe or a smaller dehiscence, leading to subtler clinical symptoms (43). These subtler symptoms could be less amenable to surgical resolution, resulting

TABLE 4 Clinical and demographic characteristics by postoperative vestibular symptom status.

	Postoperative vestibular symptom status		*P*-value
	Resolved $N = 68$ (51.5%)	Persistent (at least 1) $N = 64$ (48.5%)	
Patient characteristics			
Sex			0.823
Male	30 (44.1%)	27 (42.2%)	
Female	38 (55.9%)	37 (57.8%)	
Age at surgery, median (y)	52.4	50.6	0.370
PMH DM	5 (7.4%)	5 (7.8%)	1.000
PMH HTN	22 (32.4%)	21 (32.8%)	0.955
PMH obesity	12 (17.6%)	10 (15.6%)	0.755
PMH seizures	2 (2.9%)	3 (4.7%)	0.673
Migraine diagnosis	14 (20.6%)	26 (41.3%)	**0.010***
Prior ear surgery or infection	6 (9.2%)	7 (11.5%)	0.774
Head Trauma	12 (18.2%)	11 (21.2%)	0.686
Brain fog	4 (5.9%)	9 (16.7%)	0.076
Symptom duration prior to SCD diagnosis (mean, SD), months	40.4 (51.5)	37.2 (40.5)	0.764
Duration of follow up (mean, SD), months	22.1 (32.7)	13.4 (97.5)	0.263
Chief complaint			0.745
Auditory	38 (58.5%)	38 (61.3%)	
Vestibular	27 (41.5%)	24 (38.7%)	
Number of preoperative auditory symptoms (mean, SD)	3.4 (2.0)	4.3 (2.5)	**0.040***
Number of preoperative vestibular symptoms (mean, SD)	2.6 (1.5)	3.3 (1.7)	**0.011***
Pre-op ABG 250 Hz (dB)	25.9 (17.6)	21.6(13.6)	0.141
Pre-op ABG 500 Hz (dB)	17.7 (14.2)	15.0 (12.3)	0.215
Pre-op ABG 1000 Hz (dB)	13.3 (12.7)	12.8 (10.6)	0.825
Pre-op ABG 2000 Hz (dB)	4.4 (9.5)	3.5 (4.7)	0.521
Pre-op ABG 4000 Hz (dB)	5.9 (9.5)	4.6 (6.1)	0.350
Pre-op PTA dB	23.8 (15.3)	20.5 (14.6)	0.231
Pre-op cVEMP 500 Hz (dB HL)	64.5 (11.2)	67.6(13.4)	0.234
Pre-op cVEMP 750 Hz (dB HL)	65.7 (11.5)	67.2 (12.9)	0.562
Pre-op cVEMP 1000 Hz (dB HL)	67.2 (12.9)	70.6 (12.5)	0.167
SCD/operative characteristics			
Radiologic Laterality			**0.034***
Right	23 (36.5%)	16 (25.4%)	
Left	29 (46.0%)	23 (36.5%)	
Bilateral	11 (17.5%)	24 (38.1%)	
SCD Location			**0.612**
Lateral upslope	17 (25.8%)	13 (20.3%)	
Arcuate eminence	37 (56.1%)	42 (65.6%)	
Medial downslope	10 (15.2%)	7 (10.9%)	

(Continued)

TABLE 4 (Continued)

	Postoperative vestibular symptom status		*P*-value
	Resolved $N = 68$ (51.5%)	Persistent (at least 1) $N = 64$ (48.5%)	
SPS	1 (1.5%)	2 (3.1%)	
Arcuate+SPS	1 (1.5%)	0 (0.0%)	
SCD arc length, mean (SD)	4.4 (1.9)	3.9 (1.7)	0.177
SCD linear length, mean (SD)	4.1 (1.6)	3.7 (1.5)	0.180
Surgical Approach			0.197
Middle fossa craniotomy	65 (95.6%)	57 (89.1%)	
Transmastoid	3 (4.4%)	7 (10.9%)	
OSH Revision case	0 (0.0%)	8 (14.0%)	**0.002***
Underwent revision post index case	8 (11.9%)	11 (17.2%)	0.461

Bolded values with an ∗ indicate a statistically significant result.

TABLE 5 Patient characteristics associated with postoperative persistent auditory symptoms on multivariable binary logistic regression**.

	Risk of persistent auditory symptoms OR (95% CI)	*P*-value
PMH seizures		0.999
No	*1 (Reference)*	
Yes	$\sim 14^{8}$ (0.00–∞)	
Chief complaint		0.063
Auditory	*1 (Reference)*	
Vestibular	2.63 (0.95- 7.30)	
SCD laterality		0.828
Unilateral	*1 (Reference)*	
Bilateral	1.14 (0.36–3.63)	
Preop PTA dB	1.03 (0.99–1.07)	0.154
Preop cVEMP 1000 Hz	1.05 (1.01–1.10)	**0.028***

OR, odds ratio; CI, confidence interval; PMH, past medical history; ABG, air-bone gap; SCD, superior canal dehiscence. Preoperative PTA and cVEMP were continuous variables with OR results referring to ascending (higher) values. **Variables found significant on univariate analysis and clinically relevant variables included. Bolded values with an ∗ indicate a statistically significant result.

TABLE 6 Patient characteristics associated with postoperative persistent vestibular symptoms on multivariable binary logistic regression**.

	Risk of persistent vestibular symptoms OR (95% CI)	*P*-value
Migraines		**0.039***
No	*1 (Reference)*	
Yes	2.50 (1.19–7.96)	
Laterality		
Unilateral	*1 (Reference)*	**0.016***
Bilateral	3.08 (1.24–7.65)	
Number of preoperative auditory symptoms	1.14 (0.96–1.35)	0.144
OSH revision case		
No	*1 (Reference)*	
Yes	$\sim 14^{9}$ (0.00–∞)	0.999

**Variables found significant on univariate analysis and clinically relevant variables are included. Bolded values with an ∗ indicate a statistically significant result.

in persistent postoperative auditory symptoms. Alternatively, patients with higher preoperative thresholds may have developed more robust central compensatory mechanisms to cope with vestibular dysfunction (8, 63). These compensatory pathways may continue to generate symptoms even after the anatomical defect has been corrected (64). Nevertheless, an association between elevated cVEMP thresholds and persistent auditory symptoms post-SCD repair challenges our traditional understanding of the condition. Other literature correlating VEMP data with symptom persistence is limited. Efforts made to improve the efficacy of cVEMP testing have shown that 2, 000-Hz tone bursts improve the detection of SCD, however, these studies have not been systematically applied during patient follow-up (65). These underscore the need for a comprehensive, nuanced approach when interpreting diagnostic tests and evaluating patient symptoms. It also emphasizes the need for future studies to focus on a deeper understanding of the interplay between objective tests and symptomatology to optimize diagnostic accuracy and postoperative care.

Revision surgeries

In our cohort, patients that underwent revision surgery were more likely to experience persistent postoperative vestibular symptoms. Similar findings of less favorable outcomes with revision SCD surgery have been reported. Mozaffari et al. (66) studied 20 patients who underwent revision SCD repair and reported persistent symptoms of vertigo (67%), aural fullness (60%) and

dizziness. Sharon et al. (67) evaluated 23 revision cases out of which only 35% of patients reported complete symptom resolution, as compared to ∼66% of patients (out of 33) undergoing primary repair (16). Possible explanations involve an added surgical trauma to the inner ear labyrinth or neural structures from repeating surgeries and scar tissue from initial surgery increasing revision surgery associated trauma (67, 68). Additionally, it is possible that patients selected for revision surgeries represent a subset with more severe or complex SCDS, which could inherently be associated with a higher rate of symptom persistence. Consideration of the above results is imperative for comprehensive patient evaluation and counseling prior to revision surgery.

Patient questionnaires

Similar to prior studies conducted by our institution, symptom reporting was conducted via a questionnaire administered by a clinician. Self-reporting systems are susceptible to significant bias. SCDS is an exceptionally variable condition, making clinical assessment of symptoms very challenging for clinicians. Some attempts have been made to standardize questionnaires. A recent standardized survey was developed in 2018, the Gopen-Yang Superior Semicircular Canal Dehiscence Questionnaire, which includes sections on general quality of life, internal amplified sounds, dizziness and tinnitus, with scores of 0–100 points (69). It is described as a holistic, patient-centered self-assessment; however, it was only used preoperatively. Our survey, although similar in content and focus, was used both pre- and postoperatively in order to provide insight into patient recovery. Validated questionnaires that have been previously used to quantify symptom presentation and resolution include the Autophony Index Dizziness Handicap Inventory (AIDHI), Hearing Handicap Inventory (HHI) and Tinnitus Handicap Inventory (70–73). However, these surveys were designed with the focus of specific symptoms, not a specific etiology. The Dizziness Handicap Inventory (DHI) and Headache Impact Test (HIT-6), were recently described as methods for assessing pre- and postoperative symptoms following surgical repair of cochlea-facial nerve dehiscence (74). A 2017 systematic review by Naert et al. (75) of 66 articles involving 431 patients with SCDS aggregated the 22 most commonly reported preoperative symptoms to be used as a basis for creation of a validated outcome-measure. Our questionnaire included 19 symptoms (11 auditory and 8 vestibular symptoms) with about 14 overlapping symptoms with Naert's 22-item list. No additional validated SCD patient-reported outcome measures have been described and the overall use of standard surveys for patients with diagnosed SCDS is limited. The inconsistent correlation between objective measures including audiometric and cVEMP data and SCD size and location with patient-reported symptoms in our study as well as past studies is noteworthy (31, 55). This further highlights the need for a robust standardized validated survey creating a patient-reported outcome measure to be used throughout clinical and/or surgical management which would allow for a more consistent and objective analysis of this highly subjective and variable condition. A more standardized and comprehensive system for measuring symptoms may improve symptom tracking, progression, and improvement following surgery.

Limitations

There are noteworthy strengths and limitations for our study. First, this is one of the larger surgical SCDS cohorts evaluated both preoperatively and perhaps even more importantly postoperative allowing with both objective testing and symptom questionnaires. As discussed previously, patient symptoms were collected using a comprehensive but not yet validated questionnaire with a binary (yes/no) response limiting evaluation of symptom severity. The survey did not specifically include a question regarding postoperative resolution of chief complaint and as such, this was information we gathered from the EMR which could have been subject to a greater variability of interpretation. A more holistic representation of patient experience could be captured with a much-needed patient-reported outcome measure including additional quality-of-life assessment and grading of symptom severity. Given that only 13 patients reported postoperative persistence of their primary symptom which would subject analyses to low power bias, we focused the analyses on all persistent symptoms (which given the above were largely secondary). Furthermore, as some patients described more than one primary symptom, a separate primary symptom persistence analysis was not included. Additionally, the time-distinction between symptom persistence and prolonged postoperative recovery is not well defined in the literature, and our study (with a median follow up of 9 months and IQR 24.0 months) may have captured some prolonged recovery symptoms that could have resolved with a longer follow-up. Nevertheless, these findings can still be used for patient counseling. While only higher cVEMP thresholds, history of migraines and bilateral radiologic SCD continued to show a statistically significant association with secondary symptom persistence, we reported on and discussed history of revision cases, elevated BMI and seizures found significant only on univariate analysis due to their clinical significance and relevance gleaned from other studies. Reduced sample size available for the multivariate analysis (due to missing information) could have also contributed to lack of carried statistical significance. Additionally, symptom persistence can be partially in setting of a contralateral thin (though not dehiscent) SSC which was not a variable we were able to control for. We included multiple statistical analyses which could have increased the probability of false positive findings. The different analyses were pursued in order to thoroughly investigate and present the comprehensive variables our dataset captured.

Finally, our research was subject to all the inherent limitations of a retrospective cohort study and is potentially less generalizable given its single-center population of surgeons and patients.

Conclusion

Although surgical repair has been shown to be highly effective and safe in the management of SCDS patients, our study shows that the chance of persistent or even new symptoms following surgery is an important consideration when counseling patients considering

operative management. There are many limits to assessing how well a patient may respond to surgery including non-standardized radiologic evaluation, highly variable presenting symptoms and severity, as well as non-standardized clinical evaluation. The persistence of certain symptoms and the identification of potential associated factors including migraines, PTA thresholds, cVEMP thresholds, bilateral SCD and revision cases emphasize the importance of individualized patient counseling and management strategies. Despite the extensive literature on a variety of diagnostic testing, radiologic assessment, clinical presentation and surgical outcomes, there is a lack of consensus across centers. Future research should focus on prospective disease-specific validated patient symptom and quality-of-life survey data collection as a means to create standardized patient-reported outcome measures.

Data availability statement

The raw data supporting the conclusions of this article will be made available by the authors, without undue reservation.

Ethics statement

The studies involving humans were approved by the Massachusetts General Brigham Institutional Review Board. The studies were conducted in accordance with the local legislation and institutional requirements. Written informed consent for participation was not required from the participants or the participants' legal guardians/next of kin in accordance with the national legislation and institutional requirements.

Author contributions

LB: Conceptualization, Data curation, Formal analysis, Investigation, Methodology, Writing – original draft, Writing – review & editing. SS: Conceptualization, Data curation, Formal analysis, Investigation, Methodology, Writing – original draft, Writing – review & editing. AG: Data curation, Writing – review & editing. JC: Data curation, Formal analysis, Methodology, Writing – review & editing. KS: Data curation, Writing – review & editing. DL: Conceptualization, Methodology, Writing – review & editing.

Funding

The author(s) declare that no financial support was received for the research, authorship, and/or publication of this article.

Conflict of interest

The authors declare that the research was conducted in the absence of any commercial or financial relationships that could be construed as a potential conflict of interest.

Publisher's note

Supplementary material

The Supplementary Material for this article can be found online at: https://www.frontiersin.org/articles/10.3389/fneur.2024.1336627/full#supplementary-material

References

1. Ung N, Chung LK, Lagman C, Bhatt NS, Barnette NE, Ong V, et al. Outcomes of middle fossa craniotomy for the repair of superior semicircular canal dehiscence. *J Clin Neurosci.* (2017) 43:103–7. doi: 10.1016/j.jocn.2017.05.003

2. McCall AA, McKenna MJ, Merchant SN, Curtin HD, Lee DJ. Superior canal dehiscence syndrome associated with the superior petrosal sinus in pediatric and adult patients. *Otol Neurotol Oct.* (2011) 32:1312–9. doi: 10.1097/MAO.0b013e31822e5b0a

3. Nieto P, Gallois Y, Molinier CE, Deguine O, Marx M. Surgical treatments of superior semicircular canal dehiscence: a single-centre experience in 63 cases. *Laryngoscope Investig Otolaryngol.* (2021) 6:1414–20. doi: 10.1002/lio2.684

4. Elms HL, Canick JE, Kaylie DM. What approach minimizes hearing loss in superior semicircular canal dehiscence repair? *Laryngoscope.* (2023) 133:1784–5. doi: 10.1002/lary.30705

5. Schwartz SR, Almosnino G, Noonan KY, Hartl RMB, Zeitler DM, Saunders JE, et al. Comparison of transmastoid and middle fossa approaches for superior canal dehiscence repair: a multi-institutional study. *Otolaryngol Head Neck Surg.* (2019) 161:130–6. doi: 10.1177/0194599819835173

6. Nguyen T, Lagman C, Sheppard JP, Romiyo P, Duong C, Prashant GN, et al. Middle cranial fossa approach for the repair of superior semicircular canal dehiscence is associated with greater symptom resolution compared to transmastoid approach. *Acta Neurochir.* (2018) 160:1219–24. doi: 10.1007/s00701-017-3346-2

7. Minor LB. Clinical manifestations of superior semicircular canal dehiscence. *Laryngoscope.* (2005) 115:1717–27. doi: 10.1097/01.mlg.0000178324.55729.b7

8. Eberhard KE, Chari DA, Nakajima HH, Klokker M, Caye-Thomasen P, Lee DJ. Current trends, controversies, and future directions in the evaluation and management of superior canal dehiscence syndrome. *Front Neurol.* (2021) 12:638574. doi: 10.3389/fneur.2021.638574

9. Mikulec AA, Poe DS, McKenna MJ. Operative management of superior semicircular canal dehiscence. *Laryngoscope.* (2005) 115:501–7. doi: 10.1097/01.mlg.0000157844.48036.e7

10. Vlastarakos PV, Proikas K, Tavoulari E, Kikidis D, Maragoudakis P, Nikolopoulos TP. Efficacy assessment and complications of surgical management for superior semicircular canal dehiscence: a meta-analysis of published interventional studies. *Eur Arch Otorhinolaryngol.* (2009) 266:177–86. doi: 10.1007/s00405-008-0840-4

11. Beyea JA, Agrawal SK, Parnes LS. Transmastoid semicircular canal occlusion: a safe and highly effective treatment for benign paroxysmal positional vertigo and superior canal dehiscence. *Laryngoscope.* (2012) 122:1862–6. doi: 10.1002/lary.23390

12. Thomeer H, Bonnard D, Castetbon V, Franco-Vidal V, Darrouzet P, Darrouzet V. Long-term results of middle fossa plugging of superior semicircular canal dehiscences: clinically and instrumentally demonstrated efficiency in a retrospective series of

16 ears. *Eur Arch Otorhinolaryngol.* (2016) 273:1689–96. doi: 10.1007/s00405-015-3715-5

13. Rodgers B, Lin J, Staecker H. Transmastoid resurfacing versus middle fossa plugging for repair of superior canal dehiscence: Comparison of techniques from a retrospective cohort. *World J Otorhinolaryngol Head Neck Surg.* (2016) 2:161–7. doi: 10.1016/j.wjorl.2016.11.001

14. Brantberg K, Bergenius J, Mendel L, Witt H, Tribukait A, Ygge J. Symptoms, findings and treatment in patients with dehiscence of the superior semicircular canal. *Acta Otolaryngol.* (2001) 121:68–75. doi: 10.1080/000164801300006308

15. Zhao YC, Somers T, van Dinther J, Vanspauwen R, Husseman J, Briggs R. Transmastoid repair of superior semicircular canal dehiscence. *J Neurol Surg B Skull Base.* (2012) 73:225–9. doi: 10.1055/s-0032-1312713

16. Niesten ME, McKenna MJ, Grolman W, Lee DJ. Clinical factors associated with prolonged recovery after superior canal dehiscence surgery. *Otol Neurotol.* (2012) 33:824–31. doi: 10.1097/MAO.0b013e3182544c9e

17. Agrawal Y, Migliaccio AA, Minor LB, Carey JP. Vestibular hypofunction in the initial postoperative period after surgical treatment of superior semicircular canal dehiscence. *Otol Neurotol.* (2009) 30:502–6. doi: 10.1097/MAO.0b013e3181a32d69

18. Phillips DJ, Souter MA, Vitkovic J, Briggs RJ. Diagnosis and outcomes of middle cranial fossa repair for patients with superior semicircular canal dehiscence syndrome. *J Clin Neurosci.* (2010) 17:339–41. doi: 10.1016/j.jocn.2009.06.021

19. Suresh K, Garcia A, Bartholomew RA, Song Y, Lee DJ. Auditory and vestibular symptom improvement with surgery for superior canal dehiscence syndrome. *Otolaryngol Head Neck Surg.* (2023) 169:1005–11. doi: 10.1002/ohn.359

20. Remenschneider AK, Owoc M, Kozin ED, McKenna MJ, Lee DJ, Jung DH. Health utility improves after surgery for superior canal dehiscence syndrome. *Otol Neurotol.* (2015) 36:1695–701. doi: 10.1097/MAO.0000000000000886

21. Alkhafaji MS, Varma S, Pross SE, Sharon JD, Nellis JC, Santina CC, et al. Long-term patient-reported outcomes after surgery for superior canal dehiscence syndrome. *Otol Neurotol.* (2017) 38:1319–26. doi: 10.1097/MAO.0000000000001550

22. Goddard JC, Wilkinson EP. Outcomes following semicircular canal plugging. *Otolaryngol Head Neck Surg.* (2014) 151:478–83. doi: 10.1177/0194599814538233

23. Pereira D, Leonardo A, Duarte D, Oliveira N. Bilateral superior semicircular canal dehiscence: bilateral conductive hearing loss with subtle vestibular symptoms. *BMJ Case Rep*. (2020) 13:042. doi: 10.1136/bcr-2019-233042

24. Jacky Chen CH, Nguyen T, Udawatta M, Duong C, Romiyo P, Sheppard JP, et al. Clinical assessment of patients with bilateral superior semicircular canal dehiscence. *World Neurosurg.* (2019) 126:e1549–52. doi: 10.1016/j.wneu.2019.03.205

25. Yang HH, Yang I, Gopen QS. First-side and second-side repair of bilateral superior canal dehiscence. *Laryngoscope*. (2023) 8:31118. doi: 10.1002/lary.31118

26. Mozaffari K, Willis SL, Unterberger A, Duong C, Hong M, De Jong R, et al. Superior semicircular canal dehiscence outcomes in a consecutive series of 229 surgical repairs with middle cranial fossa craniotomy. *World Neurosurg.* (2021) 156:e229–34. doi: 10.1016/j.wneu.2021.09.038

27. Jung DH, Lookabaugh SA, Owoc MS, McKenna MJ, Lee DJ. Dizziness is more prevalent than autophony among patients who have undergone repair of superior canal dehiscence. *Otol Neurotol.* (2015) 36:126–32. doi: 10.1097/MAO.0000000000000531

28. Harris PA, Taylor R, Thielke R, Payne J, Gonzalez N, Conde JG. Research electronic data capture (REDCap)–a metadata-driven methodology and workflow process for providing translational research informatics support. *J Biomed Inform.* (2009) 42:377–81. doi: 10.1016/j.jbi.2008.08.010

29. Harris PA, Taylor R, Minor BL, Elliott V, Fernandez M, O'Neal L, et al. The REDCap consortium: Building an international community of software platform partners. *J Biomed Inform.* (2019) 95:103208. doi: 10.1016/j.jbi.2019.103208

30. Chemtob RA, Noij KS, Qureshi AA, Klokker M, Nakajima HH, Lee DJ. Superior canal dehiscence surgery outcomes following failed round window surgery. *Otol Neurotol.* (2019) 40:535–42. doi: 10.1097/MAO.0000000000002185

31. Noij KS, Wong K, Duarte MJ, Masud S, Dewyer NA, Herrmann BS, et al. Audiometric and cVEMP thresholds show little correlation with symptoms in superior semicircular canal dehiscence syndrome. *Otol Neurotol.* (2018) 39:1153–62. doi: 10.1097/MAO.0000000000001910

32. Watters KF, Rosowski JJ, Sauter T, Lee DJ. Superior semicircular canal dehiscence presenting as postpartum vertigo. *Otol Neurotol.* (2006) 27:756–68. doi: 10.1097/01.mao.0000227894.27291.9f

33. Noij KS, Duarte MJ, Wong K, Cheng YS, Masud S, Herrmann BS, et al. Toward optimizing cervical vestibular evoked myogenic potentials (cVEMP): combining air-bone gap and cVEMP thresholds to improve diagnosis of superior canal dehiscence. *Otol Neurotol.* (2018) 39:212–20. doi: 10.1097/MAO.0000000000001655

34. Lookabaugh S, Kelly HR, Carter MS, Niesten MEF, McKenna MJ, Curtin H, et al. Radiologic classification of superior canal dehiscence: implications for surgical repair. *Otol Neurotol.* (2015) 36:118–25. doi: 10.1097/MAO.0000000000000523

35. Yoo W, Mayberry R, Bae S, Singh K, Peter He Q, Lillard JW. A study of effects of multicollinearity in the multivariable analysis. *Int J Appl Sci Technol.* (2014) 4:9–19.

36. Carey JP, Migliaccio AA, Minor LB. Semicircular canal function before and after surgery for superior canal dehiscence. *Otol Neurotol.* (2007) 28:356–64. doi: 10.1097/01.mao.0000253284.40995.d8

37. Schubert MC, Migliaccio AA, Della Santina CC. Dynamic visual acuity during passive head thrusts in canal planes. *J Assoc Res Otolaryngol.* (2006) 7:329–38. doi: 10.1007/s10162-006-0047-6

38. Janky KL, Zuniga MG, Carey JP, Schubert M. Balance dysfunction and recovery after surgery for superior canal dehiscence syndrome. *Arch Otolaryngol Head Neck Surg.* (2012) 138:723–30. doi: 10.1001/archoto.2012.1329

39. Ward BK, Agrawal Y, Nguyen E, Della Santina CC, Limb CJ, Francis HW, et al. Hearing outcomes after surgical plugging of the superior semicircular canal by a middle cranial fossa approach. *Otol Neurotol.* (2012) 33:1386–91. doi: 10.1097/MAO.0b013e318268d20d

40. Ziylan F, Kinaci A, Beynon AJ, Kunst HP. A Comparison of surgical treatments for superior semicircular canal dehiscence: a systematic review. *Otol Neurotol.* (2017) 38:1–10. doi: 10.1097/MAO.0000000000001277

41. Barber SR, Cheng YS, Owoc M, Lin BM, Remenschneider AK, Kozin ED, et al. Benign paroxysmal positional vertigo commonly occurs following repair of superior canal dehiscence. *Laryngoscope.* (2016) 126:2092–7. doi: 10.1002/lary.25797

42. Agrawal Y, Minor LB, Schubert MC, Janky KL, Davalos-Bichara M, Carey JP. Second-side surgery in superior canal dehiscence syndrome. *Otol Neurotol.* (2012) 33:72–7. doi: 10.1097/MAO.0b013e31823c9182

43. Niesten MEF, Hamberg LM, Silverman JB, Lou KV, McCall AA, Windsor A, et al. Superior canal dehiscence length and location influences clinical presentation and audiometric and cervical vestibular-evoked myogenic potential testing. *Audiol Neurootol.* (2014) 19:97–105. doi: 10.1159/000353920

44. Niesten MEF, Stieger C, Lee DJ, Merchant JP, Grolman W, Rosowski JJ, et al. Assessment of the effects of superior canal dehiscence location and size on intracochlear sound pressures. *Audiol Neurootol.* (2015) 20:62–71. doi: 10.1159/000366512

45. Schutt CA, Neubauer P, Samy RN, Pensak ML, Kuhn JJ, Herschovitch M, et al. The correlation between obesity, obstructive sleep apnea, and superior semicircular canal dehiscence: a new explanation for an increasingly common problem. *Otol Neurotol.* (2015) 36:551–4. doi: 10.1097/MAO.0000000000000555

46. Berkiten G, Gürbüz D, Akan O, Tutar B, Koşar Tunç M, Karaketir S, et al. Dehiscence or thinning of bone overlying the superior semicircular canal in idiopathic intracranial hypertension. *Eur Arch Otorhinolaryngol.* (2022) 279:2899–904. doi: 10.1007/s00405-021-07020-z

47. Jung SY, Shim HS, Hah YM, Kim SH, Yeo SG. Association of metabolic syndrome with sudden sensorineural hearing loss. *JAMA Otolaryngol Head Neck Surg.* (2018) 144:308–14. doi: 10.1001/jamaoto.2017.3144

48. Kenning TJ, Willcox TO, Artz GJ, Schiffmacher P, Farrell CJ, Evans JJ. Surgical management of temporal meningoencephaloceles, cerebrospinal fluid leaks, and intracranial hypertension: treatment paradigm and outcomes. *Neurosurg Focus.* (2012) 32:E6. doi: 10.3171/2012.4.FOCUS1265

49. Jan TA, Cheng YS, Landegger LD, Lin BM, Srikanth P, Niesten MEF, et al. Relationship between surgically treated superior canal dehiscence syndrome and body mass index. *Otolaryngol Head Neck Surg.* (2017) 156:722–7. doi: 10.1177/0194599816686563

50. Sugerman HJ, DeMaria EJ, Felton WL, Nakatsuka M, Sismanis A. Increased intra-abdominal pressure and cardiac filling pressures in obesity-associated pseudotumor cerebri. *Neurology.* (1997) 49:507–11. doi: 10.1212/WNL.49.2.507

51. Goddard JC, Meyer T, Nguyen S, Lambert PR. New considerations in the cause of spontaneous cerebrospinal fluid otorrhea. *Otol Neurotol.* (2010) 31:940–5. doi: 10.1097/MAO.0b013e3181e8f36c

52. Cheng YS, Raufer S, Guan X, Halpin CF, Lee DJ, Nakajima HH. Superior canal dehiscence similarly affects cochlear pressures in temporal bones and audiograms in patients. *Ear Hear.* (2020) 41:804–10. doi: 10.1097/AUD.0000000000000799

53. Mikulec AA, McKenna MJ, Ramsey MJ, Rosowski JJ, Herrmann BS, Rauch SD, et al. Superior semicircular canal dehiscence presenting as conductive hearing loss without vertigo. *Otol Neurotol.* (2004) 25:121–9. doi: 10.1097/00129492-200403000-00007

54. Merchant SN, Rosowski JJ. Conductive hearing loss caused by third-window lesions of the inner ear. *Otol Neurotol.* (2008) 29:282–9. doi: 10.1097/MAO.0b013e318161ab24

55. Chien WW, Janky K, Minor LB, Carey JP. Superior canal dehiscence size: multivariate assessment of clinical impact. *Otol Neurotol.* (2012) 33:810–5. doi: 10.1097/MAO.0b013e318248eac4

56. Saliba I, Maniakas A, Benamira LZ, Nehme J, Benoit M, Montreuil-Jacques V. Superior canal dehiscence syndrome: clinical manifestations and radiologic correlations. *Eur Arch Otorhinolaryngol.* (2014) 271:2905–14. doi: 10.1007/s00405-013-2711-x

57. Rosengren SM, Colebatch JG, Young AS, Govender S, Welgampola MS. Vestibular evoked myogenic potentials in practice: Methods, pitfalls and clinical applications. *Clin Neurophysiol Pract.* (2019) 4:47–68. doi: 10.1016/j.cnp.2019.01.005

58. Noij KS, Rauch SD. Vestibular evoked myogenic potential (VEMP) testing for diagnosis of superior semicircular canal dehiscence. *Front Neurol.* (2020) 11:695. doi: 10.3389/fneur.2020.00695

59. Hunter JB, Patel NS, O'Connell BP, Carlson ML, Shepard NT, McCaslin DL, et al. Cervical and ocular VEMP testing in diagnosing superior semicircular canal dehiscence. *Otolaryngol Head Neck Surg.* (2017) 156:917–23. doi: 10.1177/0194599817690720

60. Mau C, Kamal N, Badeti S, Reddy R, Ying YM, Jyung RW, et al. Superior semicircular canal dehiscence: Diagnosis and management. *J Clin Neurosci.* (2018) 48:58–65. doi: 10.1016/j.jocn.2017.11.019

61. Zuniga MG, Janky KL, Nguyen KD, Welgampola MS, Carey JP. Ocular versus cervical VEMPs in the diagnosis of superior semicircular canal dehiscence syndrome. *Otol Neurotol Jan.* (2013) 34:121–6. doi: 10.1097/MAO.0b013e31827136b0

62. Milojcic R, Guinan JJ Jr, Rauch SD, Herrmann BS. Vestibular evoked myogenic potentials in patients with superior semicircular canal dehiscence. *Otol Neurotol.* (2013) 34:360–7. doi: 10.1097/MAO.0b013e31827b4fb5

63. Iversen MM, Rabbitt RD. Biomechanics of third window syndrome. *Front Neurol.* (2020) 11:891. doi: 10.3389/fneur.2020.00891

64. Mantokoudis G, Saber Tehrani AS, Wong AL, Agrawal Y, Wenzel A, Carey JP. Adaptation and compensation of vestibular responses following superior canal dehiscence surgery. *Otol Neurotol.* (2016) 37:1399–405. doi: 10.1097/MAO.0000000000001196

65. Noij KS, Herrmann BS, Guinan JJ Jr, Rauch SD. Toward optimizing cVEMP: 2,000-Hz tone bursts improve the detection of superior canal dehiscence. *Audiol Neurootol.* (2018) 23:335–44. doi: 10.1159/000493721

66. Mozaffari K, Ghodrati F, Pradhan A, Ng E, Ding K, Rana S, et al. Superior semicircular canal dehiscence revision surgery outcomes: a single institution's experience. *World Neurosurg.* (2021) 156:e408–14. doi: 10.1016/j.wneu.2021.09.083

67. Sharon JD, Pross SE, Ward BK, Carey JP. Revision surgery for superior canal dehiscence syndrome. *Otol Neurotol.* (2016) 37:1096–103. doi: 10.1097/MAO.0000000000001113

68. Limb CJ, Carey JP, Srireddy S, Minor LB. Auditory function in patients with surgically treated superior semicircular canal dehiscence. *Otol Neurotol.* (2006) 27:969–80. doi: 10.1097/01.mao.0000235376.70492.8e

69. Voth BL, Sheppard JP, Barnette NE, Ong V, Nguyen T, Chen CHJ, et al. The Gopen-Yang Superior Semicircular Canal Dehiscence Questionnaire: development and validation of a clinical questionnaire to assess subjective symptoms in patients undergoing surgical repair of superior semicircular canal dehiscence. *J Laryngol Otol.* (2018) 132:1110–8. doi: 10.1017/S0022215118002219

70. Jacobson GP, Newman CW. The development of the dizziness handicap inventory. *Arch Otolaryngol Head Neck Surg.* (1990) 116:424–7. doi: 10.1001/archotol.1990.01870040046011

71. Ventry IM, Weinstein BE. The hearing handicap inventory for the elderly: a new tool. *Ear Hear.* (1982) 3:128–34. doi: 10.1097/00003446-198205000-00006

72. Newman CW, Weinstein BE, Jacobson GP, Hug GA. The hearing handicap inventory for adults: psychometric adequacy and audiometric correlates. *Ear Hear.* (1990) 11:430–3. doi: 10.1097/00003446-199012000-00004

73. Newman CW, Jacobson GP, Spitzer JB. Development of the tinnitus handicap inventory. *Arch Otolaryngol Head Neck Surg.* (1996) 122:143–8. doi: 10.1001/archotol.1996.01890140029007

74. Wackym PA, Balaban CD, Zhang P, Siker DA, Hundal JS. Third window syndrome: surgical management of cochlea-facial nerve dehiscence. *Front Neurol.* (2019) 10:1281. doi: 10.3389/fneur.2019.01281

75. Naert L, Van de Berg R, Van de Heyning P, Bisdorff A, Sharon JD, Ward BK, et al. Aggregating the symptoms of superior semicircular canal dehiscence syndrome. *Laryngoscope.* (2018) 128:1932–8. doi: 10.1002/lary.27062

frontiers | Frontiers in Neurology

TYPE Original Research
PUBLISHED 15 March 2024
DOI 10.3389/fneur.2024.1376949

OPEN ACCESS

EDITED BY
Kunio Mizutari,
National Defense Medical College, Japan

REVIEWED BY
Takaomi Kurioka,
National Defense Medical College, Japan
Helge Rask-Andersen,
Uppsala University, Sweden

*CORRESPONDENCE
Tsukasa Ito
✉ tuito@med.id.yamagata-u.ac.jp

RECEIVED 26 January 2024
ACCEPTED 23 February 2024
PUBLISHED 15 March 2024

CITATION
Kubota T, Ito T, Furukawa T, Matsui H, Goto T, Shinkawa C, Matsuda H, Ikezono T and Kakehata S (2024) Clinical course of five patients definitively diagnosed with idiopathic perilymphatic fistula treated with transcanal endoscopic ear surgery.
Front. Neurol. 15:1376949.
doi: 10.3389/fneur.2024.1376949

Clinical course of five patients definitively diagnosed with idiopathic perilymphatic fistula treated with transcanal endoscopic ear surgery

Toshinori Kubota[1,2], Tsukasa Ito[1]*, Takatoshi Furukawa[1,3], Hirooki Matsui[1], Takanari Goto[1], Chikako Shinkawa[1], Han Matsuda[4], Tetsuo Ikezono[4] and Seiji Kakehata[1]

[1]Department of Otolaryngology, Head and Neck Surgery, Yamagata University Faculty of Medicine, Yamagata, Yamagata, Japan, [2]Department of Otolaryngology, Yonoezawa City Hospital, Yonezawa, Yamagata, Japan, [3]Department of Otolaryngology, Yamagata Prefectural Shinjyo Hospital, Shinjo, Yamagata, Japan, [4]Department of Otolaryngology, Saitama Medical University, Iruma-gun, Saitama, Japan

Objectives: An idiopathic perilymphatic fistula (PLF) can be difficult to diagnose because patients present with sudden sensorineural hearing loss (SSHL) and/or vestibular symptoms without any preceding events. In such cases, we currently test for cochlin-tomoprotein (CTP) to confirm the diagnosis of idiopathic PLF because CTP is only detected in the perilymph. In this study, we report the clinical course of five patients definitively diagnosed with idiopathic PLF who underwent PLF repair surgery using transcanal endoscopic ear surgery (TEES).

Patients and methods: Five patients were initially treated with intratympanic dexamethasone for SSHL, at which time a CTP test was also performed (preoperative CTP test). Due to refractory hearing loss and/or fluctuating disequilibrium, PLF repair surgery using TEES was performed to seal the oval and round windows using connective tissue and fibrin glue. These patients were diagnosed with definite idiopathic PLF based on pre- or intra-operative CTP test results (negative, < 0.4 ng/mL; intermediate, 0.4–< 0.8 ng/mL; and positive, > 0.8 ng/mL). We evaluated pre- and intra-operative CTP values, intraoperative surgical findings via a magnified endoscopic view, and pre- and post-operative changes in averaged hearing level and vestibular symptoms.

Results: Pre- and intra-operative CTP values were positive and intermediate in three patients, positive and negative in one patient, and negative and positive in one patient. None of the patients had intraoperative findings consistent with a fistula between the inner and middle ears or leakage of perilymph. Only two patients showed a slight postoperative recovery in hearing. Four patients complained of disequilibrium preoperatively, of whom two had resolution of disequilibrium postoperatively.

Conclusion: A positive CTP test confirms PLF in patients without obvious intraoperative findings. The CTP test is considered more sensitive than endoscopic fistula confirmation. We consider that CTP test results are important indicators to decide the surgical indication for idiopathic PLF repair surgery. In our experience with the five cases, two of them showed improvements in both hearing and vestibular symptoms.

KEYWORDS

idiopathic perilymphatic fistula, cochlin-tomoprotein, transcanal endoscopic ear surgery, sudden sensorineural hearing loss, disequilibrium

1 Introduction

A perilymphatic fistula (PLF) is defined as an abnormal communication between the perilymph-filled inner ear and the air-filled space of the middle ear. A PLF can be caused by internal or external trauma, but it can also be idiopathic. The diagnostic criteria for PLF in Japan were revised by the Intractable Hearing Loss Research Committee of the Ministry of Health, Labor, and Welfare in 2016. The PLF criteria in Japan acknowledge that idiopathic cases exist.

Idiopathic PLF can be difficult to diagnose because patients present with sudden sensorineural hearing loss (SSHL) and/or vestibular symptoms without any abnormalities demonstrated on an MRI or CT scan. In such cases, we currently test for cochlin-tomoprotein (CTP) in the middle ear to confirm idiopathic PLF because CTP is detected only in perilymph (1, 2). Suspected idiopathic PLF has been surgically treated via microscopic ear surgery (MES), but MES is not guaranteed to resolve SSHL and vestibular symptoms. Transcanal endoscopic ear surgery (TEES), however, offers a less invasive option for such patients, and TEES may have the potential to visualize fistulas/microfissures more clearly than MES. In this study, we report the clinical course of five patients definitively diagnosed with idiopathic PLF who were treated with PLF repair surgery using the TEES technique.

2 Patients and methods

2.1 Patients

The five patients (three male individuals and two female individuals; age range, 15–83 years; median age, 52.0 years) we present were initially treated with intratympanic dexamethasone (IT-DEX) for SSHL at Yamagata University Hospital between 2014 and 2017. IT-DEX was performed in the hospital for 8 consecutive days (3). Hearing levels were not completely recovered in all cases. These patients had refractory hearing loss and/or fluctuating disequilibrium; idiopathic PLF was considered based on the CTP test results at the time of IT-DEX and the course of hearing levels and/or vestibular symptoms. After informed consent, we performed a PLF repair surgery using the TEES technique to seal the inner ear windows with the hope of improving hearing and vestibular symptoms.

2.2 Diagnostic criteria for PLF

The Japanese PLF diagnostic criteria, which were revised by the Intractable Hearing Loss Research Committee of the Ministry of Health, Labor, and Welfare in 2016, were used to diagnose PLF in the current study (Table 1) (4). These criteria for PLF show that PLF is definitively diagnosed based on symptoms and positive laboratory findings. PLF symptoms include hearing loss, tinnitus, and vestibular symptoms. There are two laboratory findings of significance in patients with PLF: visual identification of a fistula between the middle and inner ears by microscope or endoscope; and a biochemical test that detects perilymph-specific proteins, including CTP, from the middle ear.

2.3 CTP test

Ikezono et al. (1) identified CTP as a perilymph-specific protein. Therefore, the detection of CTP in the middle ear is consistent with a PLF with perilymph leakage. CTP was quantified using polyclonal antibody ELISA with a specimen obtained from the middle ear cavity. The middle ear cavity was rinsed three times repeatedly with 0.3 mL of saline, and then saline was collected as a specimen for the CTP test. The cutoff criteria tested by polyclonal antibody ELISA are shown in Table 1 (negative, < 0.4 ng/mL; intermediate, 0.4–< 0.8 ng/mL; and positive, > 0.8 ng/mL). The sensitivity and specificity of the CTP test by polyclonal antibody ELISA are 86.4 and 100%, respectively (2).

All the samples were measured by T.I. in a blinded fashion, using a quality-controlled, standardized methodology established in collaboration with the central pathology lab (SRL Inc.).

The CTP test using polyclonal antibody ELISA was a prospective clinical study that was conducted with the approval of the Ethics Committee of Yamagata University (H28-303) and Saitama Medical University Hospital (IRB No. 13086). Informed consent was given by the patients. CTP tests were performed twice, as follows: the first during the IT-DEX procedure (preoperative CTP test) and the second during the TEES procedure (intraoperative CTP test).

The CTP test was performed in all patients who underwent IT-DEX for SSHL and provided informed consent for the CTP test. The CTP-positive rate for SSHL in our institutions during the study period was 15.1% (8/53). PLF repair surgery was performed in four of eight CTP-positive patients.

2.4 PLF repair surgery using the TEES technique

Our indications for idiopathic PLF repair surgery were as follows: Surgical indication 1: Patients with symptoms and/or test results suggestive of PLF, such as progressive hearing loss [Table 1 (4)]. Surgical indication 2: Patients with a positive CTP test whose hearing has not completely recovered. Surgical indication 3: Patients with positive CTP results and recurring hearing loss and/or vestibular symptoms.

PLF repair surgery using the TEES technique was performed under general anesthesia. Angled rigid endoscopes (0 and 30 degrees) with an outer diameter of 2.7 mm (KARL STORZ, Tuttlingen, Germany) were used. Images were recorded through a full high-definition (HD) camera (KARL STORZ), which was attached to the endoscope lens, and these images were displayed on a full HD monitor.

TABLE 1 Diagnostic criteria in Japan for PLF.

A. Symptoms
Hearing impairment, tinnitus, aural fullness, and vestibular symptoms are observed in cases who had preceding events, as listed below:
(1) Coexisting or pre-existing middle and/or inner ear diseases (trauma, cholesteatoma, tumor, anomaly, SCCD, etc.) middle and/or inner ear surgeries
(2) Barotrauma caused by antecedent events or external origin (e.g., blasting, diving, or flying)
(3) Barotrauma caused by antecedent events of internal origin (e.g., nose-blowing, sneezing, straining, or carrying heavy objects)
B. Laboratory findings
(1) Microscopic/endoscopic inspection
Visual identification of fistula(s) between the middle and inner ear by a microscope or endoscope. Fistulas can develop at the cochlear window, vestibular window, fracture site, microfissure, malformation, destruction in the bony labyrinth caused by inflammation, etc.
(2) Biochemical test
Perilymph-specific protein is detected in the middle ear
C. Reference
(1) A perilymph-specific protein, e.g., Cochlin-tomoprotein (CTP) detection test. After myringotomy, the middle ear is rinsed with 0.3 mL of saline three times, the fluid recovered (middle ear lavage (MEL)) and tested by polyclonal antibody ELISA. The cutoff criteria are: 0.4 < CTP negative; 0.4 ≤ CTP <0.8 intermediate; 0.8 ≤ CTP positive
(2) Idiopathic cases may exist
(3) The following symptoms and/or test results may be observed:
1. Streaming water-like tinnitus or feeling of running water in the middle ear
2. Popping sound can be heard at the onset
3. Nystagmus and/or vertigo induced by pressure application to the middle ear (Hennebert's phenomenon, fistula sign)
4. Imaging studies may show a fistula in the bony labyrinth or pneumolabyrinth
5. Progression of hearing impairment, tinnitus, aural fullness may be acute, progressive, fluctuating, or recurrent
6. The main complaints can be vestibular symptoms without hearing impairment
D. Differential diagnosis
Inner ear diseases have known causes, such as viral infection, genetics, and vestibular schwannoma.
E. Diagnosis
Probable PLF: Only symptoms listed in A
Definite PLF: Symptoms and laboratory findings listed in B

In the patient with right ear disease, a tympanomeatal flap was elevated with a circumferential incision from the 6 o'clock to the 12 o'clock position (Figure 1A). After elevation of the tympanomeatal flap, the middle ear was checked for the presence or absence of perilymphatic leakage for approximately 10 min (Figures 1B,C). The middle ear cavity was rinsed three times with 0.3 mL of saline for the CTP detection test. A minimum transcanal atticotomy was performed to clear the surgical field around the oval window. The mucosa around the oval and round windows was scratched for the attachment of the connective tissue graft. The area surrounding the stapes and round window niche was sealed with connective tissue obtained from the postauricular subcutaneous area (Figures 1D,E). Finally, fibrin glue was used to fix the connective tissue. The tympanomeatal flap was put back, and the external ear canal was then packed with chitin sheets, Gelfoam sponges soaked in antibiotic eardrops, and Merocel sponges.

2.5 Assessment of hearing levels and vestibular symptoms

Hearing tests and vestibular symptom assessments were performed preoperatively and postoperatively. Changes in hearing levels in each patient were assessed using the criteria established by the Acute Severe Hearing Loss Study Group, which are as follows: "Complete recovery" signifies recovery to a hearing level within 20 dB in pure tone audiometry (PTA) or to the same hearing level as the unaffected side; "Marked recovery" refers to more than 30 dB of recovery in PTA; "Slight recovery" is a recovery of 10–29 dB; and "No response" corresponds to a recovery of less than 10 dB (5). Changes in vestibular symptoms were assessed on the basis of the patient's subjective complaints, and the results were categorized as unchanged, progressing, or demonstrating marked improvement. Patient data were thoroughly analyzed and followed up for more than 6 months postoperatively (range, 0.7–4.2 years; median, 2.1 years).

3 Results

Table 2 shows the clinical courses for the five patients. The indication for surgery in each case was determined from the following events: Patient #1 had progressive hearing loss. Patient #2 had a positive CTP result and no recovery in hearing. Patient #3 showed marked recovery in hearing after IT-DEX, but he had recurrent disequilibrium. Patient #4 showed no recovery in hearing after IT-DEX, and he had recurrent disequilibrium. Patient #5 showed hearing improvement to 43 dB after IT-DEX but then experienced repeated hearing loss and disequilibrium (Table 3).

The association between pre- and intra-operative CTP values was positive and negative in 1 patient (patient #3), positive and intermediate in 3 patients (#2, #4, and #5), and negative and positive in 1 patient (#1). No fistulas were identified during endoscopic surgery in any patients. Two patients showed a postoperative slight recovery in hearing (#1, #4.). Four patients complained of disequilibrium

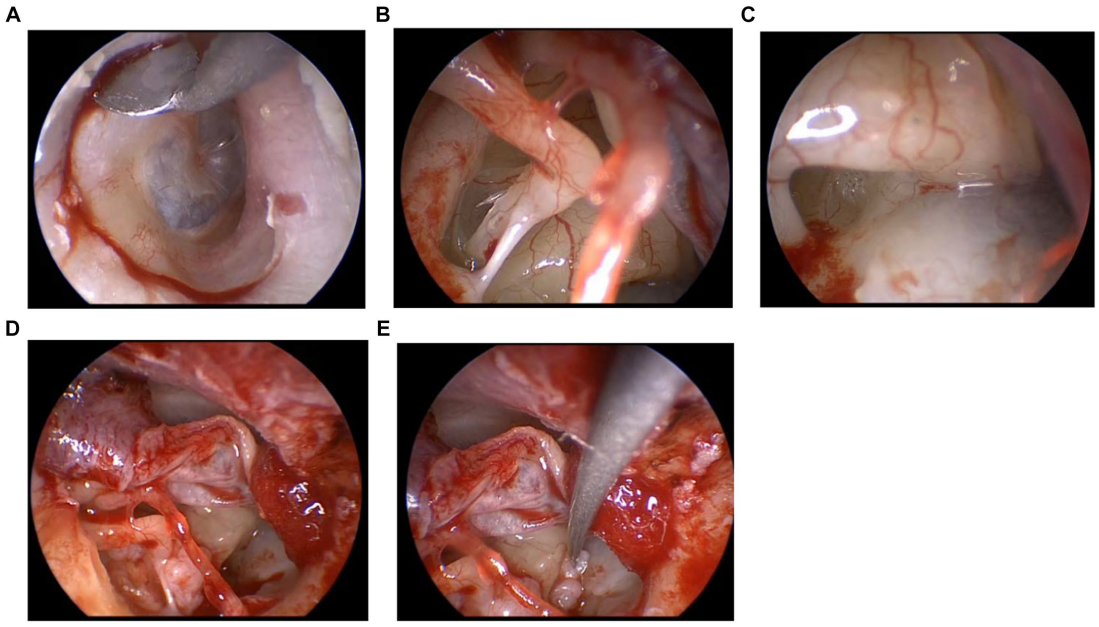

FIGURE 1
(A) Tympanomeatal flap was elevated. **(B)** Observation of the oval window. **(C)** Observation of the round window. **(D)** Sealing the area surrounding the stapes with connective tissue. **(E)** Sealing the round window niche with connective tissue.

preoperatively, of whom two had demonstrated marked improvement of disequilibrium postoperatively (patients #1 and #5).

4 Discussion

PLFs are classified into four categories according to etiology in Japan (Table 4) (4). A Japanese multicenter study involving 497 cases with suspected PLFs reported that 125 cases were classified as category 1, 28 as category 2, 77 as category 3, and 192 as category 4. The CTP-positive rate has been reported to be 8–50% for category 1 (depending on the type of disorder), 14% for category 2, 23% for category 3, and 19% for category 4 (4). Sasaki et al. reported that the CTP-positive rate was 20% in 56 SSHL patients with no apparent antecedent event and significantly higher CTP values in those aged 60 years and older (6). The presence of idiopathic PLF pathology corresponding to category 4 was considered to be present, as evidenced by the recognition of a case in category 4 in which CTP positivity led to a definitive diagnosis of PLF.

The five patients evaluated in this study underwent CTP testing twice (once at the time of IT-DEX [preoperative CTP test] and once at the time of PLF repair surgery using TEES [intraoperative CTP test]). Changes in the status of PLF can be inferred from changes in pre- and intra-operative CTP values. A patient who is preoperatively CTP-positive and intraoperatively CTP-intermediate indicates the possibility of persistent or recurrent PLF. We assumed that perilymphatic leakage and spontaneous closure of the PLF were repeated in patient #5, thus the hearing and disequilibrium improved after surgery, even after 727 days from the onset of the disease to the surgical treatment. A patient who was preoperatively CTP-positive and intraoperatively CTP-negative suggested the possibility of spontaneous PLF closure. A patient who was preoperatively CTP-negative and intraoperatively CTP-positive indicated the possibility that the PLF closed spontaneously and reoccurred or that the preoperative CTP test was a false-negative. It is important to note that a CTP-negative does not rule out the PLF, because the condition of the PLF can change during the clinical course of the patient.

Among the five patients with idiopathic PLF in this study, none of the patients achieved complete hearing recovery after IT-DEX treatment. Sasaki et al. (6) reported that CTP-positive patients with SSHL had a significantly worse hearing recovery rate after IT-DEX treatment. Although steroids may be more easily transmitted to the inner ear in PLF conditions, the results of the study suggest that steroids may be less effective in the treatment of idiopathic PLF. The therapeutic efficacy of steroids in idiopathic PLF is unclear.

We have been using TEES for ear surgery since September 2011. In recent years, TEES has gained popularity and is being applied to different types of middle ear diseases, including PLF, as a result of advances in imaging technology, including full HD video systems. TEES using a full HD video system offers a number of advantages over MES, such as a wide field of view, higher magnification of fine anatomic structures, and clear visualization of anatomic areas that are located in blind spots when viewed through a microscope (7–9). Matuda et al. reported a category 2 PLF case with a congenital dehiscence of the stapes footplate (10). In contrast, the patients in the present study were definitively diagnosed with PLF based on the CTP test results, but a fistula could not be confirmed, even via a magnified endoscopic view. In the diagnosis of idiopathic PLF, the CTP test is considered more sensitive than endoscopic fistula confirmation.

Surgical treatment of idiopathic PLF (in which no fistula can be identified) involves sealing the round and oval windows using connective tissue, temporal fascia, or tragal perichondrium (11). Based on our experiences, PLF repair surgery using TEES for idiopathic PLF can be performed without complications under clear

10.3389/fneur.2024.1376949

TABLE 2 Clinical courses of five patients.

No.	Age	Gender	Symptoms	Time to IT-DEX (day)	Time to surgery (day)	Preoperative CTP test (ng/ml)	Intraoperative CTP test (ng/ml)	Fistula finding at surgery	Hearing levels Pre IT-DEX	Hearing levels Preoperative	Hearing assessment Post IT-DEX	Hearing levels Postoperative	Hearing assessment Postoperative	Improvement of vestibular symptoms
1.	15	Female	Hearing loss, disequilibrium	6	19	<0.20	1.13	None	89 dB	111 dB	No response	99 dB	Slight recovery	Demonstrating marked improvement
2.	43	Male	Hearing loss	12	58	0.81	0.48	None	77 dB	77 dB	No response	84 dB	No response	-
3.	52	Male	Hearing loss, disequilibrium	8	192	3.44	<0.20	None	83 dB	37 dB	Marked recovery	38 dB	No response	unchanged
4.	81	Male	Hearing loss, disequilibrium	35	416	1.85	0.53	None	48 dB	51 dB	No response	47 dB	No response	unchanged
5.	83	Female	Hearing loss, disequilibrium	3	727	1.00	0.48	None	57 dB	69 dB	Slight recovery*	43 dB	Slight recovery	Demonstrating marked improvement

*Patient #5 showed hearing improvement to 33 dB after IT-DEX, but then experienced repeated hearing loss and disequilibrium. She had no hearing loss or disequilibrium attacks for 2.5 years after surgery.

visualization and a wide field of view. Heilen et al. (12) reported that there is no significant hearing improvement after exploratory tympanotomy with sealing of the round window for patients with SSHL. Prenzler et al. (13) reported that exploratory tympanotomy with sealing of the round and oval windows is useful in patients with profound SSHL. Matsuda et al. stated that indications for idiopathic PLF repair surgery are patients whose chief complaint is sustained vestibular symptoms, and the onset or exacerbation of vestibular symptoms was accompanied by sudden, fluctuating, and progressive hearing loss. They reported that the surgery was performed in seven patients, with five showing improved vertigo within 1 week and one within 1 month (14). In our experience with TEES repair surgery, two of five patients showed improvements in both hearing and vestibular symptoms, but patient #2 showed no response in hearing, and 2 patients (#3 and #4) showed unchanged vestibular symptoms. Taking into account these reports and the results of the current study, it is unclear whether sealing inner ear windows for idiopathic PLF improves hearing loss or vestibular symptoms. Large multicenter studies are needed to determine the treatment efficacy of PLF repair surgery via TEES or MES for idiopathic PLF.

The timing of repair surgery is another treatment issue for PLF patients. The need for early PLF repair surgery is unclear because some PLFs may close spontaneously. Matsuda et al. (14) reported that the time to surgery was significantly shorter in cases with good hearing recovery of more than 10 dB postoperatively compared to those with no improvement. We should consider early PLF repair surgery as a treatment option for CTP-positive patients whose hearing and vertigo do not improve after systemic steroid administration or IT-DEX. The efficacy of early PLF repair surgery in patients with idiopathic PLF should be evaluated in further studies.

The CTP test is a sensitive and useful examination in the diagnosis of idiopathic PLF and in determining the indications for PLF repair surgery, but it has a major shortcoming; specifically, it takes approximately 1 month to obtain test results. Thus, early diagnosis and early surgical treatment are difficult in patients with idiopathic PLFs because they have no apparent antecedent events associated with PLFs. The development of rapid testing methods for CTP is desirable in the future. If early diagnosis of idiopathic PLF becomes possible, surgical treatment can be performed earlier and surgical outcomes can be improved. Another limitation of the CTP test is that a positive CTP result may be derived from residual CTP in the middle ear cavity even after the PLF has been closed, but the development of rapid tests for CTP may reduce this limitation.

5 Conclusion

We evaluated five patients definitively diagnosed with idiopathic PLF who underwent PLF repair surgery using TEES. PLF repair surgery using TEES can visualize potential fistulas/microfissures more clearly than MES; however, we have not identified any in these five cases. The CTP test is considered more sensitive than endoscopic fistula confirmation. We consider that CTP test results are important indicators to decide the surgical indication for idiopathic PLF repair surgery. In our experience with five cases, two of them showed improvements in both hearing and vestibular symptoms.

TABLE 3 Surgical indications for idiopathic PLF repair surgery in our institution.

Surgical indication 1: Patients with symptoms and/or test results suggestive of PLF, such as progressive hearing loss.
(Patient #1)
Surgical indication 2: Patients with positive CTP results and hearing not completely recovered.
(Patient #2)
Surgical indication 3: Patients with positive CTP results and recurrent hearing loss and/or vestibular symptoms.
(Patients #3, #4, and #5)

TABLE 4 Categorization of PLF used in Japan.

Category 1: linked to trauma, middle and inner ear diseases, middle, and/or inner ear surgeries
Category 2: linked to barotrauma caused by antecedent events of external origin (such as flying or diving)
Category 3: linked to barotrauma caused by antecedent events of internal origin (such as straining, sneezing, or coughing)
Category 4: has no apparent antecedent event

Data availability statement

The raw data supporting the conclusions of this article will be made available by the authors, without undue reservation.

Ethics statement

The studies involving humans were approved by the Ethics Committee of Yamagata University and Saitama Medical University Hospital. The studies were conducted in accordance with the local legislation and institutional requirements. Written informed consent for participation in this study was provided by the participants' legal guardians/next of kin. Written informed consent was obtained from the individual(s) for the publication of any potentially identifiable images or data included in this article.

Author contributions

TK: Writing – review & editing, Writing – original draft, Methodology, Investigation, Data curation, Conceptualization. TsI: Writing – review & editing, Writing – original draft, Supervision, Methodology, Investigation, Data curation, Conceptualization. TF: Writing – review & editing, Writing – original draft, Investigation. HiM: Writing – review & editing, Writing – original draft, Investigation. TG: Writing – review & editing, Writing – original draft, Investigation. CS: Writing – review & editing, Writing – original draft, Investigation. HaM: Conceptualization, Formal analysis, Funding acquisition, Methodology, Writing – original draft, Writing – review & editing. TeI: Conceptualization, Formal analysis, Funding acquisition, Investigation, Methodology, Supervision, Writing – original draft, Writing – review & editing. SK: Writing – review & editing, Methodology, Writing – original draft, Supervision, Conceptualization.

Funding

The author(s) declare financial support was received for the research, authorship, and/or publication of this article. This study was supported by the Ministry of Health, Labour, and Welfare, Japan (H29-Nanchitou (Nan)- Ippan-031) (TeI) (http://www.mhlw.go.jp/english/).

Conflict of interest

Saitama Medical University, where HaM and TeI are affiliated, holds the patents for the hCTP ELISA test. This fact did not influence the results of the study.

The remaining authors declare that the research was conducted in the absence of any commercial or financial relationships that could be construed as a potential conflict of interest.

Publisher's note

All claims expressed in this article are solely those of the authors and do not necessarily represent those of their affiliated organizations, or those of the publisher, the editors and the reviewers. Any product that may be evaluated in this article, or claim that may be made by its manufacturer, is not guaranteed or endorsed by the publisher.

References

1. Ikezono T, Shindo S, Sekiguchi S, Hanprasertpong C, Li L, Pawankar R, et al. Cochlin-tomoprotein, a novel perilymph specific protein and a potential marker for the diagnosis of perilymphatic fistula. *Audiol Neurootol.* (2009) 14:338–44. doi: 10.1159/000212113

2. Ikezono T, Matsumura T, Matsuda H, Shikaze S, Saitoh S, Shindo S, et al. The diagnostic performance of a novel ELISA for human CTP (Cochlin-tomoprotein) to detect perilymph leakage. *PLoS One.* (2018) 13:e0191498. doi: 10.1371/journal.pone.0191498

3. Kakehata S, Sasaki A, Futai K, Kitani R, Shinkawa H. Daily short-term intratympanic dexamethasone treatment alone as an initial or salvage treatment for idiopathic sudden sensorineural hearing loss. *Audiol Neurootol.* (2011) 16:191–7. doi: 10.1159/000320269

4. Matsuda H, Sakamoto K, Matsumura T, Saito S, Shindo S, Fukushima K, et al. A nationwide multicenter study of the Cochlin Tomo-protein detection test: clinical characteristics of perilymphatic fistula cases. *Acta Otolaryngol.* (2017) 137:S53–9. doi: 10.1080/00016489

5. Kanzaki J, Inoue Y, Ogawa K, Fukuda S, Fukushima K, Gyo K, et al. Effect of single-drug treatment on idiopathic sudden sensorineural hearing loss. *Auris Nasus Larynx*. (2003) 30:123–7. doi: 10.1016/S0385-8146(03)00009-9

6. Sasaki A, Ikezono T, Matsuda H, Araki R, Matsumura T, Saitoh S, et al. Prevalence of Perilymphatic fistula in patients with sudden-onset sensorineural hearing loss as diagnosed by Cochlin-Tomoprotein (CTP) biomarker detection: its association with age, hearing severity, and treatment. *Eur Arch Otorrinolaringol*. (2024) 257:490–2.

7. Tarabichi M. Endoscopic management of acquired cholesteatoma. *Am J Otol*. (1997) 18:544–9.

8. Ito T, Kubota T, Watanabe T, Futai K, Furukawa T, Kakehata S. Transcanal endoscopic ear surgery for pediatric population with a narrow external auditory canal. *Int J Pediatr Otorhinolaryngol*. (2015) 79:2265–9. doi: 10.1016/j.ijporl.2015.10.019

9. Morita Y, Tono T, Sakagami M, Yamamoto Y, Matsuda K, Komori M, et al. Nationwide survey of congenital cholesteatoma using staging and classification criteria for middle ear cholesteatoma proposed by the Japan Otological society. *Auris Nasus Larynx*. (2019) 46:346–52. doi: 10.1016/j.anl.2018.10.015

10. Matsuda H, Tanzawa Y, Sekine T, Matsumura T, Saito S, Shindo S, et al. Congenital membranous stapes footplate producing episodic pressure-induced Perilymphatic fistula symptoms. *Front Neurol*. (2020) 11:585747. doi: 10.3389/fneur.2020.585747

11. Sarna B, Abouzari M, Merna C, Jamshidi S, Saber T, Djalilian HR. Perilymphatic fistula: a review of classification, etiology, diagnosis, and treatment. *Front Neurol*. (2020) 11:11. doi: 10.3389/fneur.2020.01046

12. Heilen S, Lang CP, Warnecke A, Lenarz T, Durisin M. Exploratory tympanotomy in sudden sensorineural hearing loss for the identification of a perilymphatic fistula – retrospective analysis and review of the literature. *J Laryngol Otol*. (2020) 134:501–8. doi: 10.1017/S0022215120000948

13. Prenzler NK, Schwab B, Kaplan DM, El-Saied S. The role of explorative tympanotomy in patients with sudden sensorineural hearing loss with and without perilymphatic fistula. *Am J Otolaryngol*. (2018) 39:46–9. doi: 10.1016/j.amjoto.2017.10.006

14. Matsuda H, Hornibrook J, Ikezono T. Assessing the efficacy of perilymphatic fistula repair surgery in alleviating vestibular symptoms and associated auditory impairments. *Front Neurol*. (2023) 14:14. doi: 10.3389/fneur.2023.1269298

frontiers | Frontiers in Neurology

TYPE Original Research
PUBLISHED 19 June 2024
DOI 10.3389/fneur.2024.1393648

OPEN ACCESS

EDITED BY
Michael Strupp,
Ludwig Maximilian University of Munich, Germany

REVIEWED BY
Franca Wagner,
University Hospital of Bern, Switzerland
Hans Thomeer,
Utrecht University, Netherlands
Munetaka Ushio,
Japan Community Healthcare Organization (JCHO), Japan

*CORRESPONDENCE
Masafumi Sawada
✉ sawada.masafumi@1972.saitama-med.ac.jp
Tetsuo Ikezono
✉ ikezono.tetsuo@1972.saitama-med.ac.jp

RECEIVED 29 February 2024
ACCEPTED 31 May 2024
PUBLISHED 19 June 2024

CITATION
Sawada M, Matsuda H, Tanzawa Y, Sakamoto K, Kudo H, Nakashima M and Ikezono T (2024) Practicality of multilayer round window reinforcement in the surgical management of superior semicircular canal dehiscence syndrome: a case report of long-term follow-up.
Front. Neurol. 15:1393648.
doi: 10.3389/fneur.2024.1393648

Practicality of multilayer round window reinforcement in the surgical management of superior semicircular canal dehiscence syndrome: a case report of long-term follow-up

Masafumi Sawada*, Han Matsuda, Yasuhiko Tanzawa, Kei Sakamoto, Hiroe Kudo, Masato Nakashima and Tetsuo Ikezono*

Department of Otolaryngology and Neuro-Otology, Saitama Medical University Hospital, Saitama, Japan

Several surgical techniques have been documented for approaching and repairing superior semicircular canal dehiscence syndrome (SCDS). These techniques encompass the trans-middle cranial fossa, transmastoid, endoscopic approaches, and round window reinforcement (RWR). RWR entails the placement of connective tissue with or without cartilage and around the round window niche, restricting the round window's movement to minimize the 3rd window effect and restore the bony labyrinth closer to its normal state. We employed the multilayer RWR technique, resulting in significant postoperative improvement and long-lasting effects for 3.7 years in 2 cases. Here, we present the clinical findings, surgical procedures, and the effectiveness of multilayer RWR. This technique can be the initial choice for surgical treatments of SCDS due to its high effectiveness, longer-lasting effect, and minimal risk of surgical complications.

KEYWORDS

SCDS, round window reinforcement, long-term effect, superior petrosal sinus, bilateral

Introduction

Patients with bony labyrinth dehiscence may manifest vestibular and auditory symptoms and cognitive dysfunction, referred to as otic capsule dehiscence syndrome (OCDS) (1). The surgical treatment has demonstrated remarkable efficacy in alleviating these symptoms, rendering OCDS a prominent topic in neuro-otology over the past two decades. Initially identified as superior semicircular canal dehiscence syndrome (SCDS) by Minor et al., SCDS is characterized by a defect in the bone labyrinth of the superior canal (SC), exposing the perilymphatic space to the base of the skull. This SCD acts as the "3rd mobile window" in the inner ear, where external stimuli, such as sound and pressure, can lead to changes in the endolymphatic perfusion of the SC, resulting in distressing symptoms. Patients with SCDS present with a variety of symptoms, with some experiencing more auditory and others

experiencing more vestibular complaints. Symptoms may include sound-or pressure-induced vertigo, which is time-locked to the stimulus. Sound-induced vertigo (Tullio phenomenon) involves the induction of disequilibrium and visual field movement (oscillopsia) in response to acoustic stimuli of low frequency. This symptom has a significant impact on patients' quality of life. Patients may also complain of bone conduction hyperacusis and pulsatile tinnitus.

Surgical intervention for SCDS is generally reserved for patients whose symptoms significantly impact their daily lives. The surgical approaches for addressing SCDS encompass trans-middle cranial fossa, transmastoid, and endoscopic techniques. Various methods have been employed to repair the bone defect, including plugging, resurfacing, and capping (2–4). A relatively recent technique known as round window reinforcement (RWR) has also emerged as a viable option for SCDS treatment. RWR involves the placement of connective tissue with or without cartilage around the round window niche, aiming to bring the bone labyrinth closer to its normal state while limiting the round window's movement, thus improving symptoms. Despite the limited number of reports on RWR, it has demonstrated utility as a minimally invasive technique for SCDS treatment (5–7).

However, the recurrence of the symptoms post-surgery was the main criticism of RWR; we have developed a multilayer RWR method, which yielded significant symptom improvement that persisted for an impressive 3.7 years, defying the prevailing medical consensus.

The incidence of SCDS has been reported to range from 0.5 to 2% in Europe (8). Its prevalence in Asia remains unknown but is presumed to be rare. In our department, only two cases of SCDS necessitated surgical treatment over the past decade, and both cases underwent multilayer RWR; this report presents the clinical findings, surgical procedures, and postoperative outcomes of these two cases, accompanied by a review of the existing literature.

Surgical approach

After discussing treatment options, past cure rates, and potential complications, the patients opted for multilayer RWR as the initial surgical procedure, which does not involve a craniotomy or mastoidectomy (Figure 1). Particularly in Case 1, we explained to the patient that SPS-type SCDS complicates securing the visual field during a middle cranial fossa approach. The multilayer RWR technique incorporated modifications of the technique previously reported by Wackym et al. (6). An intra-meatal incision was made, and loose areolar tissue was harvested at the site of the incision. Subsequently, a portion was thinly spread using a compression device and cut into 3–5 mm pieces. Cartilage was harvested with perichondrium from the tragus meticulously thinned with a scalpel, and cut into approximately 2–3 mm diameters in round shapes. Upon accessing the middle ear, a CO_2 laser (Lumenis Spectra II, Lumenis Inc., San Jose, CA) was utilized to remove the mucosa surrounding the round window niche meticulously. A small piece of thinly sliced cartilage with perichondrium was positioned to fit within the bony overhang of the niche space, facing the perichondrium side toward the RW so that the cartilage would not damage the RW membrane. Tiny fragments of cartilage, approximately 0.25 mm in size, were positioned around the initial cartilage to fill the gaps with the bone and stabilize the structure. Additionally, thinned connective tissue was applied to envelop the first cartilage and these additional pieces, extending over the exposed bone surrounding the niche so that it would adhere to the bony surface. Subsequent layers of additional sliced cartilage were placed on top to prevent migration. Fibrin glue (Beriplast P, CSL Behring, King of Prussia, PA) was used to secure these materials in place (6).

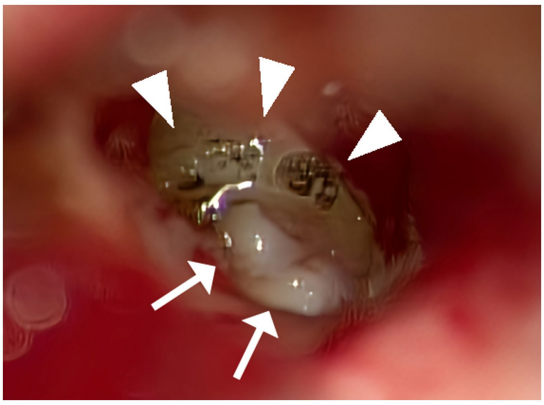

FIGURE 1
Multilayer RWR techniques. A CO_2 laser was utilized to remove the mucosa surrounding the round window niche meticulously (allow head). A small piece of thinly sliced cartilage with perichondrium was positioned to fit within the bony overhang of the niche space. Tiny fragments of cartilage were positioned around the initial cartilage to fill the gaps with the bone and stabilize the structure (allow). Thinned connective tissue was applied over the exposed bone surrounding the niche so that it would adhere to the bony surface.

Clinical assessment

We have evaluated the patients using pure tone audiometry (125 Hz, 250 Hz, 500 Hz, 1 k Hz, 2 k Hz, 4 k Hz, 8 k Hz were measured), ocular vestibular evoked myogenic potentials (oVEMP) in response to air-conducted sound and high-resolution CT scans (HRCT). The patients underwent helical high-resolution computed tomography of the temporal bone with 0.6 mm of the slice thickness in the axial plane. The images were reconstructed in planes parallel to the superior semicircular canal (Pöschl plane) and orthogonal to the canal (Stenver plane), and a head and neck radiologist diagnosed the presence of dehiscence.

We have used three questionnaires: the dizziness handicap inventory (DHI) and the Vertigo Symptom Scale Short Form (VSS-sf), which are widely used. The DHI evaluates handicaps due to dizziness in daily life. An improvement of 18 points or more is considered to represent a minimal clinically important difference (MCID) (9). The VSS-sf was developed to measure symptom frequency over 1 month, with the primary goal of assessing therapeutic effect, and has been used in clinical trials (10, 11). In VSS-sf, the higher the total score from 0 to 60, the more severe the symptoms; a score of 12 or more is considered severe (12). The Niigata PPPD Questionnaire (NPQ), recently developed for PPPD diagnosis, has proven beneficial for this purpose (13). The NPQ asks patients about factors that induce vertigo/dizziness in three categories: upright posture/walking, movement, and visual stimulation. Not only for PPPD diagnosis but in our daily clinical practice, we utilize the NPQ to identify the triggers of a patient's vestibular symptoms

(discussed below). To rule out perilymphatic fistula (PLF), the intraoperative inspection was performed to identify the possible fistula and perilymph-specific protein CTP detection test (14) was performed.

Cases

Illustrative case 1

Chief complaint: unsteadiness

History of present illness

The onset of symptoms began 5 years before the initial visit, with intermittent episodes of unsteadiness (Table 1). These episodes had minimal impact on the patient's daily life. However, approximately 5 months before the first visit, the symptoms escalated to a point where the patient could not take more than a few steps without experiencing severe unsteadiness. Activities such as using elevators or traveling by car exacerbated these symptoms. Over time, the symptoms progressively deteriorated. Even in the absence of accelerative stimuli from vehicles or elevators, the patient sustained symptoms akin to motion sickness for several months. The episodes of unsteadiness fluctuated, with some days being better than others. Additionally, the patient reported experiencing heightened sensitivity to children's loud voices, especially in the left ear. The patient's concentration had significantly declined, making tasks like reading challenging. Due to these symptoms, the patient, a carpenter working at heights, was unable to continue working and had to take medical leave. A HRCT scan raised suspicion of SCD, leading to a referral to our department.

Clinical assessment

Upon examination, the patient scored 36 points on DHI, 14 points on VSS-sf, and 52 points on NPQ. Neuro-otological examination revealed a left-sided low-frequency air-bone gap of approximately 30 dB on pure tone audiometry (Figure 2). An enhanced response was observed in the left side oVEMP with an asymmetry ratio of 82.5%. HRCT revealed a dehiscence of SPS-type only on the left side in the reconstructions on the Pöschl plane, and surgical intervention was indicated.

Surgical approach and outcome

The multilayer RWR technique was chosen as the treatment. No intraoperative fistula was identified, and intraoperative CTP testing was negative. Following the surgery, there was a notable improvement in symptom scores within 8 days. No deterioration was observed up to 1,367 days (3.7 years) postoperatively (Figure 3). Notably, the low-tone air-bone gap and VEMP asymmetry ratio did change following surgery (Figure 2).

Illustrative case 2

Chief complaint: sound-induced vertigo

History of present illness

Seven years before the initial consultation, the patient experienced the onset of sound-induced vertigo following a car accident (rear-end collision) (Table 1). Her symptoms notably worsened, primarily when she served as an emcee at sports events held in large venues. This exacerbation occurred in a time-locked manner due to exposure to intense auditory stimuli such as drum rolls, applause, and cheering. During these events, she reported a resonant sensation within her right ear and a sound-induced swaying sensation. Furthermore, she described experiencing severe oscillopsia, wherein the audience appeared to undulate like waves. Additionally, there were episodes during which she perceived spatial disorientation as if the ground and sky had inverted. Her symptoms intensified during airplane take-offs and landings, as well as while ascending in an elevator, leading to severe unsteadiness, necessitating the use of handrails for support.

Clinical assessment

At the time of examination, the patient's symptom scores were as follows: 28 points on DHI, 28 points on VSS-sf, and 50 points on NPQ. Neuro-otological examination revealed a 15 dB air-bone gap (Figure 2). An enhanced response was observed in the right side oVEMP with an asymmetry ratio of 91%. HRCT showed dehiscence of the superior semicircular canal on both sides in the reconstructions on the Pöschl plane (Figure 4). Based on her symptoms and oVEMP results, a diagnosis of right-sided SCDS was made, and surgical treatment was recommended.

Surgical approach and outcome

The patient underwent multilayer RWR surgery. No intraoperative fistula was identified, and intraoperative CTP testing was negative. Following the procedure, there was a remarkable improvement in symptom scores within 11 days postoperatively, and no worsening was observed up to 1,346 days (3.7 years) postoperatively (Figure 3). The enhanced oVEMP

TABLE 1 Patients demographics, history, third window syndrome symptoms, physical findings, and results of diagnostic studies.

Patient (age at surgery)	Sex	Diagnosis	HRCT	Low-frequency air-bone gap	Enhanced VEMP responses	Sound-induced symptom	Preceding trauma	Hearing internal sound	Length of postoperative follow up
Case 1 (43 years old)	M	Lt SPS type SCDS	Lt SPS type	Lt	Lt	Unsteadiness	No	Voice resonant	3.7 years
Case 2 (61 years old)	F	Rt SCDS	Bilateral side	Bilateral	Rt	Vertigo and oscillopsia	Car accident (rear-end collision)	Auto-phony	3.7 years

N/A, not available.

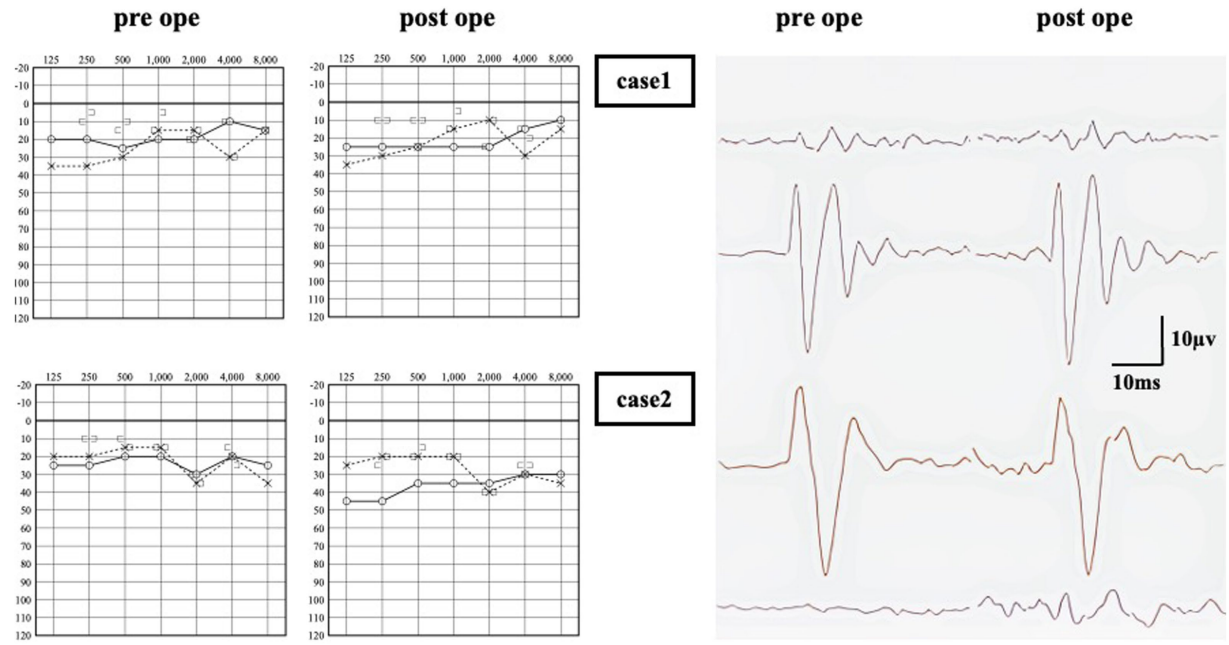

FIGURE 2
Audiometry of pre and post operation. In Case 1, no significant change in air-conduction (AC) thresholds between pre and post-surgery. An response was observed in the left side oVEMP, and no significant change was observed after surgery. In Case 2, there was a decrease in AC thresholds on the surgical side, resulting in a 15–25 dB air-bone gap in the low frequency range. An enhanced response was observed in oVEMP on the right side only, and no significant change was observed after surgery.

responses did not show improvement after surgery. The air conduction in pure tone audiometry at lower frequencies increased by 10 dB (Figure 2).

Discussion

In these 2 cases, characteristic symptoms and findings such as pressure and/or sound-induced vertigo and nystagmus, and air-bone gaps at low tones were identified, and an HRCT scan and VEMP were conducted and confirmed the diagnosis of SCDS. Their symptoms were severe and had a considerable impact on their personal and professional lives.

Patients with larger dehiscence (≥2.5 mm) were significantly more likely to exhibit vestibulocochlear symptoms/signs, enhanced VEMP responses, and objective vestibular findings compared to subjects with smaller bony defects (15). In Case 2, bilateral dehiscences were present, but the symptomatic cause was identified on the right side, with a size of 4.0 mm. The left side, measuring 2.2 mm, was not implicated in the symptoms. These findings are consistent with previous reports.

The RWR technique was developed to alleviate symptoms associated with a third window by modifying the round window (RW) compliance without directly addressing the more challenging-to-access SC. Consequently, the inner ear becomes less susceptible to sudden changes in sound and pressure. The RWR surgery reduced several symptoms of SCDS, including autophony, bone-conduction sensitivity, pulsatile tinnitus, sound or pressure-induced vestibular symptoms, and aural fullness (7, 16).

In the present study, two subjects who underwent multilayer RWR showed marked improvement in their DHI, VSS-sf and NPQ scores shortly after surgery. DHI scores showed significant decreases from 36 to 12 in Case 1 and from 28 to 0 in Case 2, indicating an improvement of more than 18 points (MCID) in both cases. VSS-fs scores, which were above 12 in both cases, indicating severe conditions, demonstrated marked improvements post-surgery, dropping to 6 and 0 points, respectively. The differential diagnosis for SCDS includes varieties of chronic vestibular disease (17), including Meniere's disease, perilymph fistula, age-related unsteadiness, and persistent postural-perceptual dizziness (PPPD). The NPQ is initially developed to assist in diagnosing PPPD and assesses symptom exacerbation in response to three characteristic factors: upright posture/walking, movement, and visual stimulation. When the cutoff is set at 27 points (total score = 72), the sensitivity of PPPD diagnosis is 70%, and the specificity is 68%. In both cases, NPQ scores exceeded the cutoff of 27 points, 52 points, and 50 points and dropped to 9 and 0, respectively. This does not mean that these cases suffered from PPPD since it is a diagnosis of exclusion. An NPQ score can exceed the cutoff in other conditions, such as SCDS, which we presented here. The routine usage of NPQ in our clinic is to analyze inducing factors. Among the 3 factors, "movement" scores are the highest in our cases (Figure 3), whereas "visual stimulation" is usually characteristic of PPPD (12), which could be helpful in the differential diagnosis of these two conditions.

These positive outcomes persisted, with no signs of symptom aggravation or recurrence for a duration nearing 3.7 years (Figure 3). Historically, concerns have been raised regarding the durability of multilayer RWR, with failures documented as early as 6 months post-treatment (18, 19). This duration is considerably shorter than the longevity reported for other surgical approaches, such as the middle

	case1				case2		
POD	Pre-operation	8	108	1367	Pre-operation	11	243
DHI	36	28	12	12	28	2	0
DHI-P	14	10	6	8	20	2	0
DHI-E	14	12	6	2	4	0	0
DHI-F	8	6	0	2	4	0	0
VSS-sf	14	5	8	6	28	N/A	0
NPQ	52	N/A	N/A	9	50	13	0
Upright posture /Walking	17	N/A	N/A	3	15	6	0
Movement	21	N/A	N/A	4	20	2	0
Visual	14	N/A	N/A	2	15	2	0

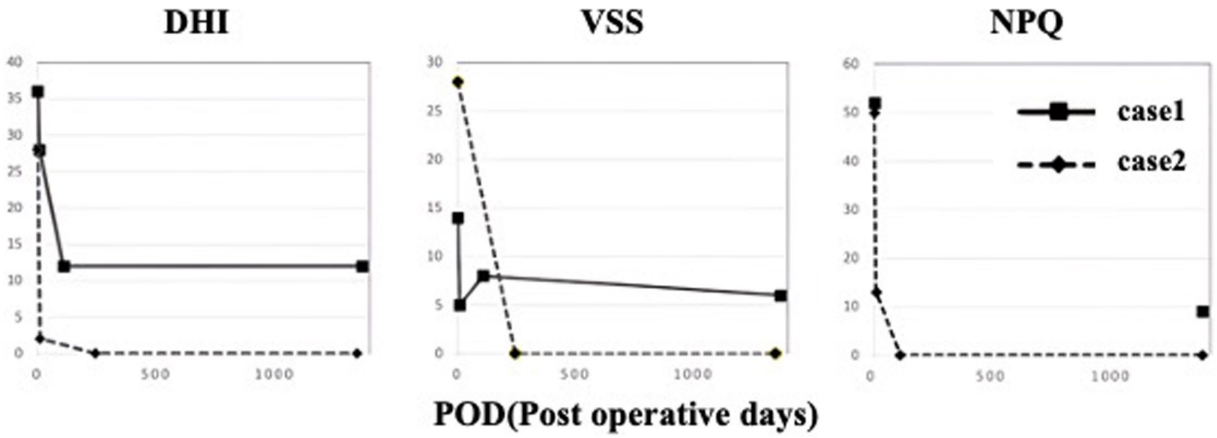

FIGURE 3
CT imaging. All reconstructed on the Pöschl plane. Case 1: This illustrates slices of the left side, the Pöschl and coronal planes. Notably, only the left side exhibited a dehiscence of SPS type. Case 2: Pöschl plane demonstrating the presence of dehiscence on both sides. Only the right side was symptomatic.

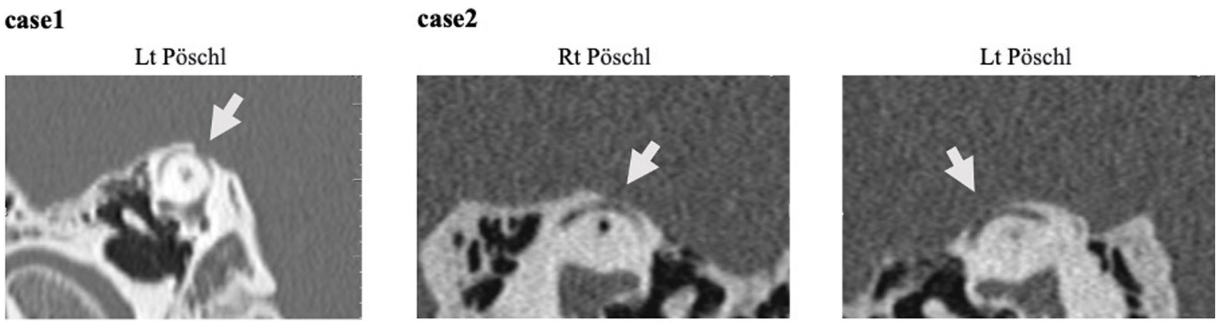

FIGURE 4
DHI & VSS score of pre and post operation. Following the RWR surgery, there was an improvement in symptom scores. In case 1, DHI from 36 to 12, with no deterioration observed up to 1,367 days (3.7 years). In case 2, DHI from 28 to 2 in 11 days, with no worsening at 1,346 days (3.7 years). VSS remained similar.

cranial fossa or transmastoid technique (20). The early failure of RWR is often ascribed to the potential for fascia graft degradation, which may undergo atrophy, resorption, or migration (21).

Addressing this issue, Wackym et al. enhanced the RWR procedure by incorporating fascia and cartilage, as well as denuding all mucosa around the RW niche using a CO_2 laser to secure the materials. The procedure was described in much greater detail than in previous publications, as clarified in reference (6). We have further adapted this procedure. We refrained from drilling off the bony overhang of the niche; instead, we utilized the niche space to fill and stabilize with the first cartilage, positioning the perichondrium toward the RWM to minimize invasiveness to the cochlea and RW membrane. 0.25 mm cartilage fragments further stabilized the first cartilage. A thinned layer of connective tissue was applied to encase the first cartilage, extending over the exposed bone encircling the niche. Additional layers of thinly sliced cartilage were superimposed to avert migration. This stratified technique augmented the graft's stability postoperatively, enabling extended-term outcomes. The follow-up period described in previous reports regarding the long-term outcomes of RWR was about 2 years, and more documentation of extended follow-up durations is needed (6).

This study carries several weaknesses. The present study is limited by the absence of a control group, either non-surgical or receiving sham surgery, which introduces the potential for a placebo effect on subjective symptoms. Regardless, our findings demonstrated that patients exhibited marked improvement post-surgery even among the 2 cases presenting chronic SCDS symptoms. This supports the inference that the observed gains are likely attributable to the surgical intervention.

In cases where RWR was performed for SCDS, it could elevate the threshold in the air-conduction testing as a surgical complication (7, 16, 22, 23). In Case 1, there was no exacerbation, while Case 2 exhibited a 20 dB exacerbation in the air-conduction testing postoperatively; however, the patient reported satisfaction due to the resolution of the debilitating vestibular dysfunction that was interfering with daily activities. Regarding cVEMP and oVEMP, postoperative testing revealed normalization of responses on the operated side after surgical plugging (24). Previous reports lacked detailed descriptions of postoperative VEMP changes in cases where RWR was performed. In our two cases, the enhanced responses of oVEMP did not normalize.

The RWR technique aims to alleviate symptoms associated with a third window by modifying the compliance of the round window (RW) rather than directly addressing the more challenging-to-access SC (6). The inner ear becomes less sensitive to sudden changes in sound and pressure without the dehiscence itself being repaired. It should be noted that this surgical procedure is aimed at alleviating vestibular symptoms and is not designed to improve the hearing component. Additionally, it may result in a decrease in conductive hearing. And that Medical Centers with low experience in the middle fossa approach technique should think over the RWR technique due to possible complications. Case 1 had an SPS-type dehiscence; the anatomical location of the SPS can make it challenging to maintain a visual field in the operative area and may increase the risk of surgical complications (25). Multilayer RWR is a preferable first choice, especially in SPS cases with a high risk of surgical complications with conventional methods.

Conclusion

We successfully treated two cases of SCDS with the multilayer RWR technique, resulting in significant improvement in subjective symptoms and quality of life during the early postoperative period, with these benefits lasting for at least approximately 3.7 years. The primary limitation of this study is that it includes only two cases, which may limit the conclusiveness of our findings. Another limitation of this technique is the potential for no improvement or even deterioration of the conductive component of hearing, despite the alleviation of vestibular symptoms. However, RWR carries a lower risk of complications such as intracranial injury, cerebrospinal fluid leakage, sensorineural hearing loss, and infection than conventional methods. It can also effectively alleviate symptoms without requiring craniotomy. Considering these factors, the multilayer RWR technique can be a favorable choice for initial surgery in the treatment of SCDS.

Data availability statement

The datasets presented in this study can be found in online repositories. The names of the repository/repositories and accession number(s) can be found in the article/supplementary material.

Ethics statement

Written informed consent was obtained from the individual(s), and minor(s)' legal guardian/next of kin, for the publication of any potentially identifiable images or data included in this article.

Author contributions

MS: Writing – original draft, Writing – review & editing. HM: Investigation, Writing – review & editing. YT: Investigation, Writing – review & editing. KS: Investigation, Writing – review & editing. HK: Investigation, Writing – review & editing. MN: Writing – review & editing, Investigation. TI: Conceptualization, Supervision, Writing – review & editing.

Funding

The author(s) declare that no financial support was received for the research, authorship, and/or publication of this article.

Conflict of interest

The authors declare that the research was conducted in the absence of any commercial or financial relationships that could be construed as a potential conflict of interest.

Publisher's note

References

1. Wackym PA, Wood SJ, Siker DA, Carter DM. Otic capsule dehiscence syndrome: superior semicircular canal dehiscence syndrome with no radiographically visible dehiscence. *Ear Nose Throat J*. (2015) 94:E8–9. doi: 10.1177/014556131509400802

2. Bi WL, Brewster R, Poe D, Vernick D, Lee DJ, Eduardo Corrales C, et al. Superior semicircular canal dehiscence syndrome. *J Neurosurg*. (2017) 127:1268–76. doi: 10.3171/2016.9.JNS16503

3. Minor LB, Solomon D, Zinreich JS, Zee DS. Sound-and/or pressure-induced vertigo due to bone dehiscence of the superior semicircular canal. *Arch Otolaryngol Neck Surg*. (1998) 124:249. doi: 10.1001/archotol.124.3.249

4. Palma Diaz M, Cisneros Lesser J, Vega AA. Superior semicircular canal dehiscence syndrome – diagnosis and surgical management. *Int Arch Otorhinolaryngol*. (2017) 21:195–8. doi: 10.1055/s-0037-1599785

5. Wackym PA, Balaban CD, Zhang P, Siker DA, Hundal JS. Third window syndrome: surgical Management of Cochlea-Facial Nerve Dehiscence. *Front Neurol*. (2019) 10:1281. doi: 10.3389/fneur.2019.01281

6. Wackym PA, Balaban CD, Mackay HT, Wood SJ, Lundell CJ, Carter DM, et al. Longitudinal cognitive and neurobehavioral functional outcomes before and after repairing otic capsule dehiscence. *Otol Neurotol*. (2016) 37:70–82. doi: 10.1097/MAO.0000000000000928

7. Silverstein H, Kartush JM, Parnes LS, Poe DS, Babu SC, Levenson MJ, et al. Round window reinforcement for superior semicircular canal dehiscence: a retrospective multi-center case series. *Am J Otolaryngol*. (2014) 35:286–93. doi: 10.1016/j.amjoto.2014.02.016

8. Carey JP, Minor LB, Nager GT. Dehiscence or thinning of bone overlying the superior semicircular canal in a temporal bone survey. *Arch Otolaryngol Neck Surg*. (2000) 126:137. doi: 10.1001/archotol.126.2.137

9. Jacobson GP, Newman CW. The development of the dizziness handicap inventory. *Arch Otolaryngol Head Neck Surg*. (1990) 116:424–7. doi: 10.1001/archotol.1990.01870040046011

10. Yardley L, Barker F, Muller I, Turner D, Kirby S, Mullee M, et al. Clinical and cost effectiveness of booklet based vestibular rehabilitation for chronic dizziness in primary care: single blind, parallel group, pragmatic, randomised controlled trial. *BMJ*. (2012) 344:e 2237. doi: 10.1136/bmj.e2237

11. Yardley L, Masson E, Verschuur C, Haacke N, Luxon L. Symptoms, anxiety and handicap in dizzy patients: development of the vertigo symptom scale. *J Psychosom Res*. (1992) 36:731–41. doi: 10.1016/0022-3999(92)90131-K

12. Yardley L, Donovan-Hall M, Smith HE, Walsh BM, Mullee M, Bronstein AM. Effectiveness of primary care–based vestibular rehabilitation for chronic dizziness. *Ann Intern Med*. (2004) 141:598–605. doi: 10.7326/0003-4819-141-8-200410190-00007

13. Yagi C, Morita Y, Kitazawa M, Nonomura Y, Yamagishi T, Ohshima S, et al. A validated questionnaire to assess the severity of persistent postural-perceptual dizziness (PPPD): the Niigata PPPD questionnaire (NPQ). *Otol Neurotol*. (2019) 40:e747–52. doi: 10.1097/MAO.0000000000002325

14. Ikezono T, Matsumura T, Matsuda H, Shikaze S, Saitoh S, Shindo S, et al. The diagnostic performance of a novel ELISA for human CTP (Cochlin-tomoprotein) to detect perilymph leakage. *PLoS One*. (2018) 13:e0191498. doi: 10.1371/journal.pone.0191498

15. Pfammatter A, Darrouzet V, Gartner M, Somers T, Dinther JV, Trabalzini F. A superior semicircular canal dehiscence syndrome multicenter study: is there an association between size and symptoms? *Otol Neurotol*. (2010) 31:447–54. doi: 10.1097/MAO.0b013e3181d27740

16. Chemtob RA, Noij KS, Qureshi AA, Klokker M, Nakajima HH, Lee DJ. Superior canal dehiscence surgery outcomes following failed round window surgery. *Otol Neurotol*. (2019) 40:535–42. doi: 10.1097/MAO.0000000000002185

17. Ward BK, Van de Berg R, Van Rompaey V, Bisdorff AR, HT E, Welgampola MS, et al *Society ICVD Proposal Superior Semicircular Canal Dehiscence Syndrome (SCDS)*. (2016). [in press].

18. Thomeer H, Bonnard D, Castetbon V, Franco-Vidal V, Darrouzet P, Darrouzet V. Long-term results of middle fossa plugging of superior semicircular canal dehiscences: clinically and instrumentally demonstrated efficiency in a retrospective series of 16 ears. *Eur Arch Otorrinolaringol*. (2016) 273:1689–96. doi: 10.1007/s00405-015-3715-5

19. Mau C, Kamal N, Badeti S, Reddy R, Ying YLM, Jyung RW, et al. Superior semicircular canal dehiscence: diagnosis and management. *J Clin Neurosci*. (2018) 48:58–65. doi: 10.1016/j.jocn.2017.11.019

20. Alkhafaji MS, Varma S, Pross SE, Sharon JD, Nellis JC, Santina CCD, et al. Long-term patient-reported outcomes after surgery for superior canal dehiscence syndrome. *Otol Neurotol*. (2017) 38:1319–26. doi: 10.1097/MAO.0000000000001550

21. Shaia WT, Diaz RC. Evolution in surgical management of superior canal dehiscence syndrome. *Curr Opin Otolaryngol Head Neck Surg*. (2013) 21:497–502. doi: 10.1097/MOO.0b013e328364b3ff

22. Silverstein H, Van Ess MJ. Complete round window niche occlusion for superior semicircular canal dehiscence syndrome: a minimally invasive approach. *Ear Nose Throat J*. (2009) 88:1042–56. doi: 10.1177/014556130908800808

23. Succar EF, Manickam PV, Wing S, Walter J, Greene JS, Azeredo WJ. Round window plugging in the treatment of superior semicircular canal dehiscence. *Laryngoscope*. (2018) 128:1445–52. doi: 10.1002/lary.26899

24. Rinaldi V, Portmann D. Vestibular-evoked myogenic potentials after superior semicircular canal obliteration. *Rev Laryngol Otol Rhinol*. (2011) 132:85–7.

25. McCall AA, McKenna MJ, Merchant SN, Curtin HD, Lee DJ. Superior canal dehiscence syndrome associated with the superior petrosal sinus in pediatric and adult patients. *Otol Neurotol*. (2011) 32:1312–9. doi: 10.1097/MAO.0b013e31822e5b0a

frontiers | Frontiers in Neurology

TYPE Original Research
PUBLISHED 28 October 2024
DOI 10.3389/fneur.2024.1476004

OPEN ACCESS

EDITED BY
Enis Alpin Guneri,
Dokuz Eylül University, Türkiye

REVIEWED BY
Joel Alan Goebel,
Washington University in St. Louis, United States
Paul R. Kileny,
University of Michigan, United States

*CORRESPONDENCE
Todd M. Mowery
✉ tm692@rwjms.rutgers.edu

†These authors share first authorship

RECEIVED 04 August 2024
ACCEPTED 20 August 2024
PUBLISHED 28 October 2024

CITATION
Hong SS, Wackym PA, Murphy DJ, Peci E, Kiel MY, Tucker A, Carayannopoulos NL, Chandrasekar SC, Suresh N, Utku UA, Yao JD and Mowery TM (2024) Model of superior semicircular canal dehiscence: asymmetrical vestibular dysfunction induces reversible balance impairment.
Front. Neurol. 15:1476004.
doi: 10.3389/fneur.2024.1476004

Model of superior semicircular canal dehiscence: asymmetrical vestibular dysfunction induces reversible balance impairment

Sean S. Hong[1†], P. Ashley Wackym[1,2†], Damian J. Murphy[1], Eran Peci[1], Matthew Y. Kiel[1], Aaron Tucker[1], Nicolas L. Carayannopoulos[1], Shrivaishnavi C. Chandrasekar[1], Nikhil Suresh[1], Umut A. Utku[1], Justin D. Yao[1,2] and Todd M. Mowery[1,2*]

[1]Department of Head and Neck Surgery & Communication Sciences, Rutgers Robert Wood Johnson Medical School, New Brunswick, NJ, United States, [2]Rutgers Brain Health Institute, New Brunswick, NJ, United States

Background: Superior semicircular canal dehiscence (SSCD) is a vestibular-cochlear disorder in humans in which a pathological third mobile window of the otic capsule creates changes to the flow of sound pressure energy through the perilymph/endolymph. The primary symptoms include sound-induced dizziness/vertigo, inner ear conductive hearing loss, autophony, headaches, and visual problems. We have developed an animal model of this human condition in the Mongolian Gerbil that uses surgically created SSCD to induce the condition. A feature that is unique in this model is that spontaneous resurfacing of the dehiscence occurs via osteoneogenesis without a subsequent intervention. In this study, we completed our assessment of this model to include reversible asymmetrical vestibular impairments that interfere with balance.

Methods: Adult Mongolian gerbils ($N = 6$) were trained to complete a balance beam task. They were also trained to perform a Rotarod task. After 10 days of training, preoperative ABR and c+VEMP testing was followed by a surgical fenestration of the left superior semicircular canal. Balance beam testing recommenced at postoperative day 6 and continued through postoperative day 15 at which point final ABR and c+VEMP testing was carried out.

Results: Behavioral comparison of preoperative and postoperative performance show a significant decrease in Rotarod performance, increased rates of falling, and an increase in time to cross the balance beam. Impairments were the most significant at postoperative day 7 with a return toward preoperative performance by postoperative day 14. This behavioral impairment was correlated with residual impairments to auditory thresholds and vestibular myogenic amplitudes at postoperative day 14.

Conclusion: These results confirm that aberrant asymmetric vestibular output in our model of SSCD results in reversible balance impairments. The level of these behavioral impairments is directly correlated with severity of the vestibular dysfunction as we have previously reported for peripheral ear physiology and cognition.

KEYWORDS

balance, dizziness, perilymph fistula, sound-induced dizziness, spatial disorientation, superior semicircular canal dehiscence

Introduction

Superior semicircular canal dehiscence (SSCD) is an inner-ear disorder characterized by a pathological third mobile window in the superior semicircular canal. First described by Minor et al. (1), SSCD presents with a variety of auditory and vestibular symptoms, including autophony, inner ear conductive hearing loss, and sound-induced dizziness/vertigo. These symptoms are often triggered by alterations in middle ear pressure or auditory stimulation (1–4). The precise mechanism by which SSCD develops remains incompletely understood. It is thought to arise from developmental abnormalities or acquired changes in bone density. The diagnosis of SSCD typically involves a combination of clinical history, physical examination, and radiologic imaging, such as high-resolution temporal bone computed tomography and vestibular evoked myogenic potentials (cervical VEMPs [cVEMPs] and ocular VEMPs [oVEMPs]) (5–14).

Previous research has expanded our understanding of the effects of vestibular dysfunction beyond the known limitations in balance, coordination, and spatial orientation. A number of studies have shown that individuals with asymmetric vestibular disorders often exhibit cognitive deficits, including impairments in attention, memory, and executive function, as well as depression (9, 15, 16). This association highlights the intricate relationship between the vestibular system and the central nervous system and warrants further investigation into the governing pathways and potential therapeutic implications of these systems.

The development of animal models has provided valuable insights into the underlying mechanisms of the various signs and symptoms observed in patients. We recently published a gerbil model of SSCD with reversible diagnostic findings characteristic of patients with the disorder (17). Other animal models of SSCD have also been created in chinchillas, guinea pigs, and rats (18–25). These models have contributed to our understanding of the pathophysiology of SSCD and have facilitated the evaluation and diagnosis of the disease. Despite these advancements, the existing models have limitations, including species-specific differences in anatomy and behavior, that warrant the establishment of animal models that more closely mimic the human condition.

The objective of this study was to expand upon our novel gerbil model of SSCD to further encompass the vestibular deficits associated with this condition. Our previous research established the gerbil model of SSCD using auditory brainstem responses (ABR) and cervical positive vestibular evoked myogenic potentials (c+VEMP), with a particular focus on capturing the cognitive impairments commonly seen in humans afflicted with this disorder and other sites of dehiscence resulting in third window syndrome (9, 10, 17, 26, 27). We have previously shown that our SSCD model results in reversible impairments in specific auditory and visual behavioral tasks assessing decision-making, suggesting a potential link between vestibular dysfunction and cognitive deficits (26). Animals with SSCD also show reversible deficits in a spatial two alternative force choice (2AFC) task where they must make a left versus right decision to receive a food reward (28). Furthermore, in that study we used neuroanatomical tracing to confirm a cross species (gerbil and mouse) vestibular behavioral circuit that modulates associative-conditioned tasks through thalamic input to the striatum. Together, these findings show how important proper vestibular function is to normal behaviors. The model provides a powerful approach for studying the central neural etiology of the cognitive behavioral symptoms reported in the human condition (9).

The same surgical techniques used in our previous studies were employed to create the SSCD in a new group of gerbils, with a focus on translating the vestibular deficits, in particular the sound-induced vestibular dysfunction (Tullio phenomenon). In our study, gerbils were trained and tested on the balance beam and Rotarod to assess vestibular function. We observed significant effects of SSCD on time on the Rotarod, time to cross the balance beam, and on falls off the beam. Furthermore, the severity of this balance behavioral impairment was highly correlated with auditory thresholds and vestibular output (c+VEMP amplitudes). By combining physiological measures (ABR and c+VEMP) with direct vestibular testing, we sought to provide a more comprehensive animal model of SSCD that could serve as a foundational model for further study of SSCD and central processes subserving the observed behavioral changes.

Materials and methods

Animals

A total of 6 adult male and female Mongolian gerbils *Meriones unguiculatus* (3 males and 3 females) were used in this study. All animals were housed in the same vivarium facility under a 12/12 dark cycle with *ad libitum* access to food and water. All animals were trained to perform the behavioral balance tasks and completed electrophysiologic testing preoperatively. The animals then received superior semicircular canal fenestration to create the SSCD. All experiments were reviewed and approved by Rutgers University Institutional Animal Care and Use Committee.

Surgical creation of superior semicircular canal dehiscence

Animals were anesthetized with isoflurane and prepared for stereotaxic surgery. An incision was made over the nuchal muscles on the left side of the head just posterior to the pinna. The nuchal muscles were then sharply and bluntly dissected to expose the left superior bulla. A 5.0 mm opening was made with a 1.5 mm diamond bur. For the SSCD surgery, a 2.0 mm fenestration of the labyrinthine bone was made on the apex of the superior canal, without violating the endolymphatic duct. The open bulla was then sealed with Sterile

Silastic (Dow Chemical Company, Midland, MI, USA) to partition the air-filled bulla from the overlying neck muscles thereby restoring the normal air-filled middle ear and avoiding a true conductive hearing loss. Condensation on the Silastic seal's interior surface was deemed indicative of this restoration of function. Finally, the reattached muscles were glued to the skull with Medbond tissue glue (Stoelting Co., Wood Dale, IL, USA) which allowed for c+VEMP testing after the procedure. The incision was closed with a running locked 4–0 Vicryl suture (Ethicon US, LLC, New Brunswick, NJ, USA) and topical antibiotic was applied to the wound.

Balance beam task

The balance beam apparatus (Panlab Harvard Apparatus, Barcelona, Spain) consisted of a wide beam (6 cm by 120 cm), elevated above the ground, with a covered safe box located at one end. Gerbils were placed on the beam and their ability to maintain balance while traversing its length was observed and recorded using an overhead camera. The SMART 3.0 video tracking software (Panlab Harvard Apparatus, Barcelona, Spain) was employed to precisely measure parameters such as latency to the box and to fall, providing quantitative data for statistical analysis. A multi-field speaker (MF1, Tucker-Davis Technologies, Alachua, FL, USA) was placed 5 cm from the starting position, elevated 6 inches directly above using a tripod. Infrared beams were placed under the speaker to trigger the playback of 90 dB broadband noise from the speaker for 3 s. Gerbils were trained on the balance beam for 3 days and then underwent recorded trials for 5 days before surgery. Testing resumed after surgery at days 6–8 and 13–15 denoted as postoperative 7 and postoperative day 14, respectively, throughout the manuscript and Figures.

Rotarod task

The Rotarod (Med Associates Inc., Fairfax, VT, USA) was used to further assess vestibular function and balance. The gerbils were placed on the rod, which accelerated from 3 to 30 rpm over 2 min in a linear manner. The length of time on the rod was recorded with a maximum cutoff of 5 min. At 5 min animals were removed from the Rotarod and returned to the cage. Animals were tested three times daily in the morning at least 2 h prior to the balance beam test.

Auditory brainstem response testing

Animals were anesthetized with isoflurane (1.0%) and placed in a small sound chamber (IAC, Sound Room Solutions, Inc., Glen Cove, NY, USA). Auditory brainstem response (ABR) recordings were made by inserting pin electrodes subcutaneously at the vertex of the skull and just caudal to the right pinna; the ground electrode was inserted into the base of the tail. BioSigRZ software and the TDT ABR system (Tucker-Davis Technologies, Alachua, FL, USA) were used to collect ABR data. A 10-cm tube (closed field) was inserted into the ear and placed at the opening of the ear canal. The left ear of the animal was stimulated via multi-field speaker (MF1, Tucker-Davis Technologies, Alachua, FL, USA) at 1, 2, 4, 8, and 16 kHz tones [90–20 dB SPL (10 dB steps)], 5 ms, 2 ms linear ramp rise-fall times at 25 Hz. Traces were averaged across 512 (threshold) sweeps. Thresholds for each frequency were measured as the last dB SPL (i.e., 10 dB SPL resolution stimulus level) that elicited a tone-induced ABR.

Sound-induced cervical positive vestibular evoked myogenic potential (c+VEMP) testing

Sound-induced otolithic stimulation and evoked intramuscular excitatory potential recordings were collected by inserting pin electrodes into the neck extensor muscles (splenius capitus *m.*), with the reference electrode placed at the vertex of the skull. BioSigRZ software and the TDT ABR system were used to collect c+VEMP data. A 10-cm tube capable of delivering 100 dB SPL (see TDT specs, Closed Field) was inserted into the ear and placed at the opening of the ear canal. The left ear of the animal was stimulated via multi-field speaker (MF1, Tucker-Davis Technologies) at 2 kHz (100 to 80 dB SPL [5 dB steps], 5 ms, 2 ms linear ramp rise-fall times sampled at 25 kHz). Traces were averaged across 512 (threshold) sweeps. The c+VEMPs were recorded under low-isoflurane anesthesia (<1.5%), near conditions of wakefulness. The c+VEMP was measured when it appeared under the condition of stimulation of air-conducted sound at 2 kHz and 100 dB. Peak amplitudes were measured by subtracting the peak of the negative N1 wave (in μV) from the later positive P1 wave.

Condenser brightfield stereomicroscopy

After the final ABR and c+VEMP recordings were collected at postoperative day 14, the animals were euthanized (Euthasol 300 mg/kg) and perfused for histology. Each animal's heart was accessed through the diaphragm. The right atrium was cut, and 20 mL of room-temperature phosphate-buffered saline (1 M) was perfused through the left ventricle. This was followed by 20 mL of cold paraformaldehyde (4%). After perfusion, the animals were decapitated. The left bulla was dissected and immersed in paraformaldehyde (4%). The superior (anterior) semicircular canal was imaged using a condenser brightfield stereomicroscope through the opening into the bulla on a Revolve R4 microscope (ECHO, San Diego, CA, USA). A scale bar was added to each image in the ECHO annotation software. Images were exported to Canvas X for analysis of the dehiscence site. The percentage of bone regrowth via osteoneogenesis was derived as a ratio of the original 2.0 mm fenestration. For each animal the bone regrowth was classified between 0 and 100% as the percentage of 2.0 mm regrowth as follows: 0% (no regrowth), 1–25% (0.1–0.49 mm), 26–49% (0.50–0.99 mm), 50–74% (1.0–1.49 mm), 75–99% (1.5–1.99 mm), full resurfacing was 100% (2.0 mm). Given the interval of time (postoperative day 14) all animals fell into easily discernable categories between 25 and 75% regrowth/resurfacing.

Statistical analysis

Statistical analyses were performed using JMP software (SAS, Carey, NC, USA) and SPSS (IBM, Armonk, New York, USA).

Figures were generated using JMP software. To test the main effects of SSCD on balance beam and Rotarod performance ANOVAs with *post-hoc* analysis using the Tukey Honestly Significant Difference (HSD) test was used. A linear regression analysis was used to calculate adjusted R^2 scores when correlating data within groups. For all analyses, statistical significance was determined at the $p < 0.05$ level or greater. Data in the Figures display group mean ± SEM or actual data points (e.g., regression analysis).

Results

In this study we used 3 male and 3 female Mongolian gerbils (*Meriones unguiculatus*) that had received a semicircular canal dehiscence to explore vestibular paradigm balance impairments. None of these animals demonstrated circling behavior or complete loss of hearing after creation of the SSCD. Animals were pretrained on a Rotarod and a wide balance beam task, followed by SSCD. Retesting occurred on postoperative day 5–7 ($Post_7$) and 13–15 ($Post_{14}$), which represent the peak dysfunction and beginning of recovery from physiological impairment, respectively.

Superior semicircular canal dehiscence-induced balance impairments during balance beam and Rotarod tasks

Animals were trained to cross a balance beam without falling off or tested on time to fall on a Rotarod task (Figure 1). After five testing sessions the experimental animals had a 2.0 mm semicircular canal dehiscence created (Figure 1A). This was used to induce an asymmetric vestibular impairment, which was still present at postoperative day 14 as an inner ear conductive hearing loss that produces elevated auditory thresholds across all frequencies (Mean ± SEM; preoperative thresholds 31.6 ± 2.1 vs. postoperative day 14 thresholds 45.6 ± 2.5, $p < 0.001$) (Figure 1B) and increased c+VEMP amplitudes at 2 kHz stimulation (preoperative amplitudes 340 ± 17 μv vs. postoperative day 14 amplitudes 480 ± 24 μv, $p < 0.001$) (Figure 1C).

For each day of testing, the animal was placed on the far end of the beam and completed the task by running the beam's length to the enclosure on the opposite end. This was repeated and measured five times. There was a significant increase in time to cross with each trial compared to the first trial for preoperative testing, postoperative testing at day 7 and day 14 (Mean ± SEM; Trial 1, 50.9 ± 7.2 ms vs. Trial 2, 60.9 ± 7.7 ms vs. Trial 3, 86.6 ± 10.0 ms vs. Trial 4, 111.2 ± 13.1 ms vs. Trial 5, 138.6 ± 16.4 ms, *p* values all <0.05). This amounted to a group

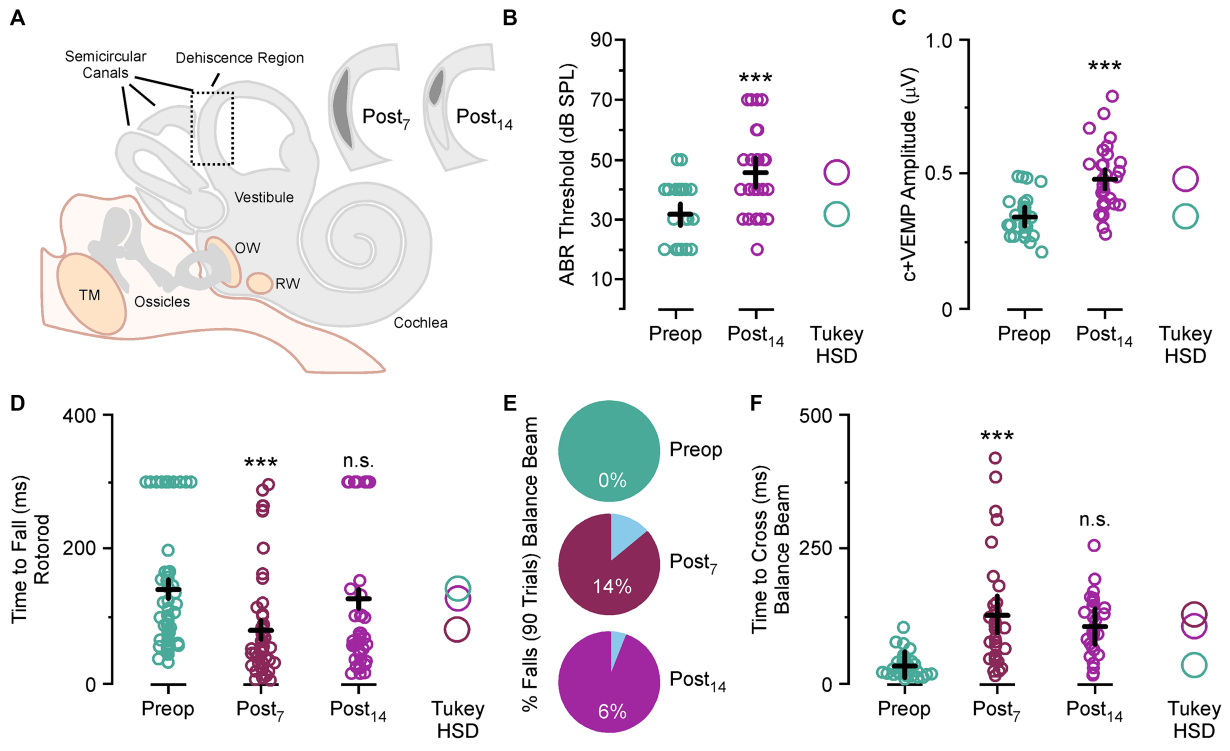

FIGURE 1
Superior semicircular canal dehiscence (SSCD)-induced balance impairment. **(A)** Diagram showing the location, size, and spontaneous bone regrowth/resurfacing of the dehiscence at postoperative day 7 and 14. **(B)** Scattergram showing a significant increase in ABR thresholds at postoperative day 14. **(C)** Scattergram showing a significant increase in c+VEMP amplitudes at postoperative day 14. **(D)** Scattergram showing significantly faster fall times for the Rotarod task at postoperative day 7 and slight impairment at postoperative day 14 compared to preoperative fall times. **(E)** Pie charts showing the rate of balance beam falls at postoperative day 7 and 14 compared to preoperative rates. **(F)** Scattergram showing the significantly longer times to cross on the balance beam task at postoperative days 7 and 14 compared to preoperative crossing times. ABR, auditory brainstem response; c+VEMP, cervical positive vestibular evoked potential; dB SPL, decibel sound pressure level; n.s., not significant; ms, millisecond; OW, oval window; $Post_7$, postoperative day 7 (dark purple); $Post_{14}$, postoperative day 14 (light purple); Preop, preoperative (teal); R^2_{adjust}, adjusted r-squared; RW, round window; TM, tympanic membrane; Tukey HSD, Tukey Honestly Significant Difference. ***p<0.001.

average increase in time to cross for Trial 2 at 64%, Trial 3 at 158%, Trial 4 at 221% and trial 5 at 368%. This trend was seen in every animal before and after surgical creation of the SSCD.

For this task a noise stimulus was played after the animal broke a beam five centimeters from the starting platform. In our previous study we show a significant increase in sound driven (2 kHz tone) c+VEMP amplitude (17) that is indicative of stimulus evoked asymmetrical vestibular output. This occurs through shunting of the sound wave energy via the dehiscence, which also dampens cochlear hair cell activation and leads to the inner ear conductive hearing loss. We hypothesized that this phenomenon might contribute to symptom expression, so we designed the experiment to assess whether noise-induced changes could be detected behaviorally in the SSCD animal model. In preoperative training the noise stimulus was introduced to reduce startle effects to the noise after SSCD. For each five-trial session the stimulus was triggered on Trial 3. As we saw a linear function in the increase in time to cross for each travel, we did not see a significant effect of noise on preoperative travel times (Trial 2, 23.6 ± 3.7 ms vs. Trial 3, 27.7 ± 3.9 ms; $p > 0.1$; Trial 3, 27.7 ± 3.9 ms vs. Trial 4, 37.8 ± 5.0 ms; $p > 0.1$). For postoperative trials the noise stimulus was played on Trial 1, 2, 4 and 5. Thus to test for a significant effect of noise onset after SSCD we would expect to see faster travel times for Trial 3 compared to Trial 2; however, we only observed the linear increase from Trial 2 to Trial 3 for postoperative day 7 (Trial 2, 89.4 ± 16.4 ms vs. Trial 3, 121.4 ± 20.8 ms; $p > 0.1$) and postoperative day 14 (Trial 2, 69.7 ± 14.2 ms vs. Trial 3, 110.7 ± 16.1 ms; $p > 0.1$) seen in preoperative testing. This suggested the noise stimulus induced no delay on time to cross and the non-noise trial did not show any savings in time to cross.

Despite not having a noise effect, we did observe impaired balance postoperatively (Figure 1D). For the Rotarod task, animals fell more often (preoperative fall rate, 79% vs. postoperative day 7 fall rate, 96%) and significantly faster (Mean ± SEM preoperative time to fall, 141.4 ± 12.6 ms vs. postoperative day 7, 80.6 ± 12.1, $p < 0.001$) at postoperative day 7. There was no significant difference in fall rate (preoperative fall rate, 79% vs. postoperative day 14 fall rate, 70%) or time to fall (Mean ± SEM preoperative time to fall, 141.4 ± 12.6 ms vs. postoperative day 14, 126.7 ± 16.0, $p > 0.1$) at postoperative day 14. The bimodal distribution of the postoperative day 14 data is indicative of differences in the rate of bone resurfacing between animals as we have previously noted (17). Removal of outlier sessions where the animals stayed on the Rotarod throughout the entire session shows that compared to preoperative time to fall there were significant increases in fall time for animals that did fall at postoperative day 14 (Mean ± SEM preoperative time to fall, 96.1 ± 6.5 ms vs. postoperative day 14, 54.8 ± 6.4, $p < 0.01$).

For the wide beam balance task, not a single animal fell preoperatively over 90 trials; however, we did see fall rates of 14 and 6% after SSCD. These falls always happened on noise stimulus trials; however, incidence rates were too low to draw any conclusions about sound-induced falling. In Figure 1E, we show that there was a significant adverse effect of SSCD on time to cross at postoperative day 7 (Mean ± SEM; preoperative time to cross 34.2 ± 22 ms vs. postoperative day 7 time to cross 128.3 ± 34 ms, $p < 0.001$) and postoperative day 14 (preoperative time to cross 34.2 ± 22 ms vs. postoperative day 14 time to cross 106.3 ± 28 ms, $p < 0.001$). It did take the animals longer to cross on postoperative day 7 vs. postoperative day 14, but this was not significant (postoperative day 7 time to cross 128.3 ± 34 ms, $p <$ vs. postoperative day 14 time to cross 106.3 ± 28 ms, $p > 0.1$). We found the same trend with the Rotarod studies (Figure 1F). Again, the time to fall for postoperative day 7 was significantly faster than preoperative times (preoperative time to fall 141 ± 13 ms vs. postoperative day 7 time to fall 80 ± 34 ms, $p < 0.001$). There was a faster fall time at postoperative day 14; however, this was not significant (preoperative time to fall 141 ± 13 ms vs. postoperative day 14 time to fall 126 ± 27 ms, $p > 0.1$). Time to fall was significantly faster at postoperative day 7 compared to postoperative day 14 (postoperative day 7 time to fall 80 ± 34 ms vs. postoperative day 14 time to fall 126 ± 27 ms, $p < 0.05$). All together, we found an effect of SSCD on balance; and the impact on balancing behavior is highest at the peak of the SSCD induced physiological, spatial, and cognitive impairments we have previously reported (17, 26, 28).

ABR and c+VEMP measurements correlate with balance impairment

To verify the involvement of vestibular dysfunction with balance beam and Rotarod measured impairments we correlated the ABR and c+VEMP thresholds and amplitudes as a function of physiological severity versus behavioral impairment at the end of postoperative testing (Figure 2). ABR and c+VEMP measurements were not recorded for postoperative day 6–8 as the animals are very sensitive to anesthesia and we did not want these affects to influence behavior. We also did not include c+VEMP threshold data as these occur below the lowest dB SPL measured by our apparatus (20 dB SPL) in our animal model. As previously reported (17) we observed a significant correlation between each animal's auditory threshold and their c+VEMP amplitude (Figure 2A). These are measured as percentage postoperative changes from preoperative baselines (ABR = 0.4 + 0.84 × c+VEMP; adjusted r-squared = 0.57, $p < 0.05$). There is also a correlation between ABR thresholds and time to fall during Rotarod testing at postoperative day 14 (ABR = 0.19–0.16 × time to fall; adjusted r-squared = 0.71, $p < 0.05$) (Figure 2B). There was also a correlation between ABR thresholds and time to fall during Rotarod testing at postoperative day 14 (ABR = 0.19–0.16 × time to fall; adjusted r-squared = 0.71, $p < 0.05$) (Figure 2B). A much stronger correlation is seen for c+VEMP amplitudes and time to fall from the Rotarod at postoperative day 14 (c+VEMP = 0.18–0.17 × time to fall; adjusted r-squared = 0.90, $p < 0.01$) (Figure 2C). The time to fall from the Rotarod was correlated with the time to cross the balance beam for postoperative day 14 animals (time to cross = 0.58–0.18 × time to fall; adjusted r-squared = 0.63, $p < 0.05$) (Figure 2D). The same trends that were observed for time to fall on the Rotarod apply to time to cross on the wide balance beam (Figures 2E,F). There was a significant correlation between ABR thresholds and time to cross at postoperative day 14 (ABR threshold = 0.25 + 0.78 × time to cross; adjusted r-squared = 0.79, $p < 0.05$) as well as between c+VEMP and time to cross (c+VEMP = −0.22 + 0.72 × time to cross; adjusted r-squared = 0.73, $p < 0.05$). All together these correlations showed a strong connection between SSCD-induced changes to peripheral physiology and Rotarod and balance beam performance impairment.

Condenser brightfield stereomicroscopy

To verify the involvement of bone regrowth status with physiological and behavioral impairments at postoperative day 14

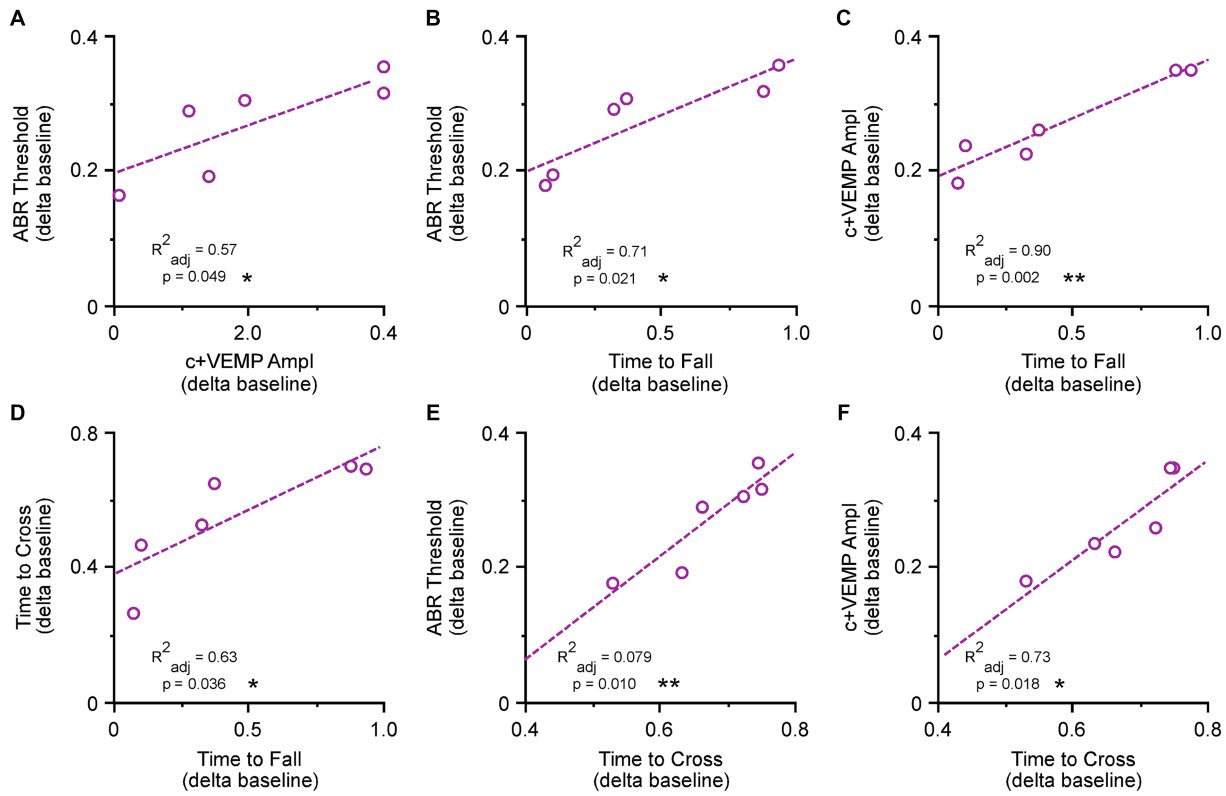

FIGURE 2
Correlations between superior semicircular canal dehiscence (SSCD)-induced changes to peripheral inner ear function and behavioral balance performance at postoperative day 14 (light purple). **(A)** Scatterplot showing correlation between ABR thresholds and c+VEMP amplitudes. **(B)** Scatterplot showing correlation between ABR thresholds and time to fall in the Rotarod task. **(C)** Scatterplot showing correlation between c+VEMP amplitudes and time to fall in the Rotarod task. **(D)** Scatterplot showing correlation between time to cross in the balance beam task and time to fall in the Rotarod task. **(E)** Scatterplot showing correlation between ABR thresholds and time to cross in the balance beam task. **(F)** Scatterplot showing correlation between c+VEMP amplitudes and time to cross in the balance beam task. ABR, auditory brainstem response; c+VEMP, cervical positive vestibular evoked potential; R^2_{adjust}, adjusted r-squared. *p<0.05, **p<0.01.

we correlated ABR thresholds, c+VEMP amplitudes, time to fall on the Rotarod task, and time to traverse the beam task (Figure 3). As previously reported (17), bone regrowth/resurfacing via osteoneogenesis commences shortly after fenestration with the bone being completely resurfaced by 1 month (Figure 3A). The status of bone regrowth at postoperative day 14 is typically between 25 and 50%. In the current study we confirmed the same trend (Figure 3B). Again, we saw significant correlations between the percentage of bone regrowth and ABR thresholds (regrowth = 1.04–2.15 × ABR threshold; adjusted r-squared = 0.59, $p < 0.05$) (Figure 3C) and a highly significant correlation for c+VEMP amplitudes (regrowth = 1.15–2.63 × c+VEMP amplitude; adjusted r-squared = 0.91, $p < 0.01$) (Figure 3D). For the Rotarod task there was a significant correlation between percentage bone regrowth and time to fall (regrowth = 0.66–0.45 × time to fall; adjusted r-squared = 0.79, $p < 0.05$) (Figure 3E). Finally, for the balance beam task there was a significant correlation between percentage of bone regrowth and time to traverse (regrowth = 1.83–2.03 × time to traverse; adjusted r-squared = 0.79, $p < 0.05$) (Figure 3F).

Discussion

In patients with SSCD, sound-induced symptoms are a common component of their clinical presentation (13, 14, 29). Often referred to as the Tullio phenomenon, sound-induced vestibular dysfunction is the result of abnormal shunting of sound pressure from the cochlea out through the dehiscent superior semicircular canal, creating a pathologic third mobile window (9, 28–33). Studies have demonstrated that in addition to inner ear conductive hearing loss, patients exhibit these balance impairments and vertigo from sudden, loud sounds along with abnormal vestibular-evoked myogenic potentials (VEMPs) (5, 6, 9, 13, 18, 34–37). Surgical plugging and correction of the dehiscence often leads to the resolution of sound-induced symptoms with preserved hearing thresholds (5, 9, 38–40).

In addition to our previous work developing the gerbil SSCD model (17, 26), other animal models have effectively demonstrated and explored the mechanisms behind the auditory deficits, namely the inner ear conductive hearing loss found in SSCD, in fat sand rats, guinea pigs and chinchillas (18–22, 41). Studies in mice have also investigated the effect of different vestibular lesions (labyrinthectomy, absent otoliths) on Rotarod and balance beam performance (42–47). To our knowledge, the present study is the first to directly assess and reproduce the vestibular deficits found in SSCD.

In this report we expanded upon the auditory and vestibular electrophysiology findings as well as the cognitive and spatial behavioral impairments observed in our animal model of SSCD (17, 26, 28). With our model established to date, the only remaining elements needed to replicate the human experience with SSCD was to

10.3389/fneur.2024.1476004

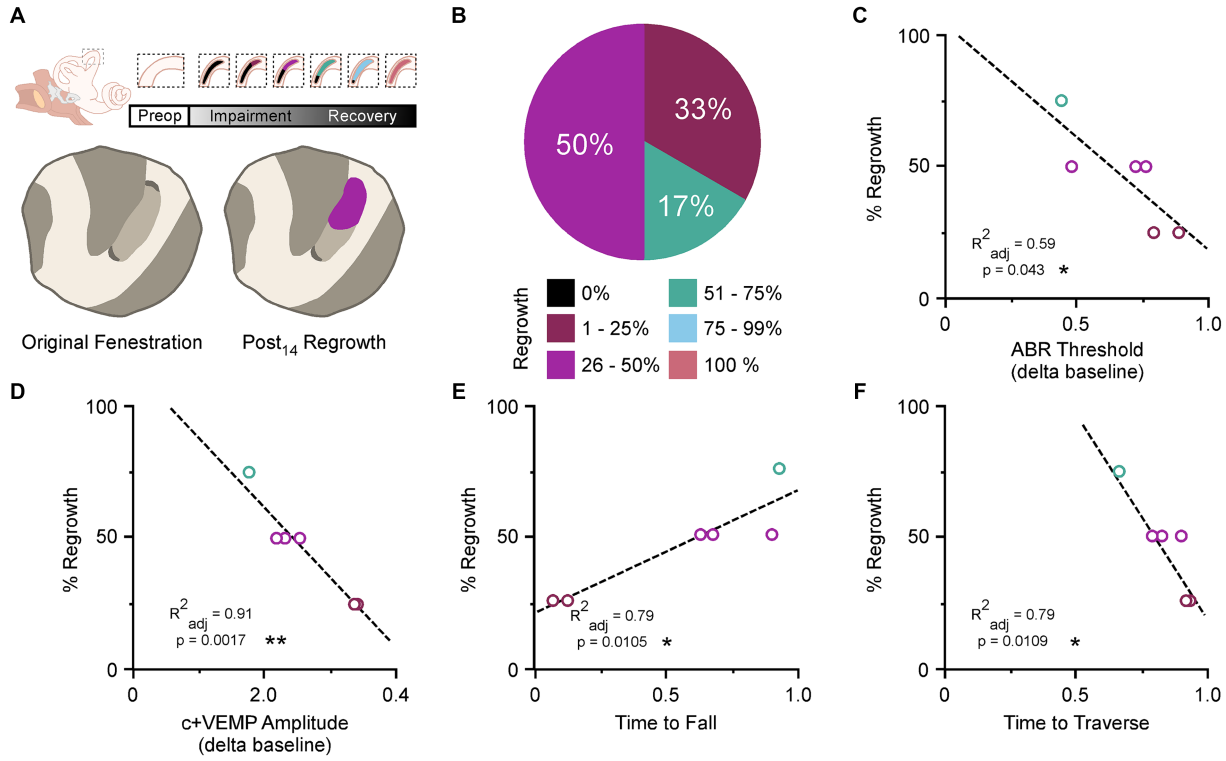

FIGURE 3
Correlation between bone regrowth, behavioral, and physiological impairment. **(A)** Diagram showing the general association between bone resurfacing and physiological impairment (*top*). Cartoon showing example of original fenestration and the typical regrowth associated with postoperative day 14 (*bottom*). **(B)** Pie chart showing the percentage of regrowth in fenestrated canals at each level of classification for postoperative day 14. **(C)** Correlation between percentage of bone regrowth and the percent ABR threshold shifts at postoperative day 14. **(D)** Correlation between percentage of bone regrowth and the percent c+VEMP amplitude shifts at postoperative day 14. **(E)** Correlation between percentage of bone regrowth and the time to fall on the Rotarod task at postoperative day 14. **(F)** Correlation between percentage of bone regrowth and the time to cross the balance beam at postoperative day 14. %, percentage; ABR, auditory brainstem response; c+VEMP, cervical positive vestibular evoked potential; $Post_{14}$, postoperative day 14; Preop, preoperative. *p<0.05, **p<0.01.

demonstrate vestibular dysfunction and sound-induced vestibular dysfunction.

After training the animals to balance on a Rotarod and to cross a wide beam, we completed the surgical creation of a SSCD and subsequently tested balance behavioral impairments during the peak (postoperative day 7) and beginning of recovery from the pathological third mobile window (postoperative day 14). We found significant effects of SSCD on time on the Rotarod, time to cross the balance beam, and on falls off the beam. Finally, the severity of this balance behavioral impairment was highly correlated with auditory thresholds and otolithic vestibular evoked responses (c+VEMP amplitudes). Together, these findings suggests that the recovery status of the dehiscence (and how large it is) will determine the severity of the balance impairments in this model. This makes it an ideal model for testing a wide variety of hypotheses associated with asymmetric vestibular dysfunction in humans due to SSCD.

To measure the degree of spontaneous resurfacing of the SSCD, we performed condenser brightfield stereomicroscopy. We then correlated the change on ABR thresholds, change in c+VEMP amplitudes, time to fall during the Rotarod task and the time to traverse during the balance beam task. For all four of these correlations, there was a statistically significant correlation between the degree of resurfacing and the electrophysiological measures and the behavioral measures.

A potential weakness of the present study is that some of the observed behavioral balance impairments could have resulted from postoperative serous labyrinthitis rather than the SSCD alone. Our inclusion–exclusion criteria excluded animals who exhibited persistent circling behavior, poor feeding and drinking behavior and loss of ABR and c+VEMP function. It is also the case that the elevated c+VEMP amplitudes would not be expected if a serous labyrinthitis impaired otolithic function after SSCD. We also minimized this effect by delaying the initial post SSCD testing for 6 days to allow for recovery after the surgical procedure. Administration of corticosteroids postoperatively was considered but not included in the study protocol because effective intralabyrinthine corticosteroid levels in gerbils has not been studied after intraperitoneal delivery, nor has a dosing regimen been studied in these animals.

Another potential weakness of our model is that the temporal lobe dura and temporal lobe is not resting on the SSCD as it likely does in patients with this disorder. An animal model of a human condition is our best approximation of human pathology, which is imperfect. In our model, there is no covering of the surgically created third mobile window, but rather the perilymph is exposed to the humid environment of the reconstructed bulla. In designing our model, we considered covering the dehiscence site; however, we were concerned about inducing an inflammatory reaction and serous labyrinthitis, so we did not do this. We do know from our initial two

papers establishing this animal model of SSCD that there are measured changes in ABR and c+VEMP that are reversible much like surgical management of SSCD patients experience, as well as reversible cognitive function changes (17, 26). For these reasons we did not cover the dehiscence site in the present series of experiments.

In our gerbil model of SSCD, the experimental reproduction of sound-induced vestibular symptoms would have served as a more accurate representation of human symptoms. While we observed more sound-induced dysfunction, these differences did not reach statistical significance. There are two possibilities to explain this, which are likely related. Either the sample size was too small to capture a small effect, or the acute sound exposure was not adequate to elicit the expected sound-induced vestibular dysfunction. One limitation of this study is that the speaker utilized could not consistently produce sound levels above 90 dB or adequately reproduce lower frequencies sound at that dB SPL. Thus, it is possible that an essential frequency range known to induce vestibular dysfunction symptoms in patients with SSCD were not delivered to the gerbils with SSCD (2, 25, 48). Future studies should address this by employing more powerful and lower-frequency sound sources to more accurately model the sound-induced vestibular dysfunction found in patients with SSCD. Future work in this animal model will focus on directly investigating the Tullio phenomenon (nystagmus), as well as the effect of SSCD on cochlear function. The development of scleral search coils for use in gerbils would also provide the opportunity to measure sound-induced nystagmus in this experimental model. Here, we plan to utilize electrocochleography around the timelines established in our vestibular paradigms to investigate how dehiscence will affect cochlear summating potentials and action potentials throughout recovery (resurfacing).

Conclusion

The findings reported herein help to further establish the Mongolian gerbil as an appropriate model for understanding the specific effects of SSCD on vestibular function. Our gerbil model reproduced the vestibular deficits seen in patients with SSCD, as evidenced by increased beam-crossing times and increased Rotarod times on postoperative day 7 (acute phase of impairment) with improvement corresponding to the onset of dehiscence recovery. These findings build upon the gerbil SSCD model showing an increase in both ABR thresholds, as a proxy for inner ear conductive hearing loss, and elevated c+VEMP amplitudes, mimicking the abnormal physiological measures found in the human disorder along this same timeline. We subsequently demonstrated that these measures, specifically c+VEMP amplitudes, had negative and reversible correlations with decision-making, suggesting potential CNS deficits resulting from the SSCD, again along this 7-day peak with the onset of recovery corresponding to behavior returning toward preoperative levels. Finally, even though we do not observe increased sound-induced vestibular dysfunction, it should be noted that a general impairment to balance is present regardless of auditory stimulation, and this is also what patients with SSCD experience. This finding is similar to the cognitive and spatial behavioral impairments which is also what patients with SSCD experience, which do not require sound-induced stimulus to become manifest.

Data availability statement

The raw data supporting the conclusions of this article will be made available by the authors, without undue reservation.

Ethics statement

The animal study was approved by Rutgers University Institutional Animal Care and Use Committee. The study was conducted in accordance with the local legislation and institutional requirements.

Author contributions

SSH: Data curation, Formal analysis, Methodology, Validation, Writing – review & editing. PAW: Project administration, Resources, Supervision, Validation, Writing – original draft, Writing – review & editing, Conceptualization, Formal analysis, Funding acquisition, Investigation, Methodology. DJM: Data curation, Investigation, Validation, Writing – review & editing. EP: Data curation, Investigation, Validation, Writing – review & editing. MYK: Data curation, Investigation, Validation, Writing – review & editing. AT: Data curation, Investigation, Validation, Writing – review & editing. NLC: Data curation, Investigation, Validation, Writing – review & editing. SCC: Data curation, Investigation, Validation, Writing – review & editing. NS: Data curation, Investigation, Validation, Writing – review & editing. UAU: Data curation, Investigation, Validation, Writing – review & editing. JDY: Formal analysis, Methodology, Supervision, Validation, Writing – original draft, Writing – review & editing. TMM: Conceptualization, Formal analysis, Investigation, Methodology, Project administration, Resources, Software, Supervision, Validation, Writing – original draft, Writing – review & editing.

Funding

The author(s) declare financial support was received for the research, authorship, and/or publication of this article. This work was supported by the Rutgers Health Chancellor Scholar Award to PAW.

Conflict of interest

The authors declare that the research was conducted in the absence of any commercial or financial relationships that could be construed as a potential conflict of interest.

The author(s) declared that they were an editorial board member of Frontiers, at the time of submission. This had no impact on the peer review process and the final decision.

Publisher's note

References

1. Minor LB, Solomon D, Zinreich JS, Zee DS. Sound- and/or pressure-induced vertigo due to bone dehiscence of the superior semicircular canal. *Arch Otolaryngol Head Neck Surg*. (1998) 124:249–58. doi: 10.1001/archotol.124.3.249

2. Cremer PD, Minor LB, Carey JP, Della Santina CC. Eye movements in patients with superior canal dehiscence syndrome align with the abnormal canal. *Neurology*. (2000) 55:1833–41. doi: 10.1212/WNL.55.12.1833

3. Minor LB. Clinical manifestations of superior semicircular canal dehiscence. *Laryngoscope*. (2005) 115:1717–27. doi: 10.1097/01.mlg.0000178324.55729.b7

4. Merchant SN, Rosowski JJ. Conductive hearing loss caused by third-window lesions of the inner ear. *Otol Neurotol*. (2008) 29:282–9. doi: 10.1097/MAO.0b013e318161ab24

5. Welgampola MS. Evoked potential testing in neuro-otology. *Curr Opin Neurol*. (2008) 21:29–35. doi: 10.1097/WCO.0b013e3282f39184

6. Watson SR, Halmagyi GM, Colebatch JG. Vestibular hypersensitivity to sound (Tullio phenomenon): structural and functional assessment. *Neurology*. (2000) 54:722–8. doi: 10.1212/WNL.54.3.722

7. Belden CJ, Weg N, Minor LB, Zinreich SJ. CT evaluation of bone dehiscence of the superior semicircular canal as a cause of sound- and/or pressure-induced vertigo. *Radiology*. (2003) 226:337–43. doi: 10.1148/radiol.2262010897

8. Wackym PA, Wood SJ, Siker DA, Carter DM. Otic capsule dehiscence syndrome: superior canal dehiscence syndrome with no radiographically visible dehiscence. *Ear Nose Throat J*. (2015) 94:E8–9. doi: 10.1177/014556131509400802

9. Wackym PA, Balaban CD, Mackay HT, Wood S, Lundell C, Carter D, et al. Longitudinal cognitive and neurobehavioral functional outcomes before and after repairing otic capsule dehiscence. *Otol Neurotol*. (2016) 37:70–82. doi: 10.1097/MAO.0000000000000928

10. Wackym PA, Balaban CD, Zhang P, Siker DA, Hundal JS. Third window syndrome: surgical management of cochlea-facial nerve dehiscence. *Front Neurol*. (2019) 10:1281. doi: 10.3389/fneur.2019.01281

11. Wackym PA, Balaban CD, Ikezono T, Agrawal Y, (Eds). (2021). Third window syndrome. Lausanne: Frontiers Media SA, pp. 1–230.

12. Schwartz T, Lindemann TL, Mongelluzzo G, Wackym PA, Gadre AK. Gray-scale inversion on high resolution computed tomography of the temporal bone: an observational study. *Ann Otol Rhinol Laryngol*. (2021) 130:1125–31. doi: 10.1177/0003489421996844

13. Ward BK, Carey JP, Minor LB. Superior canal dehiscence syndrome: lessons from the first 20 years. *Front Neurol*. (2017) 8:177. doi: 10.3389/fneur.2017.00177

14. Naert L, van R, van P, Bisdorff A, Sharon J, Ward B, et al. Aggregating the symptoms of superior semicircular canal dehiscence syndrome. *Laryngoscope*. (2018) 128:1932–8. doi: 10.1002/lary.27062

15. Smith PF, Zheng Y. From ear to uncertainty: vestibular contributions to cognitive function. *Front Integr Neurosci*. (2013) 7:84. doi: 10.3389/fnint.2013.00084

16. Popp P, Wulff M, Finke K, Rühl M, Brandt T, Dieterich M. Cognitive deficits in patients with a chronic vestibular failure. *J Neurol*. (2017) 264:554–63. doi: 10.1007/s00415-016-8386-7

17. Wackym PA, Balaban CD, Van Osch OJ, Morris B, Tamakloe MA, Salvatore V, et al. New model of superior semicircular canal dehiscence with reversible diagnostic findings characteristic of patients with the disorder. *Front Neurol*. (2023) 13:1035478. doi: 10.3389/fneur.2022.1035478.;

18. Hirvonen TP, Carey JP, Liang CJ, Minor LB. Superior canal dehiscence: mechanisms of pressure sensitivity in a chinchilla model. *Arch Otolaryngol Head Neck Surg*. (2001) 127:1331–6. doi: 10.1001/archotol.127.11.1331

19. Carey JP, Hirvonen TP, Hullar TE, Minor LB. Acoustic responses of vestibular afferents in a model of superior canal dehiscence. *Otol Neurotol*. (2004) 25:345–52. doi: 10.1097/00129492-200405000-00024

20. Songer JE, Rosowski JJ. A mechano-acoustic model of the effect of superior canal dehiscence on hearing in chinchilla. *J Acoust Soc Am*. (2007) 122:943–51. doi: 10.1121/1.2747158

21. Songer JE, Rosowski JJ. A superior semicircular canal dehiscence-induced air-bone gap in chinchilla. *Hear Res*. (2010) 269:70–80. doi: 10.1016/j.heares.2010.07.002

22. Attias J, Nageris BI, Shemesh R, Shvero J, Preis M. Superior canal dehiscence effect on hearing thresholds: animal model. *Otolaryngol Head Neck Surg*. (2011) 145:648–53. doi: 10.1177/0194599811410535

23. Tong BS, He ZY, Ding CR, Yang JM, Wang J, Han Z, et al. Mechanisms of hearing loss in a Guinea pig model of superior semicircular canal dehiscence. *Neural Plast*. (2018) 2018:1258341. doi: 10.1155/2018/1258341

24. Dlugaiczyk J, Burgess AM, Goonetilleke SC, Sokolic L, Curthoys IS. Superior canal dehiscence syndrome: relating clinical findings with vestibular neural responses from a Guinea pig model. *Otol Neurotol*. (2019) 40:e406–14. doi: 10.1097/MAO.0000000000001940

25. Curthoys IS, Smith CM, Burgess AM, Dlugaiczyk J. A review of neural data and modelling to explain how a semicircular canal dehiscence (SCD) causes enhanced VEMPs, skull vibration induced nystagmus (SVIN), and the Tullio phenomenon. *Audiol Res*. (2023) 13:418–30. doi: 10.3390/audiolres13030037

26. Mowery TM, Wackym PA, Nacipucha J, Dangcil E, Stadler R, Tucker A, et al. Superior semicircular canal dehiscence and subsequent closure induces reversible impaired decision-making. *Front Neurol*. (2023) 14:1259030. doi: 10.3389/fneur.2023.1259030

27. Chari DA, Juliano AF, Jung DH. Radiologically-proven new development of superior semicircular canal dehiscence associated with development of superior semicircular canal dehiscence syndrome. *Otol Neurotol*. (2021) 42:285–9. doi: 10.1097/MAO.0000000000002912

28. Smith JB, Hong SS, Murphy DJ, Dangcil E, Nacipucha J, Tucker A, et al. Neuroanatomical mapping of the gerbil corticostriatal sensory, motor and thalamostriatal parafascicular nucleus inputs reveals a thalamic relay for vestibular information across the striatum. *eNeuro*. (2024) 11:ENEURO.0273-24.2024. doi: 10.1523/ENEURO.0273-24.2024

29. Baloh RW. Superior semicircular canal dehiscence syndrome: leaks and squeaks can make you dizzy. *Neurology*. (2004) 62:684–5. doi: 10.1212/01.WNL.0000118644.59800.6A

30. Basura GJ, Cronin SJ, Heidenreich KD. Tullio phenomenon in superior semicircular canal dehiscence syndrome. *Neurology*. (2014) 82:1010. doi: 10.1212/WNL.0000000000000217

31. Dumas G, Curthoys IS, Castellucci A, Dumas L, Perrin P, Schmerber S. A bone-conducted Tullio phenomenon – a bridge to understand skull vibration induced nystagmus in superior canal dehiscence. *Front Neurol*. (2023) 14:1183040. doi: 10.3389/fneur.2023.1183040

32. Ostrowski VB, Byskosh A, Hain TC. Tullio phenomenon with dehiscence of the superior semicircular canal. *Otol Neurotol*. (2001) 22:61–5. doi: 10.1097/00129492-200101000-00012

33. Pullicino R, Grech R. Tullio phenomenon in superior semicircular canal dehiscence (SSCD). *BMJ Case Rep*. (2015) 2015:bcr2015213674. doi: 10.1136/bcr-2015-213674

34. Aw ST, Todd MJ, Halmagyi GM. Latency and initiation of the human vestibuloocular reflex to pulsed galvanic stimulation. *J Neurophysiol*. (2006) 96:925–30. doi: 10.1152/jn.01250.2005

35. Lempert T, von Brevern M. Episodic vertigo. *Curr Opin Neurol*. (2005) 18:5–9. doi: 10.1097/00019052-200502000-00003

36. Rosengren SM, Aw ST, Halmagyi GM, Todd NP, Colebatch JG. Ocular vestibular evoked myogenic potentials in superior canal dehiscence. *J Neurol Neurosurg Psychiatry*. (2008) 79:559–68. doi: 10.1136/jnnp.2007.126730

37. Niesten ME, McKenna MJ, Herrmann BS, Grolman W, Lee DJ. Utility of cVEMPs in bilateral superior canal dehiscence syndrome. *Laryngoscope*. (2013) 123:226–32. doi: 10.1002/lary.23550

38. Shaia WT, Diaz RC. Evolution in surgical management of superior canal dehiscence syndrome. *Curr Opin Otolaryngol Head Neck Surg*. (2013) 21:497–502. doi: 10.1097/MOO.0b013e328364b3ff

39. Mau C, Kamal N, Badeti S, Reddy R, Ying YM, Jyung RW, et al. Superior semicircular canal dehiscence: Diagnosis and management. *J Clin Neurosci*. (2018) 48:58–65. doi: 10.1016/j.jocn.2017.11.019

40. Michailidou E, Rüegg PO, Karrer T, Korda A, Weder S, Kompis M, et al. Hearing results after transmastoid superior semicircular canal plugging for superior semicircular canal dehiscence: a meta-analysis. *Audiol Res*. (2023) 13:730–40. doi: 10.3390/audiolres13050065

41. Nageris BI, Attias J, Shemesh R, Hadar T, Preis M. A third window of the posterior semicircular canal: an animal model. *Laryngoscope*. (2010) 120:1034–7. doi: 10.1002/lary.20831

42. Machado ML, Kroichvili N, Freret T, Philoxène B, Lelong-Boulouard V, Denise P, et al. Spatial and non-spatial performance in mutant mice devoid of otoliths. *Neurosci Lett*. (2012) 522:57–61. doi: 10.1016/j.neulet.2012.06.016

43. Tung VW, Burton TJ, Quail SL, Mathews MA, Camp AJ. Motor performance is impaired following vestibular stimulation in ageing mice. *Front Aging Neurosci*. (2016) 8:12. doi: 10.3389/fnagi.2016.00012

44. Kim G, Nguyen N, Kim KS. Postural control in paw distance after labyrinthectomy-induced vestibular imbalance. *Med Biol Eng Comput*. (2020) 58:3039–47. doi: 10.1007/s11517-020-02276-9

45. Shaabani M, Lotfi Y, Karimian SM, Rahgozar M, Hooshmandi M. Data on galvanic-evoked head movements in healthy and unilaterally labyrinthectomized rats. *Data Brief*. (2016) 9:338–44. doi: 10.1016/j.dib.2016.08.048

46. Negishi-Oshino R, Ohgami N, He T, Ohgami K, Li X, Kato M. cVEMP correlated with imbalance in a mouse model of vestibular disorder. *Environ Health Prev Med*. (2019) 24:39. doi: 10.1186/s12199-019-0794-8

47. Modi AD, Parekh A, Patel ZH. Methods for evaluating gait associated dynamic balance and coordination in rodents. *Behav Brain Res*. (2024) 456:114695. doi: 10.1016/j.bbr.2023.114695

48. Luecke VN, Buchwieser L, Zu Eulenburg P, Marquardt T, Drexl M. Ocular and cervical vestibular evoked myogenic potentials elicited by air-conducted, low-frequency sound. *J Vestib Res*. (2020) 30:235–47. doi: 10.3233/VES-200712

49. Stewart CE, Kanicki AC, Altschuler RA, King WM. Vestibular short-latency evoked potential abolished by low-frequency noise exposure in rats. *J Neurophysiol*. (2018) 119:662–7. doi: 10.1152/jn.00668.2017

Frontiers in Neurology

Explores neurological illness to improve patient care

The third most-cited clinical neurology journal explores the diagnosis, causes, treatment, and public health aspects of neurological illnesses. Its ultimate aim is to inform improvements in patient care.

Discover the latest Research Topics

See more →

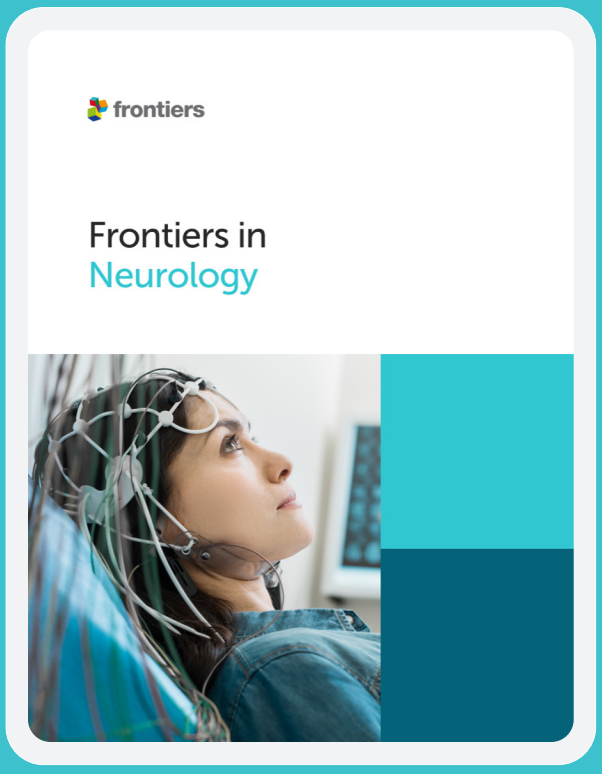

Frontiers

Avenue du Tribunal-Fédéral 34
1005 Lausanne, Switzerland
frontiersin.org

Contact us

+41 (0)21 510 17 00
frontiersin.org/about/contact